Using multi-omic approaches to identify modulators of Alzheimer's disease risk

By

Mabel Seto

Dissertation

Submitted to the Faculty of the

Graduate School of Vanderbilt University

in partial fulfillment of the requirements

for the degree of

DOCTOR OF PHILOSOPHY

in

Pharmacology

May 13, 2022

Nashville, Tennessee

Approved:

Joey Barnett, Ph.D.

Jennifer Below, Ph.D.

Paul Newhouse, M.D.

Jerri Rook, Ph.D.

Doug Ruderfer, Ph.D.

Timothy Hohman, Ph.D.

Dedication

I dedicate this dissertation to my family and friends. For without them, I could not have completed this work at all.

Acknowledgements

I would like to acknowledge the Vanderbilt Interdisciplinary Graduate Program and the Vanderbilt Department of Pharmacology for supporting me throughout my graduate career. I would especially like to acknowledge the National Institutes of Health Training Grant in Pharmacological Sciences (T32GM07628) that financially supported me from 2016 to 2018 as well as the following funding sources that supported my work: K01AG049164, K24AG046373, R21AG059941, R01AG059716, R01AG034962, R01HL111516, R01NS100980, R01AG056534, RF1AG15819 from the Intramural Research Program, the National Institute on Aging, the National Institutes of Health, the Vanderbilt University Advanced Computing Center for Research and Education (ACCRE) instrumentation grant (S10OD023680), the Vanderbilt Institute for Clinical and Translational Research (VICTR) grant (UL1TR000445, UL1TR002243). Finally, I would like to acknowledge all the mentors, trainees, and staff at the Vanderbilt Memory and Alzheimer's Center for creating such a wonderful, supportive, and collaborative training environment. I could not have wished for more.

TABLE OF CONTENTS

Page

Dedication ii

Acknowledgements iii

LIST OF TABLES x

LIST OF FIGURES xiii

LIST OF ABBREVIATIONS xv

CHAPTER 1: Introduction 1

1.1 Overview 1

1.2 Alzheimer's Disease 2

1.2.1 Discovery of Alzheimer's Disease 3

1.2.2 Amyloid Pathology 4

1.2.3 Tau Pathology 6

1.2.4 Amyloid Cascade Hypothesis 7

1.2.5 Current Therapeutics for Alzheimer's Disease 9

1.3 Resilience to Alzheimer's Disease 12

1.3.1 Inclusion Criteria 14

1.3.3 Evidence Categories 16

1.3.4 Introduction to Overview of Protective Genes and Variants 16

1.3.5 Amyloid Precursor Protein A673T: Reduced Pathologic Aβ generation 18

1.3.6 Apolipoprotein E 19

1.3.7 Protection in the Presence of *APOE*-ε4 22

1.3.8 Lipid Signaling and Homeostasis 24

1.3.9 Endosome and Lysosome Regulation 26

1.3.10 Synaptic Dysfunction 27

1.3.11 Immunity and Inflammation 30

1.4 Aims of the Project 33

CHAPTER 2: Identification of common genetic variants that modify the association between Alzheimer's disease biomarkers and hippocampal volume 36

2.1 Introduction....36

2.2 Materials and Methods....38

2.2.1 Participants 38

2.2.2 Genotyping and Quality Control Procedures....39

2.2.3 Mayo Clinic Study of Aging GWAS Data Acquisition, QC, and Imputation...40

2.2.4 Hippocampal Volume Standardization and Slope Calculation 40

2.2.5 Mayo Clinic Study of Aging MRI....41

2.2.6 CSF Biomarker Standardization....43

2.2.7 Amyloid Positron Emission Tomography 43

2.2.8 Statistical Analyses....45

2.2.9 Functional Annotation 48

2.2.10 Colocalization Analysis....48

2.2.11 Post-hoc *SEMA5B* Analyses....49

2.2.12 MAGMA Pathway Analysis....49

2.3 Results....50

2.3.1 *APOE* Allele Associations with Hippocampal Atrophy....50

2.3.2 *APOE* Allele Interactions with Baseline CSF Aβ42 51

2.3.3 Variant Interactions with Baseline CSF Aβ42 52

2.3.4 Replication of the rs62263260 Interaction with Amyloid Load in the Mayo Clinic Study of Aging....54

2.3.5 Sensitivity Analyses of rs62263260 56

2.3.6 Functional Annotation of rs62263260....56

2.3.7 Post-Hoc Analysis of *SEMA5B* expression in Brain 58

2.3.8 Gene and Pathway Results for the SNP x CSF Aβ42 GWAS....59

2.3.9 Single polymorphism nucleotide interactions with baseline levels of CSF phosphorylated tau....62

2.3.10 Functional annotation of rs114376431 62

2.3.11 Gene and Pathway Results for the SNP x CSF p-tau GWAS....63

2.4 Discussion 66
2.4.1 Variants on chromosome 3 drive increased susceptibility to amyloid-dependent neurodegeneration 66
2.4.2 Variants on chromosome 3 modify the association between CSF p-tau and hippocampal atrophy 68
2.4.3 Pathway results implicate DNA damage and repair as modifiers of amyloid-related brain atrophy 69
2.4.4 Pathway results implicate endolysosomal function as a modifier of tau-related neurodegeneration 69
2.4.5 *APOE*-ε4 carriers exhibit increased susceptibility to neurodegeneration in the presence of amyloidosis 70
2.4.6 Strengths and Limitations 70
2.4.7 Conclusion 71
2.4.8 Future directions 72

CHAPTER 3: Examining transcriptomic modifiers of the *APOE*-ε4 effects on cognition 73

3.1 Introduction 73

3.2 Materials and Methods 75
3.2.1 Participants 75
3.2.2 Neuropsychological Assessment 76
3.2.3 RNA Extraction, Library Preparation, and Sequencing 76
3.2.4 RNAseq Alignment and Quality Control 77
3.2.5 Biomarker Quantification 79
3.2.6 Statistical Analyses for Analysis 1 80
3.2.7 Sensitivity Analyses for Analysis 1 81
3.2.8 Post-hoc Biomarker Analyses 81

3.3 Analysis 1: Gene x *APOE*-ε4 Interaction Results on Cognition 82
3.3.1 *RNASE6* Interacts with *APOE*-ε4 on Cognition 82
3.3.2 Replication in ROS/MAP 82
3.3.3 Post-Hoc Analyses with Biomarkers 84
3.3.4 Discussion 88
3.3.5 Strengths and Limitations 91

3.4 Analysis 2: Investigating the relationship between *RNASE6* and other inflammatory biomarkers 93
3.4.1 CSF and Plasma Inflammatory Biomarker Quantification....95
3.4.2 Statistical Analyses....95
3.4.3 Summary of Preliminary Results....95
3.4.4 Discussion and Future Directions....97
3.5 Chapter Conclusion and Future Directions....99
CHAPTER 4: Leveraging weighted gene co-expression network analysis (WGCNA) as a tool for AD drug discovery....102
4.1 Introduction....102
4.1.1 Introduction to Weighted Gene Co-Expression Network Analysis....104
4.1.2 Introduction to Predicted Gene Expression (PrediXcan)....104
4.2 Materials and Methods....105
4.2.1 Participants....105
4.2.2 Cognitive Measures....105
4.2.3 Neuropathology....106
4.2.4 RNA sequencing and Processing....106
4.2.5 Gene Co-Expression Network Analysis....107
4.2.6 Tissue-Specific Predicted Gene Expression (PrediXcan)....107
4.2.7 Functional Annotation....109
4.2.8 Note on Statistical Analyses....109
4.3 Analysis 1: Logsdon et al., 2019 module associations with hallmarks of AD....110
4.3.1 Statistical Analyses....110
4.3.2 Participant Demographics....111
4.3.3 Module association with AD Hallmarks....111
4.3.4 Predicted gene expression module association with AD hallmarks....111
4.3.5 Grey60 module hub gene and GO-term analysis....112
4.3.6 Discussion....115
4.4 Analysis 2: Evaluation of predicted gene expression as a tool to generate and replicate gene co-expression network analyses....116
4.4.1 Network generation and evaluation....117

4.4.2 Modularity is not maintained when using predicted expression values 118
4.4.3 Discussion.....119
4.5 Analysis 3: Examining Logsdon et al., 2019 module interactions with *APOE*-ε4 positivity on hallmarks of AD.....121
4.5.1 Statistical Analyses.....121
4.5.2 Four modules interact with *APOE*-e4 positivity on cross-sectional cognition 122
4.5.3 Hub gene and GO-term analysis.....123
4.5.4 Discussion.....123
4.6 Chapter Conclusion.....128
4.6.1 Future Directions 130
CHAPTER 5: Concluding Remarks 131
APPENDIX A.....139
A.1 Acknowledgements.....139
A.2 Funding Sources 139
A.3 Appendix Tables 140
APPENDIX B 152
B.1 Acknowledgements 152
B.2 Funding Sources.....152
B.3 Appendix Tables 155
APPENDIX C 167
C.1 Acknowledgements 167
C.2 Funding Sources.....167
APPENDIX D.....169
D.1 Acknowledgments.....169
D.2 Funding Sources.....169

D.3 Supplemental Methods.....171
D.3.1 Generation of the gene co-expression network published by Logsdon et al., 2019.....171

REFERENCES 174

LIST OF TABLES

Page

Table 1.1: Summary of reviewed protective variants and genes 17

Table 2.1: Summary of imputation and quality control measures performed on each genotype dataset 42

Table 2.2: Dataset characteristics by analysis (CSF and PET) 47

Table 2.3: Participant characteristics by diagnosis 51

Table 2.4: Breakdown of combined GWAS dataset by cohort 52

Table 2.5: *APOE*-ε4 and *APOE*-ε2 associations with baseline hippocampal volume 53

Table 2.6: Variant interactions with CSF β-Amyloid 54

Table 2.7: Sensitivity Analyses for SNP x β-Amyloid GWAS 57

Table 2.8: *coloc* results for genes within 1Mb of rs62263260 58

Table 2.9: Transcription factor binding sites disrupted by SNPs within the rs62263260 locus 59

Table 2.10: Transcription factor binding sites disrupted by SNPs within the rs1162169741 locus 63

Table 3.1: Demographics of participants in VMAP who have CSF data 79

Table 3.2: Demographics for samples from each brain region in ROS/MAP 81

Table 3.3: Comparison of participant characteristics between VMAP and ROS/MAP 83

Table 3.4: Sensitivity analysis results for the *RNASE6* x *APOE*-ε4 interaction on baseline memory 84

Table 3.5: Interaction results of *RNASE6* expression and *APOE*-ε4 positivity on global cognition at last visit in ROS/MAP brain regions 85

Table 3.6: Summary of inflammatory biomarkers in VMAP 96

Table 3.7 *RNASE6* main effect and *RNASE6* interaction results with inflammatory biomarkers 97

Table 4.1: Summary of participant demographics for WGCNA analyses 112

Table 4.2: Summary of modules that are associated with hallmarks of AD.....113

Table 4.3: Significant module x *APOE*-ε4 interactions on cross-sectional cognition.....122

Table 4.4: Results of hub gene and GO-term analyses for the purple, cyan, salmon, and magenta modules.....123

Table A.1: Table of all protective SNPs identified up to 2020.....140

Table B.1: Top 20 suggestively significant ($p < 1x10^{-5}$) SNPs in the SNP x CSF Aβ42 GWAS on baseline hippocampal volume.....155

Table B.2: Top 20 suggestively significant ($p < 1x10^{-5}$) SNPs in the SNP x CSF Aβ42 GWAS on annual change in hippocampal volume.....156

Table B.3: Top 20 suggestively significant ($p < 1x10^{-5}$) SNPs in the SNP x CSF p-tau GWAS on baseline hippocampal volume.....157

Table B.4: Top 20 suggestively significant ($p < 1x10^{-5}$) SNPs in the SNP x CSF p-tau GWAS on annual change in hippocampal volume.....158

Table B.5: All suggestively significant ($p < 1x10^{-5}$) SNPs in the SNP x CSF tau GWAS on baseline hippocampal volume.....159

Table B.6: Top 20 suggestively significant ($p < 1x10^{-5}$) SNPs in the SNP x CSF tau GWAS on annual change in hippocampal volume.....160

Table B.7: Top 20 MAGMA gene associations using summary statistics from SNP x CSF Aβ42 GWAS on annual change in hippocampal volume.....161

Table B.8: Top 20 MAGMA gene associations using summary statistics from SNP x CSF Aβ42 GWAS on annual change in hippocampal volume when including *APOE4* status as a covariate in the GWAS.....162

Table B.9: Top 20 MAGMA pathway associations using summary statistics from SNP x CSF Aβ42 GWAS on annual change in hippocampal volume.....163

Table B.10: Top 20 MAGMA pathway associations using summary statistics from SNP x CSF Aβ42 GWAS on annual change in hippocampal volume when including *APOE4* status as a covariate in the GWAS.....164

Table B.11: Top 20 MAGMA gene associations using summary statistics from SNP x CSF p-tau GWAS on annual change in hippocampal volume.....165

Table B.12: Top 20 MAGMA pathway associations using summary statistics from SNP x CSF p-tau GWAS on annual change in hippocampal volume..... 166

LIST OF FIGURES

Page

Figure 1.1: Artistic depiction of amyloid and tau pathology 4

Figure 1.2: APP cleavage pathways 5

Figure 1.3: Schematic of Braak staging for neurofibrillary tangles 6

Figure 1.4: Theoretical schematic for the amyloid cascade hypothesis 8

Figure 1.5: A summary of genes containing rare and common variants that contribute to AD risk 12

Figure 1.6: Hypothetical framework for resistance and resilience to AD 13

Figure 1.7: Summary of literature search for protective variants and results 15

Figure 1.8: Theoretical contributors to resilience 18

Figure 2.1: Density plots of hippocampal volume distribution pre- and post-standardization 42

Figure 2.2: Density plots of CSF total tau and phosphorylated tau pre-and post-harmonization 44

Figure 2.3: Density plots of normalized amyloid measures 45

Figure 2.4: *APOE*-ε4 allele carriers have smaller hippocampal volumes at baseline and worse atrophy in the presence of high levels of brain amyloid pathology 53

Figure 2.5: Three SNPs in an intronic region of the *SEMA5B* gene significantly modify the association between baseline beta-amyloid and hippocampal atrophy 55

Figure 2.6: A plot demonstrating how the index SNP, rs62263260, modifies the association between standardized baseline PET amyloid levels and hippocampal atrophy in ADNI 56

Figure 2.7: Violin plots adapted from the NIH Gene-Tissue Expression (GTEx) Project showing the normalized expression of *SEMA5B* in esophageal, testicular, and brain tissue 57

Figure 2.8: Hippocampal pyramidal neurons in Alzheimer's disease brains express less *SEMA5B* than those from cognitively normal controls. 60

Figure 2.9: Summary of nominally significant MAGMA gene- and pathway-level results for the SNP x CSF Aβ42 GWAS. 61

Figure 2.10: Three SNPs on chromosome 3 significantly modify the association between CSF baseline p-tau levels and hippocampal atrophy. 64

Figure 2.11: Summary of nominally significant MAGMA gene- and pathway-level results for the SNP x CSF p-tau GWAS. 65

Figure 3.1: *APOE*-ε4 allele carriers in VMAP have worse baseline cognition in the presence of higher levels of *RNASE6* expression....84

Figure 3.2: *APOE*-ε4 allele carriers in ROS/MAP have worse global cognition in the presence of higher levels of *RNASE6* expression....85

Figure 3.3: Amyloid and tau positivity drives poorer cognitive performance at baseline....86

Figure 3.4: Amyloid-positive individuals in ROS/MAP expressing higher levels of *RNASE6* have worse baseline cognition....87

Figure 3.5: CSF biomarker levels are modulated by *RNASE6* expression 91

Figure 3.6: *RNASE6* is in a co-expression network module with *TREM2* and *MS4A* 92

Figure 3.7: *RNASE6* expression modifies baseline CSF sTREM2 levels....98

Figure 3.8: *RNASE6* expression is associated with baseline plasma CRP levels, but not other inflammatory biomarkers....101

Figure 4.1: Summary of novel module associations with hallmarks of AD....114

Figure 4.2: Higher expression of genes in the grey60 module are protective against tau burden and cognitive decline 114

Figure 4.3: Network diagram of the grey60 module....115

Figure 4.4: Dendrogram of network created with predicted expression values 118

Figure 4.5: Modularity is not maintained when using predicted expression 120

Figure 4.6: Four unique modules interact with *APOE*-ε4 positivity on cross-sectional cognition....124

Figure D.1: Heatmap demonstrating correspondence of our network modules and the previously published Logsdon modules....172

Figure D.2: Histogram demonstrating the highest percentage of gene overlap in each module between our network and the Logsdon modules....173

LIST OF ABBREVIATIONS

Listed in order of appearance:

AD, Alzheimer's disease
EOAD, early-onset Alzheimer's disease
LOAD, late-onset Alzheimer's disease
Aβ; Aβ42, $A\beta_{1-42}$, beta-amyloid
NFT, neurofibrillary tangles
PET, positron emission tomography
CSF, cerebrospinal fluid
CNS, central nervous system
NMDA, *N*-methyl-D-aspartate
GWAS, genome-wide association study
LDL, low-density lipoprotein
OR, odds ratio
SNP, single nucleotide polymorphism
MCI, mild cognitive impairment
LD, linkage disequilibrium
p-tau, phosphorylated tau
FLTD, frontotemporal lobar degeneration
MRI, magnetic resonance imaging
RNAseq, RNA sequencing
WGCNA, weighted gene co-expression network analysis
ADNI, Alzheimer's Disease Neuroimaging Initiative
VMAP, Vanderbilt Memory and Aging Project
WRAP, Wisconsin Registry for Alzheimer's Prevention
BIOCARD, Biomarkers of Cognitive Decline Among Normal Individuals
MCSA, Mayo Clinic Study of Aging
PC, principal component
QC, quality control
MAF, minor allele frequency
ICV, intracranial volume
SD, standard deviation
GMM, Gaussian mixture model
SUVR, standardized uptake value ratio
eQTL, expression quantitative trait locus
mQTL, module quantitative trait locus
GTEx, NIH Genotype-Tissue Expression Portal
PheWAS, phenome-wide association study
Mb, Megabase
NC, normal cognition
HV, hippocampal volume
AMP-AD, Accelerating Medicines Partnership Program - Alzheimer's Disease
TFBS, transcription factor binding sites

FDR, false discovery rate
GO, gene ontology
KEGG, Kyoto Encyclopedia of Genes and Genomes
PID, Protein Interaction Database
EFAM, epigenomic factor of activated microglia
ROS/MAP, Religious Orders Study (ROS) and Rush Memory and Aging Project (MAP)
DLPFC, dorsolateral prefrontal cortex
PCC, posterior cingulate cortex
CN, head of the caudate nucleus
RIN, RNA integrity number
PMI, post-mortem interval
IHC, immunohistochemistry
CPM, count per million
GO:BP, GO biological process
kNN, k-nearest-neighbors
TOM, topology overlap matrix
PRS, polygenic risk score
ELCE, early-life cognitive enrichment

CHAPTER 1

INTRODUCTION

Portions of this chapter are published under the title, “Protective Genes and Pathways in Alzheimer’s Disease: Moving Towards Precision Interventions,” in *Molecular Neurodegeneration*. Supplementary materials from the publication can be found in **Appendix A.**

1.1 OVERVIEW

Alzheimer's disease is a debilitating disorder that is characterized by neurodegeneration, memory loss and cognitive impairment. Sporadic late-onset AD is the most common form of the disease, though early-onset and familial forms of AD also exist. There is no cure for Alzheimer's disease and though only one disease-modifying therapy has been FDA-approved, the other five approved therapeutics are only effective for symptom management. Despite years of efforts, AD drug discovery has been plagued by numerous challenges. Proposed therapeutics have focused on amyloidosis, with many trials being halted due to toxicity or a lack of clinical efficacy on cognitive endpoints despite successfully lowering brain amyloid levels. In addition, AD is notably heterogeneous in presentation, making therapeutic development complex.

Studies using large-scale human "-omic" datasets (e.g., genomic, transcriptomic, proteomic, etc.) provide an opportunity to better acknowledge the heterogeneity and complexity of AD. More recently, -omics have been used to reveal novel insights into the biological mechanisms behind AD, which subsequently, helped to diversify possible therapeutic targets for AD. Though mitigation of harmful pathways and/or removal of neuropathology are two possible mechanisms

of action for AD therapeutics, our group and others have suggested that examining AD from a different perspective focusing on protective pathways may provide unique opportunities for the treatment of AD as well as for precision medicine.

The present dissertation focuses on the concept of resilience to AD or protection from AD, which refers to older individuals who have less brain atrophy or cognitive impairment than expected, given a particular level of AD neuropathology. Therefore, we believe that there are genetic and molecular factors that are protecting these individuals from the downstream consequences of pathology. Leveraging a unique statistical model, we aim to identify genetic and molecular modifiers of AD risk. Briefly, we leverage genotype data to identify variant-level modifiers of AD pathology on brain atrophy, transcriptomic data to identify gene-level modifiers of *APOE* effects on cognition, and finally, gene co-expression networks to identify novel associations with hallmarks of AD. In addition to novel drug target identification, these analyses provide a proof-of-concept for how these analyses can be used for biomarker discovery. Altogether, the analyses and results within this dissertation should demonstrate that 1) there are numerous ways to link genetic discovery to biological function and 2) that multi-omics can be used to discover and to explore previous results within new contexts.

1.2 ALZHEIMER'S DISEASE

Alzheimer's disease (AD) is a chronic neurodegenerative disorder that is characterized by two main pathologies (i.e., amyloid and tau) and presents with significant cognitive impairment as it progresses.[1, 2] AD is typically diagnosed in the clinic via neuropsychological tests, brain imaging, and biomarker analysis. However, the gold standard of diagnosis is determined by

neuropathological burden at autopsy though frameworks are evolving as technology improves and the AD field becomes more knowledgeable.[3]

In 2019, an estimated 5.8 million Americans were living with AD, and it was ranked as the sixth leading cause of the death in the US as well as the most common cause of dementia among older adults.[4] AD also represents a financial burden to patients, caregivers, and their loved ones; the estimated healthcare costs totaled $305 billion in 2020.[5] Both the number of inflicted individuals and healthcare costs are expected to more than double by 2050 as the aging population increases making it clear that AD will become a major public health crisis.[6]

AD is often divided into two categories: early-onset AD (EOAD) and late-onset AD (LOAD). EOAD comprises only 1-5% of all AD cases and is classified by onset before the age of 65.[7, 8] In contrast, the overwhelming majority of AD cases are late-onset and take place in individuals over the age of 65.[7, 9] There are both sporadic and familial forms of EOAD and LOAD, where familial forms are most often associated with autosomal dominant mutations in genes such as *APP* (amyloid precursor protein), *PSEN1* (presenilin 1), *PSEN2* (presenilin 2).[7, 8, 10] However, sporadic forms of EOAD[11, 12] and LOAD have a more complex and multifactorial etiology.[8, 13-17]

1.2.1 Discovery of Alzheimer's Disease

Alzheimer's disease was discovered in 1906 by psychiatrist and neuroanatomist, Alois Alzheimer. At that time, he encountered a 50-year-old female patient who exhibited paranoia, memory disturbances, confusion, and aggressiveness. After her death, he discovered and described the two main neuropathologies of AD: beta-amyloid (Aβ) plaques and tau neurofibrillary tangles (NFTs, **Figure 1.1**),[18] which account for approximately 40 to 70% of the variance in cognition in older adults.[19] However, it was not until over 60 years later that a relationship between Aβ, tau, and dementia were fully established.[19-21]

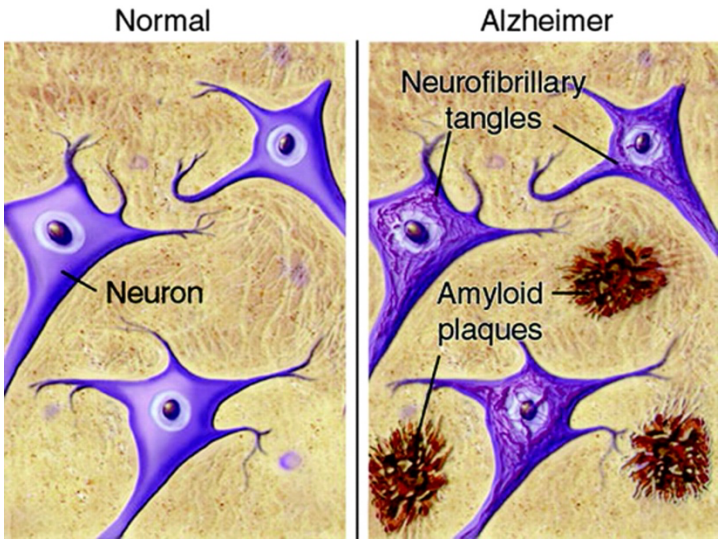

Figure 1.1: Artistic depiction of amyloid and tau pathology. Adapted from Silbert 2007.[22]

1.2.2 Amyloid Pathology

In the context of AD, Aβ comes from the proteolytic cleavage of amyloid precursor protein (APP), a single pass transmembrane protein, by β- and γ-secretase into its pathologic forms Aβ42 and Aβ40, which are 42 and 40 amino acids long, respectively (**Figure 1.2**). Though larger amounts of Aβ40 are generated via cleavage overall, it is believed that Aβ42 is more likely to aggregate due to its increased hydrophobicity in comparison to Aβ40.[23] The biological function of APP is unknown, though studies have linked APP to cell growth, cell survival, and neuronal migration.[19] APP has also been compared to Notch, a developmental protein that is also cleaved by γ-secretase.[24, 25]

Amyloid plaques, also called neuritic plaques, are extracellular and primarily consist of Aβ42.[26] It has been hypothesized that the development of neuritic plaques is due to extracellular amyloid aggregation, though it has also been suggested that plaques begin intracellularly and become extracellular after neuronal death.[23] Two types of plaques are most commonly observed in AD: diffuse and dense-core.[27] Dense-core plaques often contain neuronal nuclear material and

have been associated with synaptic loss as well as activated astrocytes and microglia.[28] In contrast, diffuse plaques are not accompanied by microglia, and it is unclear whether diffuse plaques play an independent role from dense-core plaques in the neuropathological progression of AD or whether they are observed in AD brains due to their development into dense-core plaques.[27, 28] Amyloid pathology has been linked to cognitive decline, neuroinflammation, as well as tau deposition.[21, 29-32]

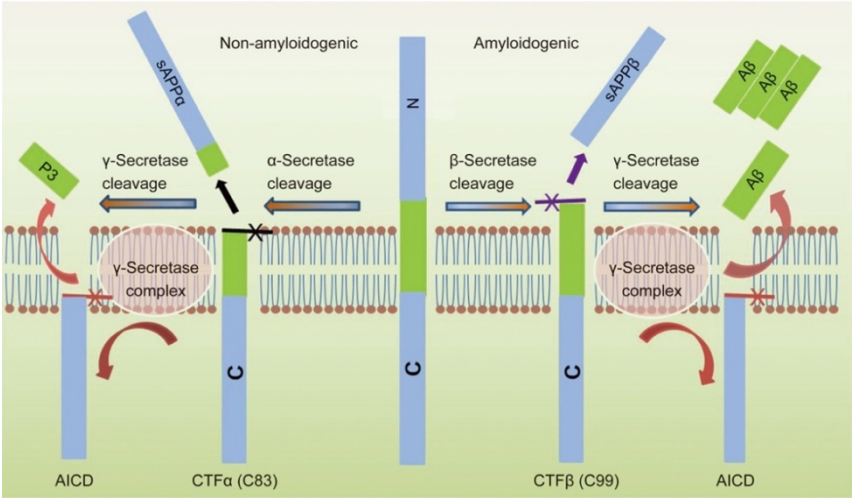

Figure 1.2. APP cleavage pathways. Adapted from Chen et al., 2017.[33] A schematic demonstrating the non-amyloidogenic and amyloidogenic cleavage pathways of human APP. CTF stands for C-terminal fragment and AICD is APP intracellular domain.

Amyloid burden has since become a biomarker for AD. Brain amyloid burden can be detected via positron emission tomography (PET) with tracers such as Pittsburgh compound B ([^{11}C]-PiB) and florbetapir ([^{18}F]-AV-45)[34] whereas cerebrospinal fluid (CSF) or plasma Aβ are most often detected via immunoassay.[35, 36] Both PET and CSF measurements of amyloid are highly correlated.[37, 38]

1.2.3 Tau Pathology

Tau is a component of the other major neuropathology of AD, neurofibrillary tangles. Tau and its associated pathologies, known as tauopathies, are also of particular interest in several neurodegenerative diseases including frontotemporal dementia, Parkinson's disease, and amyotrophic lateral sclerosis.[39-41]

The severity of neurofibrillary tangle burden within the brain can be classified via Braak staging, which is broken up into 6 progressive stages (**Figure 1.3**).[42] In stages I and II, NFTs are limited to the entorhinal cortex. In III and IV, NFTs spread to the limbic regions, including the hippocampus. Finally, in stages V and VI, NFTs can be found throughout the cortex.[42]

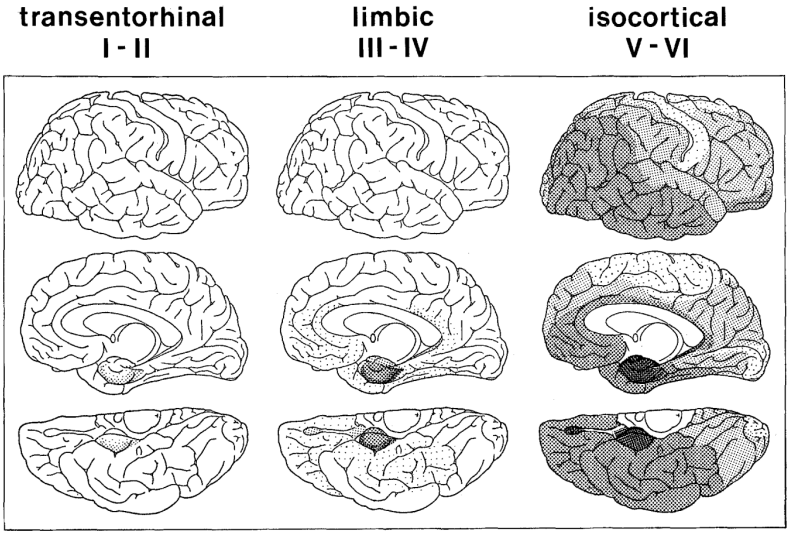

Figure 1.3. Schematic of Braak staging for neurofibrillary tangles. Adapted from Braak and Braak, 1991.[42]

Tau protein is encoded by the gene *MAPT*, microtubule associated protein tau, which is primarily expressed in neurons.[39, 43] Though the exact function of tau protein is still being characterized, it has been suggested that tau acts to stabilize microtubules within the axon.[39] In addition, studies have implicated tau in axonal transport of organelles and macromolecules.[44] Tau

is regulated by posttranslational modifications such as glycosylation, phosphorylation, and ubiquitination.[40, 45]

In 1986, tau filaments in NFTs were discovered to be abnormally hyperphosphorylated,[46] and in more recent years, as many as 40 phosphorylation sites have been identified.[20] Hyperphosphorylated tau is pathologic, and it has been shown to "seed" the formation of tau filaments when interacting with normal tau.[20] It is hypothesized that the prion-like propagation of tau filaments by hyperphosphorylated tau is how it is spread throughout the brain.[20, 40, 47] Tau pathology has also been linked to cognitive impairment and neuronal loss.[48-50]

Similar to amyloid, tau PET imaging and CSF tau immunoassays[51] are used as biomarkers for AD. Recently, several tau PET tracers have been developed so that tau progression throughout AD can be monitored.[52]

1.2.4 Amyloid Cascade Hypothesis

The amyloid cascade hypothesis posits that the abnormal aggregation of Aβ plaques precede tau filament formation and deposition. Then, both amyloid and tau pathology and downstream events instigate neuronal injury and neurodegeneration, subsequently causing cognitive impairment and memory loss (**Figure 1.4**).[53-56] This hypothesis was strongly supported by many studies[55] such as those focusing on familial EOAD, as many of the causal mutations of familial EOAD were identified in genes such as *APP*, *PSEN1*, and *PSEN2*, which are directly involved in the amyloid processing pathway.[7, 8]

Although the relationship between amyloid and tau is not fully characterized, studies have demonstrated that injection of Aβ into mouse brains caused a 5-fold increase in tau tangles near the injection sites.[57] In addition, it has been shown in a triple transgenic mouse that amyloid deposition occurs prior to tau pathology.[58] This is further supported by a rodent study

demonstrating that antibodies against tau do not affect Aβ pathology, which also suggests that amyloid is upstream of tau.[59] In humans, biomarker studies observe amyloid via PET scans and CSF prior to increases in CSF tau (**Figure 1.4**).[1, 2, 56] It should also be noted that, in the amyloid cascade framework, amyloid abnormalities can occur decades before any cognitive impairment presents.[2, 60, 61]

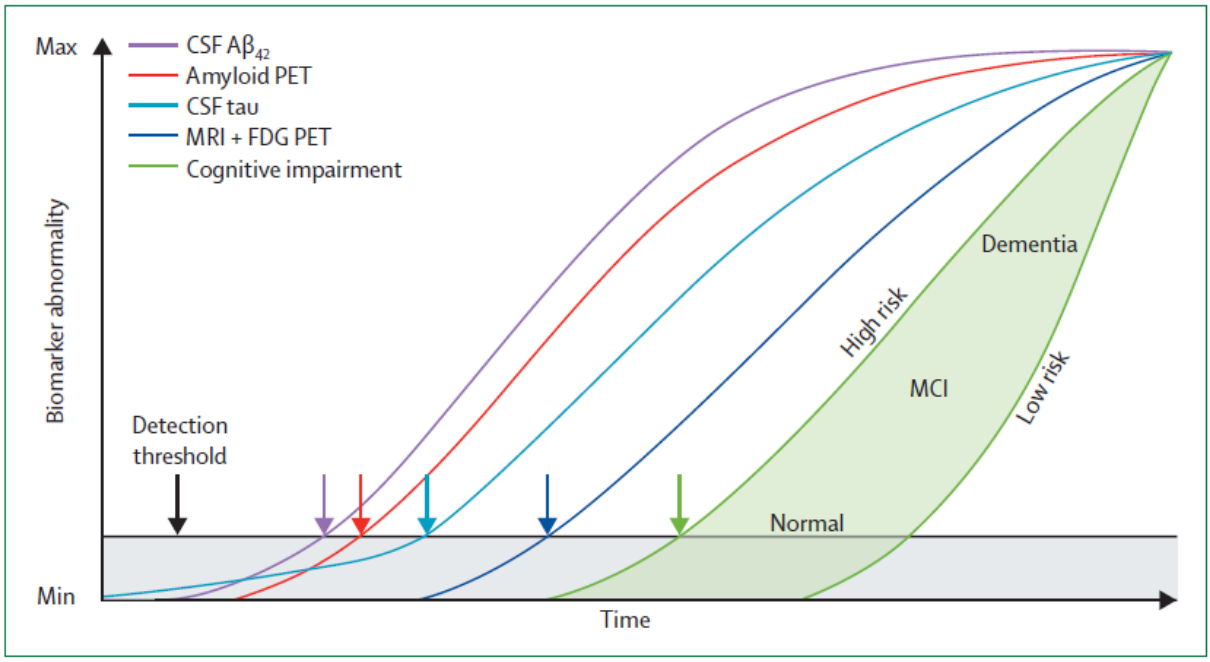

Figure 1.4. Theoretical schematic for the amyloid cascade hypothesis. Adapted from Jack et al., 2013.[2] This plot describes that biomarker abnormalities are detected in CSF Aβ42 and amyloid PET long before CSF tau abnormalities are noted and can occur decades before cognitive impairment arises.

Despite numerous studies supporting the amyloid cascade hypothesis, there is evidence to suggest that amyloid alone is not sufficient to cause AD. For example, studies have suggested that neurofibrillary tangles have a stronger correlation with cognitive impairment than neuritic plaques.[27, 56, 62] Furthermore, amyloid-focused therapeutics have largely failed in clinical trials,

despite effectively reducing amyloid burden, due to toxicity or inability to meet cognitive endpoints.[63-65]

1.2.5 Current Therapeutics for Alzheimer's Disease

There is no cure for Alzheimer's disease. AD drug discovery has been plagued by a 99.6% failure rate between the years of 2002 to 2012 with proposed therapeutics primarily focusing on amyloidosis for the past 25 years.[63, 66] In addition to the proposal of few non-amyloid-related targets, AD drug discovery is also suffering from numerous challenges including: the limitations of animal models, blood-brain barrier penetrance, and disease complexity and heterogeneity.[63, 66]

To date, there have only been 6 FDA-approved therapies specifically for AD, with the last being aducanumab in 2021.[67, 68] Aducanumab is touted as the first disease-modifying therapeutic for AD, and it is an monoclonal anti-amyloid antibody.[69] The approval of aducanumab has been controversial.[70-72] Though it has shown efficacy in reducing amyloid plaque burden,[73] it has been debated whether or not it showed efficacy in preventing cognitive decline.[70, 72] The other FDA-approved drugs for AD are as follows: Donepezil, Rivastigmine, Galantamine, Memantine, and a combination of Donepezil and Memantine.

Donepezil, Rivastigmine, and Galantamine are acetylcholinesterase inhibitors. Acetylcholine is a neurotransmitter that is essential to numerous central nervous system (CNS) functions including attention and cognition.[74-76] After neurotransmission, acetylcholine is hydrolyzed resulting in free choline which is then taken up by the pre-synaptic neuron. In both aging and AD brains, it was discovered that cholinergic function is disrupted (likely due to neuronal death), which correlated with cognitive impairment and cognitive decline.[76] Furthermore, treatment with cholinergic inhibitors such as scopolamine and atropine induce memory impairment in rats[76] and induced memory loss in young, healthy adults.[77] These studies along with numerous

others implicated cholinergic deficiency or dysfunction with cognitive impairment, supporting a "cholinergic hypothesis" of AD. Together, these studies supported the initial treatment approach of developing acetylcholinesterase inhibitors for AD. Today, Donepezil, Rivastigmine, and Galantamine remain viable treatment options for cognitive symptoms of mild to moderate AD. However, they are not disease modifying and are only effective for symptom management.[78]

Memantine is an *N*-methyl-D-aspartate (NMDA) receptor antagonist that has been approved for the treatment of moderate to severe AD as well as other disorders such as Parkinson's disease and epilepsy.[79] It can be used alone or in combination with the acetylcholinesterase inhibitor, Donepezil. Memantine functions as a low-affinity, uncompetitive antagonist for the NMDA receptor that both binds and dissipates quickly resulting in less negative effects than stronger NMDA receptor antagonists such as ketamine or MK-801.[79, 80] In clinical trials, memantine treatment resulted in better cognitive and behavioral outcomes.[81]

The NMDA receptor is activated by glutamate, the most abundant excitatory neurotransmitter in the CNS.[80] Activation of the NMDA receptor plays a major role in synaptic plasticity (i.e., long-term potentiation and long-term depression), which is considered a correlate for learning and memory.[82, 83] Though activation of the NMDA receptor is crucial for synaptic plasticity[84] and neuronal survival,[84] excessive activation also causes neuronal death.[80]

Glutamatergic and NMDA signaling are aberrant in AD; Aβ can impair glutamate reuptake and recycling as well as increase NMDA receptor currents, leading to excitotoxicity and cell death.[80] Studies have also suggested that NMDA receptor co-agonists, such as D-serine are upregulated in AD; reduction of D-serine was able to lessen both amyloid- and NMDA receptor-induced excitotoxicity.[80]

Historically, AD and AD drug discovery research has utilized a candidate gene approach, which probes a set of genes determined *a priori* that potentially contribute to AD risk or the AD endophenotype of interest.[85, 86] Though familial and candidate gene studies of *APP, PSEN1,* and *PSEN2* as well as studies supporting the amyloid cascade hypothesis[53, 54] strongly directed AD drug discovery efforts to amyloid, amyloid-focused therapeutics have not shown clinical efficacy on improving cognition in historical trials.[63-65, 67, 87] Furthermore, familial, early-onset cases of AD only make up a small percentage of all AD cases suggesting that there are factors other than amyloid that should be explored.

The recent availability of large "-omics" datasets provide a unique opportunity to overcome some of the previous challenges that have hampered drug development in AD. First, it allows for a different perspective on AD drug discovery focusing on phenotype first to identify genes and variants of interest (e.g., reverse genetic approaches, genome- or exome-wide association studies), further diversifying therapeutic targets.[64] In addition, the use of human data and human phenotypes are incredibly useful to supplement animal models, which are invaluable to drug discovery but have many limitations with regard to outcomes for AD drug discovery.[88] The boon of "-omics" data also permits systems biology-based approaches that can help to probe the etiology behind a multifactorial disease such as AD.[89]

Sporadic LOAD is complex, with numerous environmental and genetic factors contributing to the disease.[9] LOAD is highly heritable with twin studies providing estimates of $60\% < h^2 < 80\%$, [90] and to date over 40 risk loci for AD have been identified via large genome-wide association studies (GWAS), most of which are common variants with small effect sizes (**Figure 1.5**).[91-93] Although these new discoveries have provided novel insight on the biological contributors to AD, disease modifying treatments for Alzheimer's remain elusive.[63, 65, 94]

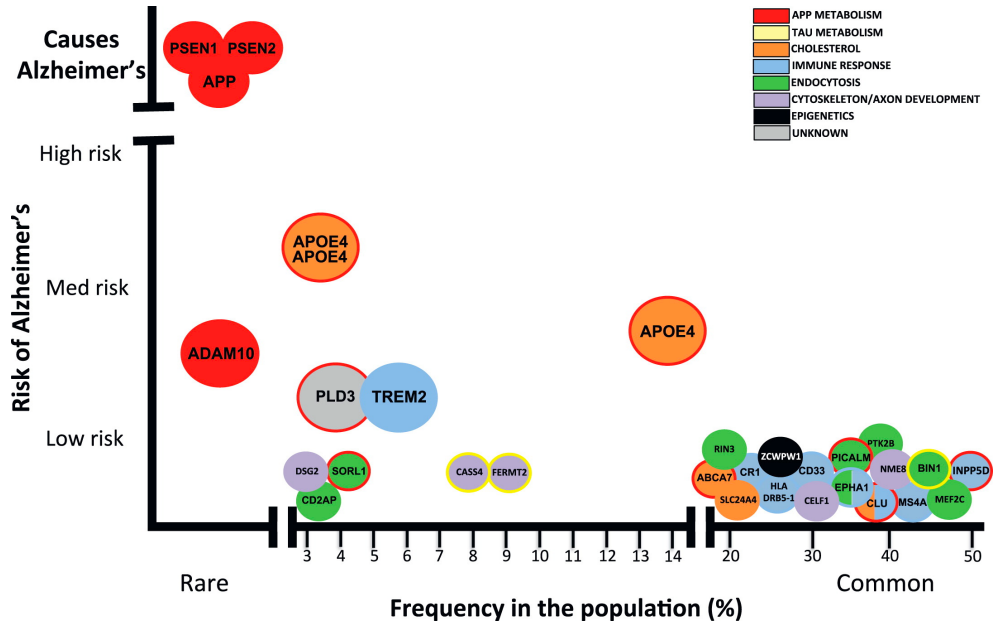

Figure 1.5. A summary of genes containing rare and common variants that contribute to AD risk. Adapted from Karch et al., 2015.[95]

1.3 RESILIENCE TO ALZHEIMER'S DISEASE

The ideas of resistance to pathology and resilience against the downstream consequences of pathology have been of particular interest in the AD field as studies continue to identify individuals with less than expected pathology, atrophy, or impairment given their age and/or neuropathological progression.[96] One such framework is presented in **Figure 1.6**. Protective factors can be defined as genetic[97] or environmental features[98] that reduce the risk that an individual will develop clinical AD. However, as our ability to measure the full neuropathological cascade of AD has expanded, the theoretical models have matured to include factors that protect from pathology, factors that protect against cognitive decline, and factors that protect against the downstream neurodegenerative cascade in AD (e.g., tau-related neurodegeneration).[99]

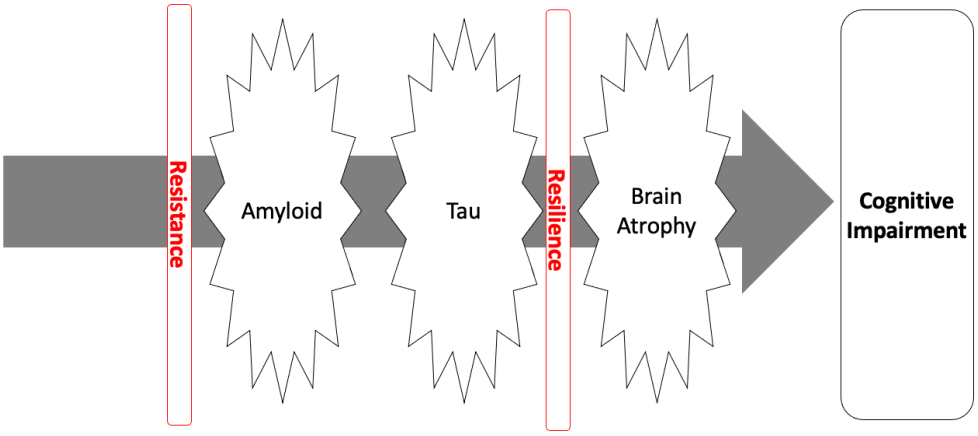

Figure 1.6. Hypothetical framework for resistance and resilience to AD. In brief, resistance can be defined as having less pathology than expected whereas resilience can be defined as less atrophy or cognitive impairment than expected given a level of pathology.

Resilience to AD, also known as asymptomatic or preclinical AD, is a phenomenon that in which individuals present with the neuropathological hallmarks of AD, but do not show clinical signs of cognitive impairment. In fact, as many as 70% of cognitively unimpaired older adults have some amount of AD pathology present in the brain at death, and as many as 30% of cognitively unimpaired older adults meet neuropathological criteria for autopsy-confirmed AD.[100-102] A shift in focus from AD risk to resilience presents an opportunity to uncover novel biological mechanisms of AD and to identify promising therapeutic targets for intervention. Such an approach has been transformative in other fields. For example, five loss-of-function variants in *PCSK9* that are associated with extremely low-density lipoprotein (LDL) cholesterol levels were identified in participants of the Dallas Heart Study.[103] These mutations led to the development of proprotein convertase subtilisin/kexin type 9 (PCSK9) inhibitors, which are currently used to treat statin-resistant hypercholesterolemia.[94, 104] In a similar way, uncovering and characterizing the

genetic factors that protect against AD could lead to new therapeutic discoveries – in which pre-existing biological pathways could be modulated for treatment.

Protective factors contributing to resilience are broadly defined within the literature. In large genome-wide association studies looking at AD cases in comparison to controls, protective variant alleles and/or genes may be defined as those with odds ratio (OR) < 1 (as examples: [91, 92, 105, 106]). In studies using continuous outcomes, protective variants and/or genes may be defined as those associated with a delay in disease onset[107, 108] or those associated with less pathology than expected.[109] Additionally, protective genetic factors may arise through associations with known protective phenotypes such as longevity,[110] cognitive reserve,[111] educational attainment,[112] or brain reserve.[111, 113] Cognitive reserve has been defined by Stern et al.,[114] as the "adaptability of cognitive processes that help to explain differential susceptibility of cognitive abilities to brain aging, pathology, or insult," whereas brain reserve is described as the "neurobiological capital (i.e., number of neurons) that allows individuals to better cope with brain aging and pathology before clinical or cognitive changes arise."[114] Characterizing the manner in which genetic factors protect against AD is critical to advance the field. Genes may protect by reducing neuropathological burden, or by providing a more optimal response to high levels of neuropathology, or even by providing a higher biological or cognitive baseline that might buffer against the clinical manifestation of the first stages of AD.[109] In this section, we will review, summarize, and carefully interrogate the evidence for emerging molecular pathways of protection to AD.

1.3.1 Inclusion Criteria

To identify AD protective or resilience variants and genes, we performed an initial PubMed search using the search terms: "protective variant Alzheimer", "protective SNP Alzheimer's Disease", "protective GWAS Alzheimer", and "SNP reduced risk AD", which yielded a total of

817 search results. The search results were further filtered manually to those that were relevant and in scope of this review (**Figure 1.7**). More specifically, we looked for previously identified variants in large GWAS and meta-analyses, case-control, cohort, or family studies, and rare variant analyses. Additionally, we included genes and variants that were previously reviewed or identified in the following papers: Andrews et al., 2019[97] and Ouellette et al., 2020.[115] Although many protective single nucleotide polymorphisms (SNPs) and genes have been identified within the literature (see **Appendix A.3**), we have limited our discussion in this review to those with published functional evidence beyond genetic discovery analyses alone.

"Functional evidence" includes (but is not limited to): additional analyses within the discovery manuscript, papers that replicated the original results, papers examining the biological effects of the variant of interest, papers that examine the annotated or referenced gene in the context of AD, and referenced literature that helps with interpretation and directionality of the biological mechanisms behind protection.

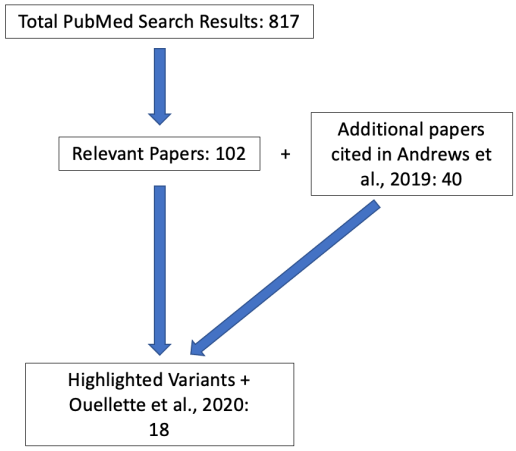

Figure 1.7. Summary of literature search for protective variants. A schematic demonstrating how search results were refined to those highlighted in the review.

1.3.3 Evidence Categories

For each highlighted variant, the strength of evidence for their mechanism of action is varied; the categories may be defined: "variant-level", "gene-level", and "pathway-level." For example, the mechanistic evidence for non-coding common variants may be limited to replication in different cohort studies. For this "variant-level" evidence, we look to additional literature to suggest a putative functional gene near or within the locus and a biological pathway. Other variants may have "gene-level" evidence, such that the functional gene within the region is well-established or that they cause an amino acid change within the encoded protein. For these variants, we look to literature to help us interpret directionality of effect and the biological pathway(s) behind protection. The strongest variants have all three facets of evidence (including "pathway-level"); they have been replicated, they are annotated, and their function and mechanism of protection are well-studied. The level of evidence for each highlighted variant and gene is included in **Table 1.1**.

1.3.4 Introduction to Overview of Protective Genes and Variants

Similar to AD risk, there are both protective biological and environmental contributors to resilience (**Figure 1.8**). In the following sections, we will focus on a selection of genes and variants that directly mediate the cellular response to AD pathology or downstream cellular stressors of pathology in the brain (**Table 1.1**). These genes also represent viable disease-modifying targets for AD, which could be modulated during and/or after pathological onset, but before cognitive impairment. Many of the genes and variants reviewed in this publication were initially identified in genome-wide association studies and meta-analyses of AD. A comprehensive list of protective variants and genes identified to date in such studies are included in **Appendix A.3**

Table 1.1: Summary of reviewed protective variants and genes						
rsID[A]	Allele[B]	CPRA[B]	MAF[C]	Gene	Evidence	Reference
rs63750847	C > T	21:27269932:C:T	0.0001	*APP*	Pathway	[116]
rs7412	C > T	19:45412079:C:T	0.087	*APOE*-ε2	Pathway	[117]
rs121918393	C > A	19:45412013:C:A	0	*APOE3ch*	Gene	[107]
rs9536314	T > G	13:33628138:T:G	0.147	*KL (*Klotho-VS*)*	Gene	[118]
rs9527025	G > C	13:33628193:G:C	0.168	*KL (*Klotho-VS*)*	Gene	[118]
rs10553596	T > -	10:115439641:T:-	0.19	*CASP7*	Gene	[119]
rs2230806	C > T	9:107620867:C:T	0.29	*ABCA1*	Pathway	[120]
rs72973581	G > A	19:1043103:G:A	0.05	*ABCA7*	Pathway	[121]
rs11218343	T > C	11:121435587:T:C	0.052	*SORL1*	Gene	[122]
rs142787485	A > G	2:26358156:A:G	0.0406	*RAB10*	Variant	[123]
rsID[A]	Allele[B]	CPRA[B]	MAF[C]	Gene	Evidence	Reference
rs3851179	T > C	11:85868640:T:C	0.361	*PICALM*	Variant	[124]
rs3796529	C > T	4:57797414:C:T	0.194	*REST*	Gene	[125]
rs72824905	C > T	16:81942028:C:T	0.007	*PLCG2*	Gene	[106]
rs3747742	T > C	6:41162518:T:C	0.306	*TREML2*	Gene	[105]
rs1990621	C > G	7:12283873:C:G	0.447	*TMEM106B*	Variant	
-	-			*MS4A* cluster	Variant	[126]
-	-			*BDNF*	Pathway	[127]
-	-			*Dlgap2*	Gene	[128]

[A] rsID is given for all variants except for reviewed genes whose wild-type forms are protective or for those in a multi-gene cluster (major > minor). [B] Allele information from dbSNP (https://www.ncbi.nlm.nih.gov/snp/) and/or confirmed in the referenced literature. [C] Minor allele frequency information from dbSNP (ALFA project - global, https://www.ncbi.nlm.nih.gov/snp/docs/gsr/alfa/) and/or confirmed in the referenced literature.
Abbreviations: CPRA, chromosome, position, reference allele, alternative allele; MAF, minor allele frequency.

For this section, it should be noted that for common variants, one allele (often the minor allele) will be associated with protection from AD whereas the other allele will be associated with risk. When discussing protective variants, the effective allele will be given in the text unless otherwise stated. In addition, the definitive mechanism of action may not be known for all common variants, so functional evidence is used to help interpret the acting gene within the region as well as the directionality of its mechanism of action.

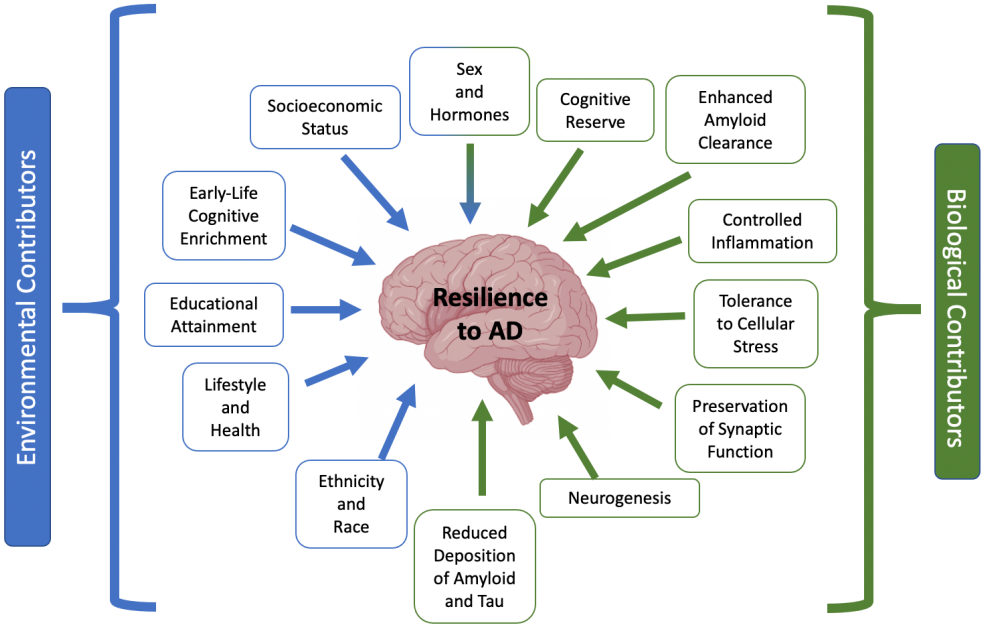

Figure 1.8. Theoretical contributors to resilience. A schematic demonstrating possible environmental and biological contributors to resilience to AD. The review focuses largely on proposed protective, biological pathways.

1.3.5 Amyloid Precursor Protein A673T: Reduced Pathologic Aβ generation

APP, located on chromosome 21, is a gene that encodes amyloid precursor protein (APP). Aβ peptides are formed by the proteolytic cleavage of APP by α-, β-, and γ-secretases, and this processing pathway is also the source of neurotoxic Aβ, a major component of Alzheimer's disease. To date, there are over 60 identified mutations in the *APP* gene, with a large majority existing within coding regions.[129] Over 25 of these mutations are pathogenic and increase the risk of autosomal dominant Alzheimer's disease through increasing Aβ production and oligomerization and reducing its clearance.[129]

Though mutations in *APP* are often associated with an increased incidence of familial early-onset Alzheimer's disease, Jonsson et al., identified a missense mutation within the *APP* gene in an elderly Icelandic population that was both protective against Alzheimer's disease and

associated with a slower decline in cognitive function among cognitively normal individuals [94, 116]. The identified variant is a rare SNP, rs63750847, that results in a substitution from alanine to threonine at position 673 of the protein (henceforth reported as p.A673T), which is near its β-secretase cleavage site.[116] Protection conferred by p.A673T is also further supported by *in vitro* studies demonstrating that the p.A673T allele results in a suboptimal β-secretase cleavage site that reduces production of pathologic Aβ by 50% in comparison to wild-type cells and delayed Aβ aggregation.[130, 131] In addition, a study within a Finnish male sample found that *APP* p.A673T carriers had 28% lower plasma levels of Aβ40 and Aβ42 compared to their age and *APOE* matched controls.[132] Altogether, there is strong gene- and pathway-level evidence that p.A673T is protective, and the data also suggest that a reduced amyloid burden throughout life is protective against AD as well.

The p.A673T allele is extremely rare,[133-135] so it has not been verified whether it exhibits the same protective effect in non-Nordic populations. For example, the carrier frequency for p.A673T was only 0.018% in the US white population[134] and was found to be absent in a large Chinese sample[136] suggesting the protective effect of the allele may be limited to individuals of Nordic descent.

1.3.6 Apolipoprotein E

The gene *APOE*, located on chromosome 19, encodes the protein Apolipoprotein E (APOE). There are three polymorphic alleles of *APOE*: *APOE*-ε2, ε3, and ε4, with estimated global allele frequencies of 8%, 78%, and 14%, respectively.[137] Well-established in the literature, *APOE*-ε4 is known as the greatest common genetic risk factor for AD,[138-141] in which individuals carrying even one *APOE*-ε4 allele have up to 3 times increased risk for AD in comparison to ε3/ε3 homozygotes. Carrying two *APOE*-ε4 alleles can increase risk by up to 15-fold.[142, 143]

In contrast, *APOE*-ε2 is a protective factor against AD.[117, 144] The magnitude of protection has been debated within the literature due to differences between neuropathologically- and clinically confirmed AD cases (i.e., individuals exhibiting clinical symptoms may be assigned to the AD group in a case-control study, though they do not meet neuropathological criteria for AD).[142] A recent study with neuropathological samples by Reiman et al., demonstrated that the prevalence of AD was extremely low in *APOE*-ε2 homozygotes such that carriers of *APOE*-ε2 are 2.5 (ε2/ε3) to 8 (ε2/ε2) less likely to develop AD.[142] The proposed mechanism by which *APOE*-ε2 provides protection from AD is through reduced Aβ aggregation and improved Aβ clearance.[144, 145] However, the biological mechanisms underlying how *APOE*-ε2 enhances Aβ clearance have not yet been confirmed. One possible hypothesis of clearance is that APOE-ε2-Aβ complexes are more efficiently endocytosed and cleared within cells via their interaction with LDLR (low-density lipoprotein receptor), LRP1 (LDL receptor-related protein 1), and HSPGs (heparan sulfate proteoglycans), though this is still debated in the field.[144-146]

In addition to Aβ clearance, recent literature suggests that *APOE* may also be involved in the spreading of tau downstream of amyloidosis. Arboleda-Velasquez et al. identified an individual with both an autosomal dominant AD mutation in *PSEN1* (presenilin 1, p.E280A) and two alleles of a rare mutation within *APOE*-ε3, called the Christchurch mutation (*APOE3ch*, p.R136S), who experienced a multi-decade-long delay in the onset of cognitive symptoms despite having widespread amyloid deposition throughout the brain as measured by PET. Although heterozygous individuals were present in the cohort, homozygosity of *APOE3ch* was required for protection. Interestingly, tau deposition (as measured by flortaucipir) was limited to the medial temporal and occipital lobes.[107] So far, these data suggest that the brain can withstand the widespread deposition

of amyloid for a long period of time if tau deposition is limited before the onset of cognitive impairment.

Like APOE-ε2, the APOE3ch protein displays similar protein-protein interactions with the LDLR and HSPG receptors, suggesting that it may offer protection through the same molecular mechanisms. For example, APOE3ch protein displays impaired binding affinity for HSPGs, and it has been suggested that this altered affinity may be responsible for its effects on tau deposition.[107] Recent studies by Therriault et al., examined the interaction of *APOE*-ε4 and Aβ on CSF and brain levels of tau supporting a probable relationship between *APOE* allele (e.g., *APOE3ch*) and tau deposition.[147, 148] This relationship is further supported by Shi et al., who demonstrated that of tau transgenic mice expressing *APOE*-ε4 had higher tau levels and more neurodegeneration than mice expressing *APOE*-ε2 or *APOE*-ε3.[149] However, elucidation of the processes behind *APOE3ch*'s inhibition of tau spreading requires further study.

Given *APOE*'s involvement in AD, it has been explored as a potential therapeutic target for AD treatment. Anti-APOE-ε4 antibodies and antisense oligonucleotides that reduce brain APOE-ε4 levels have been explored, with positive results in reducing Aβ plaque burden.[150, 151] In addition, therapeutics that modulate APOE function to make it more "APOE-ε3-like" or "ε2-like" have been explored with relatively positive results *in vitro* and in murine models,[150] though there are important considerations with regard to lipid health as homozygous ε2 carriers are likely to have a higher incidence of type III hyperlipoproteinemia.[152] However, efforts to target APOE therapeutically for AD have been somewhat limited due to its widespread expression throughout the body (i.e., brain and periphery) and its broad function in biological processes related to adipose function, fertility, and metabolism.[153, 154] A comprehensive review of APOE signaling in AD has been published previously, including the proposal of numerous therapeutic strategies.[155] The

emergence of *APOE3ch* suggests that modifying APOE function and protein interactions (e.g., APOE-ABCA1, APOE-HSPG, APOE-Aβ) through antibodies or small molecules may be the most promising pathway for protection.[155]

1.3.7 Protection in the Presence of *APOE*-ε4

As aforementioned, individuals carrying at least one copy of *APOE*-ε4 have significantly increased risk for AD and mortality.[156] However, not every *APOE*-ε4 carrier develops AD, suggesting that there are factors that confer protection in these higher-risk individuals.[157] Supporting this hypothesis, studies have identified variants that are protective from AD despite *APOE*-ε4 carriership.

An allele of the gene, Klotho (*KL*), named Klotho-VS was first implicated in human aging by Arking et al., in 2002.[158] Klotho-VS is a haplotype containing two missense variants in linkage disequilibrium (LD): rs9536314 (p.F352V) and rs9527025 (p.C370S) [118]. Though it has been debated within the literature,[159, 160] one allele of Klotho-VS has been associated with protective phenotypes such as: slower cognitive decline,[160, 161] greater cortical volume,[162] and reduced amyloid burden.[163] Most recently, a study by Belloy et al., suggested that a single allele of Klotho-VS reduces AD risk by 1.3 times in *APOE*-ε4 carriers in comparison to *APOE*-ε4 carriers without Klotho-VS.[118] The authors also recapitulated previous findings that *APOE*-ε4-carrying Klotho-VS heterozygotes had reduced amyloid burden.

Klotho is involved in numerous biological functions, including growth-factor mediated signaling, calcium homeostasis, synaptic function, autophagy, cellular survival, and others.[164, 165] Higher levels of Klotho have been associated with longer life spans[166] and decreased markers of cellular aging (e.g., lower epigenetic age, higher telomerase activity).[167, 168] Interestingly, heterozygotes with the -VS haplotype appear to have increased levels of Klotho and lower AD risk

in comparison to homozygotes, suggesting that there is a protective range of Klotho.[118] At this time, there is no established connection between Klotho and APOE function in clearance, though Klotho appears to mediate amyloid clearance via autophagic pathways that interact with APOE.[169-172] Interestingly, Zhao et al. demonstrate that Klotho overexpression can reduce tau phosphorylation as well as improve Aβ clearance in a mouse model of AD, which suggests that Klotho can also reduce the neuropathological burden of amyloid and tau independently of APOE.[173] Though the evidence implicating Klotho-VS in AD is relatively strong, the exact biological pathway by which Klotho-VS is protective requires further study.

In another study identifying modifiers of AD risk in *APOE*-ε4 carriers, *APOE*-ε4 homozygotes carrying a common loss-of-function variant in *CASP7* (rs10553596) had roughly 2-fold reduced risk of AD compared to noncarriers.[119] rs10553596 represents a TT deletion within the coding region of *CASP7*; this causes both a leucine to serine amino acid change at position 44 of the protein as well as premature termination at position 133. Though caspase 7 is the likely functional gene, we can only speculate why this particular variant preferentially protects *APOE*-ε4 carriers. Caspase 7's most well-established role is within the apoptotic cascade; however, it has been suggested that caspase 7 plays an integral role in the activation of microglia without initiating cell death.[174] Therefore, the loss of caspase 7 function may reduce aberrant microglial activation, thus limiting neuroinflammation, neurotoxicity, or cell death in response to pathology.[174-176]

However, neither of the variants of *KL* (Klotho) or *CASP7* are protective in the absence of *APOE*-ε4, suggesting that the protective effects may only be seen under higher pathologic burden.[118, 119] Broadly, Klotho-VS and caspase 7 (rs10553596) appear to exhibit protection via increasing cellular tolerance of stress,[177, 178] though elucidation of their true therapeutic potential requires further examination.

1.3.8 Lipid Signaling and Homeostasis

APOE is also highly involved in lipid metabolism,[153] and its major role in AD suggests that lipid signaling is an important etiological pathway of AD. Throughout the body, lipids play major roles in the structure and integrity of the cellular membrane, as well as endo- and exocytosis of macromolecules.[179] In the brain, studies suggest that they also play roles in blood-brain barrier function, inflammation, and myelination, among other processes.[179] Variants within lipid-related genes have been associated with both risk and resilience to AD, some of which include (but are not limited to) the following genes: *APOE,*[155] *ABCA1,*[180, 181]*ABCA7*,[182] and *SORL1*,[183] which will be discussed further below. The protective SNPs identified within *SORL1*, *ABCA7*, and *ABCA1* further support a hypothesis that much of the genomic protection against AD relies on efficient clearance of pathology.

ABCA1 encodes a protein of the same name (ABCA1, ATP-binding cassette transporter ABCA1) that mediates cholesterol efflux and APOE lipidation.[184] Two variants in ABCA1, rs2230805 and rs2230806, were identified as protective variants via a case-control study in a Hungarian sample [120]. Both rs2230805 and rs2230806 cause a non-synonymous amino acid change (p.L158L and p.R219K, respectively) and these SNPs are in strong LD (D': 0.92; r^2: 0.766).[120] There has been some debate within the literature about whether rs2230805 and rs2230806 are truly protective;[181] however, there is evidence that the rs2230806/p.R219K variant delays the onset of LOAD by 1.7 years on average.[108] Functional studies suggest that ABCA1 deficiency increases Aβ deposition and exacerbates cognitive impairment in mice, especially in rodents expressing *APOE*-ε4,[185] so the protective effect may be mediated by increased expression of ABCA1 or a gain-of-function in ABCA1 protein leading to enhanced lipidation of APOE.

ABCA7 (ATP-binding cassette transporter, ABCA7) is also a gene within the same ATP-binding cassette transporter family.[186] A common variant in *ABCA7*, rs72973581 (Study MAF = 4.3%[121]), results in a glycine to serine substitution at position 215 (p.G215S) and has been shown to reduce AD risk by roughly half.[121] Though *ABCA7* mediates lipid efflux and regulates lipid homeostasis similar to *ABCA1*, its protective effect appears to take a different path; ABCA7 has a function in phagocytosis and APP processing.[186] For example, microglia from *Abca7*-deficient mice exhibit reduced capacity for phagocytosis and increased activation of β-secretase, resulting in higher levels of Aβ40 and Aβ42.[187-189]

A protective variant was also identified within the *SORL1* (sortillin-related receptor 1) gene, which is a receptor for APOE.[190] More specifically, rs11218343-C is an intronic variant within *SORL1*, and the minor allele was associated with protection from AD in a genome-wide meta-analysis of Caucasian, Japanese, Korean, and Han Chinese individuals.[122] SORL1 is a member of the LDLR protein family as well as the vacuolar protein sorting 10 (VPS10) domain receptor family of proteins; it is suggested that SORL1 binds soluble Aβ and directs it to lysosomes for eventual degradation.[191] Though it is unclear how the minor allele rs11218343-C affects *SORL1* expression because it is in a non-coding region, SORL1 loss-of-function or deficiency has been associated with AD.[192-194] Therefore, a gain-of-function may be protective against AD. In addition, the gene-gene interaction between *APOE* and *SORL1* may also mediate amyloid clearance.[195, 196]

Similar to potential therapeutics that aim to increase the protective potential of APOE, targeting ABCA1, ABCA7, and SORL1 with activators (i.e., positive allosteric modulators, partial agonists, agonists) or increasing their expression may mimic the protective effect of the identified variants.[197, 198] Again, there are also *ABCA1*, *ABCA7*, and *SORL1* variants that increase the risk of AD,[180-183] emphasizing the importance of lipid homeostasis in the neuropathological progression

of AD. On the other hand, these protective variants suggest that lipid-mediated endocytosis and phagocytosis are important for amyloid clearance.

1.3.9 Endosome and Lysosome Regulation

As aforementioned, lipid homeostasis is also connected to cellular trafficking.[199] Dysregulation of cellular trafficking (e.g., endosomal-lysosomal pathways, among others) has been associated with neurodegenerative disorders including AD,[200] Parkinson's disease, and amyotrophic lateral sclerosis,[201] and variants within trafficking genes have been identified in large-scale GWAS and meta-analyses of AD.[91-93] From APP processing[202] and amyloid clearance[203] to neurotransmission,[204] maintenance of cellular trafficking could both be a cause and/or consequence of mechanisms protecting individuals from AD.

RAB10 (Ras-related protein Rab-10) encodes a protein of the same name that is a small GTPase and a key regulator of cellular trafficking.[205] The protective variant, rs142787485-G, is located in the 3' untranslated region of the *RAB10* gene and reduces AD risk by up to 1.7 times.[123] Though it is unclear whether the protective effect of rs142787485-G is through reduced *RAB10* expression, mRNA levels of *RAB10* are increased in AD, and there is evidence that RAB10 may also play a direct role in APP processing.[123, 206] In support of these hypotheses, *in vitro* studies demonstrate that shRNA-mediated knockdown of *rab10* in mouse neuroblastoma cells results in a reduction of amyloid.[123] RAB10 has also been associated with the retromer complex, which mediates clearance of pathology.[206] However, RAB10 is also involved in other cellular functions such as the maintenance of endoplasmic reticulum morphology, axonogenesis, and neurotransmitter release, making it difficult to pinpoint its exact contribution to neuroprotection.[206, 207]

A variant in the *PICALM* (phosphatidylinositol-binding clathrin assembly protein, PICALM) locus, rs3851179-A, exhibits protection from AD in numerous studies of European-decent (Caucasian/non-Hispanic white) participants (OR = 0.3 - 0.9).[208, 209] However, it should be noted that this protective effect appears to be limited to *APOE*-ε4 non-carriers.[124] A clathrin-interacting protein, PICALM plays a major role in clathrin-mediated endocytosis, which can facilitate neurotransmission through receptor recycling and degradation.[210, 211] Variants in the *PICALM* locus have also been associated with increased risk of AD, [212, 213] though the pathogenic mechanisms are still unclear. Ando et al. imply that *PICALM* is abnormally cleaved and downregulated in AD brains.[214] Other studies have suggested that PICALM modulates APP processing and Aβ clearance,[211] and inducible pluripotent stem cell experiments have supported those findings.[215] Though the functional gene in the region has not been definitively demonstrated, these studies suggest rs3851179-A mediates protection through increased expression of *PICALM* and improved Aβ clearance, perhaps, through endocytic mechanisms.[215, 216]

Though the protective effects of the *RAB10* and *PICALM* variants appear to point toward APP processing and Aβ trafficking and clearance, both proteins also play important roles in synaptic function and neurotransmission. Therefore, *RAB10* and *PICALM* may also implicate additional biological pathways that help preserve synaptic function in the presence of stressors such as AD pathology, as expanded upon in the next section.

1.3.10 Synaptic Dysfunction

Synaptic dysfunction is a hallmark of AD as well as many other neurodegenerative disorders, and it is believed to occur even before marked neurodegeneration and downstream cognitive impairment.[200, 217] Amyloid and tau burden are associated with synapse loss and dysfunction through both direct (e.g., tau-associated mitochondrial disruption) and indirect (e.g.,

neuroinflammation) pathways.[217] Synaptic plasticity is an important, biological correlate of learning and memory;[218] therefore, processes preserving synaptic density and function (even in the presence of pathology) are likely to be protective. There is notable genetic evidence of such protection from human genetic studies.

A transcriptional regulator, REST *(*restrictive element-1 silencing transcription factor), has been of interest with regard to neuronal development and brain aging. REST is a repressor of numerous genes including pro-apoptotic genes and others that mediate the cellular response to stress and to AD neuropathology.[219] *In vitro*, REST deficiency results in increased cellular damage and cell death relative to wild type, especially in response to cellular stressors such as hydrogen peroxide and Aβ.[219] Though *REST* expression in older adults (aged 73 to 106) is increased when compared to young adults (aged 20 to 35), its expression is significantly reduced in individuals with mild cognitive impairment (MCI) and AD compared to controls.[219] A missense variant in exon 4 of *REST*, rs3796529-T, has been associated with slower hippocampal atrophy in individuals with MCI.[220] As REST mediates a wide array of biological processes, the effect mediated by rs3796529-T has not yet been confirmed. However, evidence suggests that higher levels of *REST* are beneficial due to its regulatory role in neurogenesis and neurodifferentiation as well as its ability to improve cellular tolerance to stress; therefore, rs3796529-T may result in a gain-of-function or an increase of *REST* expression.[221, 222]

BDNF (brain-derived neurotrophic factor), an important protein for neural development, neurogenesis, and synaptic growth,[223] is a downstream target of REST.[224] BDNF is also necessary for learning and memory,[225] which is often impaired in AD; studies have suggested that BDNF is important for synaptic plasticity (such as long-term potentiation) in the hippocampus.[225] On average, individuals with AD have lower circulating levels of BDNF than controls, though there

has been some debate within the literature.[226] In support of a protective role, Weinstein et al. demonstrated that higher levels of peripheral BDNF decreased AD risk, with the highest levels reducing risk by up to two-fold.[127] In addition, conditional *BDNF* expression in 5xFAD mice was able to rescue cognitive deficits and synaptic function.[227] Furthermore, *BDNF* overexpression was shown to be neuroprotective against amyloid *in vitro*[228] and was able to reduce Huntington-like phenotypes in mice.[229]

A risk allele of *BDNF* has also been identified: rs6265-A or p.V66M.[230, 231] In addition to increased risk of sporadic AD, studies suggest that p.V66M increases the severity of cognitive decline, hippocampal atrophy, and neuropathological burden in autosomal dominant AD.[232-234] p.V66M negatively affects the secretion of BDNF,[235] which supports the hypothesis that therapeutics increasing the efficacy, expression, or secretion of BDNF are expected to be protective.

The evidence for synaptic pathways also extends beyond human genomic discovery approaches. *Dlgap2* (disks large-associated protein 2) was recently identified as a protective candidate in a novel genetically diverse mouse model of AD and confirmed in a human GWAS.[128] Proteins within the DLGAP family, such as DLGAP2, function as important scaffolding proteins within the post-synaptic density and have been linked to neurological and psychiatric disorders including schizophrenia, AD, and Parkinson's disease.[236] DLGAPs also play a role in modulating neuronal transmission though synaptic scaling.[236] Similar to BDNF, lower levels of DLGAP2 have been associated with AD as well as increased cognitive decline.[128] Additionally, a risk variant within *DLGAP2* (rs6992443) was identified in a study examining the association of known epigenetically modified genes with LOAD.[237] Together, these data suggest that higher levels of DLGAP2 are likely to protect synaptic function. Another protein within the DLGAP family,

DLGAP1 (also known as GKAP) is a nominated AD drug target on the Agora platform, which is a database of nominated targets for AD therapeutics, and increased expression is predicted to be protective, similar to *DLGAP2*.[238] Aβ has been shown to mediate the degradation of DLGAP1 through phosphorylation by CDK5.[239] Therefore, biological factors or therapeutics preventing the phosphorylation and/or degradation of DLGAP1 could help preserve synaptic function in the presence of pathology. Altogether, these variants and proteins support the idea that increased tolerance to cellular stress and continued maintenance of synaptic function are two interconnected mechanisms behind neuroprotection from AD and resilience.

1.3.11 Immunity and Inflammation

Neuroinflammation has been linked to overall pathophysiological changes within the brain during AD progression.[240] Microglia, the resident immune cells of the brain, are responsible in part for the clearance of amyloid through phagocytosis and the activation of additional immune cells. When the pathological burden in the brain is insurmountable by the immune system, inflammation becomes chronic and damaging to neurons due to the prolonged secretion of pro-inflammatory cytokines and factors by microglia.[240] Though many of the aforementioned protective variants primarily mediate amyloid clearance, variants that are able to modulate neuroinflammation (i.e., temper its damaging effects) are also likely to be protective. In addition, it should be noted that risk variants of *PLCG2*[241] and the *MS4A* gene cluster[242, 243] (discussed below) have been discovered.

PLCG2 encodes phospholipase C gamma 2 (PLCγ2), which is expressed in microglia and granule cells within the brain.[244] A rare variant of *PLCG2* (rs72824905-G or P522R) reduces AD risk by nearly two-fold.[106, 245] PLCγ2 is a member of the phospholipase C-gamma family, and as such, cleaves phosphatidylinositol 4,5-bisphosphate (PIP_2) into its products, inositol triphosphate (IP3) and diacylglycerol (DAG), that then propagate downstream signaling.[246] Though canonical

phospholipid signaling serves a broad number of functions, PLCγ2 has been implicated in immune function and is believed to be in the same signaling pathway as *TREM2*,[106] which has been identified as a genetic risk factor of AD.[247] The nonsynonymous amino acid change, p.P522R, appears to lie in a regulatory region of PLCγ2 and results in a hypermorphic form of the protein though the biological mechanism behind its neuroprotective effect is still unclear.[244] It should be noted, however, that increased inflammation is a double-edged sword; other gain-of-function mutations in PLCγ2 have been associated with autoimmune disorders.[248]

Similar to *PLCG2*, *TREML2* (triggering receptor expressed on myeloid cell-like 2) is expressed by microglia.[249, 250] rs3747742-C (p.S144G) is a protective, missense coding variant within the *TREML2* gene.[105] Another protective, intergenic SNP between neighboring genes *TREM2* and *TREML2*, rs9381040, is in high LD with rs3747742 (D': 0.86; r^2: 0.67) and has a similar odds ratio as rs3747742 (OR=0.92 and 0.93, respectively).[105] rs3747742-C has been associated with lower levels of baseline CSF total tau as well as a slower rate of increase in CSF total tau levels, though there was no association with CSF levels of phosphorylated tau (p-tau) or amyloid.[251] In contrast, Benitez et al., demonstrate that rs3747742 and rs9381040 are both associated with lower levels of CSF p-tau, and their conditional analyses suggest that rs3747742 and rs9381040 represent the same signal.[105] TREML2 plays a pro-inflammatory role;[249] studies have shown that activated microglia and inflammatory cytokines are connected to tau pathology, [252] suggesting that rs3747742-C reduces TREML2 activity though more studies are required to determine the exact mechanism by which the variant confers protection.[251]

Another case-control study focusing on variants within the *MS4A* and *TREM* gene clusters demonstrated that a set of variants within the *MS4A* (membrane-spanning 4A) gene cluster were twice as frequent in controls than in AD cases.[126] Further investigation of the identified variants

suggested that protection is conferred through a loss-of-function of MS4A family proteins, [126] though additional studies are needed. However, *MS4A* genes have been previously associated with AD risk.[242, 243] Moreover, high levels of *MS4A6A* expression have been associated with elevated Braak scores.[253] There is also evidence that the *MS4A* locus plays a role in modulating *TREM2* expression, particularly soluble CSF TREM2 (sTREM2) levels. A GWAS of CSF sTREM2 by Deming et al. suggested that protective *MS4A* gene cluster variants increased CSF sTREM2, which was associated with reduced AD risk and a delayed age-at-onset.[254] Together, these data functionally connect the *TREM2* and *MS4A* gene clusters and represent a potential mechanism by which inflammation can be modulated in the brain.

rs1990621, a variant within the *TMEM106B* (transmembrane protein 106B) locus, has been associated with neuronal protection in individuals with neurodegenerative disorders including AD.[255] rs1990621 is in high LD with rs3173615 (p.T185S, $r^2 = 0.98$),[255] which was identified as a protective variant for frontotemporal lobar degeneration (FLTD), the second most-common cause of dementia in older adults.[256] rs1990621 is also in high LD with rs1990622 ($r^2 = 0.98$),[255] which has been previously linked with familial, progranulin-related FLTD.[257] TMEM106B is a lysosomal protein that has been associated with aging and age-associated inflammation, and the risk alleles appear to be pro-inflammatory, perhaps through modulation of progranulin.[258, 259] However, the mechanism behind TMEM106B-mediated protection is unclear as TMEM106B expression is reduced in AD brains,[256] but the risk alleles increase its mRNA expression in FLTD.[260] Altogether, TMEM106B-mediated protection from AD appears to be complex and requires further study.

AD drug discovery efforts have begun to include targets outside of amyloid and amyloid processing, with an increase in immune-modulating therapeutics. As of February 2020, 3 out of the 18 drugs in Phase 3 clinical trials have targeted inflammation with a focus on reducing

neuroinflammation and increasing clearance of amyloid.[64] As of November 2020, these trials were still ongoing. However, it is likely that the efficacy of an inflammatory-focused drug is dependent on the state (i.e., early/late) of disease.[261, 262]

1.4 AIMS OF THE PROJECT

The present dissertation focuses on leveraging multiple domains of data from longitudinal aging studies (e.g., genomic, transcriptomic, cognitive, biomarker, neuroimaging) to identify novel genetic and molecular factors contributing to AD and resilience to AD. One goal of the dissertation is to investigate how the aforementioned data modalities can be combined to link molecular biology to human phenotypes and behavior and to better understand complex diseases such as AD. In addition, we aim to identify modulators of AD risk for the purposes of elucidating the biological basis of resilience to AD in addition to presenting novel therapeutic targets for AD drug discovery. All analyses and results within this project should be interpreted in the context of sporadic late-onset AD.

One major focus of our group is on resilience to AD (described above in section **1.2**), which is described, in part, as a phenomenon in which individuals present with sufficient quantities of amyloid and tau pathology to have autopsy-confirmed AD,[101, 102, 263] but never experience cognitive impairment during late-life. Alternatively, a resilient individual could be described as someone who has less than expected neurodegeneration or cognitive decline given a particular amount of neuropathology. Therefore, we hypothesize that there are protective factors that underlie these individuals' resilience to pathology and other AD risk factors such as *APOE*-ε4, which are related to worse outcomes.[264-267] To probe this hypothesis, we leverage computational models to

identify novel genomic-, transcriptomic-, and network-level factors that confer protection from brain atrophy or cognitive decline in the presence of risk factors like pre-existing amyloid and tau pathology. We also hypothesize that the same computational tools used in our analyses can be applied independently, or in concert, to further advance therapeutic avenues for AD.

The proposed aims for this dissertation are as follows: **Aim 1: Identify genetic variants that confer neuroprotection from AD pathology.** AD pathology is strongly linked to neurodegeneration,[1-3, 268-271] however, not all individuals who are biomarker positive will suffer from significant brain atrophy and cognitive decline. Therefore, we are interested in identifying common genetic variants that slow, or diminish, the relationship between neuropathology and brain atrophy. Leveraging genotype, neuroimaging, and CSF biomarker data from 4 longitudinal aging cohorts,[272-275] I will perform a genome-wide association study to identify SNPs that modify the association between amyloid and tau measured in CSF and brain atrophy measured by hippocampal volume via MRI.

Aim 2: Identify gene transcripts that confer protection from the effects of *APOE*-ε4. The *APOE*-ε4 allele is associated with increased risk of AD in addition to worse cognitive outcomes.[276] However, there are individuals who do not experience cognitive decline despite carrying *APOE*-ε4 suggesting that there are protective factors mitigating the increased risk. Leveraging both blood and brain transcriptomics from two well-characterized aging cohorts, I aim to identify genes via RNA sequencing (RNAseq) that modify the association between *APOE*-ε4 positivity and cognitive outcomes such as memory and executive function.

Aim 3: Evaluate the reproducibility of Weighted Gene Co-Expression Network Analysis (WGCNA) and identify modules that modify *APOE*-ε4 effects on hallmarks of AD. To determine whether WGCNA is a robust and reproducible computational method, I will rebuild

a previously published gene co-expression network[277] using bulk brain RNAseq and compare it to the original network. Then, using the same defined co-expression modules, I aim to identify novel functional domains that modify the relationship between *APOE*-ε4 positivity and amyloid and tau burden at autopsy as well as cognition. In addition, we also leverage the PrediXcan method to determine whether predicted gene expression data is suitable for gene co-expression network generation and/or replication.

Altogether, the above aims should not only demonstrate the viability of each computational method separately as a tool by which to probe the biology of complex disorders such as AD, but also as methods that can be used together to link genetics to biological functions as well as for biomarker and novel therapeutic target discovery. Over the following chapters, we will unpack each aim in more detail beginning with **Aim 1**, in which we identify two novel loci on chromosome 3 that interaction with CSF amyloid and p-tau, respectively on annual change in hippocampal volume (**Chapter 2**). In **Chapter 3**, we describe **Aim 2** and implicate an innate immunity gene, *RNASE6*, in cognitive decline as well as discuss how blood transcriptomics may be used as a biomarker to monitor brain changes. We perform gene network-based analyses in **Chapter 4**; immune signaling and macromolecule biosynthesis are two biological processes associated with cognition and cognitive decline when identifying co-expression modules that modulate *APOE*-ε4 effects on hallmarks of AD. Finally, in **Chapter 5**, we offer a summary of up-and-coming research domains in the AD field and how they may transform therapeutics, treatment, and precision medicine for AD.

CHAPTER 2

IDENTIFICATION OF COMMON GENETIC VARIANTS THAT MODIFY THE ASSOCIATION BETWEEN ALZHEIMER'S DISEASE BIOMARKERS AND HIPPOCAMPAL VOLUME

Portions of this chapter are published under the title, "Exploring common genetic contributors to neuroprotection from amyloid pathology," in *Brain Communications*. Acknowledgements and full funding details for this chapter can be found in **Appendix B**.

2.1 INTRODUCTION

Canonically, the neuropathological progression of AD has been described as follows (**Figure 1.4**): amyloid abnormalities occur prior to tau abnormalities, then, amyloid and tau together along with other downstream biological processes (e.g., inflammation), result in neurodegeneration and subsequently, cognitive impairment.[1-3]

Though Alzheimer's disease is typically diagnosed clinically via cognitive tests,[3, 278] many other CNS disorders can also present with memory loss and cognitive impairment. Thus, AD can only be definitively diagnosed via examining brain neuropathology burden at autopsy. As biomarkers become more readily available and accessible to monitor brain changes over time, new frameworks have been developed to allow for the consideration of AD as a heterogeneous and dynamic disease and to improve screening for AD risk in living individuals who are clinically normal. One such framework is the "A/T/N system" in which the main biomarkers of AD: amyloid, tau, and neurodegeneration are given binary classifications (i.e., positive, or negative) such that an A+/T+/N+ individual has both amyloid and tau pathology as well as neurodegeneration.

The A/T/N system can also capture individuals with asymptomatic Alzheimer's disease, or preclinical Alzheimer's disease, in which individuals present with the neuropathological hallmarks of Alzheimer's such as amyloid, tau, and/or neurodegeneration, but do not yet show clinical signs of cognitive impairment.[100-102] Asymptomatic individuals may also be amyloid and tau positive, yet have no markers of neurodegeneration despite increased risk of AD. Some of these individuals may prove to be resilient. Modifiable risk factors that contribute to resilience have been a major focus of the field, including factors like educational attainment that have been leveraged as proxy measures in classical cognitive reserve literature.[111] Resilience has also been defined in two parts: better than expected cognitive function given the overall level of Alzheimer's disease pathologies (i.e., cognitive resilience) and less than expected brain atrophy given the level of Alzheimer's pathologies (i.e., brain resilience).[99] While modifiable lifestyle factors certainly contribute to such resilience,[279, 280] there is also emerging evidence from our group and others' that resilience is heritable and may have a genetic basis.[107, 264-267]

One notable example is the apolipoprotein E (*APOE*) polymorphic alleles, as *APOE*-ε2 allele carriers have reduced Alzheimer's disease risk.[117, 141, 281] In addition, recent studies have suggested that the genetic architecture of resilience is distinct from that of clinical Alzheimer's disease with only a small contribution of *APOE*,[282] suggesting that uncovering the genetic architecture of resilience may provide new insight into genomic pathways of protection.

The present analytical approach will further probe the genetic basis of resilience by identifying common genetic variants that modify the well-established association between biomarkers of Alzheimer's disease neuropathology and downstream neurodegeneration.[1-3, 283] For this study, we will leverage CSF biomarkers of Alzheimer's disease neuropathology (i.e., tau, phosphorylated tau (p-tau), beta-amyloid (Aβ42)) as well as PET biomarkers of amyloid-β, which

have previously been shown to be strongly associated with downstream hippocampal atrophy.[1-3, 283, 284] In addition, we will leverage hippocampal volume measured with magnetic resonance imaging (MRI) as our proxy measure of neurodegeneration.[285, 286]

2.2 MATERIALS AND METHODS

2.2.1 Participants

Data for mega-analysis were acquired from four longitudinal studies of aging and Alzheimer's disease that include CSF biomarkers of Alzheimer's neuropathology, genotype data, and neuroimaging. The studies are as follows: the Alzheimer's Disease Neuroimaging Initiative (ADNI), Vanderbilt Memory and Aging Project (VMAP), Wisconsin Registry for Alzheimer's Prevention (WRAP), and the Biomarkers of Cognitive Decline Among Normal Individuals (BIOCARD) study. Data from the Mayo Clinic Study of Aging (MCSA) was used for replication. Consent for each participant was acquired by each longitudinal aging study independently.

The ADNI database (adni.loni.usc.edu) was launched in 2003 as a public-private partnership, led by Principal Investigator Michael W. Weiner, MD. The primary goal of ADNI has been to test whether serial MRI, PET, other biological markers, and clinical and neuropsychological assessment can be combined to measure the progression of MCI and early AD. ADNI enrolls participants who are 55 to 90 years of age (www.adni-info.org). VMAP was launched at Vanderbilt University Medical Center. The study enrolls individuals with MCI, as well as age-, sex-, and race-matched cognitively normal counterparts. Participants are excluded if they are not eligible for MRI or have a history of neurological or cardiovascular disease.[272] WRAP

began at the University of Wisconsin-Madison in 2001. WRAP enrolls individuals who are cognitively normal, 40 to 65 years of age, have a parental history of AD, and an increased risk for the disease. In 2004, WRAP began recruitment of cognitively normal individuals without a self-reported parental history of AD.[274] The BIOCARD study is currently located at Johns Hopkins School of Medicine. BIOCARD enrolls participants who were middle-age and cognitively intact. The study is enriched for individuals who had a first-degree relative with AD.[287] The MCSA is a population-based prospective study of older adults residing in Olmsted County, Minnesota.[288, 289] Individuals have been enrolled serially starting in 2004, with multimodal clinical and biomarker data obtained at longitudinal visits based on study protocols.

2.2.2 Genotyping and Quality Control Procedures

Genotyping was performed by each study on different genotyping platforms (see **Table 2.1**). Genotyping data were limited to non-Hispanic white individuals whose principal components (PCs) overlayed with individuals of European ancestry using the 1000 Genomes CEU reference panel. Quality control (QC) was performed on genotype data from each cohort separately using PLINK software (version 1.9b_5.2).[290] Before imputation, single nucleotide polymorphisms (SNPs) with genotyping efficiency <95%, minor allele frequency (MAF) <1%, or deviation from Hardy-Weinberg equilibrium ($p<1x10^{-6}$) were excluded. Furthermore, we excluded participants whose call rate was <99%, who exhibited an inconsistency between reported and genetic sex, or who exhibited excess relatedness (PI_HAT>0.25). We also removed individuals who were outliers based on their ancestral PCs (calculated with EIGENSOFT version 7.2.1)[291] or who were statistical outliers in heterozygosity rate (>5 SD).

Imputation was performed on the Michigan Imputation Server[292] using the HRC r1.1.2016 reference panel (Build 37) and SHAPEIT phasing. Imputed genetic data were further filtered for

imputation quality (r^2>0.9) and biallelic SNPs. To create the joint dataset, we merged genotype data from ADNI, VMAP, WRAP, and BIOCARD, excluding multiallelic SNPs, duplicate SNPs, SNPs that were not present in all datasets, and SNPs with genotyping efficiency <99%. Additional participants were excluded for relatedness or outlying PCs, resulting in a dataset consisting of 1065 individuals and 5,891,064 variants.

2.2.3 MCSA GWAS Data Acquisition, QC, and Imputation

GWAS data for 1783 MCSA participants was acquired using DNA from peripheral blood samples and via the Illumina Infinium Global Screening Array-24 v2.0. Standard SNP-level QC filters were applied using PLINK, including call rate ≥95%, Hardy-Weinberg Equilibrium (p≥1 x 10-5), and MAF ≥1%. Subject-level QC filters included call rate ≥98%, sex checks versus clinical data, Caucasian ancestry determined through STRUCTURE version 2.3.4, and ensuring no cryptic first- or second-degree relatedness (PLINK identity by descent PI_HAT<0.25). Genome-wide imputation was performed with the Michigan Imputation Server using Minimac version 4-1.0.2 and the HRC reference panel. Following additional post-imputation QC filters including SNP call rate ≥95%, sample call rate ≥98%, Hardy-Weinberg Equilibrium (p≥1 x 10-6), MAF≥1%, stringent imputation quality measure (r2≥0.8), and removal of SNPs with duplicate or no identifying rs number, data was available for 6153814 SNPs and 1727 MCSA participants.[293]

2.2.4 Hippocampal Volume Standardization and Slope Calculation

MRI was performed at each study site; acquisition and processing protocols are published elsewhere.[272, 274, 294, 295] We excluded images that failed visual QC, that were taken >90 days prior to CSF acquisition, or that were statistical outliers (>5 SD).

Total hippocampal volume was harmonized across studies using a two-step procedure, and the standardization of all hippocampal volume measurements were based on the first MRI scan of

cognitively normal participants at baseline. First, raw hippocampal volume measurements were adjusted to remove the effects of sex and intracranial volume (ICV). All study cohorts were subset to individuals who were cognitively normal at the time of their first MRI scan. Using a linear regression, the slopes (β) of the associations between ICV, sex, and total hippocampal volume and the interaction between ICV and sex (ICV x sex) on total hippocampal volume in cognitively normal individuals, were calculated using the following model: Total Hippocampal Volume ~ ICV + Sex + ICV x Sex. Hippocampal volume for all subjects was then adjusted for the above confounders by subtracting the mean-centered effects of ICV, sex, and ICV x sex from the total hippocampal volume. We performed this adjustment because ICV is associated with hippocampal volume, and ICV also strongly differs by sex.[296]

Second, we calculated Z-scores using the mean and standard deviation (SD) of the adjusted volume from cognitively normal participants at baseline, resulting in our standardized hippocampal volume variable (**Figure 2.1**). Data from ADNI1 and ADNI2 were harmonized separately to account for differences in scanner strength (1.5T vs 3T).

2.2.5 Mayo Clinic Study of Aging MRI

MRI for MCSA participants was acquired on 3T scanners (General Electric Healthcare, Waukesha, WI, USA) using protocols aligned with ADNI.[297] Information for acquisition and processing has been described elsewhere.[298-300] Hippocampal volume and ICV were derived using FreeSurfer (version 5.3).

Table 2.1: Summary of imputation and quality control measures performed on each genotype dataset							
		Pre-QC		**Pre-imputation**		**Post-imputation**	
Dataset	Platform	N	# of variants	N	# of variants	N	# of variants
ADNI 1	Illumina 610-Quad	757	620,901	666	536,557	666	6,577,704
ADNI 2	Illumina OmniExpress	432	730,525	430	641,075	430	6,662,117
ADNI WGS	Illumina Omni 2.5M (WGS Platform)	812	2,379,855	807	1,480,134	807	7,298,856
ADNI (merged)	(merge)	1903	7,571,217	N/A	N/A	1,247	7,849,615
BIOCARD	Illumina OmniExpress	261	730,525	193	638,868	190	6,559,742
WRAP	Illumina Multi-Ethnic Genotyping Array	1340	1,779,819	1198	898,220	1,198	10,499,994
VMAP	Illumina Infinium Expanded Multi-Ethnic Genotyping Array (MEGA^{EX})	352	1,842,793	261	770,719	256	6,760,400
Note: Since genetic data for ADNI were obtained on multiple platforms, QC and imputation were completed on each set separately and were merged after post-imputation filters. For these merged sets, number of samples and variants immediately after merging and after additional filtering for overlap and relatedness are in the "Pre-QC" and "Post-imputation" columns respectively.							

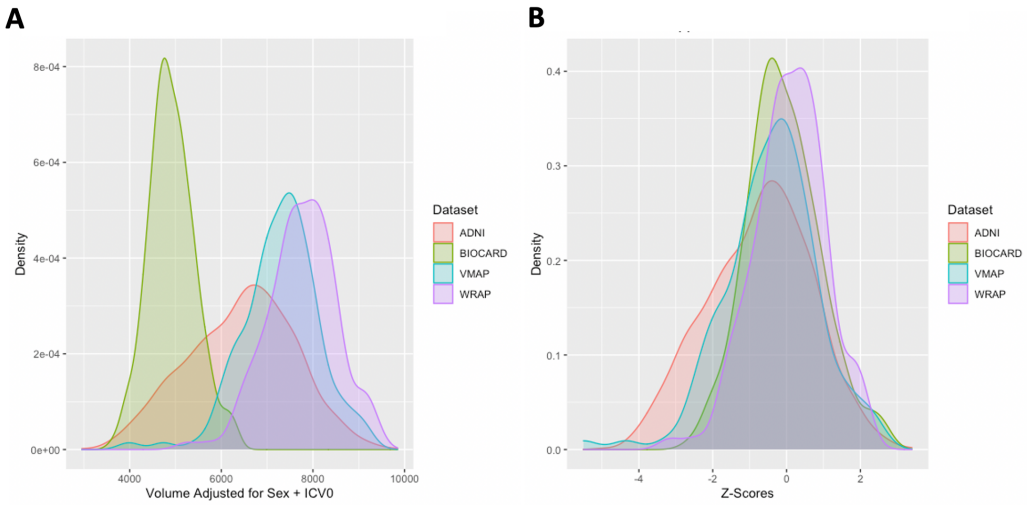

Figure 2.1. Density plots of hippocampal volume distribution pre- and post-standardization per study. The plots are colored by dataset for visualization. The density is presented on the y-axis. **A)** Pre-standardized distribution of hippocampal volumes adjusted for sex and intracranial volume (in mm^3). **B)** Distribution of hippocampal volume Z-scores after standardization. All measures were centered and standardized using the mean and standard deviation of adjusted hippocampal volumes of cognitively normal participants.

2.2.6 CSF Biomarker Standardization

CSF acquisition via lumbar puncture and biomarker quantification was performed by each longitudinal aging study. Acquisition and quantification protocols have been reported by each study.[272, 274, 287, 295]

Standardized CSF tau (total tau) and p-tau values were quantified as Z-scores based on the mean and standard deviation of tau measurements from participants who are cognitively normal (**Figure 2.2**).

CSF Aβ42 was harmonized using a two-component Gaussian mixture model (GMM)[301] due to the bimodal nature of the data. The mean and standard deviation estimated from the predicted amyloid negative gaussian distribution in cognitively normal individuals was used to standardize all values (**Figure 2.3A**). We and others have published extensively on this method to harmonize positron emission tomography (PET) and CSF amyloid measures.[301-303]

2.2.7 Amyloid Positron Emission Tomography

To support our findings, we leveraged amyloid PET data from MCSA participants measured with Pittsburgh compound B ([^{11}C]-PiB), as described elsewhere.[289, 304] We also examined amyloid PET data from ADNI measured with Pittsburgh compound B ([^{11}C]-PiB) and florbetapir ([^{18}F]-AV-45). Additional details on acquisition and pre- and post-processing pipelines can be found on the ADNI website (www.adni-info.org). Mean standardized uptake value ratio (SUVR) values were standardized using a similar two-component GMM as aforementioned, following previously published methods (**Figure 2.3B**).[301, 305]

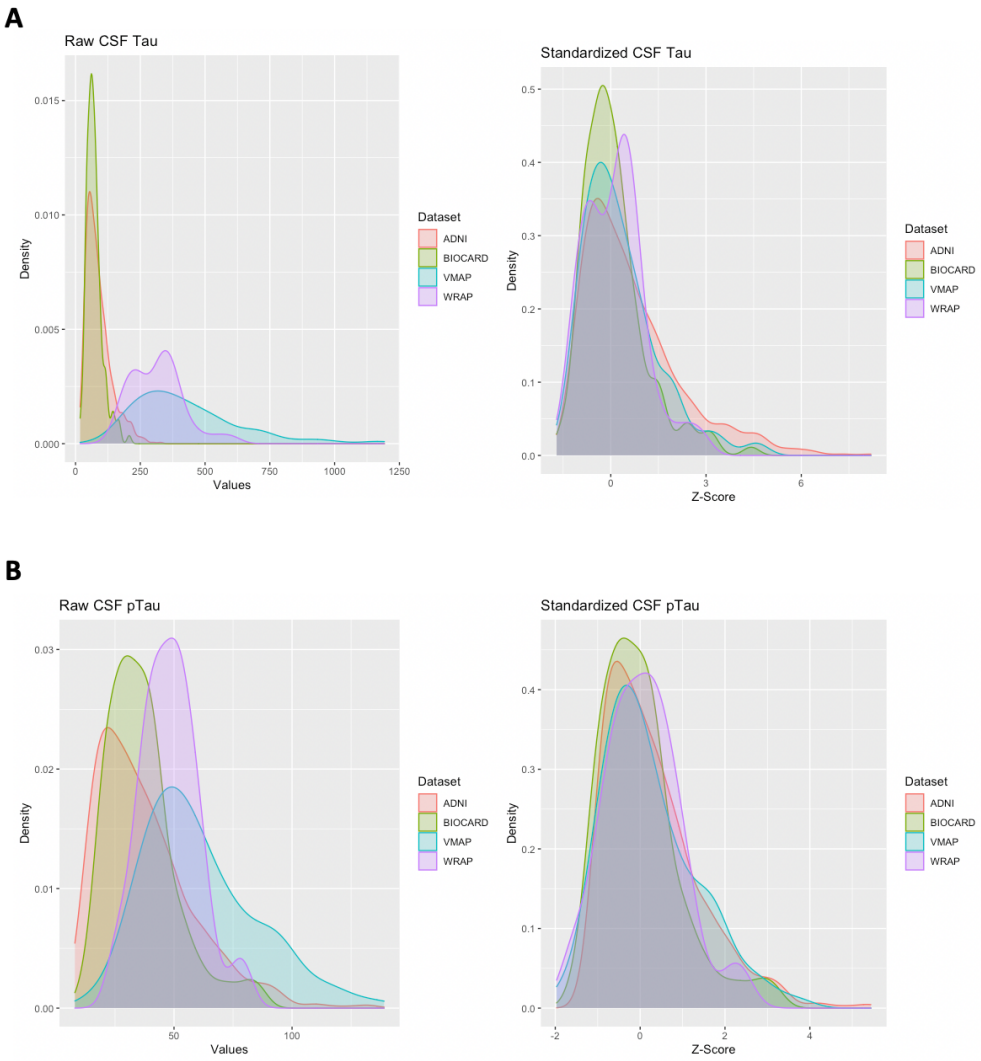

Figure 2.2. Density plots of CSF total tau and phosphorylated tau pre- and post-harmonization. A) Density plot of raw CSF total tau colored by dataset (left). Density plot after standardization (right). **B)** Density plot of raw CSF phospho-tau colored by dataset (left). Density plot after standardization (right). Both CSF total tau and p-tau levels were centered and standardized using the mean and standard deviation of CSF levels of cognitively normal participants. The density is presented on the y-axis.

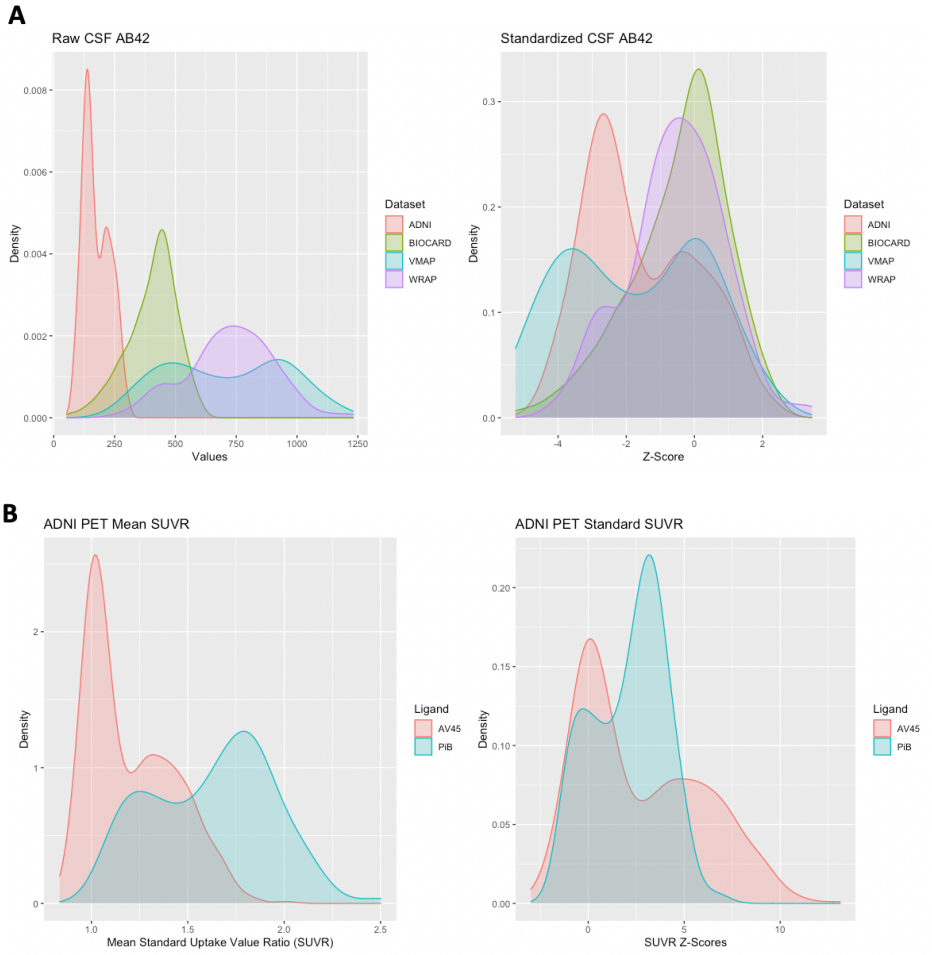

Figure 2.3. Density plots of normalized amyloid measures. All measures were centered and standardized using the mean and standard deviation of the amyloid negative gaussian distribution within study from a mixture model. **A)** Density plot of **r**aw CSF Aβ42 values colored by dataset (left). Density plot after harmonization (right), where the x-axis represents Z-scores. **B**) Left and right panels represent amyloid PET standard uptake value ratios pre- and post- harmonization. These density plots are colored by ligand.

2.2.8 Statistical Analyses

GWAS were conducted using the joint dataset (see above) with PLINK and R (version 3.6.0). Both baseline hippocampal volume and annual change in hippocampal volume were used as continuous outcomes. The annual change in hippocampal volume was determined using linear mixed-effects regression, where the intercept and slope (time from baseline MRI scan) were entered as both fixed and random effects. Covariates for the GWAS included age at first MRI, sex,

and the first three ancestral PCs (calculated using EIGENSOFT version 7.2.1)[291] to account for unmeasured population stratification. For computational efficiency, we extracted the hippocampal volume slopes from mixed-effects regression models and entered them as continuous outcomes in a linear regression with PLINK. The interaction term between each SNP and continuous CSF biomarker levels (i.e., amyloid and tau) was used to identify variants that modified the association between Aβ42 and/or tau and annual change in hippocampal volume. All variants were tested using additive coding. Genome-wide significance was set *a priori* to $p<5x10^{-8}$.[306] Although this linear regression approach was more computationally feasible, the full linear mixed-effects model has multiple advantages including the estimation of both intercepts and slopes in the same model. For that reason, we did run the full linear-mixed effects model for all variants meeting genome-wide significance ($p<1x10^{-8}$) to ensure our results are not driven by the two-stage analytical approach and to have a model that aligns with the linear mixed-effects model used in our independent replication. Sensitivity analyses included *APOE*-ε4 allele count, MRI scanner strength, and a variable for cohort as additional covariates.

To validate the candidate locus discovered in our primary analyses, we also tested the target SNP, rs62263260, using additive coding in the independent dataset from MCSA (n=808). Replication analyses used a mixed-effects linear regression to examine the SNP interaction with baseline amyloid PET standardized uptake value ratio (SUVR), against longitudinal hippocampal volume as the outcome and including age, sex, and ICV as covariates. In this model, ICV was included as an additional covariate because hippocampal volume measurements were not adjusted for the effect of ICV in MSCA.

We also leveraged amyloid PET data from ADNI (n=667) testing the SNP interaction with standardized mean SUVR on the same hippocampal outcome. Covariates included age, sex, and

PET tracer. Both linear and linear mixed-effects regression models were used. Harmonization across tracers was completed leveraging a GMM as previously published (**Figure 2.3B**).[307]

Finally, we used a linear regression model to assess the interaction between *APOE* allele count (ε4 additive coding and ε2 dominant coding due to few homozygous carriers) with CSF amyloid on cross-sectional and longitudinal hippocampal volume (n=1537, **Table 2.2**).

Table 2.2: Dataset characteristics by analysis (CSF and PET)

	Combined CSF Dataset[a]	CSF GWAS Dataset	ADNI PET Total
N	1537	1065	667
Age at baseline	70.3±8.8	70.8±8.7	73.4±7.1
Sex, % female	48%	47%	44%
% *APOE*-ε4 carriers	42%	40%	41%
% *APOE*- ε2 carriers	10%	10%	10%
NC (persons)	734	490	220
MCI (persons)	637	475	398
AD (persons)	176	100	49
	Combined CSF Dataset[a]	CSF GWAS Dataset	ADNI PET Total
Std. CSF Aβ42	-1.31±1.7	-1.34±1.7	2.53±3.07
Std. CSF Tau	0.49±1.5	0.49±1.4	N/A
Std. CSF p-Tau	0.25±1.1	0.23±1.1	N/A
Neuroimaging Measurements (MRI)			
Std. Hippocampal Volume	-0.55±1.3	-0.58±1.3	-0.62±1.3
Std. Hippocampal Vol. Slopes	-0.13±0.1	-0.14±0.1	-0.16±0.1

Note: Data given as mean ± standard deviation unless otherwise noted.

2.2.9 Functional Annotation

Expression quantitative trait locus (eQTL) annotation was performed using the NIH Genotype-Tissue Expression (GTEx) Portal[308] and brain cortex eQTL data from Sieberts et al. When assessing eQTL p-values for the 44 available tissues within GTEx, we performed Bonferroni correction to account for multiple comparisons (significant $p<0.0011$). Additional annotation leveraged both INFERNO (http://inferno.lisanwanglab.org/) and the Brain xQTL Serve database (http://mostafavilab.stat.ubc.ca/xqtl/). We also leveraged phenome-wide association study (PheWAS) results via the Pheweb browser (http://r2.finngen.fi/, data freeze 2) of the FinnGen study, a biobank project that combines genotype data from 96,499 samples with electronic health records from Finnish health registries. Information on their study has been reported online (https://finngen.gitbook.io/documentation/).

2.2.10 Colocalization Analysis

To examine genes in the region of the rs62263260 locus, we performed colocalization analysis using summary statistics from the SNP x CSF Aβ42 GWAS and brain cortex eQTL data from Sieberts et al., (i.e., dorsolateral prefrontal cortex, temporal cortex)[309] as well as eQTL data from GTEx v8 (i.e., tissues where rs62263260 was a statistically significant eQTL for any gene: esophagus muscularis, testis, brain anterior cingulate cortex BA24). Using coloc (version 3.2-1),[310, 311] we performed colocalization in a 1 Megabase (Mb) window around the lead SNP, rs62263260 with default priors.[311] All protein coding genes within that window (Chromosome 3, 123175327: 122175327) were tested. A posterior probability greater than 80% (PP4 > 0.8) is indicative of colocalization.[310, 311] Colocalization analyses was not performed for our p-tau result, rs116216974, as it was not an eQTL and is within an intergenic region.

2.2.11 Post-hoc *SEMA5B* Analyses

To assess whether *SEMA5B* expression differs by AD diagnosis, we utilized summaries of case/control analyses from the Accelerating Medicines Partnership Program for Alzheimer's (AMP-AD). Data from this project are made freely available online (https://agora.adknowledgeportal.org).

Furthermore, we examined neuronal *SEMA5B* expression data. Pyramidal neuron expression data for these analyses was obtained from the NIH Gene Expression Omnibus (https://www.ncbi.nlm.nih.gov/geo/). Additional details on brain collection, expression profiling, and microarray analysis are described elsewhere.[312-315] Tissues include the entorhinal cortex, hippocampus, medial temporal gyrus, posterior cingulate cortex, primary visual cortex, and superior frontal gyrus.

Repeated measures ANOVA was used to evaluate differences in *SEMA5B* expression in AD patients compared to controls across brain regions. Covariates included age, sex, and brain region. Post-hoc paired comparisons within each region were performed leveraging independent samples t-tests (one-tailed). We corrected for multiple comparisons leveraging the Bonferroni procedure for the six brain regions evaluated.

2.2.12 MAGMA Pathway Analysis

Gene and pathway analyses were conducted using MAGMA version 1.08.[316] Gene test analyses used the SNP-wise mean model specified in MAGMA. Results were corrected for multiple comparisons using the false-discovery rate (FDR) procedure. Gene sets for MAGMA analyses leveraged data from the Gene Ontology (GO) project,[317] Kyoto Encyclopedia of Genes and Genomes (KEGG),[318-320] REACTOME,[321, 322] BIOCARTA,[323] and the Protein Interaction Database (PID)[324] totaling 12,195 sets.

2.3 RESULTS

Participant characteristics stratified by diagnosis are presented in **Table 2.3**. We observed statistically significant differences between participants in each diagnostic category as expected except for the average number of follow-up visits. Participants in the BIOCARD and WRAP studies are younger than those enrolled in ADNI and VMAP, which may partially explain differences in biomarker levels and hippocampal volumes (**Table 2.4**). Additionally, ADNI includes more participants that have been diagnosed with MCI and Alzheimer's disease than in VMAP, WRAP, or BIOCARD. Using the composite dataset, we performed GWAS to identify common SNPs that modify the association between baseline CSF biomarkers (i.e., amyloid and tau) and baseline hippocampal volume as well as annual change in hippocampal volume. No significant interactions with baseline CSF total tau were identified. All suggestively significant loci ($p<1x10^{-5}$) are displayed in **Appendix B Tables B.1-6**. We also expand on a study by Chiang et al.[325] that explored whether *APOE*-ε4 allele status modified the association between baseline CSF amyloid and longitudinal changes in hippocampal volume.

2.3.1 *APOE* Allele Associations with Hippocampal Atrophy

APOE results are presented in **Table 2.5.** As expected, *APOE*-ε4 allele count was associated with lower baseline hippocampal volume ($\beta=-0.43$, $p<2x10^{-16}$) and faster atrophy ($\beta=-0.03$, $p<2x10^{-16}$). Additionally, *APOE*-ε2 carriers have greater hippocampal volume at baseline ($\beta=0.25$, $p=0.02$) and slower atrophy ($\beta=0.02$, $p=0.0002$) compared to non-carriers.

Table 2.3: Participant characteristics by diagnosis					
	NC	MCI	AD	Total[a]	p-value
N	490	475	100	1065	
Age at baseline	68.4±9.3	72.5±7.3	74.5±8.4	70.8±8.7	< 0.001
Sex, % female	53%	39%	48%	47%	0.002
% *APOE*-ε4 carriers	29%	47%	67%	41%	< 0.001
% *APOE*-2 carriers	13%	9%	3%	10%	< 0.001
Std. CSF Aβ42	-0.75±1.6	-1.70±1.7	-2.52±1.3	-1.34±1.7	< 0.001
Std. CSF Tau	0.08±1.0	0.64±1.5	1.81±1.7	0.49±1.4	<0.001
Std. CSF p-tau	-0.03±0.9	0.37±1.1	0.78±1.2	0.23±1.1	<0.001
Number of Visits	3.46±1.83	4.00±1.86	2.80±1.22	3.64±1.83	0.9
Neuroimaging Measurements (MRI)					
Std. Hippocampal Volume	-0.01±1.0	-0.84±1.3	-2.1±1.3	-0.58±1.3	< 0.001
Std. Hippocampal Vol. Slopes	-0.10±0.1	-0.15±0.1	0.21±0.1	-0.14±0.1	< 0.001

Analysis of variance (ANOVA) analyses indicated significant differences ($p<0.05$) across diagnostic groups for all demographic categories except for the average number of visits. Values given are mean ± standard deviation unless otherwise noted. [a]Consists of participants from ADNI, VMAP, WRAP, and BIOCARD.

2.3.2 *APOE* Allele Interactions with Baseline CSF Aβ42

As seen previously by Chiang et al.,[325] *APOE*-ε4 significantly interacted with baseline CSF Aβ42 (β=0.11, p=0.0004, **Figure 2.4**) on hippocampal volume such that *APOE*-ε4 carriers with higher brain amyloid burden display lower hippocampal volumes and more rapid hippocampal atrophy. We also observe an interaction between *APOE*-ε2 and baseline CSF Aβ42 on baseline hippocampal volume, though it did not survive correction for multiple comparisons. *APOE*-ε2 did not interact with CSF Aβ42 on longitudinal change in hippocampal volume. (**Table 2.5**).

Table 2.4: Breakdown of combined GWAS dataset by cohort						
	ADNI	VMAP	BIOCARD	WRAP	Total	P-value
N	702	126	140	97	1065	<0.001
%Female	44%	31%	61%	65%	47%	<0.001
Age, years	73.6±7.1	73.0±6.4	60.8±7.7	61.7±5.7	70.8±8.7	<0.001
% *APOE*-ε4 Carriers	43%	33%	35%	38%	40%	0.059
% *APOE*-ε2 Carriers	10%	10%	11%	14%	10%	0.474
Standardized Aβ42	-1.55±1.6	-1.73±2.0	-0.45±1.4	-0.55±1.4	-1.34±1.7	<0.001
Standardized p-tau	0.29±1.1	0.22±1.1	-0.002±0.9	0.07±0.9	0.23±1.1	<0.001
Hippocampal Volume	-0.81±1.4	-0.43±1.3	0.001±1.0	0.09±1.0	-0.58±1.3	<0.001
Hippocampal Slopes	-0.15±0.8	-0.15±0.1	-0.09±0.1	-0.06±0.1	-0.14±0.1	<0.001
Number of Visits	4.04±1.94	2.97±0.90	2.29±1.35	3.59±1.26	3.64±1.83	<0.001

Analysis of variance (ANOVA) analyses indicated significant differences across longitudinal aging studies for all demographic categories except for the average number of visits. Note: Values given are mean ± standard deviation unless otherwise noted.

2.3.3 Variant Interactions with Baseline CSF Aβ42

No significant interactions with CSF Aβ42 in cross-sectional analyses were observed. In longitudinal analyses, we identified a novel genetic locus on chromosome 3 (rs62263260-T, β=0.026, $p=1.46x10^{-8}$, MAF=0.12, **Table 2.6**) that is located within an intron of the *SEMA5B* gene (**Figure 2.5A, B**).

Table 2.5: *APOE*-ε4 and *APOE*-ε2 associations with baseline hippocampal volume						
Predictor	Outcome	B	SE	P value	Adj. r^2	Δr^2
APOE-ε4[a]	Baseline HV	-0.43	0.05	< 2.00e-16	0.185	0
APOE-ε4 x CSF Aβ42[b]	Baseline HV	0.11	0.03	0.0004	0.216	3.1
APOE-ε2[a]	Baseline HV	0.25	0.10	0.0168	0.146	0
APOE-ε2 x CSF Aβ42[b]	Baseline HV	-0.13	0.06	0.0435	0.201	5.5
APOE-ε4[a]	Longitudinal HV	-0.031	0.003	< 2.00e-16	0.193	0
APOE-ε4 x CSF Aβ42[b]	Longitudinal HV	0.0056	0.002	0.0024	0.248	5.5
APOE-ε2[a]	Longitudinal HV	0.0236	0.006	0.0002	0.140	0
APOE-ε2 x CSF Aβ42[b]	Longitudinal HV	-0.0054	0.004	0.152	0.235	9.5

[a] Model: Hippocampal Volume ~ Age + Sex + ***APOE***
[b] Model: Hippocampal Volume ~ Age + Sex + ***APOE* x CSF Aβ42**
Abbreviations: HV, hippocampal volume; B, beta; SE, standard error; Δr^2; change in r^2; Adj. r^2, adjusted r^2

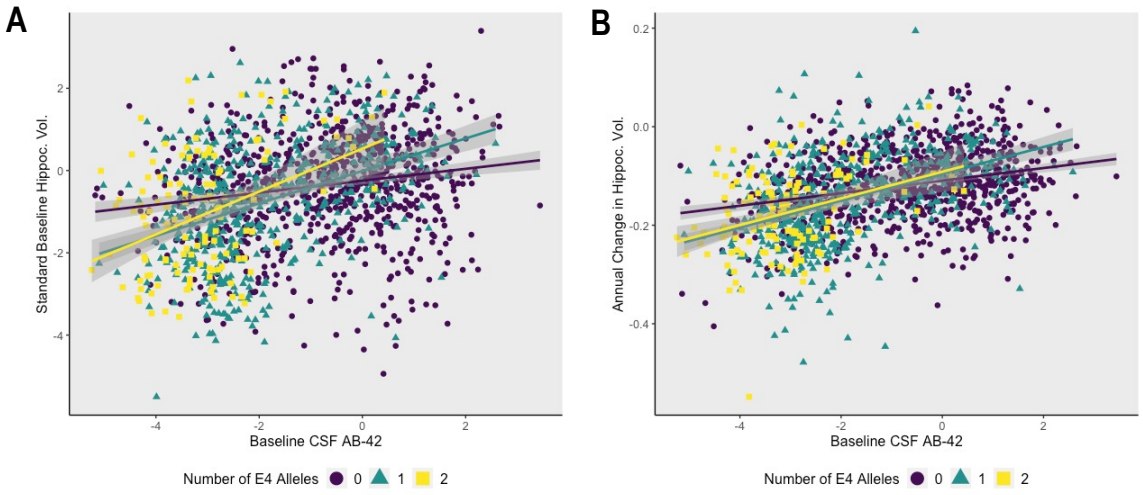

Figure 2.4. *APOE*-ε4 allele carriers have smaller hippocampal volumes at baseline and worse atrophy in the presence of high levels of brain amyloid pathology. A) A plot demonstrating how *APOE*-ε4 allele count modifies the association between Aβ42 and baseline hippocampal volume in a dose-dependent manner (β=0.11, p=0.0004). The y-axis represents baseline standardized hippocampal volume, and the x-axis represents standardized CSF levels of Aβ42 (z-scores). Points and lines are color coded by genotype, where *APOE*-ε4 heterozygotes are denoted by the green line and homozygotes are red. **B)** *APOE*-ε4 positivity increases the rate of atrophy in individuals with high brain amyloid burden (β=0.0056, p=0.0024). There appears to be no change between heterozygous and homozygous carriers of the ε4 allele.

Table 2.6: Variant Interactions with CSF Aβ42							
variant	chromosome	BP	allele	MAF	B	SE	P value
rs62263260	3	122675327	T	0.121	0.02621	0.0046	1.46e-08
rs11707826	3	122676305	T	0.122	0.02616	0.0046	1.53e-08
rs10934626	3	122676523	T	0.122	0.02616	0.0046	1.53e-08

Abbreviations: BP, base pair, MAF, minor allele frequency, B, beta; SE, standard error

Among participants harboring a high baseline brain amyloid burden (i.e., low CSF Aβ42 levels), minor allele (T) carriers of rs62263260 demonstrated a faster rate of hippocampal atrophy (**Figure 2.5C**). At lower brain amyloid levels, minor allele carriers of rs62263260 had slower rates of hippocampal atrophy. Two additional SNPs within this region reached genome-wide significance (**Table 2.6**) and are in high LD (r^2>0.8) with the index SNP, rs62263260 (**Figure 2.5B**). The main effect of rs62263260 was not significantly associated with longitudinal atrophy (p>0.1). Genome-wide significance of the rs62263260 x CSF Aβ42 interaction did not change when using linear-mixed effects regression (β=0.03, p=3.13x10^{-8}) as opposed to linear regression.

2.3.4 Replication of the rs62263260 Interaction with Amyloid Load in the Mayo Clinic Study of Aging

In the independent MCSA cohort where amyloid burden was assessed by [^{11}C]-PiB PET, rs62263260 again displayed a significant interaction with baseline brain amyloid levels to predict longitudinal hippocampal atrophy (n=808, β=-0.24, p=0.0112). Presence of the minor (T) allele was associated with a faster rate of hippocampal atrophy among those with higher baseline amyloid burden (i.e., higher levels of amyloid PET and/or lower levels of CSF amyloid), and slower rates among those with low amyloid burden validating our initial findings in the discovery dataset. Similar results to MCSA were observed when leveraging amyloid PET data from ADNI

(n=667; β=-0.0055, p=0.0045; **Figure 2.6**). Linear mixed-effects regression results (β=-0.013, p=0.013) were largely consistent with the PET results in ADNI.

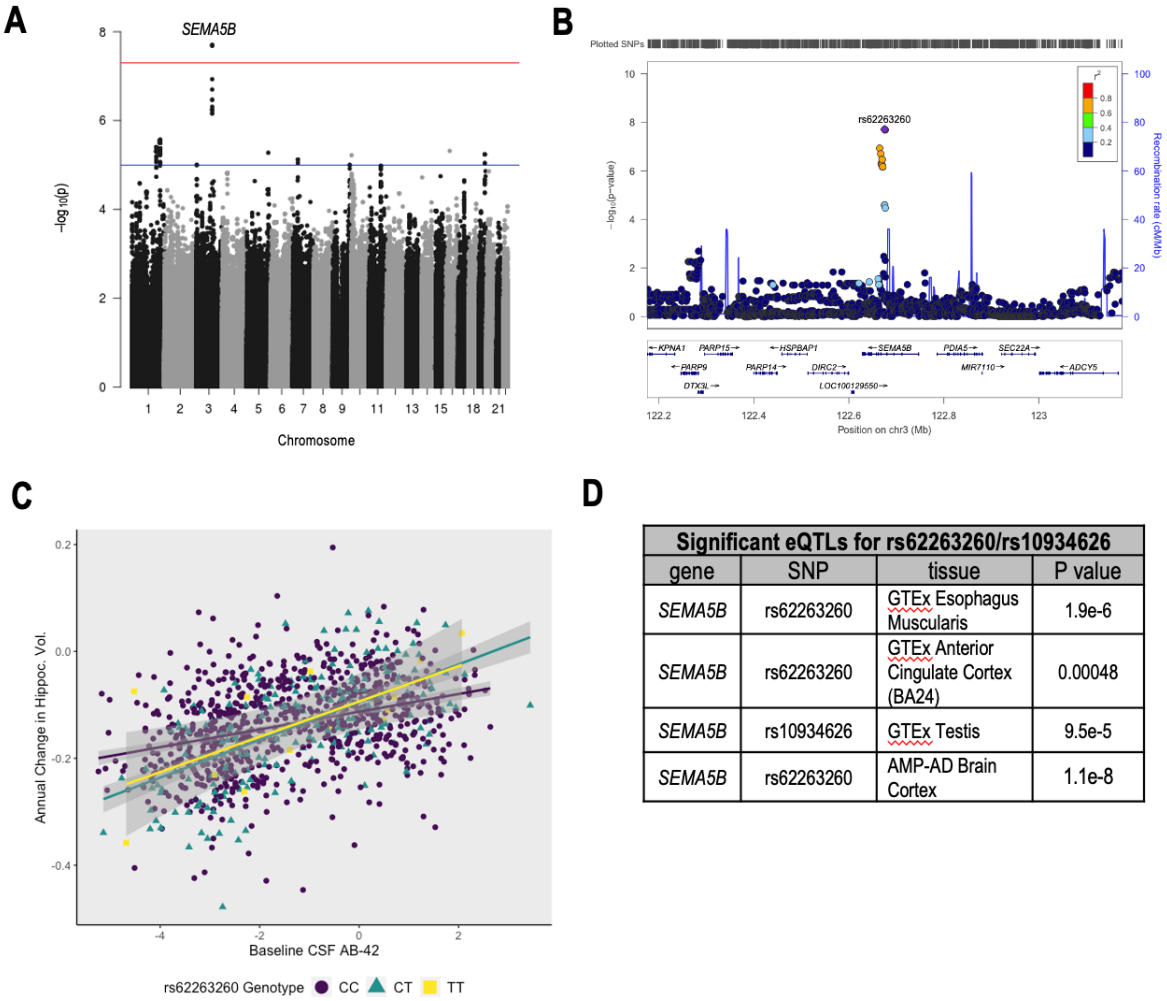

D

Significant eQTLs for rs62263260/rs10934626			
gene	SNP	tissue	P value
SEMA5B	rs62263260	GTEx Esophagus Muscularis	1.9e-6
SEMA5B	rs62263260	GTEx Anterior Cingulate Cortex (BA24)	0.00048
SEMA5B	rs10934626	GTEx Testis	9.5e-5
SEMA5B	rs62263260	AMP-AD Brain Cortex	1.1e-8

Figure 2.5. Three SNPs in an intronic region of the *SEMA5B* gene significantly modify the association between baseline beta-amyloid and hippocampal atrophy. A) The Manhattan plot of the genome-wide association study. The threshold for genome-wide statistical significance ($\alpha=5x10^{-8}$) is indicated by the red line. The blue line represents the suggestive threshold for significance ($\alpha=1x10^{-5}$). B) A LocusZoom plot of *SEMA5B* and additional genes in the 1Mb region. Points are colored by LD with the top variant, where higher r^2 values are colored in red and lower r^2 values are colored in blue based off of LD calculated in non-Hispanic whites of European descent. The diamond represents the variant with the smallest P-value. C) A plot demonstrating how the index SNP, rs62263260, modifies the association between CSF Aβ42 and hippocampal atrophy. The y-axis represents annual change in standardized hippocampal volume, and the x-axis represents standardized CSF levels of Aβ42 (z-scores). Points and lines are color coded by genotype. Individuals harboring higher levels of baseline pathology exhibit worse hippocampal atrophy (β=0.026, $p=1.46x10^{-8}$). D) Tissues where rs62263260 or rs10934626 (LD $r^2>0.9$) is a statistically significant eQTL for the *SEMA5B* gene.

2.3.5 Sensitivity Analyses of rs62263260

The rs62263260 x amyloid interaction results maintained genome-wide significance in sensitivity analyses covarying for age, sex, PC1-3, *APOE*-ε4, and scanner strength (**Table 2.7**). When covarying for age, sex, PC1-3, and study, the significance becomes slightly attenuated ($p=7.7x10^{-8}$).

2.3.6 Functional Annotation of rs62263260

The index SNP rs62263260, is a significant eQTL for the *SEMA5B* gene in the brain with associations in other tissues including the esophagus (**Figure 2.5D**). In addition, carriers of the minor allele (T) appear to have higher levels of *SEMA5B* expression compared to non-carriers (**Figure 2.7,** eQTL information from Sieberts et al., 2020).[309]

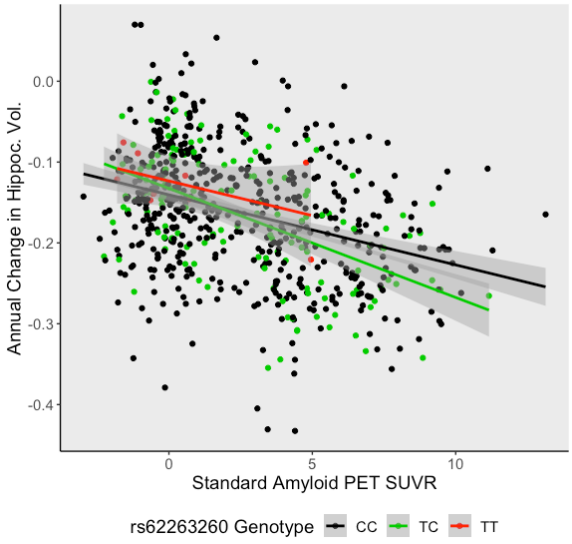

Figure 2.6. A plot demonstrating how the index SNP, rs62263260, modifies the association between standardized baseline PET amyloid levels and hippocampal atrophy in ADNI. The y-axis represents baseline standardized hippocampal volume, and the x-axis represents standardized amyloid PET SUVR. Points and lines are color coded by genotype, where rs62263260-T heterozygotes are denoted by the green line and homozygotes (TT) are red.

Table 2.7: Sensitivity Analyses for SNP x β-Amyloid GWAS				
Analysis	variant	B	SE	P value
+ *APOE4* count and scanner strength as covariates	rs62263260	0.01617	0.002761	6.30e-09
	rs11707826	0.01615	0.00276	6.54e-09
	rs10934626	0.01615	0.00276	6.54e-09
Linear mixed-effects regression	rs62263260	0.03302	0.00595	3.13e-08
	rs11707826	0.03296	0.00595	3.27e-08
	rs10934626	0.03294	0.00595	3.27e-08

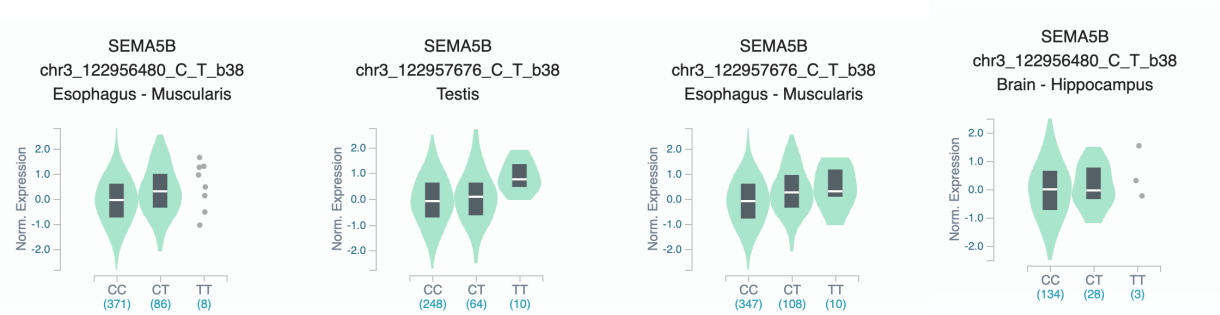

Figure 2.7. Violin plots adapted from the NIH Gene-Tissue Expression (GTEx) Project showing the normalized expression of *SEMA5B* in esophageal, testicular, and brain tissue. The plots suggest that the minor alleles of rs62263260 and rs10934626, a SNP in the same locus, are associated with an increase in Semaphorin 5B expression, especially in homozygotes. These images were obtained from the GTEx Portal on 06/15/20. In addition, the given rs62263260 *SEMA5B* eQTL beta from Sieberts et al., 2020 is β=0.318. The expression increasing allele is rs62263260-T, the minor allele.[309]

To determine whether *SEMA5B* was the acting gene in the region, colocalization analysis was performed. rs62263260 strongly colocalized with *SEMA5B* expression in the esophagus muscularis in GTEx v8 (PP4 > 0.99). In other datasets where rs62263260 or its neighboring SNPs were significant eQTLs for *SEMA5B*, colocalization results were negative (PP3 > 80%) or inconclusive (**Table 2.7**).

In addition, rs62263260 and SNPs in the surrounding region (i.e., rs11707826, rs10934626) significantly disrupted 6 transcription factor binding sites (p.fdr<0.05, **Table 2.8**),

but were not enriched for enhancer sites and were not methylation-QTLs or histone-QTLs in any queried database.

Table 2.8: *coloc* results for genes within the 1Mb region of rs62263260; only *SEMA5B* was tested in GTEx tissues because rs62263260 (or its associated SNPs) was not an eQTL for any other gene in GTEx. In GTEx, a significant eQTL is p<0.0011 after Bonferroni correction.

Sieberts et al., 2020; AMP-AD Cortex Meta-Analysis eQTL, n=1433							
Gene	**SNP**	**eQTL pvalue (FDR-corrected)**	**PP3**	**PP4**	**Best-fit SNP**	**BP Position (hg38)**	**Best-fit SNP.PP.H4**
SEMA5B	rs62263260	9.31E-07	0.9980	6.33E-05	rs2276782	3:122913049	0.8688
CCDC58	rs62263260	0.7853	0.346	0.0338	rs62263260	3:122956480	0.2711
FAM162A	rs62263260	0.4372	0.175	0.106	rs10934626	3:122957676	0.3026
WDR5B	rs62263260	0.3234	0.9980	8.93E-05	rs6438741	3:122562494	0.2564
KPNA1	rs62263260	0.9854	0.9980	3.32E-05	rs6771095	3:122472888	0.1279
PARP9	rs62263260	0.9930	0.9980	5.51E-05	rs9872708	3:122523960	0.0570
DTX3L	rs62263260	0.8757	0.136	0.0347	rs62263260	3:122956480	0.2790
PARP14	rs62263260	0.9436	0.9980	6.01E-05	rs10804558	3:122826566	0.2284
HSPBAP1	rs62263260	0.7977	0.9980	5.83E-05	rs2276775	3:122927887	0.9914
DIRC2	rs62263260	0.0680	0.9960	0.0013	rs2276781	3:122913589	0.1711
PDIA5	rs62263260	0.8578	0.449	0.0247	rs62263260	3:122956480	0.2599
SEC22A	rs62263260	0.5753	0.9970	1.31E-04	rs62263260	3:122956480	0.1934
ADCY5	rs62263260	0.9027	0.187	0.0484	rs10934626	3:122957676	0.1830
HACD2	rs62263260	0.8443	0.205	0.0353	rs62263260	3:122956480	0.2718
MYLK	rs62263260	0.9457	0.139	0.0334	rs62263260	3:122956480	0.2482
CCDC14	rs62263260	0.8065	0.278	0.0363	rs62263260	3:122956480	0.2636
GTEx v8 - Esophagus Muscularis, n=465							
Gene	**SNP**	**eQTL p-value (uncorrected)**	**PP3**	**PP4**	**Best-fit SNP**	**BP Position (hg38)**	**Best-fit SNP.PP.H4**
SEMA5B	rs62263260	0.0000019	0.0020	0.9950	rs10934626	3:122957676	0.4187
GTEx v8 - Testis, n=368							
Gene	**SNP**	**eQTL p-value (uncorrected)**	**PP3**	**PP4**	**Best-fit SNP**	**BP Position (hg38)**	**Best-fit SNP.PP.H4**
SEMA5B	rs10934626	0.000095	0.9890	0.0064	rs10934626	3:122957676	0.4900
GTEx v8 -Brain Anterior Cingulate Cortex BA24, n=147							
Gene	**SNP**	**eQTL p-value (uncorrected)**	**PP3**	**PP4**	**Best-fit SNP**	**BP Position (hg38)**	**Best-fit SNP.PP.H4**
SEMA5B	rs62263260	0.00048	9.39E-04	0.0267	rs16833588	3:122857345	1.20E-05

Note: A posterior probability greater than 80% (PP4 > 0.8) is indicative of colocalization, whereas PP3 is the posterior probability that both traits are associated with two independent SNPs.

2.3.7 Post-Hoc Analysis of *SEMA5B* Expression in Brain

Using Agora, a publicly available database powered by the AMP-AD Consortium https://agora.adknowledgeportal.org/genes/(genes-router:gene-details/ENSG00000082684), we examined whether AD diagnosis had any effect on *SEMA5B* gene expression. In multiple brain tissues including cerebellum, prefrontal cortex, and temporal cortex, *SEMA5B* expression is

decreased in AD brains in comparison to controls. To ensure that the differences observed on Agora were not due to cell type differences in the bulk tissue, we also leveraged a laser-captured neuronal gene expression dataset[312-315] to assess neuron-specific *SEMA5B* expression differences by diagnosis. Similar to the results seen on Agora, we observed a main effect of diagnosis on *SEMA5B* expression ($F(1, 152)=17.45$, $p < 0.0001$) whereby we observed lower expression of *SEMA5B* in AD compared to control neurons (**Figure 2.8**). When evaluating each region individually in post-hoc paired comparisons, we observed that the difference was particularly pronounced in the hippocampus ($T(20.768)=-2.79$, $p=0.006$).

Table 2.9: Transcription factor binding sites disrupted by SNPs within the rs62263260 locus

rsID	BP	R^2	motif_start	motif_end	tf_name	p.fdr
rs2288678	122667277	0.71	122667274	122667283	ETS1(ETS)	0.003
rs2288678	122667277	0.71	122667275	122667284	SPDEF(ETS)	0.003
rs10934625	122671316	0.71	122671310	122671321	Nur77(NR)	0.003
rs10934626	122676523	1	122676518	122676525	SCL(bHLH)	0.01
rs35989119	122671081	0.71	122671077	122671084	CRX(Homeobox)	0.022
rs2288678	122667277	0.71	122667275	122667284	ETV1(ETS)	0.033

Abbreviations: BP, base pair; R^2, measurement of linkage disequilibrium; motif_start, transcription factor motif start (in BP); motif_end, transcription factor motif end; p, p-value; p.fdr, FDR-corrected p-value

2.3.8 Gene and Pathway Results for the SNP x CSF Aβ42 GWAS

In gene level analyses, the *TOMM40* interaction with CSF Aβ42 on hippocampal atrophy was the top result ($p=1.60\text{x}10^{-5}$, p.fdr=0.28), but did not survive multiple corrections. The *TOMM40* signal was further attenuated when covarying for *APOE* as expected (p.fdr=0.74).[326]

Our top pathway-level results included the GO-term "regulation of double strand break repair" ($p=3.11\text{x}10^{-4}$) but it did not survive correction. Nominally significant gene- and pathway-level results are reported in **Figure 2.9** and **Appendix B Tables B.7-10.**

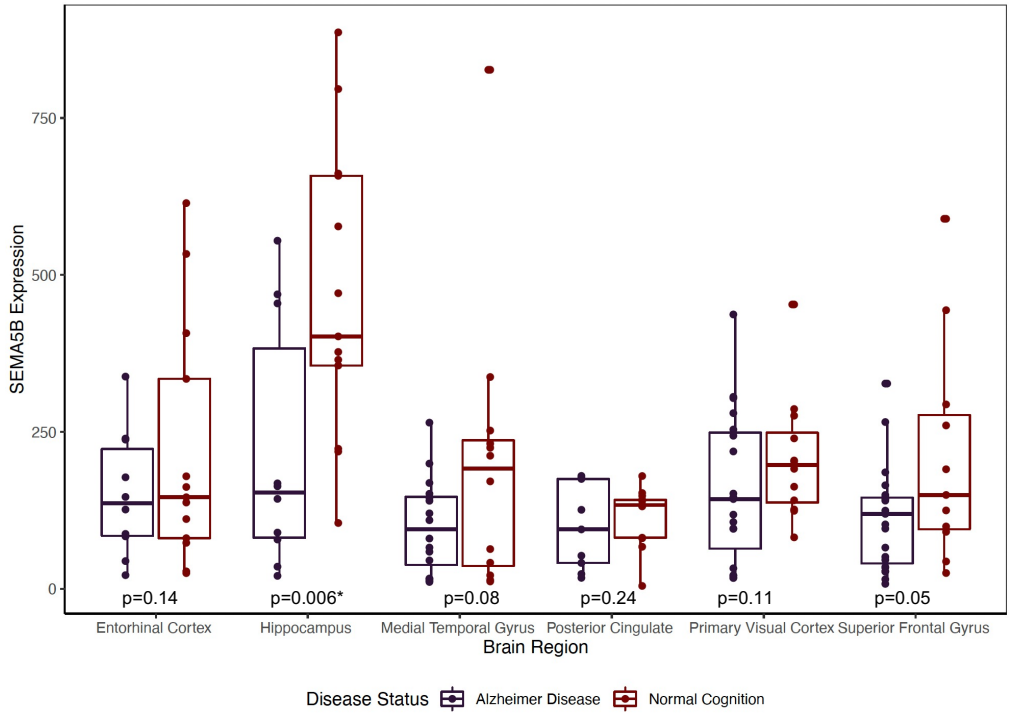

Figure 2.8. Hippocampal pyramidal neurons in Alzheimer's disease brains express less *SEMA5B* than those from cognitively normal controls. A box plot summarizing laser-captured neuronal expression of *SEMA5B* across brain regions (i.e., entorhinal cortex, hippocampus, medial temporal gyrus, posterior cingulate cortex, primary visual cortex, and superior frontal gyrus) in AD cases and controls such that each point represents a sample's *SEMA5B* expression. Across regions, we observed lower expression of *SEMA5B* in AD compared to controls ($F(1, 152)=17.45$, $p<0.0001$). In post-hoc paired comparisons, the association was particularly pronounced in the hippocampus surviving Bonferroni correction for multiple comparisons ($p=0.006$).

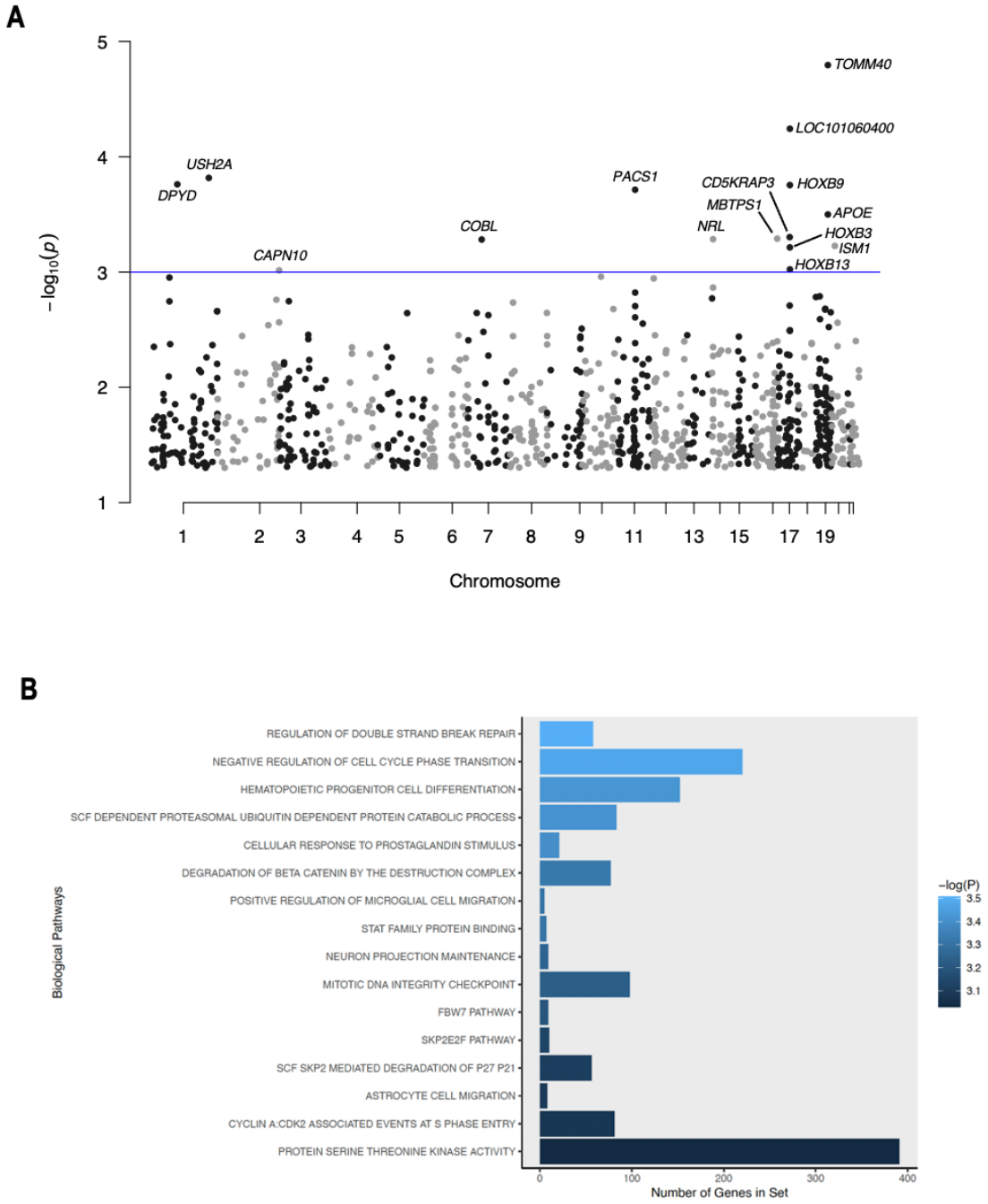

Figure 2.9. Summary of nominally significant MAGMA gene- and pathway-level results for the SNP x CSF Aβ42 GWAS. A) A Manhattan plot summarizing chromosome and p-value for all genes tested by MAGMA. The threshold for nominal significance is indicated by the blue line ($\alpha=1x10^{-3}$). *TOMM40* is the most significant result with a p-value of $1.60x10^{-5}$. **B)** A bar plot summarizing pathway-level results with $p < 1x10^{-3}$. The y-axis represents the number of genes in each pathway gene set. Bars are filled according to p-value. The most significant pathway is "regulation of double strand break repair" ($p=3.11x10^{-4}$).

2.3.9 Single polymorphism nucleotide interactions with baseline levels of CSF phosphorylated tau

We did not observe any genome-wide significant interactions with CSF p-tau on baseline hippocampal volume. In longitudinal analyses, CSF p-tau levels interacted with a locus on chromosome 3 (rs116216974-G, MAF=0.02, β=0.05619, p=2.05x10^{-8}) that is 39.8 kilobases downstream of the *SATB1* gene (**Figure 2.10A,B**). Two other SNPs, rs115028405 and rs114376431, within this same region reached genome-wide significance (p=2.05x10^{-8}), and they are in LD (r^2>0.8) with the index SNP rs116216974 (**Figure 2.10B**). Minor allele carriers of rs114376431-G have a slower rate of hippocampal atrophy among individuals harboring greater levels of brain p-tau pathology (**Figure 2.10C**). rs114376431-G alone was not significantly associated with baseline hippocampal volume or longitudinal atrophy (p>0.1). Similar to rs62263260, rs116216974 remained significant after adding *APOE*-ε4 count and MRI scanner strength as covariates to the model. However, the p-value was slightly attenuated when using a linear mixed-effects model (p=2.37x10^{-7}).

2.3.10 Functional Annotation of rs114376431

The index SNP for our p-tau locus, rs116216974, was not reported to be an eQTL, mQTL, or histone-QTL. SNPs in the surrounding region (i.e., rs114376431, rs115028405) were not enriched for enhancer or epigenomic sites, but 7 transcription factor binding sites (TFBS) identified by HOMER[327] were significantly disrupted (p.fdr<0.05, **Table 2.9**). In the FinnGen study, the minor allele of rs116216974-G is marginally associated with increased incidence of diseases of the blood and blood-forming organs (p=3.1x10^{-6}) including ICD-10 codes for nutritional and hemolytic anemias, blood disorders, and immunodeficiencies.[328]

Table 2.10: Transcription factor binding sites disrupted by SNPs within the rs116216974 locus

rsID	BP	R^2	motif_start	motif_end	tf_name	p.fdr
rs79531054	18077596	0.90	18077589	18077598	HOXD13(Homeobox)	0.004
rs79531054	18077596	0.90	18077589	18077600	TATA-Box(TBP)	0.004
rs115028405	18342494	1	18342489	18342505	Fox:Ebox(Forkhead,bHLH)	0.004
rs115028405	18342494	1	18342494	18342503	FOXA1(Forkhead)	0.037
rs116341779	18421999	0.90	18421993	18422007	Bcl6(Zf)	0.037
rs79531054	18077596	0.90	18077589	18077598	Unknown(Homeobox)	0.028
rs115028405	18342494	1	18342494	18342505	Foxa2(Forkhead)	0.04

Abbreviations: BP, base pair; R^2, measurement of linkage disequilibrium; motif_start, transcription factor motif start (in BP); motif_end, transcription factor motif end; p, p-value; p.fdr, FDR-corrected p-value

2.3.11 Gene and Pathway Results for the SNP x CSF p-tau GWAS

In gene-level analyses, *PLCB4* (phospholipase C beta 4) interaction with CSF p-tau on hippocampal atrophy was the top result ($p=1.09x10^{-5}$). Additionally, our top pathway-level results included the GO-term "endolysosome lumen" for p-tau ($p=1.13x10^{-4}$), but neither gene- nor pathway-level results survived correction for multiple comparisons. Nominally significant results are summarized in **Figure 2.11** and **Appendix B Tables B.11 and B.12**.

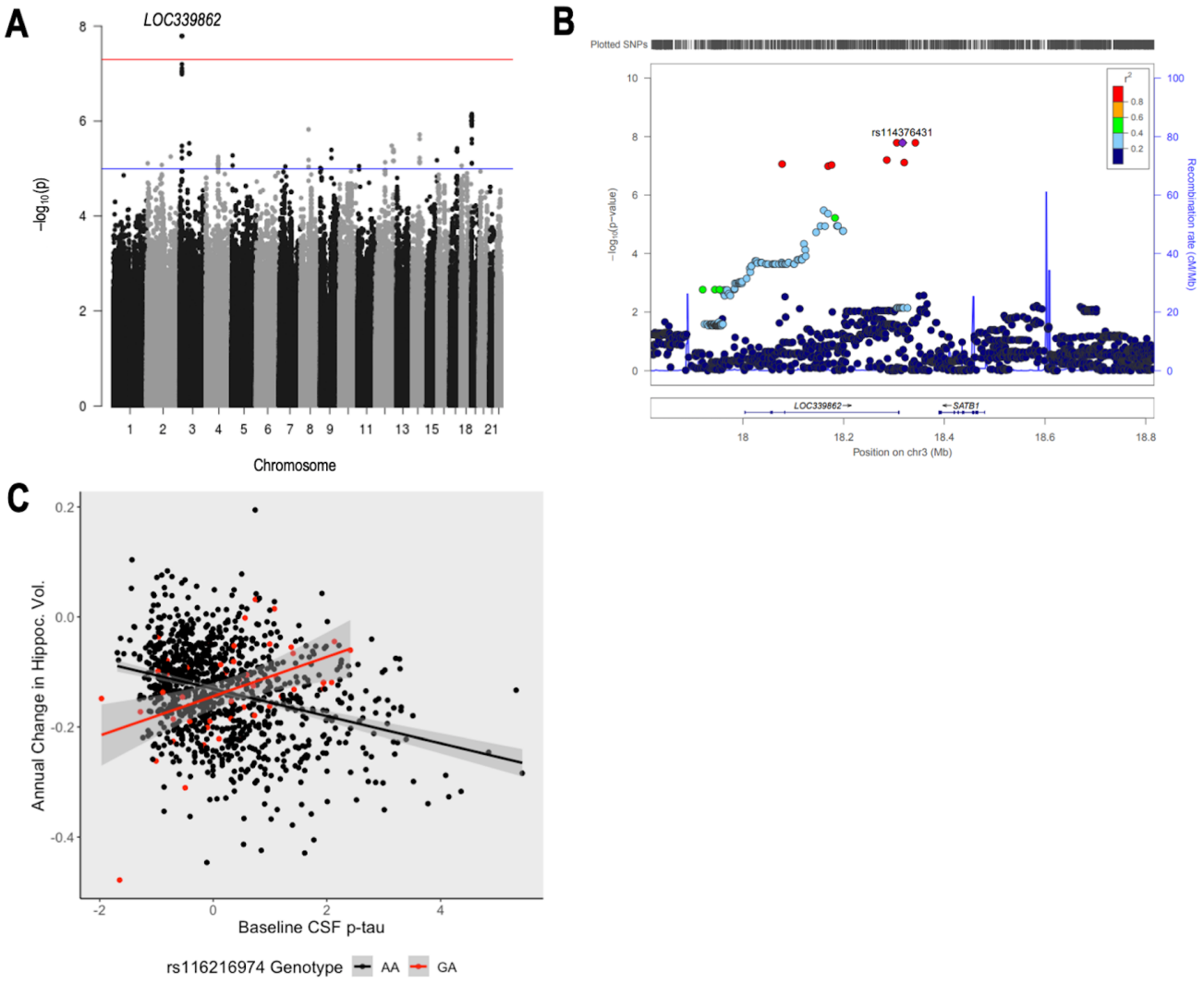

Figure 2.10. Three SNPs on chromosome 3 significantly modify the association between CSF baseline p-tau levels and hippocampal atrophy. A) The Manhattan plot of the genome-wide association study. The threshold for genome-wide statistical significance ($\alpha=5x10^{-8}$) is indicated by the red line. The blue line represents the suggestive threshold for significance ($\alpha=1x10^{-5}$). The labeled gene (*LOC339862*) is closest to the locus of interest. **B)** A LocusZoom plot of the identified locus. Our SNPs were also located downstream of the *SATB1* gene. Points are colored by LD with the top variant, where higher r^2 values are colored in red and lower r^2 values are colored in blue. The diamond represents the variant with the smallest P-value. **C)** A plot demonstrating how our SNPs modify the association between p-tau and hippocampal atrophy ($\beta=0.06$, $p=2.05x10^{-8}$). The y-axis represents annual change in standardized hippocampal volume, and the x-axis represents standardized CSF levels of p-tau (z-scores). Points and lines are color coded by genotype, where minor allele carriers are red. There were no homozygous carriers of the minor allele in our dataset.

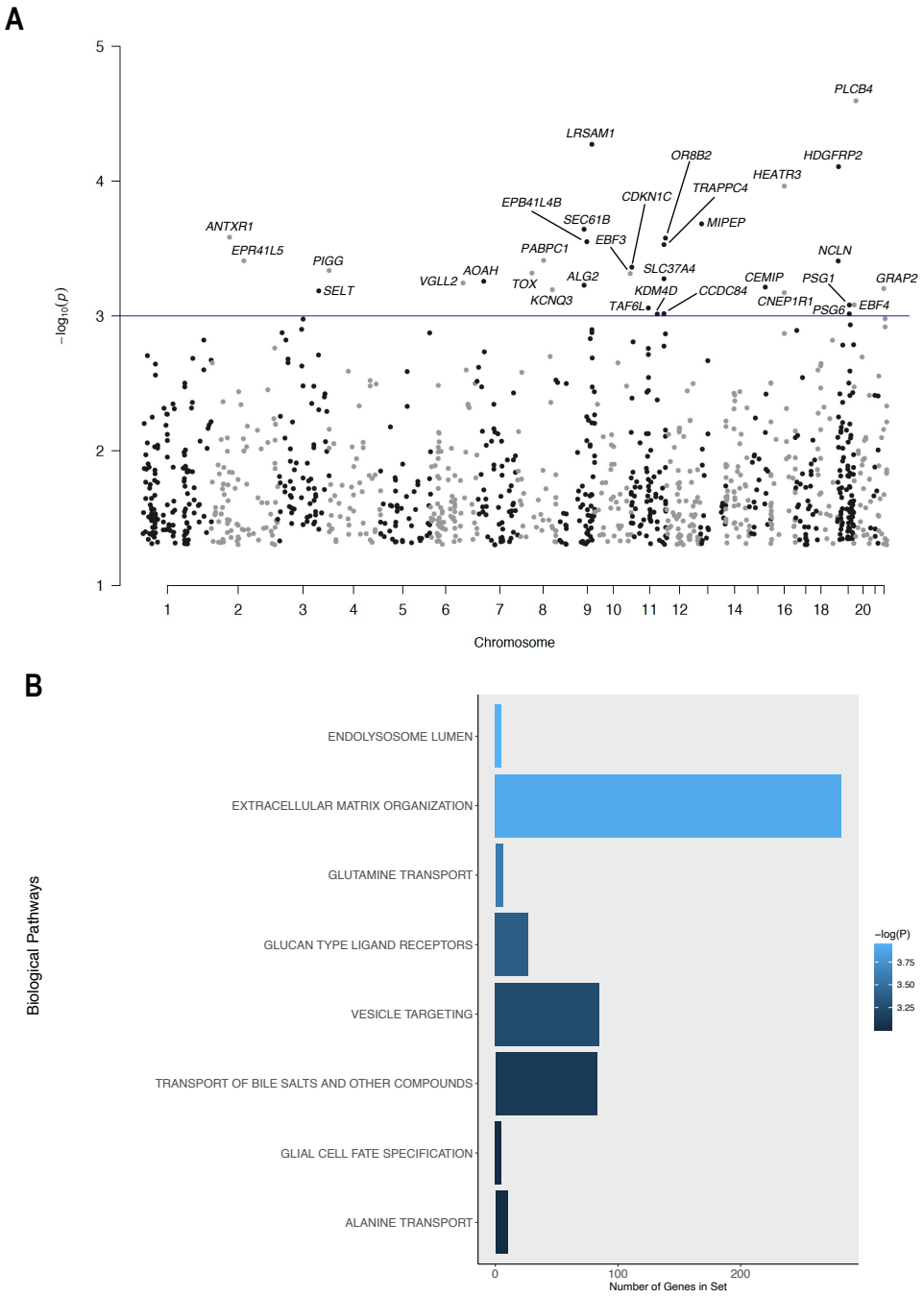

Figure 2.11. Summary of nominally significant MAGMA gene- and pathway-level results for the SNP x CSF p-tau GWAS. A) A Manhattan plot summarizing chromosome and p-value for all genes tested by MAGMA. The threshold for nominal significance is indicated by the blue line ($\alpha=1x10^{-3}$). *PLCB4* is the most significant result with a p-value of $1.09x10^{-5}$. **B)** A bar plot summarizing pathway-level results with $p < 1x10^{-3}$. The y-axis represents the number of genes in each pathway gene set. Bars are filled according to p-value. The most significant pathway is "endolysosome lumen" ($p=3.11x10^{-4}$).

2.4 DISCUSSION

We identified two novel loci that modify the association between baseline CSF biomarkers and the annual rate of hippocampal volume decline. First, minor allele (T) carriers of rs62263260 exhibit faster rates of hippocampal atrophy among individuals with biomarker evidence of amyloidosis. However, rs62263260 minor allele carriers with low amyloid burden appear to be protected from neurodegeneration compared to non-carriers. Importantly, we observed evidence of this interaction effect across PET and CSF measures of amyloidosis and replicated this interaction effect in an independent dataset. Moreover, our top variant is a strong eQTL for *SEMA5B*, a gene involved in synaptic pruning and axonal guidance. Second, we discovered that minor allele (G) carriers of rs116216974 exhibit slower rates of hippocampal atrophy in the presence of high CSF p-tau.

Additionally, we replicated previous work demonstrating that *APOE*-ε4 modifies the association between baseline CSF amyloid on both cross-sectional and longitudinal measures of hippocampal volume. Though additional studies are needed, the present results suggest that axonal guidance, synaptic pruning genes, DNA damage repair and endolysosomal function, along with *APOE,* may modulate the association between Alzheimer's pathology and downstream neurodegeneration, providing exciting targets for future mechanistic studies.

2.4.1 Variants on chromosome 3 drive increased susceptibility to amyloid-dependent neurodegeneration

Notably, our top GWAS finding rs62263260 and the additional SNPs within the region have not been linked to Alzheimer's in any previous case-control studies of clinical Alzheimer's disease and Alzheimer's risk.[91, 93] It is also not significantly associated with diagnosis in our study

(p=0.47). As in previous studies examining Alzheimer's disease endophenotypes as outcomes,[329] rs62263260 may be more related to the rate of disease progression than risk for the onset of clinical disease.

rs62263260 is a significant eQTL for the *SEMA5B* gene in two independent eQTL studies and is colocalized with *SEMA5B* in esophageal tissue. Though *SEMA5B* expression in esophageal tissue is not directly linked to neurodegeneration, it should be noted that studies leveraging the NIH GTEx portal have suggested that genetic regulation of gene expression is conserved across many tissues,[330, 331] thus, significant results in seemingly non-relevant tissues, such as the esophagus, with increased sample size (and subsequently, statistical power), could still provide insights into hypothetical disease processes. However, further study in highly relevant tissues (i.e., hippocampus) is still needed to conclusively elucidate its role in amyloid-related hippocampal atrophy. *SEMA5B* encodes semaphorin 5B (Sema5B), which is expressed in both the developing and adult hippocampus.[308, 332-334] Proteins within the semaphorin family, including Sema5B, facilitate neural development, axonal growth, and synapse maintenance.[335] Sema5B is being actively studied and is not well-characterized, but *Sema5b* knockout mice exhibit aberrant neuronal branching and axonal pathfinding defects.[336-339] In contrast, overexpression of *Sema5b* in mouse hippocampal neurons resulted in a decrease in synapse number.[332]

The direction of the *SEMA5B* association in the present manuscript is difficult to determine, though preliminary eQTL results suggest that the minor allele of rs62263260 is associated with increased expression of *SEMA5B* in tissues including the brain,[309] esophagus, and testes (**Figure 2.7**). Thus, it may be that higher expression of *SEMA5B* is associated with slower hippocampal atrophy in the absence of amyloidosis, but more rapid neurodegeneration in the presence of amyloid. In contrast to the eQTL direction of effect, there is evidence that *SEMA5B* expression is

downregulated in Alzheimer's disease brains as reported by the Agora platform (https://agora.ampadportal.org/genes) and within our post-hoc analyses, further suggesting a change over the course of disease. We hypothesize that *SEMA5B* expression and function may change as Alzheimer's disease progresses, though further mechanistic study of *SEMA5B* in relevant brain tissues is truly needed to confirm its role and function in neurodegeneration.

2.4.2 Variants on chromosome 3 modify the association between CSF p-tau and hippocampal atrophy

A variant on chromosome 3 interacted with p-tau, though did not annotate to any gene in functional analyses. One hint of function came in phenome-level analyses of the SNP which revealed a possible link between genetic drivers of anemia and neuroprotection from p-tau, such that minor allele carriers of rs116216974 appear to have a higher incidence of anemia, which also increases risk of dementia.[340-342] Given these findings, we would expect minor allele carriers of rs116216974 to have worse hippocampal atrophy, but instead, the minor allele was protective.

Nutritional anemias make up nearly one-third of all elderly anemia cases, which are treatable via nutritional supplementation.[343] Low blood vitamin B levels and high levels of homocysteine have been tied to Alzheimer's disease incidence in case-control studies, and both are inversely correlated. Therefore, one mechanism behind the neuroprotection we observed may be related to the treatment of anemia such that dietary supplementation of B-vitamin-related pathways may slow atrophy in the presence of Alzheimer's disease pathology.[344] However, the exact molecular pathways or mechanisms by which rs116216974 confers its neuroprotective effects are still unclear, and the connection to anemia and vitamin B is speculative.

2.4.3 Pathway results implicate DNA damage and repair as modifiers of amyloid-related brain atrophy

In addition to the *SEMA5B* results, we observed some evidence of a modifying role of DNA double-stranded break repair on amyloid-related hippocampal atrophy in our pathway-level results. DNA damage is suggested to play a large role in aging such that insurmountable damage (e.g., from reactive oxygen species) results in apoptosis or cellular senescence.[345, 346] The relationship between normal aging and DNA damage is well-established, and emerging evidence supports a more direct role for DNA damage in Alzheimer's disease.[347] Deficiency in repair mechanisms can occur as a result of Alzheimer's disease pathology (e.g., amyloid-related decreases in the DNA repair factor, *BRCA1* (breast cancer factor 1)) and can also enhance Alzheimer's disease pathology (e.g., aberrant CDK5 (cyclin-dependent kinase 5) activity).[347, 348]

2.4.4 Pathway results implicate endolysosomal function as a modifier of tau-related neurodegeneration

Our top pathway-level result for our CSF p-tau interaction was "endolysosome lumen." The endosomal-lysosomal system is important for the internalization, recycling, and degradation of cellular components,[349] and its dysregulation has been observed in Alzheimer's disease. Several Alzheimer's disease risk loci are implicated in endolysosomal function, (e.g., *PICALM*, *CLU*),[212, 213] and the endolysosomal network is an important clearance pathway of Alzheimer's disease pathology,[350] and there is increasing evidence that biological mechanisms that improve pathological clearance may result in a reduction of brain atrophy.[215, 216, 351]

2.4.5 *APOE*-ε4 carriers exhibit increased susceptibility to neurodegeneration in the presence of amyloidosis

APOE-ε4 is the strongest genetic risk factor for late-onset Alzheimer's disease, causing a 2- to 3-fold increased risk of Alzheimer's among heterozygous *APOE*-ε4 carriers, and up to a 15-fold increased risk among homozygous *APOE*-ε4 carriers.[142, 352] *APOE*-ε4 increases the pathological deposition and aggregation of Aβ in the brain – even in cognitively normal older adults – and has also shown evidence of independent associations with tau and cerebrovascular disease.[149, 353] Our analyses add to existing literature suggesting that carriers of *APOE*-ε4 exhibit faster hippocampal volume decline in the presence of brain amyloidosis. Interestingly, the cross-sectional effects on baseline hippocampal volume appear to occur in a dose-dependent manner. However, we do not see any difference in the association between higher levels of amyloid and neurodegeneration in *APOE*-ε4 heterozygotes compared to *APOE*-ε4 homozygotes, perhaps suggesting the additional impact of homozygous carriership on hippocampal volume was already present at baseline in these cohort studies. *APOE*-ε4 positivity has been associated with accelerated seeding of amyloid pathology and an earlier onset of amyloid positivity.[61, 354] Furthermore, it has been suggested that the length of amyloid positivity correlates positively with the rate of the future progression of disease.[61] Altogether, the results add to a growing body of literature suggesting that *APOE* contributes to the progression of Alzheimer's disease both upstream and downstream of amyloidosis.

2.4.6 Strengths and Limitations

This study has multiple strengths including the use of harmonized CSF and PET amyloid values in addition to longitudinal neuroimaging data from well-characterized aging studies. We were also able to replicate our amyloid results in an independent cohort. In this study, as well as

others, we have also demonstrated that our harmonization processes are viable for increasing sample size, laying the foundation for future large-scale genomic discovery analyses of resilience.

However, our study is not without limitations. Our sample was restricted to individuals who were highly educated, non-Hispanic white, and were free of other health comorbidities, limiting the generalizability of our results to additional populations. Though we were able to harmonize and standardize the CSF biomarker values and hippocampal volume measurements across cohorts, subtle differences remain possible due to differences in age and enrollment criteria (**Table 2.4**). Additionally, as some of our results are based on cross-sectional amyloid data, we cannot exclude that parts of our findings could be explained by the recent suggestion that *APOE* genotype could be used as a surrogate measure of time with Aβ pathology,[355] i.e., that Aβ-positive *APOE*-ε4 carriers have had Aβ pathology 10-15 years longer than Aβ-positive non-carriers, and that they therefore are further along in the neurodegenerative phase of Alzheimer's disease. This hypothesis needs to be addressed in future longitudinal studies.

2.4.7 Conclusion

In this study, we identified two novel loci on chromosome 3 that modify the association between baseline CSF Alzheimer's disease biomarker values and hippocampal atrophy. We also supported previous findings that *APOE*-ε4 was associated with baseline hippocampal volume and hippocampal atrophy in the presence of amyloid pathology. Our results highlight potential biological pathways that may be implicated in both neuroprotection from and susceptibility to Alzheimer's disease pathologies including defects in axonal branching, DNA damage, and lysosomal function.

2.4.8 Future Directions

Looking forward, further efforts to harmonize biomarker and neuroimaging data from additional cohorts will be needed to fully characterize the roles of the newly identified loci in neuroprotection from Alzheimer's pathology. As deposition and aggregation of Alzheimer's neuropathology occurs over time, it may be helpful to look at the effects of rs62263260 and rs116216974 using biomarker data at different timepoints. It may also be fascinating to examine the effects of rs62263260 and rs116216974 in early-onset AD.

Functional *in vitro* and *in vivo* studies examining *SEMA5B* function in relevant tissues will also help support our hypothesis that it is involved in amyloid-related neurodegeneration as well as elucidate its mechanism in neurodegeneration. Furthermore, additional studies are truly required to understand how rs116216974 is conferring its neuroprotective effects from tau pathology. Though rs116216974 has been connected to nutritional anemia, its mechanism of action is unclear. Future studies involving rs116216974 may examine the consequences of transcription factor binding site disruption and/or link rs116216974 to a coding gene.

CHAPTER 3

EXAMINING TRANSCRIPTOMIC MODIFIERS OF THE *APOE*-ε4 EFFECTS ON COGNITION

Portions of this chapter are currently in press under the title, "*RNASE6* is a novel modifier of *APOE*-ε4 effects on cognition," that has been submitted to *Neurobiology of Aging* in February 2022. Full acknowledgements and funding details can be found in **Appendix C.**

3.1 INTRODUCTION

The most common form of Alzheimer's disease is sporadic LOAD, which is complex in etiology and heterogeneous in clinical presentation.[7, 356] Sporadic LOAD is polygenic, and to date, over 40 risk loci for AD have been identified via large genome-wide association studies.[92, 93, 357, 358] One key genetic driver is *APOE* (apolipoprotein E), which has three common polymorphic alleles: ε2, ε3, and ε4. The *APOE*-ε4 allele is the strongest common genetic risk factor for AD.[359, 360] A single allele of *APOE*-ε4 can increase AD risk by up to 3 times compared to *APOE*-ε3, and two *APOE*-ε4 alleles can increase risk by up to 15-fold.[142, 361] In addition to increased AD risk, the *APOE*-ε4 allele is associated with increased brain amyloid and tau burden,[362] which ultimately leads to neurodegeneration and cognitive impairment.[363, 364] However, many *APOE*-ε4 carriers remain cognitively normal throughout life despite the increased AD risk,[276] suggesting that there may be neuroprotective molecular modifiers of *APOE* effects. For example, mutations within the caspase 7 (*CASP7*) and Klotho (*KL*) genes were suggested to have protective effects (e.g., reduced AD risk, slower cognitive decline) in *APOE*-ε4 carriers in comparison to non-carriers.[365] In the brain, epigenetic modifiers of *APOE*-ε4 have also been observed, such as the recently described

epigenomic factor of activated microglia (EFAM).[366] Indeed, identifying and describing *APOE* modifiers may provide critical insight into the pathophysiology of AD and provide novel targets for therapeutic intervention.

The primary function of the APOE protein is lipid transport and signaling, which plays important roles in the brain, innate immune system, and vascular system.[141, 367] Given the roles of APOE in both the peripheral and central nervous system, whole blood transcriptomics may provide an opportunity to identify novel genes and pathways that contribute to neuroprotection by modifying the effect of *APOE*. Furthermore, blood transcriptomics provide some important advantages over brain transcriptomics alone, particularly when seeking for modifiers of *APOE* effects. While transcriptomic signatures in blood do not perfectly mimic the brain,[368, 369] many of the gene networks and molecular pathways that change over the course of AD are measurable in the blood and provide a window into relevant biological cascades such as inflammation.[370] As one example, peripheral inflammation changes very early in AD and contributes to AD progression,[371, 372] with emerging evidence[373, 374] suggesting that non-CNS inflammation is particularly relevant among *APOE*-ε4 carriers.

Within this chapter, I will summarize how whole blood RNAseq from the Vanderbilt Memory and Aging Project can be used to identify modulators of *APOE* effects on cognition as well as how our findings in whole blood can be used as possible biomarkers for brain changes during the neuropathological progression of AD. After discovery and replication analyses, we aim to put our findings in a deeper biological context by considering our results within the presence of amyloid, tau, and inflammatory biomarkers. Thus, the analyses are as follows:

1. We leverage whole blood RNAseq data from VMAP to identify genes that enhance or diminish the effects of *APOE*-ε4 positivity on cognitive performance. We then extend our analyses

into the brain with bulk RNAseq data to assess whether results in blood show comparable effects within an immediately relevant tissue to AD, such as the brain. Finally, we examine our significant results in the context of AD by performing post-hoc analyses with both CSF and neuropathological measures of amyloid and tau.

2. As the discovery analyses identify *RNASE6*, an innate immunity gene, as a modifier of *APOE*-ε4 effects on cognition within whole blood, we investigate the relationship between *RNASE6* gene expression in whole blood (again, within VMAP) and both CNS and peripheral inflammatory biomarkers to better understand the biological mechanism behind our results.

3.2 MATERIALS AND METHODS

3.2.1 Participants

The Vanderbilt Memory and Aging Project (VMAP) is a longitudinal aging cohort that was established in 2012 to investigate the relationship between vascular health and brain aging. 335 individuals were enrolled; the study preferentially recruited participants with mild cognitive impairment (MCI, N=168) aged 60 and above along with matched counterparts who had normal cognition (N=167). Individuals with cognitive diagnoses other than MCI or normal cognition (NC), history of neurological disease, MRI contraindications, heart failure, major psychiatric illness, or systemic or terminal illness were excluded. At enrollment, participants underwent a comprehensive evaluation including, but not limited to, *APOE* genotyping, neuroimaging, cognitive assessment, blood draw, and optional lumbar puncture.[375]

Independent data for replication were acquired from the Religious Orders Study (ROS) and the Rush Memory and Aging Project (MAP), known as ROS/MAP collectively. The ROS began in 1994 and enrolls priests and nuns from across the United States. The MAP cohort began in 1997

and enrolls lay persons from northeastern Illinois. Both longitudinal aging studies were launched to better understand risk factors for and the neurobiology of cognitive decline and dementia. Both studies were approved by an Institutional Review Board of Rush University Medical Center. All participants were without known dementia at enrollment, agree to comprehensive neuropsychological evaluations, and sign an Anatomic Gift Act and Repository Consent to allow their data to be shared.[376] Additional ROS/MAP data can be requested via the AMP-AD (https://adknowledgeportal.synapse.org/) as well as the Rush Alzheimer's Disease Center Resource Sharing Hub (https://www.radc.rush.edu/).

3.2.2 Neuropsychological Assessment

Composite measures for memory and executive function in VMAP were generated following previously described procedures.[377, 378] Briefly, the memory composite leveraged data from the California Verbal Learning Test (2nd edition) and the Biber Figure Learning Test. The executive function composite score in VMAP was derived from the following tasks: Digit Span from the Wechsler Adult Intelligence Scale (3rd edition), Trail Making Test, Stroop Color Word Inhibition, and Controlled Oral Word Association.

The global cognition variable in ROS/MAP was generated by averaging the Z-scores of 17 neuropsychological tests across five domains of cognition (i.e., episodic, semantic, and working memory, perceptual orientation, and perceptual speed). This composite measurement has been described fully elsewhere.[379]

3.2.3 RNA Extraction, Library Preparation, and Sequencing

Vanderbilt Memory and Aging Project

Blood draws were performed in the morning under fasting conditions. Approximately 2.5 mL of whole blood were kept frozen at -80°C in a PAXgene tube (QIAGEN, 761115) until

processing [375]. RNA extraction, library preparation, and RNA sequencing were performed by the VANTAGE Core (Vanderbilt University, TN, USA). Total RNA was extracted from whole blood using the QIASymphony RNA Kit (QIAGEN, 931636), and both ribosomal RNA and hemoglobin were depleted with the NEBNext Globin and rRNA Depletion Kit (New England BioLabs, Inc., E7750). Library preparation was completed using the NEBNext Ultra Directional Library Prep Kit (New England BioLabs, Inc., E7420) before sequencing was performed using 150 base pair (bp) paired end reads on an Illumina NovaSeq 6000 (Illumina), targeting an average of 50 million reads per sample.

Religious Orders Study and Memory and Aging Project

50 mg of frozen brain tissue were dissected and homogenized in DNA/RNA shield buffer (Zymo Research, R1100). RNA was extracted from the dorsolateral prefrontal cortex (DLPFC), posterior cingulate cortex (PCC), and head of the caudate nucleus (CN) using the Chemagic RNA tissue kit (PerkinElmer, Inc. CMG-1212) on a Chemagic 360 instrument. 500 ng of total RNA was used as input for sequencing library generation and rRNA was depleted with RiboGold (Illumina, 20020599). A Zephyr G3 NGS workstation (PerkinElmer, Inc.) was utilized to generate TruSeq stranded sequencing libraries (Illumina, 20020599). Libraries were normalized for molarity and sequenced using 2 x 150 bp paired end reads on a NovaSeq 6000 (Illumina) targeting a total of 40 to 50 million reads. Additional details are previously described.[380-382] These data are available on the AMP-AD Knowledge Portal (https://www.synapse.org/#!Synapse:syn3219045).

3.2.4 RNAseq Alignment and Quality Control

RNAseq alignment and QC for both VMAP and ROS/MAP samples largely followed a previously reported procedure used by the AMP-AD Consortium.[383] Alignment was performed using STAR (version 2.5.2b) with twopassMode set to basic.[384] Reads were aligned to the Ensembl

(GRCh38, version 99) reference genome,[385] and gene counts were computed using the featureCounts[386] command from the Subread package (version 2.0.0). Summary metrics were calculated using Picard (version 2.18.27, http://broadinstitute.github.io/picard/) to evaluate sample quality and for later use as covariates.[387]

Before QC of the VMAP whole blood RNAseq, samples with RNA integrity number (RIN) less than 3.0 were excluded. In addition, genes with missing gene length or GC-content were removed, after which all gene counts were quantile normalized using the cqn R package (version 1.30.0) to remove technical variability due to gene length and GC-content.[388] At this time, gene expression values greater than three standard deviations from the mean expression for each gene were removed. Additional samples were removed if deemed principal component outliers or if missing RIN, age, sex, other demographic information, or cognition data prior to batch correction. Expression values were adjusted for batch effects using the R package limma (version 3.40.6).[389, 390] This left 60,669 genes and 324 samples in VMAP for discovery analyses.

QC of the bulk brain RNAseq from ROS/MAP followed the aforementioned pipeline. From these data, samples with RIN less than 4.0 or with post-mortem interval (PMI) greater than 24 hours were excluded. Additional samples were removed if missing covariates or cognitive data resulting in a final dataset of 535 samples.

Sensitivity analyses leveraged RNAseq data from VMAP that was additionally adjusted *(*i.e., along with quantile normalization and controlling for batch) for the following covariates using limma: sex, race, *APOE*-ε4 allele count, RIN, age, education, percentage pass-filter reads aligned, and percent coding, intergenic, intronic, and ribosomal bases.

3.2.5 Biomarker Quantification

VMAP Cerebrospinal Fluid Biomarkers

CSF was collected from 155 individuals enrolled in VMAP. A total of 151 individuals remain when samples missing covariates are removed (**Table 3.1**). Additional detail on lumbar puncture and collection is described elsewhere.[375] Beta-amyloid ($A\beta_{1-42}$, Fujirebio, 81583), total tau (Fujirebio, 81579), and tau phosphorylated at threonine 181 (p-tau, Fujirebio 81581) were quantified using commercially available immunoassays. The CSF thresholds for pathologic amyloid and tau positivity are as follows: CSF $A\beta_{1-42}$ less than 530 ng/L[391] and CSF total tau levels greater than 400 ng/L.[392]

Table 3.1: Demographics of participants in VMAP who have CSF data.

	VMAP	VMAP CSF
N	324	151
Age in Years	72.9 (7.3)	72.4 (6.3)
Memory Composite Score	-0.009 (0.97)	-0.012 (0.96)
Executive Function Score	0.002 (0.91)	0.069 (0.86)
% Male	58.0%	66.2%
Education in Years	15.8 (2.7)	16.0 (2.8)
% Normal Cognition	51.8%	52.3%
# *APOE*-ε4 Alleles (0/1/2)	211 / 92 / 21	100 / 37 / 14

Abbreviations: CSF, cerebrospinal fluid

ROS/MAP Brain Neuropathological Measures

Neuropathological outcomes included beta-amyloid (Aβ), phosphorylated tau (p-tau), neuritic plaques, and neurofibrillary tangles (NFT). Aβ and phosphorylated tau were identified via

immunohistochemistry and quantified via image analysis. The overall amyloid level is defined as the mean percent of cortex occupied by Aβ across eight brain regions (hippocampus, angular gyrus, and entorhinal, midfrontal, inferior temporal, calcarine, anterior cingulate, and superior frontal cortices). The overall tangle density is defined as the mean cortical density per mm^2 of the same eight brain regions mentioned above. Neuritic plaque and NFT burden were determined by microscopic examination of silver-stained slides across 5 brain regions (hippocampus and entorhinal, midtemporal, inferior parietal, and midfrontal cortices). These neuropathological measures were previously characterized by ROS/MAP.[376] Consortium to Establish a Registry for Alzheimer's Disease (CERAD) scores were used to determine amyloid positivity such that scores of "moderate" or "frequent" neuritic plaques were categorized as amyloid positive. Tau positivity was determined using Braak staging (Braak ≥ 4).[42, 393, 394]

3.2.6 Statistical Analyses for Analysis 1

All statistical analyses were performed using R (version 3.6.3, https://www.r-project.org/). False-discovery rate[395] was used to correct for multiple comparisons in all analyses, with family-wise α set *a priori* to 0.05. Both baseline and longitudinal memory and executive function scores were used as continuous outcome variables. Linear regression was used to assess the interaction between *APOE*-ε4 positivity (i.e., presence of at least one ε4 allele) and gene expression measured by RNAseq on cross-sectional memory performance. Linear mixed-effects regression tested the *APOE* interaction with gene expression on longitudinal memory, where the intercept and interval from baseline were entered as both fixed and random effects. Covariates in both models included baseline age and sex.

Replication analyses were performed using ROS/MAP samples. Specifically, linear regression models were used to examine the interaction between *APOE*-ε4 positivity and bulk

brain gene expression in the DLPFC, CN, and PCC (**Table 3.2**) on the last global cognition composite score before death. Covariates included post-mortem interval (PMI), sex, and age at death.

3.2.7 Sensitivity Analyses for Analysis 1

Sensitivity analyses included models with more stringent QC for VMAP whole blood RNAseq data (i.e., adjusted for batch, sex, age, RIN, percentage of coding, intronic, and intergenic bases) to determine whether the observed results were due to technical effects. Additional sensitivity analyses included stratifying by cognitive diagnosis and covarying for education because of their effects on cognitive performance.

Table 3.2: Demographics for samples from each brain region in ROS/MAP

	DLPFC	PCC	CN
N	535	322	435
Age at Death in Years	88.5±6.6	88.5±6.3	88.6±6.5
Global Cognition Composite	-0.78±1.04	-0.69±1.02	-0.76±1.1
% Male	36.8	38.5	35.4
Education in Years	16.4±3.5	16.0±2.8	16.3±3.6
% Normal Cognition	34.2	38.5	34.9
# *APOE*-ε4 Alleles (0/1/2)	411 / 118 / 6	255 / 64 / 3	333 / 97 / 5
RNASE6 expression	-0.04±0.85	-0.07±0.75	-0.03±0.74

Values are given as mean ± standard deviation unless otherwise noted. Abbreviations: DLPFC, dorsolateral prefrontal cortex; PCC, posterior cingulate cortex; CN, head of caudate nucleus

3.2.8 Post-hoc Biomarker Analyses

Given the relationship between *APOE* and AD biomarkers, we plan to examine the interaction between amyloid and tau positivity and any significant gene hits on cognition to better

understand the biological mechanisms behind our cognitive results. For these analyses, we leveraged CSF measurements of amyloid and tau in VMAP and neuropathological measurements from ROS/MAP. Covariates for these analyses included age, sex, and PMI where relevant. Using similar regression models, we also investigated whether the gene x *APOE*-ε4 interaction had any effect on baseline CSF amyloid and tau levels, covarying for age and sex.

3.3 ANALYSIS 1: GENE x *APOE*-ε4 INTERACTION RESULTS ON COGNITION

The characteristics of individuals from VMAP (N=324) and those from ROS/MAP who have DLPFC RNAseq (N=535) are presented in **Table 4.3**. Overall, a larger percentage of participants in VMAP are *APOE*-ε4 positive (34.8% versus 23.1%, respectively) and have normal cognition (51.8% versus 34.2%). VMAP participants are also younger than participants from ROS/MAP, on average. In contrast, a higher percentage of participants in ROS/MAP are tau and amyloid positive and they are more highly educated on average. It should be noted that cognition scores cannot be compared across studies because two different cognitive composites are used that are not scaled across studies. The total number of samples from each brain region in ROSMAP can be found in **Table 3.2**.

3.3.1 *RNASE6* Interacts with *APOE*-ε4 on Cognition

Of the 60,669 genes tested, expression of *RNASE6*, ribonuclease A family member K6, interacted with *APOE*-ε4 status on baseline memory in VMAP (β=-1.16, p.fdr=0.003, p.unadjusted= 4.35×10^{-8}) whereby higher *RNASE6* expression in whole blood was associated with worse memory performance at baseline among *APOE*-ε4 carriers (β=-0.96, $p=4.43 \times 10^{-8}$). In contrast, higher levels of *RNASE6* expression were nominally associated with better memory

among *APOE*-ε4 non-carriers (β=0.22, p=0.09, **Figure 3.1A**). We observed similar results for another cognitive domain, executive function (β=-0.54, p=0.008, **Figure 3.1B**). However, we did not observe any significant interactions between whole blood gene expression and *APOE*-ε4 positivity on longitudinal cognition.

Table 3.3: Comparison of participant characteristics between VMAP and ROS/MAP			
	VMAP	ROS/MAP[a]	P
N	324	535	
Age in Years[b]	72.9±7.3	88.5±6.6	$< 1x10^{-5}$
Composite Cognition Score	-0.009±0.97[c]	-0.78±1.04[d]	
% Male	58.0	36.8	$< 1x10^{-5}$
Education in Years	15.8±2.7	16.4±3.5	0.02
% Normal Cognition	51.8	34.2	$< 1x10^{-5}$
	VMAP	ROS/MAP[a]	P
# *APOE*-ε4 Alleles (0/1/2)	211 / 92 / 21	411 / 118 / 6	0.0002
% Amyloid Positive	30.4[e]	60.5	$< 1x10^{-5}$
% Tau Positive	43.0[e]	52.3	0.04

[a]Samples with dorsolateral prefrontal cortex RNAseq; demographics for other brain regions can be found at **Table 3.2**; [b]VMAP: age at baseline, ROSMAP: age at death; [c]Memory composite score at baseline; [d]Global cognition composite score at last visit before death; [e]CSF measurements only available in 151 participants. Values are given as mean ± standard deviation unless otherwise noted. Analysis of variance (ANOVA) analyses were performed to assess differences between the discovery (VMAP) and replication (ROS/MAP) datasets.

The *RNASE6* x *APOE*-ε4 interaction on baseline memory remained significant in sensitivity analyses (see section 3.2 **Materials and Methods**) when leveraging more stringent QC controlling for technical variation in RNA sequencing ($p=2.23x10^{-8}$, **Table 3.4**). The interaction also remained significant when stratifying by diagnosis (i.e., normal cognition or MCI) and covarying for education (p-values<0.00657, **Table 3.4**).

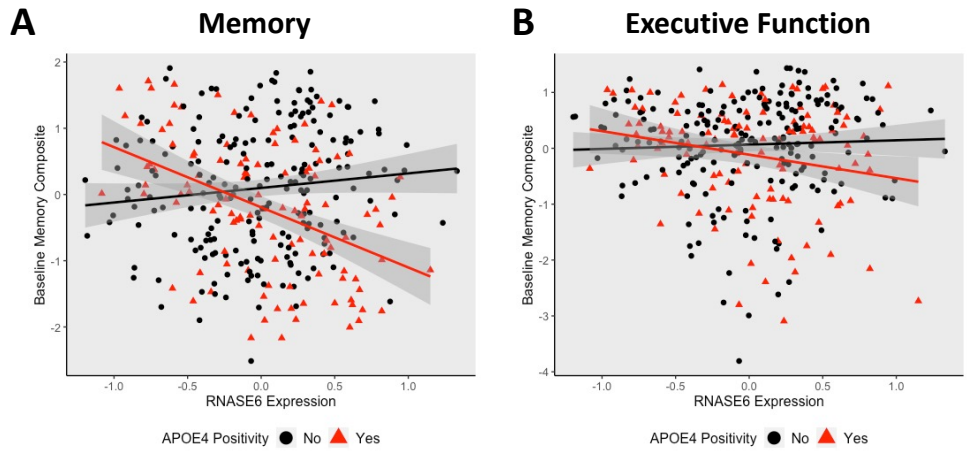

Figure 3.1. *APOE*-ε4 allele carriers in VMAP have worse baseline cognition in the presence of higher levels of *RNASE6* expression. A) A scatterplot demonstrating how *RNASE6* expression modifies the association between *APOE*-ε4 positivity and cognitive performance (β=-1.16, p=4.35x10^{-8}). Baseline composite memory scores are denoted on the y-axis; and the x-axis represents quantile normalized and batch controlled *RNASE6* expression in whole blood. Points and lines are colored by *APOE*-ε4 positivity where *APOE*-ε4 carriers are denoted by the color red. B) Baseline executive function scores are denoted on the y-axis. APOE-ε4 carriers expressing higher levels of *RNASE6* also have worse baseline executive function (β=-0.54, p=0.008).

Table 3.4: Sensitivity analysis results for the *RNASE6* x *APOE*-ε4 interaction on baseline memory

Analysis	N	B	SE	P
Original *RNASE6* x *APOE*-ε4 Interaction	324	-1.164	0.208	4.35x10^{-8}
Using Strict RNAseq QC	324	-1.197	0.209	2.23x10^{-8}
Participants with NC[a]	168	-0.580	0.211	6.57x10^{-3}
Participants with MCI[a]	128	-0.867	0.278	2.30x10^{-3}
Including Education as a Covariate	324	-1.042	0.206	7.47x10^{-7}

[a]Number of participants with normal cognition and MCI sum to 296. Individuals with a diagnosis of AD or "Other" have been removed. Abbreviations: NC = normal cognition, MCI = mild cognitive impairment, B = beta, SE = standard error, P = p-value, QC = quality control.

3.3.2 Replication in ROS/MAP

Leveraging data from an independent cohort, ROS/MAP, we examined the interaction between *RNASE6* expression in brain tissue and *APOE*-ε4 genotype on global cognition at the final

visit prior to death. Using bulk RNAseq data from 3 distinct brain regions: DLPFC, PCC, and head of the CN, we observed replication of the previous interaction on memory (β=-0.35, p=0.002) in the DLPFC (**Figure 3.2**), though the observed effects were not present in the PCC or the CN (p-values>0.3; **Table 3.5**).

Table 3.5: Interaction results of *RNASE6* expression and *APOE*-e4 positivity on global cognition at last visit in ROS/MAP brain regions

Tissue	N	B	SE	P.unadjusted
DLPFC	535	-0.349	0.11	0.002
PCC	322	-0.167	0.18	0.36
CN	435	-0.080	0.17	0.63

Abbreviations: B = beta, SE = standard error, P = p-value, DLPFC = dorsolateral prefrontal cortex, PCC = posterior cingulate cortex, CN = head of the caudate nucleus

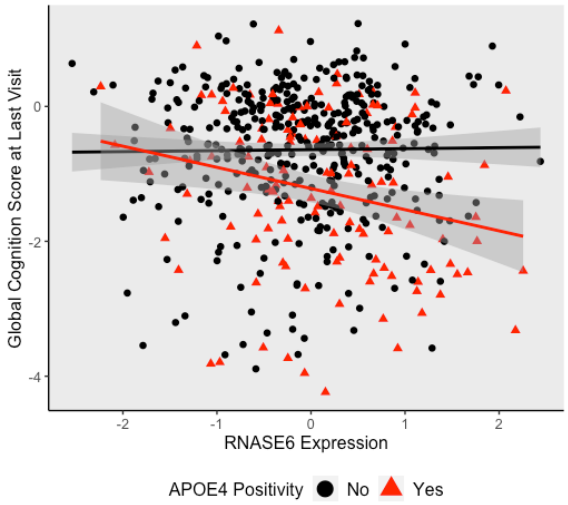

Figure 3.2. *APOE*-ε4 allele carriers in ROS/MAP have worse global cognition in the presence of higher levels of *RNASE6* expression. *RNASE6* expression in the dorsolateral prefrontal cortex is on the x-axis, the last global cognition score before death is on the y-axis. Points and lines are colored by amyloid positivity where amyloid positivity is denoted by the color red. *RNASE6* expression modifies the association between *APOE*-ε4 positivity and global cognition such that higher *RNASE6* expression predicts worse performance at the last visit before death in *APOE*-ε4 carriers (β=-0.35, p=0.002).

3.3.3 Post-Hoc Analyses with Biomarkers

Like our initial findings within VMAP, we observed an interaction with amyloid positivity whereby higher levels of *RNASE6* in blood were associated with worse baseline memory in VMAP (β=-1.14, p=0.001, **Figure 3.3A**). We also observed a similar interaction with tau positivity whereby higher levels of *RNASE6* were associated with worse baseline memory (β=-0.63, p=0.04, **Figure 3.3B**). Neither interaction was significantly associated with baseline executive function (p-values>0.1). We replicated the amyloid interaction effect in ROS/MAP DLPFC leveraging an immunohistochemical measurement of amyloid (β=-0.26, p=0.007, **Figure 3.4**), though the tau interaction did not replicate (p=0.1).

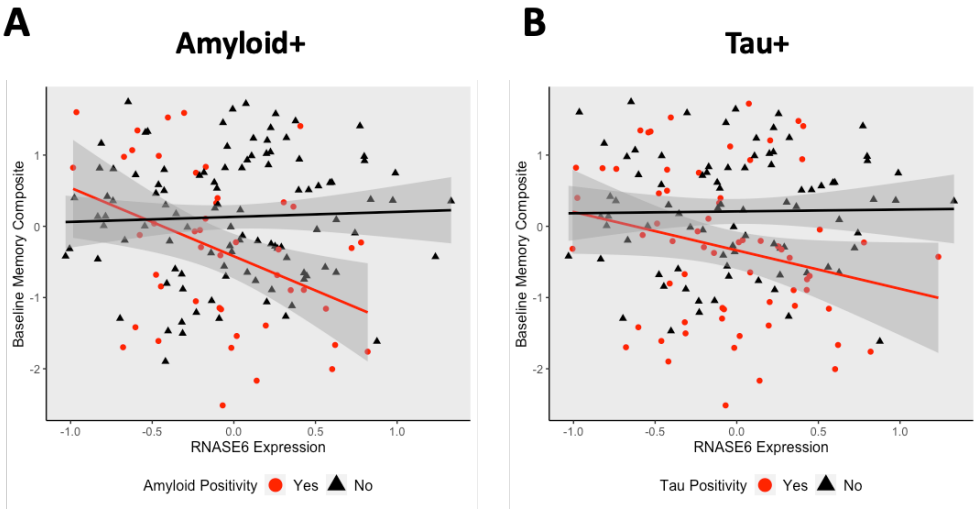

Figure 3.3. Amyloid and tau positivity drives poorer cognitive performance at baseline. A) A scatterplot demonstrating how *RNASE6* expression modifies the association between amyloid positivity and baseline memory. Amyloid-positive individuals expressing higher levels of *RNASE6* have worse baseline memory than individuals who are not amyloid-positive (β=-1.14, p=0.001). Baseline composite memory scores are denoted on the y-axis; and the x-axis represents quantile normalized and batch controlled *RNASE6* expression in whole blood. Points and lines are colored by amyloid positivity where amyloid positivity is denoted by the color red. B) Tau-positive individuals expressing higher levels of *RNASE6* also have worse baseline memory than individuals who are not tau-positive (β=-0.63, p=0.04).

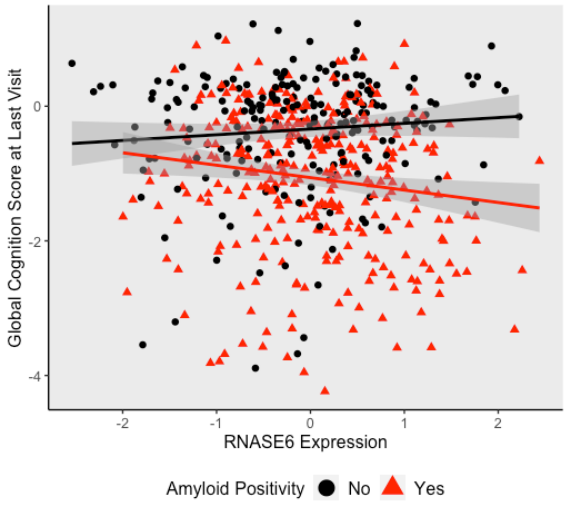

Figure 3.4. Amyloid-positive individuals in ROS/MAP expressing higher levels of *RNASE6* have worse baseline cognition. *RNASE6* expression in the dorsolateral prefrontal cortex is on the x-axis, the last global cognition score before death is on the y-axis. Points and lines are colored by amyloid positivity where amyloid positivity is denoted by the color red. Higher *RNASE6* expression predicts worse performance at the last cognitive visit before death in amyloid-positive individuals (β=-0.26, p=0.007).

We also wanted to examine whether *RNASE6* expression influenced AD biomarker levels in *APOE*-ε4 carriers and non-carriers. The main effect of *RNASE6* was significantly associated with CSF $A\beta_{1\text{-}42}$ (**Figure 3.5A**, β=91.8, p=0.02) such that higher *RNASE6* levels in blood were correlated with reduced brain amyloid burden. However, when examining the *RNASE6* x *APOE*-ε4 positivity interaction, this effect appeared to be in *APOE*-ε4 non-carriers only, though the interaction was non-significant (p=0.1, **Figure 3.5A**). Though *RNASE6* expression alone was not significantly associated with CSF tau or p-tau, it significantly modified the relationship between *APOE*-ε4 and both CSF tau (β=230.1, p=0.003) and CSF p-tau (β=22.7, p=0.01) levels such that *APOE*-ε4 carriers expressing higher levels of *RNASE6* in blood have increased tau pathology at baseline (**Figure 3.5B, C**). None of these effects were observed using neuropathological measures of amyloid and tau in ROS/MAP.

3.3.4 Discussion

In this study, we observed the significant *APOE4*-modifying effect of *RNASE6* expression, in both blood and brain tissues, on cognition. Specifically, *APOE*-ε4 carriers expressing higher levels of *RNASE6* in whole blood had worse baseline memory and executive function performance. We also replicated this novel discovery in an independent sample leveraging transcriptomic data from the dorsolateral prefrontal cortex. In addition, we found that higher *RNASE6* levels are associated with poorer memory performance in individuals that are amyloid-positive and/or tau-positive in comparison to individuals who are biomarker negative (**Figure 3A, B**). *RNASE6* also modifies the effect of *APOE*-ε4 on CSF tau and p-tau levels, such that *APOE*-ε4 carriers expressing higher levels of *RNASE6* have increased CSF tau burden.

RNASE6 is a fascinating, novel inflammatory risk factor for AD. RNASE6 protein exhibits antimicrobial activity.[396] Overexpression of endogenous *RNASE6* in mice is also associated with increased levels of reactive oxygen species as well as increased inflammatory factor secretion.[397] In addition, *RNASE6* levels are increased in individuals with AD across several brain regions including the cerebellum, inferior frontal gyrus, and temporal cortex (AMP-AD Agora; https://agora.adknowledgeportal.org/genes/(genes-router:gene-details/ENSG00000169413). It has been established within the literature that immune function plays a role in cognitive decline,[371, 372, 398] and recent evidence has implicated the importance of neuroinflammation early in the AD cascade[399] and suggests that it drives downstream neurodegeneration. Furthermore, different microglial pathways appear to be involved in the accumulation of amyloid and tau proteinopathies.[400]

As *RNASE6* is relatively understudied and the inflammatory and immunological systems are complex, we looked to alternative data sources to interpret our findings. Using publicly

available gene co-expression networks, we observed that *RNASE6* is in a brain gene co-expression module with several AD genes including *TREM2* and *MS4A6A* (AMP-AD Agora, **Figure 3.6**), which are both highly expressed in microglia.[254, 401] In publicly available microglia data published previously, both *RNASE6* and *TREM2* are upregulated in an AD-associated microglial cluster.[402, 403] Together, these results strongly suggest that *RNASE6* is also expressed within microglia.

RNASE6 was also found to be upregulated in neurofibrillary tangle-bearing neurons suggesting that it may play a role in increasing tau pathology burden.[403] However, we also observe a trend in which higher *RNASE6* expression in *APOE*-ε4 non-carriers correlates to reduced brain amyloid burden (i.e., higher CSF $A\beta_{1-42}$, **Figure 3.5A**). Though we cannot make any formal conclusions without further study, a few hypotheses can be conceptualized from this particular result. The first is that *RNASE6* may play two distinct roles in both the neuroinflammatory-related clearance and deposition of AD neuropathology in *APOE*-ε4 carriers. Alternatively, it may be that neuroinflammation has been occurring longer in individuals carrying *APOE*-ε4 due to earlier amyloid deposition in comparison to non-carriers.[355] It has also been suggested that *APOE*-ε4 expressing microglia are more likely to be pro-inflammatory and have impaired clearance activity in comparison to *APOE*-ε3 expressing microglia, not only suggesting that prolonged inflammation, but also enhanced inflammation may be partially responsible for our results.[404] Finally, our results and others suggest that *RNASE6* expression is involved in the deposition of tau neurofibrillary tangles. Thus, one possible hypothesis, downstream of beta-amyloid, perhaps, would be that increased *RNASE6* expression in *APOE*-ε4 carriers results in an increase of inflammation (via harmful, pro-inflammatory microglia) and tau neurofibrillary tangle burden resulting in worse cognitive performance (**Figure 3.7**).

It should also be noted that our significant results are restricted to cross-sectional cognitive performance. Although we looked at longitudinal outcomes, the *RNASE6* x *APOE*-ε4 interaction on cognitive performance over time is non-significant (p.unadjusted > 0.05) in whole blood and brain tissue. These data suggest that *RNASE6* expression in *APOE*-ε4 carriers may play its role prior to the onset of cognitive decline in contrast to directly modulating cognitive performance over time. However, longitudinal gene expression, cognition, and biomarker data are needed for further examination of *RNASE6* in this context. There is substantial evidence that neuroinflammatory pathways may be particularly relevant among *APOE*-ε4 carriers (reviewed in [373]), and contribute to impaired amyloid clearance,[405] enhanced gliosis,[406] and enhanced brain cytokine levels.[407] *APOE*-ε4 carriers also display prolonged inflammatory responses in comparison to non-carriers.[141] If *RNASE6* expression is indeed a surrogate for an immune response, it can be hypothesized that *APOE*-ε4 carriers have a higher susceptibility to inflammation than non-carriers and that our findings in baseline cognition may be due to prolonged inflammation, and consequently, increased neurofibrillary tangle deposition[29] before any changes to cognition.

As aforementioned, the report discussing EFAM and its impact on *APOE*-ε4[366] provides an interesting convergence of observations from the peripheral and CNS resident immune systems; future work can explore whether these two factors (EFAM and RNASE6) are independently influencing *APOE*-ε4 or may synergize. In addition, future work on *RNASE6* expression in microglia may help clarify the potential mechanistic pathway of the observed effect. It is also notable that another RNASE family gene, *RNASE13* was previously associated with executive function resilience,[408] suggesting that this family of proteins may be exciting targets for future investigation, particularly in response to pathology along an inflammatory pathway.

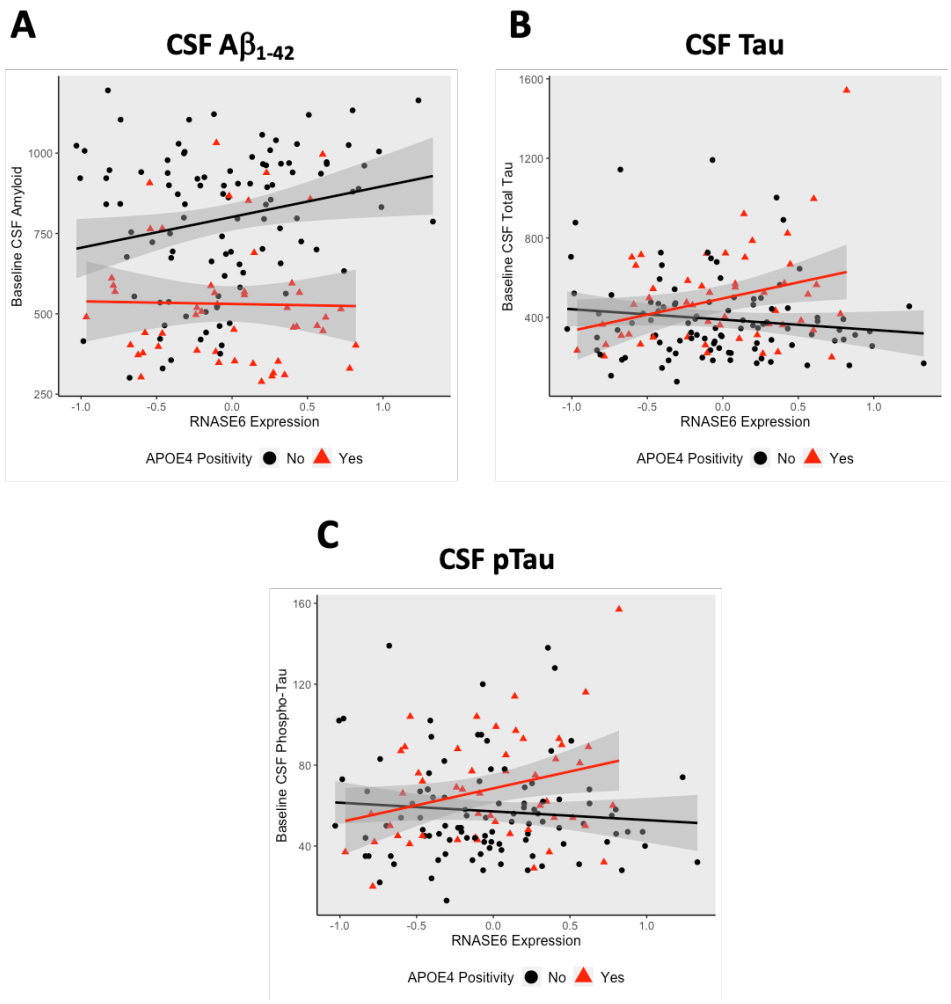

Figure 3.5. CSF biomarker levels are modulated by *RNASE6* expression. A) Brain amyloid burden is reduced in *APOE*-ε4 non-carriers when *RNASE6* expression is high (β= 91.8, p=0.02). Baseline CSF $A\beta_{1\text{-}42}$ levels are denoted on the y-axis and whole blood *RNASE6* expression is on the x-axis. CSF $A\beta_{1\text{-}42}$ levels have an inverse relationship with brain amyloid burden such that higher CSF $A\beta_{1\text{-}42}$ is indicative of lower brain amyloid levels. B) In contrast, CSF tau levels increase as *RNASE6* levels increase in *APOE*-ε4 carriers (β=230.1, p=0.003). C) CSF p-tau levels also increase as *RNASE6* levels increase in *APOE*-ε4 carriers (β=22.7, p=0.01). In all plots, CSF biomarker levels are denoted on the y-axis; and the x-axis represents quantile normalized and batch controlled *RNASE6* expression in whole blood. Points and lines are colored by *APOE*-ε4 positivity where *APOE*-ε4 carriers are denoted by the color red.

3.3.5 Strengths and Limitations

This study has multiple strengths including our multi-modal discovery analyses, independent replication, and the use of comprehensive longitudinal cognitive data from two deeply characterized aging studies. Furthermore, our findings highlight the potential of blood

transcriptomics to identify inflammatory and/or immune factors that have additional effects on the brain. Blood draws are also more accessible to individuals than in comparison to other procedures such as lumbar punctures, making similar analyses using blood transcriptomics increasingly viable in larger or more diverse populations.

However, there are limitations in our study that should be considered. The individuals in our sample are largely non-Hispanic white and highly educated, limiting the generalizability of our results. We also lack functional data to support a specific mechanism of action; it is particularly challenging given that the relationship between peripheral and brain *RNASE6* expression is not well-characterized. Along with these considerations, the gene expression and pathology data used in our analyses are both cross-sectional; we cannot make a conclusion on how *RNASE6* expression may affect AD neuropathology over time nor on how a diagnosis of AD may affect *RNASE6* expression longitudinally. Future work with data from both the periphery and the CNS will be critical to extend these exciting findings.

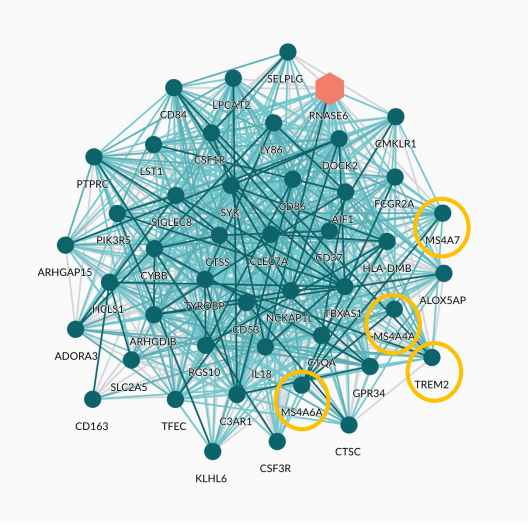

Figure 3.6. *RNASE6* is in a co-expression network module with *TREM2* and *MS4A*. This figure is adapted from Agora (https://agora.ampadportal.org/genes). *RNASE6* is highlighted in orange. Yellow circles denote *TREM2* and genes within the *MS4A* cluster.

3.4 ANALYSIS 2: INVESTIGATING THE RELATIONSHIP BETWEEN *RNASE6* AND OTHER INFLAMMATORY BIOMARKERS

Microglia and astrocytes are the immune cells of the CNS, and they express genes such as: *TREM2*, *MS4A*, and *HLA-DRB1*. Supported by the discovery of variants within these immunity-related genes in large GWAS and GWAS meta-analyses of AD risk,[91-93, 358] neuroinflammation and innate immunity have been implicated in the risk and neuropathological progression of AD.

It has been hypothesized that neuroinflammation is both beneficial and detrimental; in early stages, acute inflammatory events can help clear the CNS of pathology such as amyloid. However, chronic inflammation when pro- and anti-inflammatory signaling has been disrupted by an insurmountable burden of pathology, for example, has been associated with cognitive impairment and increased AD risk.[240]

Neuroinflammation was also thought to be a response to AD pathology and neurodegeneration within the CNS, but it has since been suggested that neuroinflammation can also precede, facilitate, and worsen the neuropathological progression of AD. For example, a recent study by Park and Barrett demonstrate in mice that gliosis may occur prior to amyloid and tau deposition.[409] Recent studies have also implicated peripheral inflammation in AD,[372, 410, 411] such that systemic inflammation has been associated with increased AD risk[372] as well as cognitive decline in late life.[410]

To better understand how *RNASE6* relates to both peripheral inflammation and neuroinflammation, we wanted to examine its relationship to neuroinflammatory CSF biomarkers soluble TREM2 (sTREM2, triggering receptor expressed on myeloid cells 2) and YKL-40 (chitinase-3-like 1) as well as plasma peripheral inflammatory biomarkers tumor necrosis factor

alpha (TNF-α), C-reactive protein (CRP), and interleukin-6 (IL-6). These preliminary analyses leveraged data using the same VMAP samples summarized in **Table 3.1**. Mean and standard deviation of inflammatory biomarkers have been included in **Table 3.5**.

Regarding neuroinflammation, TREM2 is of particular interest because variants identified within the *TREM2* gene have been associated with increased risk of AD. One such example is the R74H variant of *TREM2* that increases AD risk by approximately three-fold.[412] Furthermore, *RNASE6* is in the same gene co-expression module as *TREM2*.

TREM2 modulates inflammatory signaling and is involved in numerous microglial functions including the recruitment of microglia to amyloid plaques. sTREM2 is produced by the proteolytic cleavage or alternative splicing of TREM2. CSF levels of sTREM2 can be used as a proxy of microglial activity[413, 414] and is increased in individuals with AD as well as in individuals with inflammatory conditions such as multiple sclerosis (reviewed in Zhong et al.,).[412] Higher levels of sTREM2 have also been associated with increased tau pathology[413, 415] and protection from amyloid accumulation[416] and cognitive decline.[417] It should be noted, however, that sTREM2 levels are dynamic and AD stage-dependent,[414, 415] and its function in AD is not well-characterized making it difficult to interpret whether it is truly protective or not. CSF YKL-40 is primarily expressed by astrocytes and has been described as a probable fluid biomarker of preclinical AD.[418]

Meanwhile, plasma CRP, IL-6, and TNF-α are indicative of systemic inflammation.[419-422] CRP is a non-specific marker of inflammation, and is elevated in individuals with AD.[423] Similarly, IL-6 and TNF-α are pro-inflammatory cytokines that show evidence of being elevated in individuals with AD.[422]

3.4.1 CSF and Plasma Biomarker Inflammatory Quantification

CSF sTREM2 was quantified on site with a non-commercially available enzyme-linked immunoassay (ELISA). CSF YKL-40 was quantified using the Human Chitinase 3-like 1 Quantikine ELISA Kit (R&D Systems, Inc, Minneapolis, MN). Plasma CRP, TNFα, and IL-6 were quantified via immunoassay. Additional details on plasma and CSF collection can be found in section **3.3 Materials and Methods**.

3.4.2 Statistical Analyses

All statistical analyses were performed using R (version 3.6.3, https://www.r-project.org/). Outliers with any biomarker levels greater than 5 standard deviations above the mean were removed prior to analysis. Linear regression was used to assess the interaction between *APOE*-ε4 positivity (i.e., presence of at least one ε4 allele) and *RNASE6* expression in whole blood on baseline CSF and plasma inflammatory biomarker levels (i.e., CSF sTREM2 and YKL-40, plasma IL-6, CRP, and TNF-α). Covariates included age and sex. We also used linear models to examine the association between the aforementioned biomarkers and baseline cognition (i.e., memory and executive function) covarying for age and sex.

3.4.3 Summary of Preliminary Results

RNASE6 expression was significantly associated with baseline CSF sTREM2 levels such that higher levels of *RNASE6* resulted in lower baseline levels of CSF sTREM2 (**Table 3.6**). The *RNASE6* x *APOE*-ε4 interaction was also significant such that higher levels of *RNASE6* levels were associated with increased baseline levels of CSF sTREM2 in *APOE*-ε4 carriers (**Table 3.6**, **Figure 3.7**). In addition, *RNASE6* expression was associated with baseline levels of plasma CRP such that higher levels of *RNASE6* resulted in lower levels of plasma CRP (**Figure 3.8A**). In

contrast, *RNASE6* expression was not significantly associated with baseline CSF YKL-40 levels or baseline plasma IL-6, or TNF-α levels. Similarly, *RNASE6* expression did not significantly interact with *APOE*-ε4 positivity on the aforementioned biomarkers (**Table 3.6**, **Figure 3.8B, C, D**).

Table 3.6: Summary of inflammatory biomarkers in VMAP

	VMAP	VMAP CSF
N	321	151
Age in Years	72.8±7.3	72.4±6.3
Memory Composite Score	-0.011±0.97	-0.012±0.96
Executive Function Score	0.003±0.91	0.069±0.86
% Male	57.6%	66.2%
Education in Years	15.8±2.7	16.0±2.8
% Normal Cognition	51.7%	52.3%
# *APOE*-ε4 Alleles (0/1/2)	209 / 91 / 21	100 / 37 / 14
CSF sTREM2	*N/A*	3648.5±1809.9
CSF YKL-40	*N/A*	193519.0±64443.8
Plasma CRP	2.4±3.2	*N/A*
Plasma IL-6	3.6±2.7	*N/A*
Plasma TNF-α	6.1±2.5	*N/A*

Table 3.7: *RNASE6* main effect and *RNASE6* interaction results with inflammatory biomarkers				
Predictor	Outcome	B	SE	P
***RNASE6* Main Effect**	**CSF sTREM2**	**-668.67**	**333.76**	**0.047**
***RNASE6* x *APOE*-ε4 Positivity**	**CSF sTREM2**	**1362.23**	**615.02**	**0.028**
RNASE6 Main Effect	CSF YKL-40	-20301.0	11980.5	0.092
RNASE6 x *APOE*-ε4 Positivity	CSF YKL-40	40187.3	22076.9	0.071
RNASE6 Main Effect	Plasma IL-6	0.037	0.38	0.92
RNASE6 x *APOE*-ε4 Positivity	Plasma IL-6	0.45	0.64	0.49
***RNASE6* Main Effect**	**Plasma CRP**	**-0.93**	**0.45**	**0.04**
RNASE6 x *APOE*-ε4 Positivity	Plasma CRP	0.77	0.75	0.31
RNASE6 Main Effect	Plasma TNF-α	-0.44	0.35	0.21
RNASE6 x *APOE*-ε4 Positivity	Plasma TNF-α	0.02	0.58	0.97

Abbrevations: B, beta; SE, standard error; P, p-value

3.4.4 Discussion and Future Directions

In these preliminary analyses, *RNASE6* expression in whole blood was associated with baseline CSF sTREM2 levels such that higher *RNASE6* levels are predictive of lower baseline CSF sTREM2 (**Figure 3.7A**). *RNASE6* expression also interacted with *APOE*-ε4 positivity on CSF sTREM such that higher levels of *RNASE6* predict higher CSF sTREM2 levels in *APOE*-ε4 carriers (**Figure 3.7B**). TREM2 is primarily expressed by microglia,[424] thus suggesting that a deeper relationship may exist between *RNASE6* function and microglial activity. This relationship is further supported by the co-expression of *RNASE6* and *TREM2* in network modules (**Figure 3.6**).

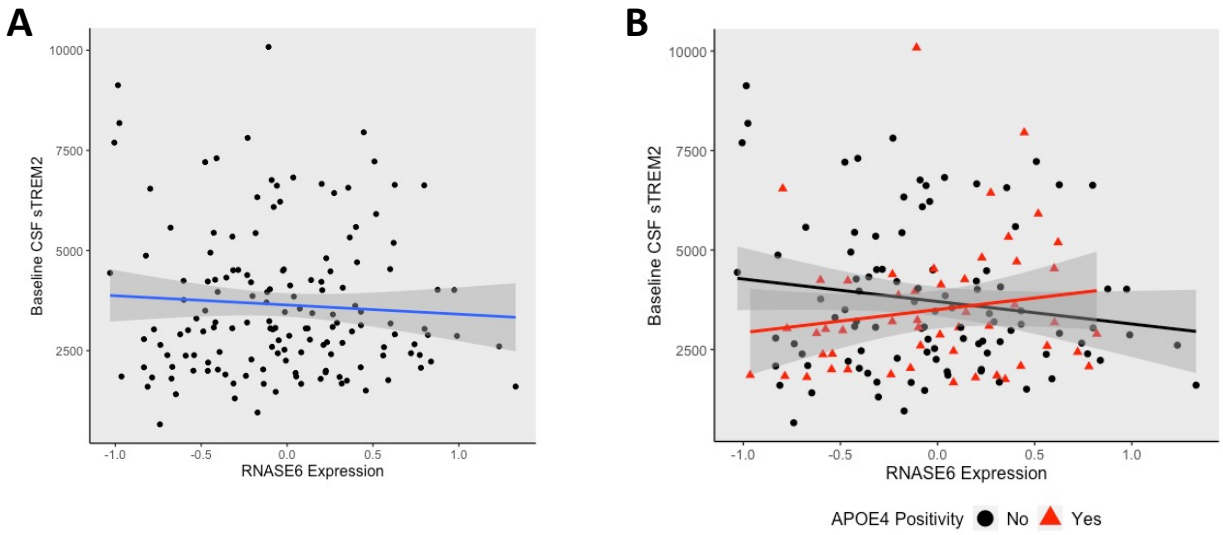

Figure 3.7. *RNASE6* expression modifies baseline CSF sTREM2 levels. A) Baseline CSF sTREM2 levels are reduced when *RNASE6* expression in whole blood is high (β=-668.7, p=0.047). Baseline sTREM2 levels are denoted on the y-axis and whole blood *RNASE6* expression is on the x-axis. B) In contrast, baseline CSF sTREM2 levels are higher when *RNASE6* expression is high in *APOE*-ε4 carriers (β=1362.2, p=0.028). Points and lines are colored by *APOE*-ε4 positivity where *APOE*-ε4 carriers are denoted by the color red.

CSF sTREM in our sample is not significantly associated with baseline memory performance or executive function ($p > 0.2$), though studies have suggested that increased CSF sTREM2 levels are both protective against cognitive decline.[416, 417, 425] It should be noted that our current available data is restricted to cross-sectional measurements, though CSF sTREM2 levels are dynamic over the course of disease limiting our ability to interpret our findings.

RNASE6 expression was inversely associated with plasma CRP such that higher levels of *RNASE6* predict lower levels of CRP (β=0.93, p=0.04, **Figure 3.8A**). Baseline CRP in our analyses was not associated with baseline memory or executive function ($p > 0.6$). As aforementioned, CRP is often considered a marker of systemic inflammation,[426] and increased levels of plasma CRP have been associated with poor cognitive function.[427] In contrast, plasma CRP is decreased in

individuals with AD and in *APOE*-ε4 carriers.[428, 429] *RNASE6* is upregulated following infection[430] and for host defense,[431] so our results are somewhat counterintuitive.

CSF YKL-40, plasma IL-6, and TNF-α (**Figure 3.8B, C, D**) were not significantly associated with *RNASE6,* nor is the *RNASE6* x *APOE*-ε4 interaction significant on YKL-40, IL-6, or TNF-α. Additionally, plasma TNF-α is not significantly associated with baseline measurements of cognition in our sample. Baseline levels of IL-6, however, are significantly associated with baseline memory (β=-0.06, p=0.004) and baseline executive function (β=-0.04, p=0.01), which supports previous studies.[432, 433]

3.5 CHAPTER CONCLUSION AND FUTURE DIRECTIONS

To conclude, our results suggest that *RNASE6* modifies the association between *APOE*-ε4 positivity and cross-sectional measures of cognition. *RNASE6*, also known as ribonuclease A family member K6, is an innate immunity gene that has been implicated in antimicrobial activity[396] and pro-inflammatory factor secretion.[397] Most excitingly, *RNASE6* is in a gene co-expression network module with microglial genes *TREM2* and *MS4A* that have been previously identified as AD risk loci. In addition, we found that *RNASE6* expression levels are correlated with CSF sTREM2 levels among *APOE*-ε4 carriers supporting the notion that *RNASE6* is expressed in microglia and that there may be a biological interaction between RNASE6 and TREM2.

Gene co-expression analyses also suggest that *RNASE6* may be involved in tau neurofibrillary tangle deposition,[403] and studies examining CSF sTREM2 have also shown that it positively correlates with CSF total tau and p-tau levels.[434, 435] Altogether, these data suggest that

RNASE6 and TREM2 may exist in the same biological pathways resulting in increased neurofibrillary tangle burden and subsequently, neurodegeneration and cognitive decline.

In addition to supporting previous analyses implicating innate immunity in cognitive decline, our results suggest that data from whole blood transcriptomics can provide information about AD-relevant biological changes that may be occurring in the brain and provide a proof-of-concept for how a similar analyses can be leveraged to identify blood-based biomarkers. We also demonstrate that network-level analyses can be useful to help interpret gene-level results in a larger biological context when literature is unavailable.

As aforementioned, additional longitudinal studies examining *RNASE6* function within the CNS and blood are necessary to understand how it is causing worse baseline cognitive performance. In addition, animal studies may be of potential benefit to elucidate the relationship between *RNASE6*, microglia, and peripheral inflammation and their roles in Alzheimer's risk and neuropathogenesis.

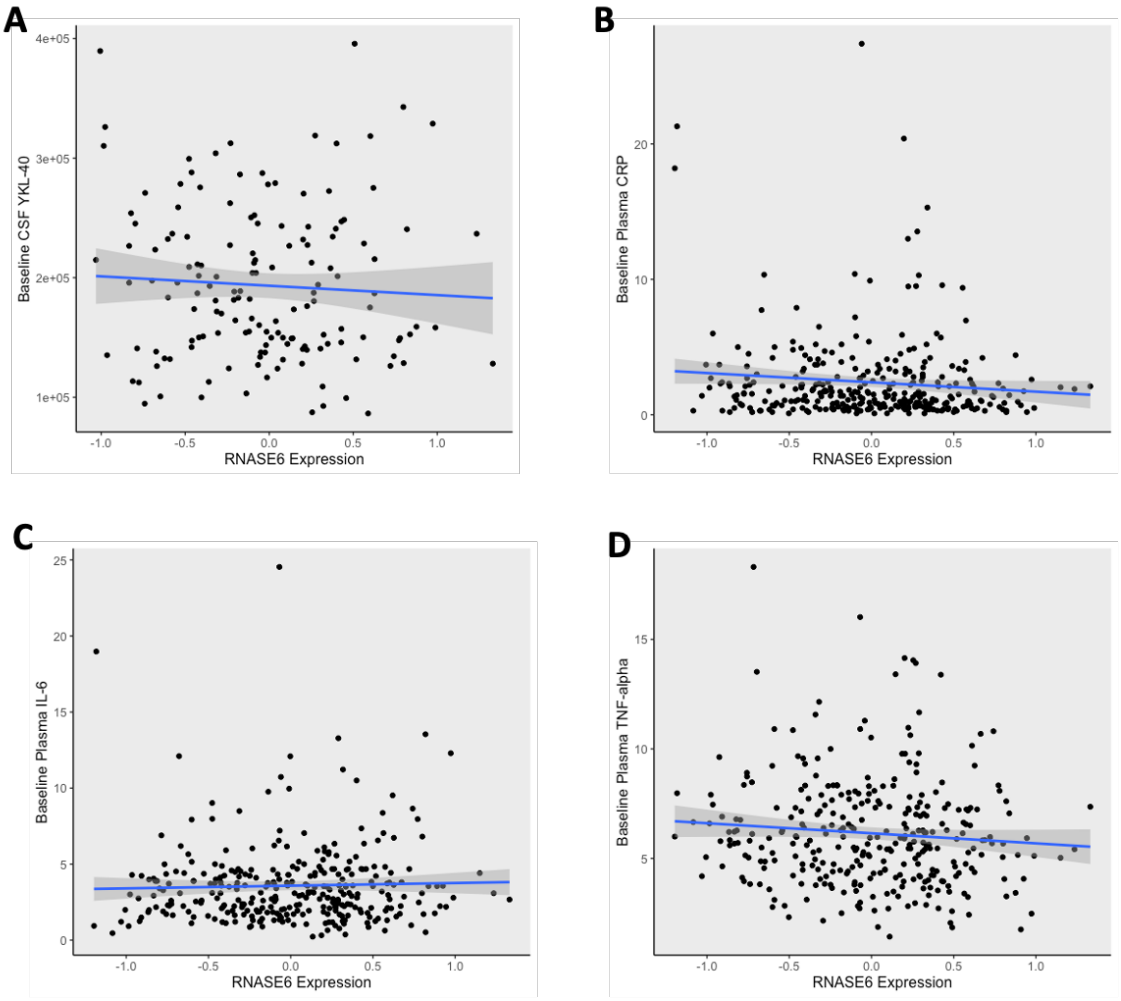

Figure 3.8. *RNASE6* expression is associated with baseline plasma CRP levels, but not other inflammatory biomarkers. Baseline biomarker levels are denoted on the y-axis and whole blood *RNASE6* expression is on the x-axis. A) Scatterplot between whole blood *RNASE6* expression and baseline CSF YKL-40. B) Scatterplot between *RNASE6* expression and baseline plasma CRP. Baseline levels of CRP are lower when *RNASE6* expression is high (β=0.93, p=0.04). C) Scatterplot between *RNASE6* expression and baseline plasma IL-6. D) Scatterplot between *RNASE6* expression and baseline plasma TNF-α.

CHAPTER 4

LEVERAGING WEIGHTED GENE CO-EXPRESSION NETWORK ANALYSIS (WGCNA) AS A TOOL FOR AD DRUG DISCOVERY

Supplemental information, full funding details and acknowledgements for this chapter can be found in **Appendix D.**

4.1 INTRODUCTION

Alzheimer's disease (AD) is a complex neurodegenerative disorder that is heterogeneous in presentation. While familial cases of Alzheimer's disease are often driven by autosomal dominant mutations in genes such as *APP*, *PSEN1*, and *PSEN2*,[436] sporadic forms of AD can be considered polygenic.[14-17] AD is 60 to 80% heritable,[90, 437, 438] and over 40 risk loci for AD have been identified in large scale GWAS and meta-analyses.[91-93, 358] Many of the recently identified loci are common variants with low effect size perhaps suggesting that numerous genes are working in concert along with lifestyle factors to affect an individual's overall sporadic AD risk.

Historically, AD and AD drug discovery research has utilized a candidate gene approach, which probes a set of genes determined *a priori* that potentially contribute to AD risk or the AD endophenotype of interest.[85, 86] Though familial and candidate gene studies of *APP, PSEN1,* and *PSEN2* as well as studies supporting the amyloid cascade hypothesis[53, 54] strongly directed AD drug discovery efforts to amyloid, amyloid-focused therapeutics have largely failed in clinical trials.[63-65, 67, 87]

More recently, the availability of large "-omics" datasets have allowed for a different perspective on AD drug discovery focusing on phenotype first to identify genes and variants of

interest (e.g., reverse genetic approaches, genome- or exome-wide association studies), which has helped to diversify drug targets.[64] In addition, the boon of "-omics" data permits systems biology-based approaches that can help to probe the etiology behind a multifactorial disease such as AD.[89]

Though approaches such as genome-wide association studies have identified numerous novel risk loci for AD,[91-93, 212, 358] linking genetic discovery to biological mechanisms remains a major challenge of the field. Identified variants can be in non-coding or intergenic regions making it difficult to assign risk variants to specific genes or functions. However, network biology methods along with others (e.g., eQTL studies, transcriptomic data) have emerged to help elucidate the functions of genetic loci.[277, 381, 439-441]

Chapter 4 focuses on using a network-based approach called WGCNA (weighted gene co-expression network analysis)[439, 442] for the identification of novel mechanisms and genetic factors that are associated with hallmarks of AD (e.g., amyloid, tau, cognitive decline). Leveraging WGCNA, we will link biological function to genetic discovery in our analyses, providing insight into the etiology of AD. Furthermore, we believe that this approach has utility for AD drug discovery. Identifying targets within the context of a network will increase the chance of finding "druggable" targets due to the highly connected nature of the modules such that a "non-druggable" protein may function alongside one that is "druggable."[443] This chapter will summarize 3 different analyses using WGCNA as well as the data described in section **4.2 Materials and Methods.** <u>The analyses are as follows:</u>

1. To validate WGCNA as a viable and robust research tool for our group, we first examined the associations between pre-defined gene co-expression network modules[277] generated from dorsolateral prefrontal cortex (DLPFC) RNA sequencing (RNAseq) from the Religious Orders Study and Memory and Aging Project (ROS/MAP) and AD endophenotypes such as

amyloid and tau burden at autopsy, cross-sectional global cognition, and annual change in cognition.

2. Next, we evaluate whether predicted gene expression values calculated via PrediXcan[444] are suitable for gene network replication and/or network building.

3. Finally, we use the same RNAseq data and pre-defined network in **Analysis 1** (above) to examine whether any co-expression modules interact with *APOE*-ε4 positivity on amyloid and tau burden at autopsy, cross-sectional global cognition, and annual change in cognition.

4.1.1 Introduction to Weighted Gene Co-Expression Network Analysis

Weighted gene co-expression network analysis (WGCNA) is just one approach by which genes can be linked to function. In WGCNA, networks are generated from gene expression data, and the overall structure of the network is determined by the strength of pairwise correlations between genes. After network generation, hierarchical clustering is used to identify biologically relevant modules, which are small groups of highly connected genes that may be functioning together.[439] The biological function of those modules can then be identified via GO-term analysis or via hub gene analysis, in which the most highly connected gene in the module becomes a surrogate for the modules' overall function.[439]

4.1.2 Introduction to Predicted Gene Expression (PrediXcan)

Gene expression can be altered by a variety of factors such as genetics, environment, and disease traits.[444] In brief, the PrediXcan technique leverages reference transcriptomes from studies such as the NIH Genotype-Tissues Expression (GTEx) project[445] to train machine learning models that can estimate the genetic contribution to gene expression. Additional details on the PrediXcan method can be found elsewhere.[444]

4.2 MATERIALS AND METHODS

4.2.1 Participants

Data were acquired from the Religious Orders Study (ROS) and the Rush Memory and Aging Project (MAP), known as ROS/MAP collectively. The ROS began in 1994 and enrolls priests and nuns from across the United States. The MAP cohort began in 1997 and enrolls lay persons from northeastern Illinois. Both longitudinal aging studies were launched to better understand risk factors of cognitive decline and AD. All participants are cognitively normal at enrollment, undergo comprehensive neuropsychological evaluations, and consent to organ donation at death. Genotypes and RNAseq data are also available for a subset of individuals. We are leveraging neuropathological data *(*i.e., brain amyloid plaques and tau neurofibrillary tangles) as well as bulk RNAseq from the DLPFC for our analyses.[381, 446]

4.2.2 Cognitive Measures

The global cognition variable was generated by averaging the Z-scores of 17 different neuropsychological tests across five domains of cognition (i.e., episodic, semantic, and working memory, perceptual orientation, and perceptual speed). This composite measurement has been previously calculated in ROS/MAP by our group and others.[379, 447] Cognitive decline, or annual change in global cognition was determined for each individual using linear-mixed effects regression, where the fixed effect is time, and the random effect is the time interval from the last visit for each participant.

4.2.3 Neuropathology

Neuropathological outcomes included beta-amyloid (Aβ), phosphorylated tau, neuritic plaques, and neurofibrillary tangles (NFT), which were previously characterized by ROS/MAP.[446] Aβ and phosphorylated tau were identified via immunohistochemistry (IHC) and quantified via image analysis. The overall amyloid level is defined as the mean percent of cortex occupied by Aβ across eight brain regions (hippocampus, angular gyrus, and entorhinal, midfrontal, inferior temporal, calcarine, anterior cingulate, and superior frontal cortices). The overall tangle density is defined as the mean cortical density per mm^2 of the same eight brain regions mentioned above. Neuritic plaque and NFT burden were determined by microscopic examination of silver-stained slides across 5 brain regions (hippocampus and entorhinal, midtemporal, inferior parietal, and midfrontal cortices). Only amyloid and tangle density are used in analyses.

4.2.4 RNA sequencing and Processing

RNA extraction from the DLPFC, library preparation, and sequencing were completed by ROS/MAP; additional details are described elsewhere.[380] Initial data processing and quality control (QC) was performed following the procedure in Logsdon et al. 2019.[277] QC is also summarized on the AMP-AD Knowledge Portal (https://www.synapse.org/#!Synapse:syn8456629). Alignment was performed with STAR using the GENCODE24 (GRCh38) reference genome and twopassMode set to Basic. Gene counts were also computed for each sample using STAR by using the GeneCounts option of the quantMode function.[384] Summary metrics were calculated using Picard (http://broadinstitute.github.io/picard/) to evaluate sample quality and to identify covariates.

Gene and sample quality control and normalization were performed as follows: genes expressing less than 1 count per million (CPM) in over 50% of samples in each diagnosis category

(AD, Control, Other) as well as genes missing gene length data and GC content were excluded. Conditional quantile normalization, with the R package cqn,[388] was performed to remove additional technical variability due to gene length and GC content. After quantile normalization, gene expression values that are greater than 3 standard deviations away from the mean expression were excluded. Sample outliers were excluded based on principal component (PC) analysis. Samples were also excluded if they were missing technical or clinical data (i.e., RNA integrity number (RIN), age, sex, etc.). After these filters, 15,582 genes in 631 samples remained.

Expression values were further normalized by adjusting for batch, sex, age of death, post-mortem interval, RIN, and the percentage of coding, intronic, and intergenic bases in an iterative manner in which expression values are adjusted for a covariate before it is included as a fixed effect in a linear model. Observation weights for covariates are calculated by the R package limma[390] and the function voom.[389]

4.2.5 Gene Co-expression Network Analysis

We built gene co-expression network modules from DLPFC bulk RNAseq based on previously reported module definitions in Logsdon et al.,[277] Module definitions from the publication are available on the AMP-AD Knowledge Portal (https://www.synapse.org/#!Synapse:syn2580853). The modules were generated using the R package, WGCNA.[439] A total of 19 modules were defined, with a minimum module size of 100 genes. Additional details on replication of the published gene network be found in **Appendix D.**

4.2.6 Tissue-Specific Predicted Gene Expression (PrediXcan)

Protocols for DNA collection, processing, and genotyping have been previously reported by ROS/MAP.[380] Genotyping was performed by ROS/MAP in four phases, and each dataset underwent the same QC and imputation processes individually prior to merging. All QC was

performed using PLINK (version 1.9b_5.2) software.[290] All genotyping data were limited to individuals of European decent. SNPs with genotyping efficiency <95%, minor allele frequency <1%, or deviation from Hardy-Weinberg equilibrium ($p<1x10^{-6}$) were excluded prior to imputation. Participants whose call rate was <99%, who had a reported versus genetic sex inconsistency, or who exhibited relatedness to another sample (PI_HAT > 0.25) were excluded in addition to individuals whose ancestral PCs were outliers when calculated with EIGENSOFT version 7.2.1.[291]

Imputation was performed on the Michigan Imputation Server using the HRC r1.1.2016 reference panel (build 37, assembly 19) and SHAPEIT phasing.[292] After imputation, genotype data were further filtered for imputation quality ($R^2>0.9$). Multiallelic and duplicate SNPs were removed prior to SNP filtering using the same thresholds as aforementioned, after which all genotyping datasets were merged. Non-overlapping SNPs and PC outliers were removed, resulting in a final dataset containing 2192 samples and 5,187,865 variants.

Tissue-specific predicted gene expression profiles were quantified using the PrediXcan method.[444] Briefly, models were built using elastic net regression to impute tissue-specific gene expression profiles from genotype data. To predict expression in ROS/MAP, we used expression models generated from the transcriptome data of CommonMind Consortium, which includes DLPFC RNAseq for 980 individuals from multiple sites including the Mount Sinai Brain Bank, University of Pennsylvania Brain Bank, University of Pittsburgh Brain Bank, and the National Institutes of Mental Health Brain Collection Core.[448] Prediction models and source code for the PrediXcan method are freely available online (https://github.com/hakyimlab/PrediXcan, http://predictdb.org/).

Prior to analyses, genes whose expression was predicted with an $R^2 < 0.8$, had 0 variance, had greater than 90% values of 0, or were outliers greater or less than 5 standard deviations of the mean were removed from the dataset. In addition, individuals missing covariates or outcomes of interest as well as individuals who were also present in our DLPFC RNAseq sample were removed from the predicted expression sample leaving a total of 760 participants and 7,245 genes (**Table 4.1**).

4.2.7 Functional Annotation

For module associations that replicated when using predicted gene expression values, hub gene analyses were performed with WGCNA (version 1.68) to better understand the biological function of the module. The network structure and hub genes were estimated using the following parameters: power=13, networkType = signed, corFnc = "cor" (parameter for Pearson correlation). Additionally, gene set enrichment was performed with the R package gprofiler2 (version 0.2.1)[449] with default parameters. GO: Biological Process (GO:BP, biomaRt releases/2021-12-15)[450] was used as the annotation source.

4.2.8 Note on Statistical Analyses

Each analysis will have its own section summarizing the statistical analyses specific to that analysis

4.3 ANALYSIS 1: LOGSDON ET AL., 2019[277] MODULE ASSOCIATIONS WITH HALLMARKS OF AD

4.3.1 Statistical Analyses

All statistical analyses were performed in R (version 3.6.1, https://www.r-project.org/). Prior to calculating the module eigengenes (i.e., the first principal component), any missing gene expression values were imputed using k-nearest-neighbors (kNN) imputation via the R package, impute (version 1.58.0).[451] The number of neighbors used for imputation was 10. Module eigengenes were scaled and zero-centered. Using the eigengenes from 19 reported AD co-expression modules,[277] we performed linear regression analyses assessing the association between the eigengenes and cross-sectional global cognition at the last visit before death, cognitive decline, and immunohistochemical measurements of amyloid and tau. Covariates included age of death, sex, education, and post-mortem interval. Correction for the number of modules was completed using Bonferroni correction ($p < 0.003$).

Our replication analyses leveraged predicted gene expression values in ROS/MAP generated using the PrediXcan method in the ROS/MAP cohort. Again, missing gene expression values were imputed using kNN and module eigengenes were scaled and centered. Using the previous module definitions described above, we performed linear regression analyses assessing the association between the eigengene of these modules and the aforementioned hallmarks of AD (i.e., cognitive decline, AD neuropathology) covarying for age of death, sex, education, and post-mortem interval.

4.3.2 Participant Demographics

Participant characteristics are presented in **Table 4.1.** Overall, participants in the discovery dataset were younger, had a shorter post-mortem interval, and had less neuropathology on average than participants in the replication dataset. It should also be noted that there are fewer genes available when using predicted expression values, as poorly predicted genes were removed prior to analyses.

4.3.3 Module association with AD hallmarks

Using bulk RNAseq data of the dorsolateral prefrontal cortex from ROS/MAP (n=625), We also identified 18 new associations with amyloid, tau, baseline global cognition, and annual change in global cognition across 10 unique modules using the module definitions reported by Logsdon et al., (**Table 4.2, Figure 4.2**). It should be noted that the module assignment colors are largely arbitrary and assigned by WGCNA, except for the "grey" module. The grey module contains genes that were not assigned to any other module; it contains genes that are not "co-expressed."

4.3.4 Predicted gene expression module association with AD hallmarks

Using genotype data from ROS/MAP, we calculated predicted expression using the PrediXcan method along with the reference transcriptome from the CommonMind Consortium.[448] Leveraging the previously published module definitions, we were able to replicate the "grey60" module association with cognitive decline (β=0.002, 1.21×10^{-5}) and IHC tau burden (β=-0.11, $p=2.54 \times 10^{-4}$) at autopsy (**Figure 4.2**). When using the module eigengene value as a proxy for all gene expression within a module, higher gene expression in the grey60 module predicts less brain tau burden and slower cognitive decline when using bulk DLPFC RNAseq data and predicted gene

expression values (**Figure 4.3**). No novel associations were identified when using predicted expression data.

Table 4.1: Summary of participant demographics for WGCNA analyses		
	Discovery	**Replication**
	ROS/MAP DLPFC RNAseq	ROS/MAP Predicted Expression
N	625	760
%Female	64%	69%
Age at death, years	**88.7±6.6**	**90.2±6.3**
Education, years	16.4±3.6	16.2±3.6
PMI, hours	**7.35±4.8**	**10.5±9.6**
Amyloid[a]	1.66±1.2	1.70±1.1
Neuritic plaques[b]	**0.70±0.5**	**0.79±0.5**
Tangles[a]	**2.15±1.3**	**2.43±1.5**
Neurofibrillary tangles[b]	**0.66±0.4**	**0.72±0.4**
Cognitive decline[c]	-0.12±0.1	-0.12±0.1
Genes Passing QC	15,882	7,245

Analysis of variance (ANOVA) analyses were used to identify significantly different characteristics between groups. Boldfaced values represent variables that are significantly different ($p<0.001$) between groups. Values given are mean ± standard deviation unless otherwise noted. [a]Pathology was quantified via immunohistochemistry. [b] Plaques and tangles were quantified via silver staining. [c]Cognitive decline was calculated via linear mixed-effects regression models where the fixed effect was time, and random effects were time between visits for each participant. Abbreviations: DLPFC, dorsolateral pre-frontal cortex; PMI, post-mortem interval, QC=quality control

4.3.5 Grey60 module hub gene and GO-term analysis

As grey60 was the only module that replicated using both observed and predicted expression, we performed both hub gene and GO-term analysis for the module. A "hub gene" describes a gene with high connectivity within the module. The most intra-connected gene for the grey60 module is *PAPOLA* (**Figure 4.4**), poly(A) polymerase alpha and the most significant GO:BP term is, "cellular response to stress" ($p=4.01x10^{-5}$).

Table 4.2: Summary of modules that are associated with hallmarks of AD				
Module Color	**outcome**	**BETA**	**SE**	**P**
red	amyloid	-0.048	0.012055	8.69×10^{-5}
grey60	amyloid	-0.067	0.019134	4.57×10^{-4}
black	amyloid	-0.05	0.014568	6.80×10^{-4}
grey	amyloid	0.0212	0.006877	1.59×10^{-3}
black	tau	-0.114	0.026325	1.62×10^{-5}
pink	tau	-0.131	0.030269	1.78×10^{-5}
brown	tau	0.0693	0.016171	2.09×10^{-5}
green	tau	-0.0976	0.023045	2.65×10^{-5}
lightcyan	tau	-0.136	0.034869	1.01×10^{-4}
greenyellow	tau	-0.122	0.031621	1.25×10^{-4}
grey60	tau	-0.127	0.034747	2.78×10^{-4}
blue	tau	-0.054	0.016253	9.46×10^{-4}
grey60	cross_cog	0.0180	0.00490985	2.80×10^{-4}
black	cross_cog	0.0137	0.00384382	3.90×10^{-4}
brown	cross_cog	-0.007	0.00229648	2.37×10^{-3}
Module Color	**outcome**	**BETA**	**SE**	**P**
grey60	long_cog	0.002	0.00045611	2.08×10^{-5}
black	long_cog	0.0014	0.00034653	3.76×10^{-5}
brown	long_cog	-0.0008	0.0002141	5.09×10^{-4}

Significant p-values after Bonferroni correction are $p < 0.003$. Abbreviations: SE, standard error; cross_cog, global cognition at last visit before death; long_cog, annual change in global cognition.

Module Color	IHC Amyloid	IHC Tau	Cross-sectional Global Cognition	Cognitive Decline
Black				
Blue				
Brown				
Green				
Green-Yellow				
Grey				
Grey60				
Light Cyan				
Pink				
Red				

Legend = Significant in discovery | Significant in discovery & replication

Figure 4.1. Summary of novel module associations with hallmarks of AD. Green is indicative of significance when using RNAseq data to build modules. Yellow is indicative of significance in both discovery and replication (i.e., predicted expression) datasets.

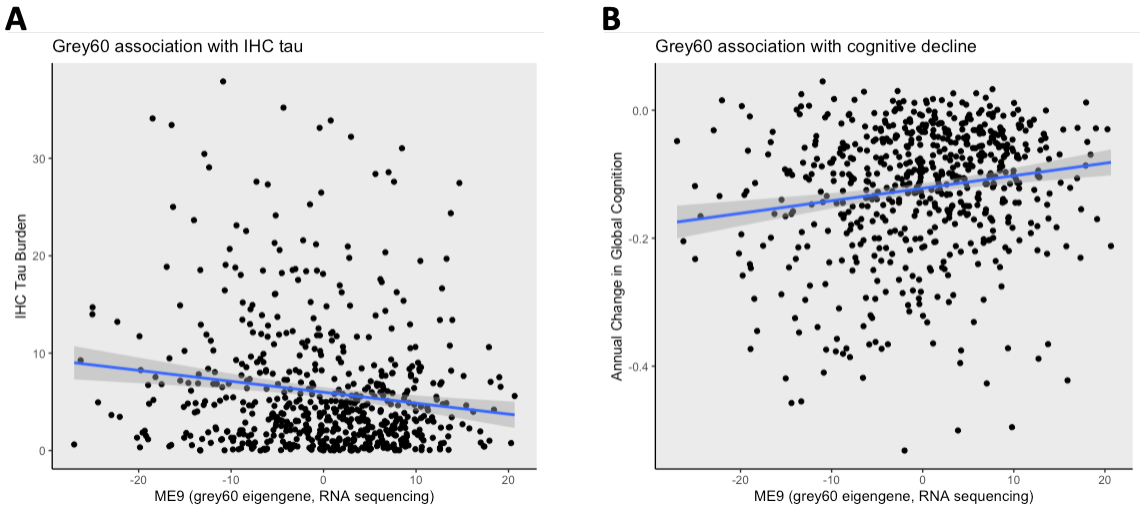

Figure 4.2. Higher expression of genes in the grey60 module are protective against tau burden and cognitive decline. A) A scatterplot exhibiting the association between the grey60 module eigengene and tau (β=-0.127, p=2.78x10^{-4}). The x-axis denotes the grey60 module eigengenes for each participant in the sample, and the y-axis denotes the immunohistochemical measurement of tau in the brain at autopsy. B) A scatterplot exhibiting the association between grey60 and cognitive decline (β=0.002, p=2.08x10^{-5}). The y-axis denotes the annual change in global cognition calculated with linear mixed-effects regression models.

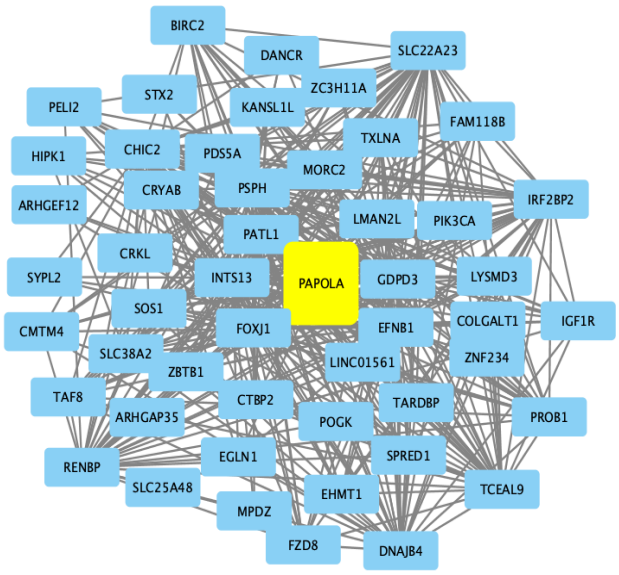

Figure 4.3. Network diagram of the grey60 module. A network diagram showing the hub gene, *PAPOLA*, in yellow, and the top 100 edges of the network.

4.3.6 Discussion

In these analyses, we have validated WGCNA as a robust and reproducible method by rebuilding a previously published gene co-expression network.[277] Full details on reproducing the network are available in **Appendix D**. In addition, we have also identified a module, grey60, that is associated with both tau burden and cognitive decline. In summary, higher expression of genes within the module predict lower tau burden at autopsy and slower cognitive decline (**Figure 4.3**). We have also replicated these associations using the predicted expression values of genes assigned to the grey60 module generated via the PrediXcan method[444] and the reference transcriptome of the CommonMind Consortium.[448]

The hub gene of the grey60 module is *PAPOLA*, which encodes a protein named poly(A) polymerase alpha. PAPOLA protein serves to poly-adenylate the 3' end of pre-mRNA. Polyadenylation subsequently stabilizes the mRNA and increases translocation of the mRNA from

the nucleus to the cytoplasm.[452] *PAPOLA* has never been classified a risk gene for AD, but evidence on Agora (AMP-AD) suggests that it is upregulated in AD brains compared to controls (https://agora.adknowledgeportal.org/genes/(genes-router:gene-details/ENSG00000090060). In addition, upstream regulators of *PAPOLA* have also been linked to *APP*.[453] It is well supported that transcriptional regulation and gene expression are changed during Alzheimer's disease,[454-457] though it is unclear exactly what role PAPOLA is playing in our results and in disease. "Cellular response to stress" is the GO-term most associated with the grey60 module, which is understandable given the context of aging and AD. However, it is quite general, limiting our ability to pinpoint a specific mechanism or function. In the future, differential expression studies examining *PAPOLA* and its downstream effects may be useful to elucidate a more specific biological mechanism in the context of AD. These future studies may also help to uncover a novel therapeutic target for AD that is co-expressed with PAPOLA but is less ubiquitously expressed overall.

4.4 ANALYSIS 2: EVALUATION OF PREDICTED GENE EXPRESSION AS A TOOL TO GENERATE AND REPLICATE GENE CO-EXPRESSION NETWORK ANALYSES

Transcriptomic datasets are often limited in sample size, especially in cohorts such as ROS/MAP where brain donation only occurs at death. Genomic datasets often have increased sample size in comparison to brain transcriptomic datasets because sample collection is less invasive for participants. Due to these limitations, we were interested in applying an emerging technique that leverages only genotype data to provide a proof-of-concept for how transcriptomic reference panels can be leveraged to apply gene co-expression networks in the context of genome-

wide association analyses. More specifically, we wanted to evaluate whether predicted expression from the frontal cortex was suitable for generating gene co-expression networks with increased sample size. For this study, we leveraged predicted expression values from ROS/MAP using the CommonMind Consortium reference transcriptome and the PrediXcan method for prediction (See section **3.3.6** in **Materials and Methods**). The sample used for this study was the same as the replication sample described above (**Table 4.1**).

4.4.1 Network generation and evaluation

The gene co-expression network was generated using WGCNA (version 1.68) in R (version 3.6.1). Prior to hierarchical clustering and module assignment, sample outliers were removed. In addition, genes whose expression was predicted with an $R^2 < 0.8$, had 0 variance, had greater than 90% values of 0, or were outliers greater or less than 5 standard deviations of the mean were removed from the dataset. The network was generated using the following function and parameters:

```
bwnet = blockwiseModules(datExpr, maxBlockSize = 8000, power = 7, networkType = "signed",
TOMType = "signed", replaceMissingAdjacencies = TRUE, minModuleSize = 30,
reassignThreshold = 1e-10, mergeCutHeight = 0.15, numericLabels = TRUE, saveTOMs =
TRUE, saveTOMFileBase = "power7_pearson_cor_test2", verbose = 5)
```

After generating the topology overlap matrix (TOM) with the blockwiseModules function, we merged any modules with a threshold of 0.15 (i.e., modules with eigengenes that are correlated with an $r > 0.85$ are merged). When examining the network generated with predicted expression data, most of the genes were assigned to the “grey” module, and co-expression was extremely low between genes with pair-wise Pearson correlations < 0.045 (**Figure 4.5**) suggesting that predicted expression values are not suitable for generating networks for co-expression analyses.

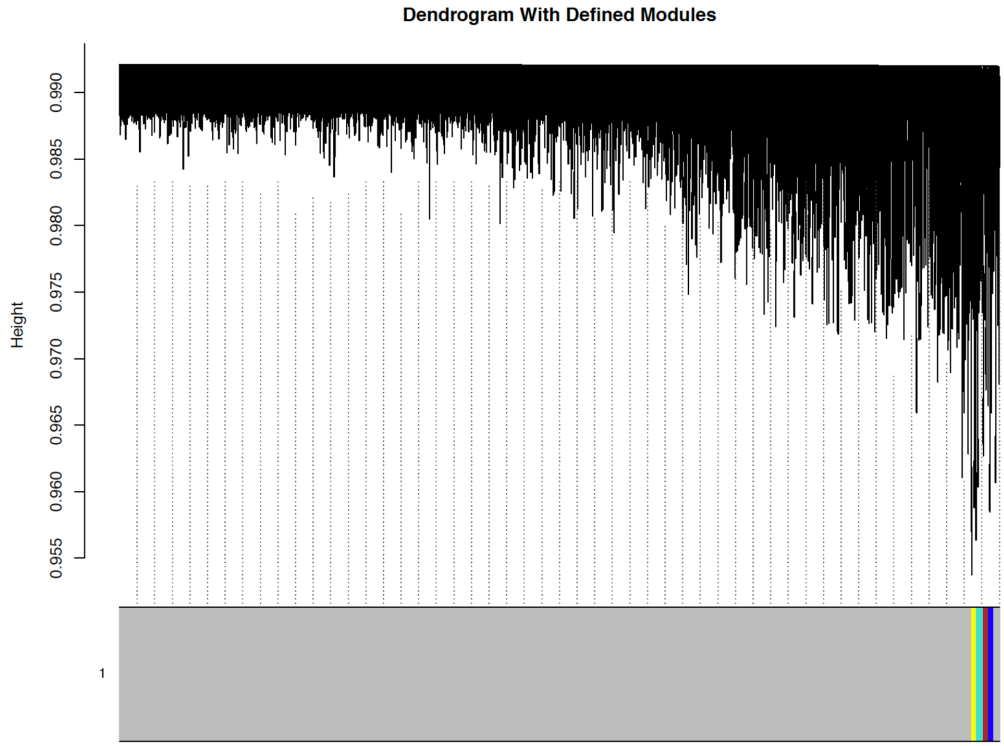

Figure 4.4. Dendrogram of network created with predicted expression values. Height is a measurement of dissimilarity (1 – correlation). The x-axis denotes the colors for assigned modules. An assignment of "grey" suggests that a gene cannot be assigned to another module due to low co-expression.

4.4.2. Modularity is not maintained when using predicted expression values

Due to our observations after attempting to generate a gene network with predicted expression values, we wanted to examine the "modularity" within the grey60 module (see section **4.3.4**). We used percent variance explained by the first principal component, or module eigengene, of a module as a proxy for modularity. In addition, we performed linear regression analyses to test the association between all genes assigned to grey60 and cognitive decline. For computational efficiency, cognitive decline, or annual change in global cognition was determined for each individual within the sample using linear-mixed effects regression, where the fixed effect is time, and the random effect is the time interval from the last visit for each participant.

When comparing RNAseq to predicted expression, we observe that the variance explained by the module eigengene is very low when using predicted expression to build the pre-defined module (**Figure 4.6A, B**). It should be noted, however, that some of the individual gene associations with cognitive decline remain significant when using either RNAseq or predicted expression (**Figure 4.6C, D**).

4.4.3 Discussion

In **Analysis 1**, we observed that the grey60 module generated with predicted expression values appears to replicate the association results of the transcriptome-generated grey60 module with cognitive decline. Due to our observations in this analysis (#2), however, it can be hypothesized that the predicted-grey60 module replication may be spurious due to the low percentage of variance explained by the module eigengene. Some of the individual predicted gene-trait associations with cognitive decline remained significant (**Figure 4.5D**), thus, the module replication may have been driven by these few genes and additional analyses can be completed to test this prediction.

We also determined that predicted expression cannot be used to create gene co-expression networks *de novo* due to poor correlation structure between genes. One possible reason for this may be that PrediXcan uses only *cis*-eQTLs for prediction.[444] However, gene expression can be influenced by both *cis*-eQTLs, which act on local genes (typically within 1 Megabase) and *trans*-eQTLs that can act on more distant genes as well as those on other chromosomes.[458] Studies posit that *trans*-eQTLs play a role in co-regulation and co-expression of numerous genes[459, 460]. Therefore, it is likely that we have removed most of the underlying network structure when using predicted expression to create a co-expression network.

Within the context of gene co-expression network analysis, I propose that predicted expression data be used with caution. Though we observed that it can recapitulate aspects of network analyses, it cannot be used to generate entire networks or to fully replicate modules. Instead, the use of predicted expression data should be limited to replication of single gene-trait associations. Interestingly, *PAPOLA*, the hub gene of grey60 is not significantly associated with cognitive decline when using RNAseq or predicted expression data (**Figure 4.5C, D**) which suggests that the most interconnected gene within a module may not always be the gene that is most associated with the phenotype of interest.[461]

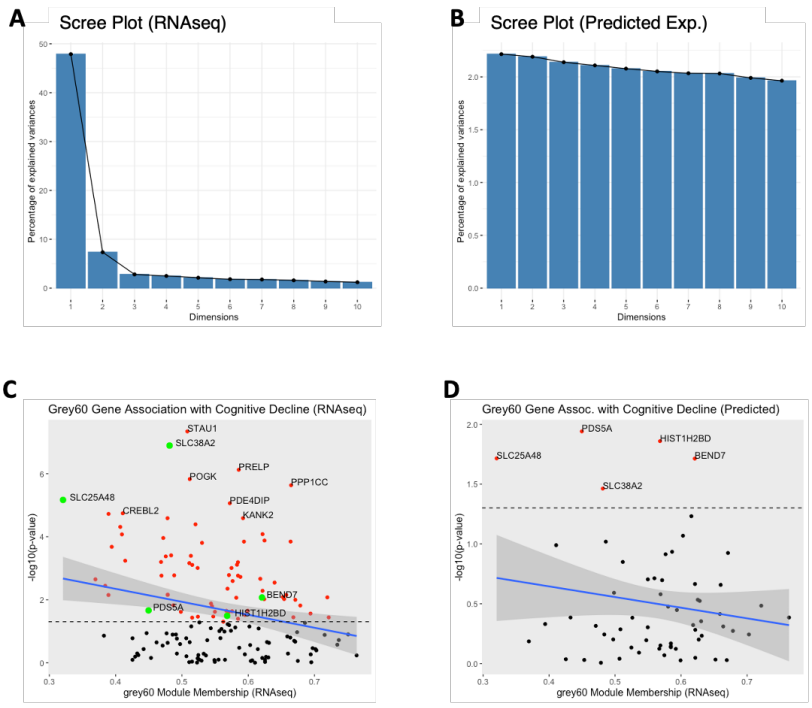

Figure 4.5. Modularity is not maintained when using predicted expression. A, B) The module eigengene more variance (0-50%) when calculated with RNAseq than it does when calculated with predicted expression values (0-2%). C) Genes within grey60 drive the module association with cognitive decline. Red = p.fdr < 0.05, green = genes also exhibiting significance in predicted expression. D) The gene-trait association exhibits a similar pattern as in RNAseq when using predicted expression values. The points in red are those with $p < 0.05$. The module association in both datasets is driven highly associated genes. Dotted line represents p=0.05.

4.5 ANALYSIS 3: EXAMINING LOGSDON ET AL., 2019[277] MODULE INTERACTIONS WITH *APOE*-ε4 POSITIVITY ON HALLMARKS OF AD

APOE-ε4 is the greatest genetic risk factor for AD, and even the presence of a single ε4 allele can result in a 3-fold increase in risk for disease.[138-141] In addition to increased AD risk, *APOE*-ε4 has been linked to negative outcomes such as increased brain amyloid deposition,[141] increased synaptic loss,[462] exacerbated tau pathology,[362, 463] and cognitive decline.[464, 465] However, many *APOE*-ε4 carriers remain cognitively normal throughout life despite the increase in AD risk,[276] suggesting that there are protective factors able to modulate *APOE*-ε4 effects. Furthermore, studies demonstrate that *APOE*-ε4 carriers have different transcriptional profiles than non-carriers suggesting that there may be biological pathways in the neuropathological progression of AD that *APOE*-ε4 carriers are more or less susceptible to in comparison to non-carriers.[466-468] Therefore, we hypothesize that using a systems biology approach such as WGCNA will not only help to identify individual genes that modify the effects of *APOE*-ε4, but also co-expressed genes or biological functions that modify *APOE*-ε4.

Again, leveraging the network published by Logsdon et al., 2019,[277] we wanted to examine whether any modules modified the relationship between *APOE*-ε4 positivity and amyloid and tau burden at autopsy, cross-sectional cognition, or cognitive decline. This analysis used ROS/MAP DLPFC RNAseq, and the sample used for this analysis is the same as the discovery sample described in **Table 4.1**.

4.5.1 Statistical Analyses

This analysis utilized the same principal components calculated in the statistical analyses described in section **4.3.1**. Using the eigengenes from 19 reported AD co-expression modules,[277]

we performed linear regression analyses assessing the interaction between the module eigengene and *APOE*-ε4 positivity (i.e., presence of at least one ε4 allele) on cross-sectional global cognition at the last visit before death, cognitive decline (calculation described in section **4.2.2**), and immunohistochemical measurements of amyloid and tau (described further in section **4.2 Materials and Methods**). Covariates included age of death, sex, education, and post-mortem interval. Correction for the number of modules was completed using Bonferroni correction ($p < 0.003$). We then performed hub gene analysis and GO-term analysis on any significant module interactions.

4.5.2 Four modules interact with *APOE*-ε4 positivity on cross-sectional cognition

We identified four co-expression network modules that modify the association between *APOE*-ε4 positivity and cross-sectional cognition at the last visit prior to death (**Table 4.3**). There were no other significant module interactions with any other tested outcome (i.e., amyloid, tau, cognitive decline).

Lower expression of genes within the purple and the cyan modules are associated with worse cross-sectional cognition in *APOE*-ε4 carriers, whereas increased expression of genes within the salmon and magenta modules are associated with worse cross-sectional cognitive performance in *APOE*-ε4 carriers (**Figure 4.6**).

Table 4.3: Significant module x *APOE*-ε4 interactions on cross-sectional cognition

Module Color	BETA	SE	P
purple	0.036	0.0081	1.16×10^{-5}
cyan	0.031	0.0099	1.49×10^{-3}
salmon	-0.036	0.0101	3.95×10^{-4}
magenta	-0.031	0.0097	1.60×10^{-3}

4.5.3 Hub gene and GO-term analysis

Hub genes and GO-terms for the purple, salmon, cyan, and magenta modules were identified following the procedure described in section **4.2.7**. The hub gene and most significant GO:BP term for each module is summarized in **Table 4.4.**

Table 4.4: Results of hub gene and GO-term analyses for the purple, cyan, salmon, and magenta modules

Module Color	Hub Gene	GO-term ID	Term Name	P-value
Purple	*YBX3*	GO:0048518	Positive regulation of biological process	1.59×10^{-26}
Cyan	*LAPTM5*	GO:0002376	Immune system process	1.16×10^{-50}
Salmon	*RTF1*	GO:0009059	Macromolecule biosynthetic process	4.50×10^{-5}
Magenta	*ATP2B1*	GO:0043412	Macromolecule modification	1.67×10^{-4}

4.5.4 Discussion

Leveraging a pre-defined gene co-expression network, we identified 4 unique module interactions with *APOE*-ε4 positivity on global cognition. When using eigengene values as a proxy for gene expression of all genes within a specific module, we observe that lower expression of genes within the purple and cyan modules result in worse cross-sectional cognitive performance in *APOE*-ε4 carriers. In contrast, higher expression of genes within the salmon and magenta modules are associated with worse cognition in *APOE*-ε4 carriers. When examining each hub gene's interaction with *APOE*-ε4 positivity, we observed inconsistency between the gene-trait association and the previously observed module-trait associations.

The hub gene of the purple module is *YBX3*, Y-box binding protein 3 (YB-3). YB-3 is a part of a family of Y-box binding proteins (YB) that bind both DNA and RNA and interact with almost all mRNA.[469, 470] The functions of YB proteins are extremely broad, and the most studied member of the protein family, YB-1, has been implicated in cell differentiation, stress response,

and translational control.[469] YB-3 is a transcriptional regulator that is believed to be negatively regulated by YB-1 and appears to have a redundant function in the absence of YB-1.[471] In addition, YB-3 appears to play a role in amino acid homeostasis and the translation of solute carrier transporters.[472]

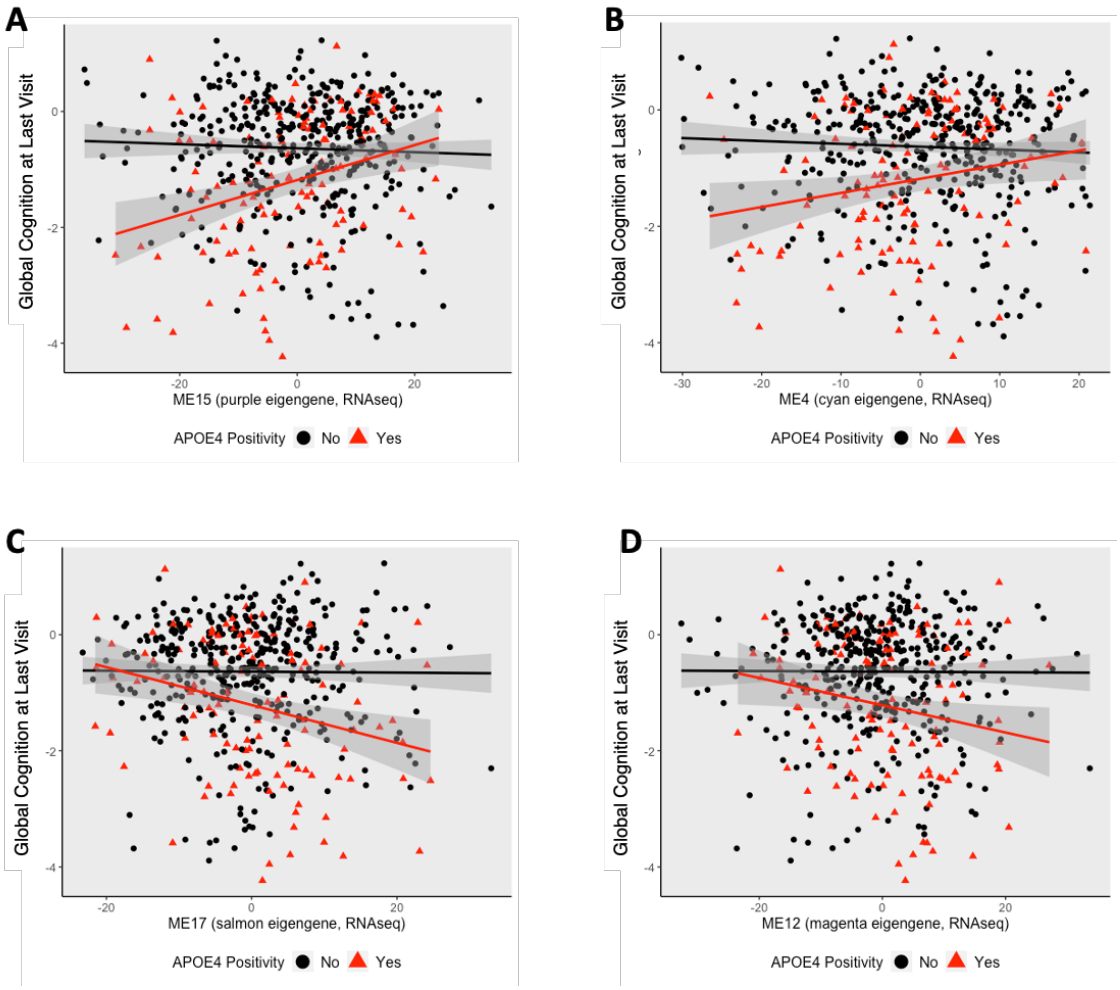

Figure 4.6. Four unique modules interact with *APOE*-ε4 positivity on cross-sectional cognition. Points and lines are colored by *APOE*-ε4 positivity where *APOE*-ε4 carriers are denoted by the color red**.** A, B) Lower eigengene values in the purple and cyan modules result in worse global cognition at the last visit before death in *APOE*-ε4 carriers. C, D) Higher eigengene values in the salmon and magenta modules results in worse cognitive performance in *APOE*-ε4 carriers.

It is almost fitting that the most significant GO-term for the purple module is "positive regulation of biological process," which is equally broad in nature. The given definition of "positive regulation of biological process," is "any process that activates or increases the frequency, rate, or extent of a biological process. Biological processes are regulated by many means; examples include the control of gene expression, protein modification or interaction with a protein or substrate molecule." Therefore, interpretation of this module is difficult without further analysis.

Sources also suggest that YB-3 is a transcriptional repressor and a negative regulator of cell death[473], so a downregulation of *YBX3* expression consistent with the purple module eigengene may result in the effects we observe in *APOE*-ε4 carriers (i.e., dysregulated cellular death resulting in cognitive impairment). Additionally, *in vitro* studies demonstrated that *APOE*-ε4 expression encourages cellular death in cultured neurons,[474, 475] supporting this hypothesis.

Paradoxically, *YBX3* is upregulated in multiple regions within AD brains (https://agora.adknowledgeportal.org/genes/(genes-router:gene-details/ENSG00000060138) in comparison to controls, which weakens this hypothesis. Though recent studies indicate that stress granules, riboprotein complexes that form as a response to environmental stressors, are becoming of interest in neurodegenerative disorders like AD. The presence of *APOE*-ε4 appears to accelerate stress granule formation in studies using a cerebral organoid.[462, 476] Although YB-3 has not been previously identified in studies of AD risk, it has been found within stress granules which may play a role in our results.[469, 476]

LAPTM5 (lysosomal-associated transmembrane protein 5), is the hub gene of the cyan module. *LAPTM5* is expressed in primarily in immune cells,[477] including microglia,[478, 479] and is thought to facilitate the transport of receptors to lysosomes,[480] phagocytosis,[479] and the positive regulation of pro-inflammatory signaling pathways.[477] Previous studies have identified *LAPTM5*

as a potential risk gene for AD,[481, 482] and co-expression network analyses have linked it to other AD-related genes, *TREM2* and *TYROBP*.[478, 479, 483] Furthermore, *Laptm5* expression is positively correlated with amyloid deposition in *APOE*-ε4-expressing mice that were fed a high-fat diet,[484] and it is upregulated in mice when amyloid plaque load is heavy[481], which is consistent with what is observed in human AD brains on Agora (https://agora.adknowledgeportal.org/genes/(genes-router:gene-details/ENSG00000162511). Though LAPTM5's mechanism of action in AD is not fully characterized, these data suggest that it may play a function in amyloid clearance or the regulation of microglia in response to amyloid.[481]

In our results, we observe poorer cognition among *APOE*-ε4-carriers expressing lower levels of *LAPTM5*. Therefore, one possible hypothesis that LAPTM5 is unable to facilitate amyloid clearance in *APOE*-ε4-carriers, and individuals expressing lower levels have increased susceptibility to *APOE*-ε4-associated risk and amyloid. In contrast to the purple module, the most significant GO-term of the cyan module is "immune system process," which is congruent with LAPTM5's biological function and continues to support previous work implicating neuroinflammation in cognitive decline among both *APOE*-ε4 carriers and non-carriers.

RTF1, RNA polymerase-associated protein, is the hub gene of the salmon module. As its protein name describes, RTF1 plays roles in activating gene transcription and histone modification.[485] When domains of RTF1 are deleted or mutated, defects in transcription can occur.[485] In a recent differential expression study examining gene expression data from AD cases and controls, *RTF1* was identified as a downregulated gene within the hippocampus and entorhinal cortex.[486] As transcriptional changes are evident within aging and AD,[486-488] it is perhaps unsurprising that a transcription-related gene would be associated with AD endophenotypes. However, our results insinuate that increased expression of *RTF1* in *APOE*-ε4 carriers results in

worse cognitive performance. As *APOE* genotype can affect transcriptional profiles alone, an interaction with *RTF1* may suggest that complex transcriptional changes are driving our results. However, further examination of genes within the salmon module will be necessary for a more detailed biological interpretation.

The most significant GO-term for the salmon module is, "macromolecular biosynthetic process," which is defined as, "the chemical reactions and pathways resulting in the formation of a macromolecule, any molecule of high relative molecular mass, the structure of which essentially comprises the multiple repetition of units derived, actually or conceptually, from molecules of low relative molecular mass," which is broad and could refer to the synthesis of mRNA transcripts or production and aggregation of beta-amyloid, which are both modulated by *APOE* genotype warranting further study.

ATPase plasma membrane Ca2+ transporting 1 (*ATP2B1)* is the hub gene of the magenta module. Its function is important for calcium homeostasis; it maintains low intracellular calcium concentration after signaling.[489] *ATP2B1* is widely expressed throughout the body (https://www.proteinatlas.org/ENSG00000070961-ATP2B1),[490] and is expressed in neurons.[491] Though it has not been previously associated with AD in any genome-wide association study, *ATP2B1* has been previously identified in a network analysis of AD[492] as well as in a mouse study examining the consequences of amyloid pathology on gene expression.[493] Calcium dysregulation has been hypothesized to contribute to AD and brain aging, and *APOE*-ε4-mediated neurotoxicity has been attributed, in part, to calcium dysregulation suggesting that that *ATP2B1* will be an interesting candidate for further study.[494, 495] Our results demonstrate that an increase in *ATP2B1* expression in *APOE*-ε4 carriers is detrimental to cognitive performance, such that *APOE*-ε4 carriers may be particularly susceptible to changes in calcium homeostasis. However, *ATP2B1*

expression is downregulated approximately 9-fold in *APOE*-ε3/ε4 individuals with AD in comparison to ε3/ε3 controls.[496] One possibility for this paradox may be that *ATP2B1* expression is decreased in individuals with AD due to significant neurodegeneration.

"Macromodule modification" is the most significant GO-term for the magenta module, and its definition is "the covalent alteration of one or more monomeric units in a polypeptide, polynucleotide, polysaccharide, or other biological macromolecule, resulting in a change in its properties." Post-translational modifications are of particular importance to biology and to AD. For example, neurofibrillary tangles are the result of post-translational hyperphosphorylation of tau.[40, 45, 497] Thus, further dissection of this module is of particular interest for future investigation.

4.6 CHAPTER CONCLUSION

In conclusion, we confirmed the robustness and reproducibility of gene co-expression network generation and analysis with WGCNA by re-creating the network published by Logsdon et al., in 2019 in **section 4.3**.[277] Using the pre-existing module definitions provided by Logsdon et al.,[277] and AMP-AD, we also identified 18 novel associations across 10 unique modules with brain amyloid and tau burden at autopsy, global cognition at the last visit prior to death, and cognitive decline which served as a proof-of-concept for our future analyses using WGCNA. The grey60 module, which was enriched for genes involved in "cellular response of stress," was of particular interest for this set of analyses because we were able to replicate our associations with tau burden and cognitive decline with predicted expression data. When using the module eigengene as a proxy for gene expression of genes within grey60, our results demonstrated that higher levels of genes within the module were protective against tau burden and cognitive decline. Unfortunately, after

further evaluating the utility of PrediXcan and predicted expression for gene co-expression network analyses in section **4.4**, we discovered that predicted expression data is not a viable option for network generation or full replication of network analyses though it is suitable for recapitulating single gene-trait associations.

In section **4.5**, we identified 4 novel module interactions with *APOE*-ε4 positivity on cross-sectional cognition using the same, previously described network.[277] In these analyses, we found that lower expression of genes within the purple and cyan modules were associated with worse cross-sectional cognition in *APOE*-ε4 carriers and that higher expression of genes within the salmon and magenta modules were associated with worse cognition in *APOE*-ε4 carriers. The hub genes of these modules were *YBX3, LAPTM5, RTF1,* and *ATP2B1* which implicated stress granules, lysosomal regulation, histone modification, and calcium homeostasis in susceptibility to *APOE*-ε4-mediated cognitive impairment. In our results, higher expression of *YBX3* and *LAPTM5* may be beneficial among *APOE*-ε4 carriers, whereas the opposite is true of *RTF1* and *ATP2B1* expression. We found no significant interactions on longitudinal cognition, again, insinuating that the biological effects are imparted prior to decline. As such, genes within the identified modules may present as suitable therapeutic targets for AD prevention rather than AD treatment once cognitive impairment occurs.

Though the analyses within this chapter have demonstrated that annotation for network modules can be broad or abstract, systems-based approaches are powerful tools for linking a single gene to a broader function because they take complex interactions into consideration. For example, the directionality of some of our module interactions are inconsistent with prior literature investigating the aforementioned hub genes as candidate genes. Evidence also suggests that the hub gene of a module, though useful in interpreting biological function, may not necessarily be

the gene that is most associated with the outcome of interest.[461] However, biological interactions between multiple genes within the module may ultimately drive our observed results though replication, further assessment of the co-expression modules, and alternate network-based approaches are necessary to truly validate this idea.

4.6.1. Future Directions

Future directions for these analyses involve performing hub gene and GO-term analysis for the other modules (**Table 4.2**) that were significantly associated with amyloid, tau, and cognition. The biological mechanisms of the grey60, purple, salmon, cyan, and magenta modules should also be further studied as the associated GO-terms were extremely broad. As those modules all contain over 100 genes each, it may be of interest to re-cluster them to get smaller modules with more specific biological annotations. In addition, the Logsdon et al., 2019[277] gene network should be evaluated for associations with resilience to AD as an alternative mechanism for discovering novel targets for AD drug discovery.[99, 282]

Finally, additional gene co-expression networks should be built in other distinct brain regions including the posterior cingulate cortex and the caudate nucleus now that additional RNAseq data from ROS/MAP is publicly available on AMP-AD. These networks can be used to evaluate region-specific transcriptome changes in the context of AD and resilience to AD. Finally, analyses should also examine the viability and utility of module-quantitative trait loci to further investigate using network analysis in the context of genome-wide association analyses.[498]

CHAPTER 5

CONCLUDING REMARKS

Portions of this chapter are published under the title, “Protective Genes and Pathways in Alzheimer’s Disease: Moving Towards Precision Interventions,” in *Molecular Neurodegeneration*.

In this dissertation, we began by examining a single polymorphism, before moving onto a single gene, and finally, to a network of interacting genes that can influence AD risk. The overarching goal of this dissertation was to utilize these three biological "levels" of human data to identify genetic and molecular modifiers of AD risk. There are strengths and limitations to each "level" of analysis described herein, but it is important to note that they are all biologically connected and can be used independently or jointly to better understand AD biology, to identify new therapeutic targets, and to propose novel biomarkers for AD.

Each analytical chapter also leveraged interaction models to identify factors that would enhance or diminish the relationships between AD risk and AD endophenotypes. In other words, we utilized statistical models to help us identify factors that could prevent brain atrophy or cognitive decline even in the presence of amyloid and/or tau pathology or an *APOE*-ε4 allele. Hence, the rationale behind this project largely relies on the idea of resistance and resilience to AD.

Overall, investigating AD from the perspective of resistance and resilience provides a unique perspective not only on the disease itself, but also for future therapeutics. To date, therapeutics in the Alzheimer’s space have largely focused on reducing pathology (particularly

amyloid) that already exists within the CNS, however, any neurodegeneration that has already occurred remains after treatment, potentially impacting trial endpoints.[63-65, 87]

Examining resistance and resilience for AD drug discovery provides an opportunity to hijack pre-existing biological pathways that are protective even in the presence of pre-existing pathology or neurodegeneration. Subsequently, therapeutics resulting from resilience research would have a therapeutic window that is less disease-stage dependent. Additionally, these therapeutics could also be catered to a patient's genetic profile (*e.g.*, *APOE*-ε4 positivity), which could uncover new possibilities for the future of precision medicine.

In summary, **Chapter 1** describes Alzheimer's disease, the current therapeutic landscape for AD, and the ideas of resistance and resilience. In **Chapter 2**, we performed a genome-wide association study to identify two novel loci on chromosome 3 that interact with baseline levels of CSF Aβ42 and CSF p-tau, respectively. We also implicate axonal guidance, synaptic pruning genes, DNA damage repair, and endolysosomal function in the neuropathological progression of AD.

Briefly, minor allele (T) carriers of rs62263260 exhibit faster rates of hippocampal atrophy among individuals with CSF biomarker evidence of amyloidosis. Excitingly, this result was replicated independently using an alternative measurement of amyloid burden, amyloid PET. rs62262360 is a robust eQTL for *SEMA5B* in tissues including the esophagus, testes, and more importantly, the brain. In two independent datasets, evidence suggested that carriers of the T-allele express higher levels of *SEMA5B* within the brain than non-carriers, which we hypothesize increases susceptibility to amyloid-mediated hippocampal atrophy.

Second, we discovered that minor allele (G) carriers of rs116216974 exhibit slower rates of hippocampal atrophy in the presence of high CSF p-tau. Unfortunately, rs116216974 was not

an eQTL for any gene limiting our ability to interpret our results and to better understand rs116216974's protective mechanism of action. Though variant-level analyses have their own benefits, linking a SNP to function can be difficult without determining the acting gene within the region. Thus, gene-level analyses follow.

In **Chapter 3**, we identified *RNASE6* (ribonuclease A family member K6), which modifies the interaction between *APOE*-ε4 positivity and baseline cognition such that *APOE*-ε4 carriers expressing higher levels of *RNASE6* have worse cognitive performance at baseline. This chapter further implicates neuroinflammation and innate immunity as potential drivers of cognitive decline as well as demonstrates the utility of whole blood transcriptomics for monitoring of brain changes during aging and the progression of AD. As *RNASE6* is an immune-related gene that is not well-characterized within the literature, we utilized publicly available gene co-expression network analyses to help provide an interpretation of our *RNASE6* x *APOE*-ε4 positivity result.

In **Chapter 4**, we rebuilt a previously published co-expression network to assess the reproducibility of gene co-expression network analysis and the WGCNA method. Using the pre-defined network, we identified novel associations with hallmarks of AD including amyloid and tau burden at autopsy and cognitive decline. We then replicated the grey60 module's association with tau and cognitive decline using predicted expression data generated via the PrediXcan method, after which we determined that predicted expression data is not suitable for *de novo* gene co-expression network generation or module replication due to a lack of a correlation structure between genes. Finally, we identify 4 unique module interactions with *APOE*-ε4 positivity on cross-sectional cognitive performance at the last visit prior to death that result in worse cognitive performance in ε4 carriers. These modules connect immune function, responses to cellular stress,

transcriptional regulation, and calcium homeostasis to cognitive decline and provide a potential pathway to identify preventative therapeutic targets for AD.

Altogether, these chapters support the idea that -omic data and computational tools can be used to identify factors that are protective in the presence of AD risk, to better understand the etiology of AD, as well as to facilitate drug discovery efforts.

Finally, we offer additional perspectives on how the AD field can rapidly advance towards precision therapeutics. First, there is a pressing need for large genomic studies that integrate detailed metrics of neuropathology, neurodegeneration, and cognitive decline. For example, our group has recently quantified a continuous measure of cognitive resilience by integrating established measures of amyloid pathology and harmonized measures of cognition.[282] Using these data, we identified variants upstream of the gene, *ATP8B1* (ATPase phospholipid transporting 8B1), that were associated with increased susceptibility to amyloid.[282] *ATP8B1* is an interesting candidate that encodes a protein by the same name that is important for modulating phospholipid composition within cellular membranes as well as maintaining bile acid homeostasis. Notably, deleterious variants were recently identified in another gene within the same family, *ATP8B4* (ATPase phospholipid transporting 8B4), via whole-exome sequencing,[499] suggesting this family of flippases may be highly relevant to AD risk and progression. Although our study was the largest GWAS of resilience completed to date, we remained vastly underpowered to fully delineate the genetic architecture of resilience, highlighting the need for large-scale collaborative efforts to expand sample sizes and identify new signals. It is also notable that we did not observe a genetic correlation between clinical AD and resilience to AD, suggesting that genetic analyses exploring the downstream consequences of pathology will uncover novel molecular contributors to AD risk and protection.

In addition to the discovery of numerous common AD risk variants with low effect sizes, the failure of numerous anti-amyloid drugs in clinical trials have demonstrated that there is no singular variant, gene, or mechanism behind sporadic AD. Polygenic risk scores (PRS) that take the complexity of sporadic AD into account could be a useful way to predict an individual's overall risk for disease. Recent studies have demonstrated the ability of PRS to predict AD with accuracy up to 84%.[13] PRS also present an exciting future for precision medicine as more genetic data are acquired and more risk loci are identified. Similar to PRS, a variant or gene with smaller effect size is unlikely to provide complete protection from AD on its own. As such, a "polygenic resilience score" combining both common and rare variants could not only help to predict individuals who are resilient from AD but could also provide new opportunities for AD drug discovery in the form of polypharmacology and/or pharmacogenetics.

One major limitation of this dissertation is that the data used for analyses primarily comes from non-Hispanic white individuals. Overall, less than 30% of all published GWAS studies have focused on minority populations (e.g., individuals of African, Latin, or Hispanic descent), and in turn, most of what is known currently about AD genetic architecture is based on studies focusing on non-Hispanic white individuals.[500] As a result, the information can only be generalized to the non-Hispanic white population, which is likely to present scientific, public health, and ethical issues that need to be addressed in the coming years.

For example, a recent study discovered that Black individuals were 35% less likely to be diagnosed with AD in comparison to non-Hispanic white individuals despite having increased AD risk.[501] Furthermore, the same study suggested that there are racial differences in symptom presentation [501] highlighting a major need to address disparities in cohort enrollment, community engagement and outreach, and scientific research.

In addition to clinical presentation, factors of AD risk and resilience can also vary across populations. For example, some studies have shown that *APOE*-ε4 alleles confer less AD risk in individuals of African descent than in non-Hispanic white individuals.[502, 503] However, African Americans are at increased risk of AD overall when compared to non-Hispanic whites.[504, 505] Though environmental differences between racial and ethnic groups (e.g., income, stress, discrimination) contribute to the pathogenesis of AD, a better understanding of the genetic architecture of AD in under-represented minority populations is scientifically and ethically critical to advance the field and enable personalized interventions.

Excitingly, emerging analyses within the past few years have not only identified novel AD risk loci in minority populations,[506] but also have supported that risk loci in non-Hispanic white populations may not confer the same risk in groups of different race and ethnicity.[502, 507] Similar studies have also identified AD protective variants. Some notable examples are: rs75002042 (OR=0.61), which is an intronic variant in the gene *FBXL7* (F-box/LRR-repeat protein 7); it was identified in a case-control study of Caribbean-Hispanic individuals,[508] and *LRIG1* (Leucine Rich Repeats and Immunoglobulin Like Domains, OR=0.54, rs2280575), which was discovered in an East Asian sample.[509] These findings, along with others, represent exciting advancements not only for minority populations but also for AD research.

Third, there is a growing literature on the genomics of educational attainment and cognitive performance that is relevant to cognitive reserve and protection from AD. In fact, educational attainment and cognitive performance are heritable[510-512]-- genetic differences can account for as much as 60% of the variation in educational attainment[513] and 70% of the variation in general cognitive ability,[514, 515] which can be apparent even in early-life. Data from studies such as the Nun Study have demonstrated that early-life linguistic ability is associated with AD neuropathology

and cognitive changes in late-life [279]. Furthermore, early-life cognitive enrichment (ELCE) was recently associated with slower age-related cognitive decline and late-life neuropathology,[516] suggesting that intervention on modifiable risk factors at a young age affects performance in old age. The fact that much of the cognitive benefits of ELCE were independent of AD neuropathology suggests there are distinct and complex pathways that promote resilience (i.e., pathology-related versus pathology-independent).[517] Fully encompassing the genetic architecture of cognitive ability into our models of AD resilience will be critical as we move to better understand the molecular pathways that protect against AD.

Fourth, AD is a disease of aging, and the strongest genetic risk factor for the disease (*APOE*) has a robust association with longevity.[518, 519] Far more work integrating the genetic architecture of longevity related traits into our models of AD are needed to better understand how these pathways intersect. For example, telomere length is strongly associated with life span, and shortened telomeres are indicative of cell aging.[520] In 2020, a drug to lengthen telomeres through transduction of human TERT (telomerase reverse transcriptase) was in Phase I clinical trials.[64] However, the direction of telomere effects, the relevant cell types, and changes over the course of age and disease remain poorly understood, providing a critical knowledge gap for future work.[521] Similarly, disentangling the effects of longevity genes on survival from the effects on neuropathological burden and age-related cognitive decline will be critical to better understand and prioritize molecular pathways that contribute to longevity and AD.

Finally, there is an incredible opportunity to advance our understandings of protection by focusing on the notable heterogeneity in the neuropathological presentation and clinical manifestation of the disease across sexes. Nearly two-thirds of diagnosed AD cases are women[505, 522] and *APOE*-ε4 is more strongly associated with clinical AD[523] and measures of tau.[524] Moreover,

AD neuropathology is more likely to clinically manifest as clinical dementia in women than in men.[525, 526] There is now emerging work implicating sex-specific genomic and transcriptomic signatures of AD in humans, and work in mouse models has implicated the important contribution of both gonadal hormone and X-chromosome effects on conferring risk and resilience to AD in a sex-specific manner. Yet, the vast majority of studies of protection in AD have not integrated sex-specific models, and the degree to which the molecular contributors to resilience differ by sex remains poorly understood.[524, 525, 527-532] Further exploration into sex differences in biological mechanisms driving resilience to AD could present a turning point for precision medicine by clarifying whether the best target pathway for intervention varies by age, biomarker status, genetic background and sex.[533]

In conclusion, sporadic AD presents immense therapeutic challenges due to the heterogeneity in the neuropathological presentation, age of onset, rate of decline, and clinical manifestation of disease. However, this same heterogeneity provides an exciting opportunity to characterize the specific molecular context in which neuroprotection is observed. The powerful stories of protection in even a single high-risk patient can transform our molecular understanding of a disease. The new identification of a protected autosomal dominant mutation carrier (i.e., *APOE3ch*) has provided exciting new directions for AD therapeutics, and we must find a way to identify such incredible stories of resilience in sporadic AD that surely are hiding in our ever-expanding cohort studies of aging and AD. We anticipate that multi-omics and computational biology will continue to be a part of that story.

APPENDIX A

This serves as the Appendix for CHAPTER 1: INTRODUCTION

A.1 ACKNOWLEDGEMENTS

The results published here are in whole or in part based on data obtained from Agora, a platform initially developed by the NIA-funded AMP-AD consortium that shares evidence in support of AD target discovery.

A.2 FUNDING SOURCES

This review was funded by K01AG049164, R01AG059716, R21AG059716, and R01AG057914.

A.3 APPENDIX TABLES

Full supplemental table including CPRA can be found here:
https://molecularneurodegeneration.biomedcentral.com/articles/10.1186/s13024-021-00452-5.

Table A.1: Table of all protective SNPs identified up to 2020.

Study	DOI/PMID	Gene	rsID
AlmeidaJFF 2018	https://doi.org/10.1007/s12031-018-1045-y	*MS4A6A*	rs610932
AlmeidaJFF 2018	https://doi.org/10.1007/s12031-018-1045-y	*CLU*	rs11136000
Andersson 2016	https://dx.doi.org/10.3233%2FJAD-160319	*SORT1*	rs17646665
Anvar 2015	https://doi.org/10.1016/j.jns.2015.09.344	*IL16*	rs4072111
Arboleda-Velasquez 2019	https://doi.org/10.1038/s41591-019-0611-3	*APOE*	rs121918393
Ayers 2016	https://doi.org/10.1186/s12864-016-2725-z	*CASP7*	rs10553596
Babenko 2018	https://dx.doi.org/10.1186%2Fs12868-018-0413-4	*APOE*	rs769449
Bao 2016	https://doi.org/10.12659/MSM.895622	*CD33*	rs3865444
Bao 2016	https://doi.org/10.12659/MSM.895622	*TOMM40*	rs157580
Belloy 2020	https://doi.org/10.1001/jamaneurol.2020.0414	*KL*	rs9536314, rs9527025
Benedet 2018	https://doi.org/10.1212/NXG.0000000000000216	*CYP2C19*	rs4388808
Benitez 2014	https://doi.org/10.1016/j.neurobiolaging.2013.12.010	*TREML2*	rs3747742
Bertram 2005	https://doi.org/10.1136/jmg.2004.024596	*TFCP2*	rs4438107
Bertram 2007	https://doi.org/10.1038/ng1934	*ACE*	rs1800764
Bertram 2007	https://doi.org/10.1038/ng1934	*ACE*	rs4291
Bertram 2007	https://doi.org/10.1038/ng1934	ACE	rs4343

Study	DOI/PMID	Gene	rsID
Bertram 2007	https://doi.org/10.1038/ng1934	*APOE*	rs405509
Bertram 2007	https://doi.org/10.1038/ng1934	*APOE*	rs440446
Bertram 2007	https://doi.org/10.1038/ng1934	*APOE*	rs449647
Bertram 2007	https://doi.org/10.1038/ng1934	*CHRNB2*	rs4845378
Bertram 2007	https://doi.org/10.1038/ng1934	*GAPDHS*	rs12984928
Bertram 2007	https://doi.org/10.1038/ng1934	*GAPDHS*	rs4806173
Bertram 2007	https://doi.org/10.1038/ng1934	*IDE*	rs2251101
Bertram 2007	https://doi.org/10.1038/ng1934	*MTHFR*	rs1801131
Bertram 2007	https://doi.org/10.1038/ng1934	*PRNP*	rs1799990
Bertram 2007	https://doi.org/10.1038/ng1934	*PSEN1*	rs165932
Bertram 2007	https://doi.org/10.1038/ng1934	*TFAM*	rs2306604
Bian 2008	https://doi.org/10.1007/s12031-008-9036-z	*NQ01*	rs1800566
Bian 2008	https://doi.org/10.1007/s12031-008-9036-z	*NQ01*	rs1800566
Boada 2012	https://doi.org/10.1016/j.neurobiolaging.2010.06.016	*ESR1*	rs3844508
Boiocchi 2015	https://doi.org/10.2174/1567205012666151027130635	*HSP70*	rs1043618
Boiocchi 2015	https://doi.org/10.2174/1567205012666151027130635	*HSP70*	rs1061581
Bratosiewicz-Wasik 2018	https://doi.org/10.1016/j.neulet.2018.07.010	*APOE*	rs449647
Bruunsgaard 2004	https://doi.org/10.1111/j.1532-5415.2004.52369.x	*TNF*	rs1800629
Bufill 2015	https://doi.org/10.1097/WAD.0000000000000002	*RELN*	rs528528
Bufill 2015	https://doi.org/10.1097/WAD.0000000000000002	*PLK2*	rs15009
Bufill 2015	https://doi.org/10.1097/WAD.0000000000000002	*PLK2*	rs702723
Burfiend 2017	https://doi.org/10.1016/j.trci.2017.05.001	*AQP4*	rs9951307

Study	DOI/PMID	Gene	rsID
Burfiend 2017	https://doi.org/10.1016/j.trci.2017.05.001	*AQP4*	rs3875089
Carrasquillo 2015	https://doi.org/10.1016/j.neurobiolaging.2014.07.042	*PICALM*	rs3851179
Carrasquillo 2017	https://doi.org/10.1016/j.jalz.2016.10.005	*TREM*	rs9357347
Cascalheira 2015	https://doi.org/10.1177/0004563214561770	*TCN2*	rs1801198
Chagnon 1999	https://doi.org/10.1002/(SICI)1096-8628(19990702)85:1%3C20::AID-AJMG6%3E3.0.CO;2-K	mitochondria	rs2853517
Chagnon 1999	https://doi.org/10.1002/(SICI)1096-8628(19990702)85:1%3C20::AID-AJMG6%3E3.0.CO;2-K	mitochondria	rs193303002
Chang 2016	https://doi.org/10.18632/oncotarget.8176	*HMGCR*	rs3846662
Chapuis 2009	https://doi.org/10.1038/mp.2009.10	*IL-33*	rs7044343
Chen 2008	https://doi.org/10.1016/j.brainres.2007.10.054	*CETP*	rs2303790
Chen 2016	https://doi.org/10.1007/s10072-016-2579-9	*PTGS2*	rs20417
Chen 2017	https://doi.org/10.1111/jgs.14537	*ESR2*	rs4986938
Chen 2017	https://doi.org/10.1111/jgs.14537	*ESR2*	rs867443
Chen 2018	https://doi.org/10.12659/MSM.907809	*EGFR*	rs730437
Chen 2018	https://doi.org/10.12659/MSM.907809	*EGFR*	rs1468727
Chen 2020	https://doi.org/10.3233/jad-191214	*SLAMF1*	rs13374761
Chou 2016	https://doi.org/10.1186/s13195-016-0222-x	*SORL1*	rs1784933
Christopher 2017	https://doi.org/10.1002/ana.25094	*PPP4R3A*	rs2273647
Combarros 2008	https://doi.org/10.1007/s00702-008-0028-5	*CYP19A1*	rs1062033
Combarros 2008	https://doi.org/10.1007/s00702-008-0028-5	*IL10*	rs1800896
Cong 2011	https://doi.org/10.1016/j.neurobiolaging.2009.01.001	*ADAM9*	rs7006414
Cong 2020	https://doi.org/10.1016/j.neurobiolaging.2020.07.005	*ERC1*	rs2968869
Correia 2009	https://doi.org/10.1016/j.neulet.2009.03.088	*HFE*	rs1800562

Study	DOI/PMID	Gene	rsID
Cui 2012	https://doi.org/10.1016/j.jocn.2011.08.036	*IDE*	rs4646958
Cui 2012	https://doi.org/10.1016/j.jocn.2011.08.036	*IDE*	rs1887922
Curtis 2020	https://doi.org/10.1111/ahg.12375	*TIAF1*	rs73986791
Curtis 2020	https://doi.org/10.1111/ahg.12375	*NDRG2*	rs199616382
Dai 2018	https://doi.org/10.1159/000492536	*CHI3L1*	rs4950928
DosSantos 2017	https://doi.org/10.1007/s12031-017-0928-7	*CD33*	rs3865444
Dumitrescu 2020	https://doi.org/10.1093/brain/awaa209	*ATP8B1*	rs2571244
Ezquerra 1997	https://doi.org/10.1016/S0304-3940(97)00328-5	*PSEN1*	rs165932
Feher 2018	https://doi.org/10.1016/j.neulet.2017.11.027	*ABCA1*	rs2230805
Feher 2018	https://doi.org/10.1016/j.neulet.2017.11.027	*ABCA1*	rs2230806
Finckh 2003	https://doi.org/10.1007/s10048-003-0157-9	*PLAU*	rs2227564
Fiocco 2010	https://doi.org/10.1212/WNL.0b013e3181d9edba	*COMT*	rs4680
Fu 2009	https://doi.org/10.1002/gps.2196	*CYP46A1*	rs3742376
Funalot 2004	https://doi.org/10.1038/sj.mp.4001584	*ECE-1*	rs213045
Galimberti 2004	https://doi.org/10.1016/j.jns.2004.07.005	*CCR2*	rs1799864
Gao 2016	https://doi.org/10.18632/oncotarget.7945	*ZCWPW1*	rs1476679
Ghani 2016	https://doi.org/10.1016/j.neurobiolaging.2016.03.009	*MS4A locus*	NA
Gongzalez 2014	https://doi.org/10.1016/j.medcli.2013.07.031	*COX2*	rs20417
He 2006	https://www.ncbi.nlm.nih.gov/pubmed/16863614	*PON1*	rs662
He 2010	https://doi.org/10.1007/s10072-009-0199-3	*IL6*	rs1800796
Hua 2013	https://doi.org/10.3109/00207454.2013.784286	*IL6*	rs1800795
Jamieson 2005	https://doi.org/10.1016/j.neulet.2004.10.038	*SLC11A2*	rs407135

Study	DOI/PMID	Gene	rsID
Janicki 2013	https://doi.org/10.1159/000343074	*CYP19*	rs4775935
Janicki 2013	https://doi.org/10.1159/000343074	*CYP19*	rs727479
Janicki 2013	https://doi.org/10.1159/000343074	*CYP19*	rs6493495
Janicki 2013	https://doi.org/10.1159/000343074	*CYP19*	rs11070843
Janicki 2014	https://doi.org/10.1159/000355559	*ESR1*	rs6902771
Janicki 2014	https://doi.org/10.1159/000355559	*ESR1*	rs3853250
Janicki 2014	https://doi.org/10.1159/000355559	*ESR1*	rs4870056
Janicki 2014	https://doi.org/10.1159/000355559	*ESR1*	rs2234693
Janicki 2014	https://doi.org/10.1159/000355559	*ESR1*	rs9340799
Janicki 2014	https://doi.org/10.1159/000355559	*ESR1*	rs9322332
Ji 2015	https://www.ncbi.nlm.nih.gov/pubmed/26770425	*MS4A6A*	rs610932
Ji 2015	https://www.ncbi.nlm.nih.gov/pubmed/26770425	*GAB2*	rs2373115
Ji 2015	https://www.ncbi.nlm.nih.gov/pubmed/26770425	*GAB2*	rs4945261
Jiang 2017	https://doi.org/10.1007/s12035-016-9706-8	*TREML2*	rs3747742
Jiao 2015	https://doi.org/10.1371/journal.pone.0144898	*BIN1*	rs744373
Jiao 2015	https://doi.org/10.1371/journal.pone.0144898	*MS4A*	rs1562990
Jiao 2015	https://doi.org/10.1371/journal.pone.0144898	*EXOC3L2*	rs597668
Jiao 2015	https://doi.org/10.1371/journal.pone.0144898	*HLA-DRB5/DRB1*	rs9271192
Jiao 2015	https://doi.org/10.1371/journal.pone.0144898	*TOMM40*	rs11556505
Jiao 2015	https://doi.org/10.1371/journal.pone.0144898	*TOMM40*	rs157581
Jin 2009	https://doi.org/10.3233/DMA-2009-0665	*ECE-1*	rs213045
Jonsson 2012	https://doi.org/10.1038/nature11283	*APP*	rs63750847

Study	DOI/PMID	Gene	rsID
Jun 2016	https://doi.org/10.1038/mp.2015.23	*KANSL1-MAPT*	rs2732703
Jun 2017	https://doi.org/10.1016/j.jalz.2016.12.012	*TSPOAP1*	rs2632516
Jun 2017	https://doi.org/10.1016/j.jalz.2016.12.012	*NFIC*	rs9749589
Keage 2010	https://doi.org/10.1093/ageing/afp210	*ACE*	rs4343
Kero 2013	https://doi.org/10.1016/j.neurobiolaging.2012.09.017	*APP*	rs63750847
Khoshbakht 2015	https://www.ncbi.nlm.nih.gov/pubmed/26306153	*IL6*	rs11556218
Khoshbakht 2015	https://www.ncbi.nlm.nih.gov/pubmed/26306153	*IL6*	rs4778889
Kok 2011	https://doi.org/10.1186/1742-2094-8-96	*CRP*	rs2794521
Koutroumani 2013	https://doi.org/10.1016/j.jns.2013.02.003	*ADRA2B*	NA
Kunkle 2018	https://doi.org/10.1101/294629	*INPP5D*	rs10933431
Kunkle 2018	https://doi.org/10.1101/294629	*ZCWPW1/NYAP1*	rs12539172
Kunkle 2018	https://doi.org/10.1101/294629	*EPHA1*	rs11762262
Kunkle 2018	https://doi.org/10.1101/294629	*CLU*	rs9331896
Kunkle 2018	https://doi.org/10.1101/294629	*SPI1*	rs3740688
Kunkle 2018	https://doi.org/10.1101/294629	*MS4A2*	rs7933202
Kunkle 2018	https://doi.org/10.1101/294629	*PICALM*	rs3851179
Kunkle 2018	https://doi.org/10.1101/294629	*SORL1*	rs11218343
Kunkle 2018	https://doi.org/10.1101/294629	*SLC24A4-RIN3*	rs12881735
Kunkle 2018	https://doi.org/10.1101/294629	*CASS4*	rs6024870
Kunkle 2018	https://doi.org/10.1101/294629	*ADAM10*	rs593742
Kunkle 2018	https://doi.org/10.1101/294629	*IQCK*	rs7185636
Kunkle 2018	https://doi.org/10.1101/294629	*ADAMTS1*	rs2830500

Study	DOI/PMID	Gene	rsID
Kwiatkowski 2016	https://doi.org/10.1159/000444643	*LIG1*	rs20579
Lalli 2015	https://doi.org/10.1038/mp.2015.131	*CCL11*	rs9909184
Lambert 2000a	https://doi.org/10.1093/oxfordjournals.hmg.a018918	*TFCP2*	rs13463
Lambert 2013	http://dx.doi.org/10.1038/ng.2802	*EPHA1*	rs11771145
Lambert 2013	http://dx.doi.org/10.1038/ng.2802	*CLU*	rs9331896
Lambert 2013	http://dx.doi.org/10.1038/ng.2802	*MS4A6A*	rs983392
Lambert 2013	http://dx.doi.org/10.1038/ng.2802	*PICALM*	rs10792832
Lambert 2013	http://dx.doi.org/10.1038/ng.2802	*CD33*	rs3865444
Lambert 2013	http://dx.doi.org/10.1038/ng.2802	*SLC24A4-RIN3*	rs10498633
Lambert 2013	http://dx.doi.org/10.1038/ng.2802	*DSG2*	rs8093731
Lambert 2013	http://dx.doi.org/10.1038/ng.2802	*MEF2C*	rs190982
Lambert 2013	http://dx.doi.org/10.1038/ng.2802	*NME8*	rs2718058
Lambert 2013	http://dx.doi.org/10.1038/ng.2802	*ZCWPW1/NYAP1*	rs1476679
Lambert 2013	http://dx.doi.org/10.1038/ng.2802	*CASS4*	rs7274581
Landgren 2012	https://doi.org/10.1007/s00702-012-0823-x	*ARC*	rs10097505
Landgren 2012	https://doi.org/10.1007/s00702-012-0823-x	*ARC*	NA
Leduc 2015	https://doi.org/10.1038/mp.2014.81	*HMGCR*	rs3846662
Li 2013	https://doi.org/10.1111/cns.12062	*LRRK2*	rs33949390
Li 2019	https://doi.org/10.1007/s00401-019-02066-0	*TMEM106B*	rs1990621
Lin 2012	https://doi.org/10.1007/s11033-011-1072-z	*HFE*	rs1799945
Liu 2014a	https://doi.org/10.1007/s12017-013-8250-1	*CLU*	rs11136000
Liu 2014a	https://doi.org/10.1007/s12017-013-8250-1	*CLU*	rs11136000

Study	DOI/PMID	Gene	rsID
Liu 2015	https://doi.org/10.3109/01677063.2015.1099651	*NTF-3*	rs6489630
Liu 2016	https://doi.org/10.1155/2016/9418163	*CHAT*	rs2177369
Liu 2017	https://doi.org/10.1038/ng.3766	*SPPL2A*	rs59685680
Logue 2018	https://doi.org/10.3389/fnins.2018.00592	*F5*	rs2027885
Logue 2018	https://doi.org/10.3389/fnins.2018.00592	*KIAA0196*	rs7817741
Logue 2018	https://doi.org/10.3389/fnins.2018.00592	*KIAA0196*	rs2272729
Logue 2018	https://doi.org/10.3389/fnins.2018.00592	*PTK2B*	rs115828696
Logue 2018	https://doi.org/10.3389/fnins.2018.00592	*SORL1*	rs3862606
Logue 2018	https://doi.org/10.3389/fnins.2018.00592	*PILRB*	rs11284139
Luedecking-Zimmer 2003	https://doi.org/10.1002/ajmg.b.10026	*LSF*	rs13463
Luo 2015	https://doi.org/10.1016/j.jns.2015.10.053	*PTSG2*	rs20417
Lupton 2014	https://doi.org/10.3233/JAD-131121	*ABCA1*	rs371168450, rs9282543, rs33918808
Lv 2008	https://doi.org/10.1016/j.neurobiolaging.2006.10.001	*APP*	rs466433
Lv 2008	https://doi.org/10.1016/j.neurobiolaging.2006.10.001	*APP*	rs364048
Ma 2009	https://doi.org/10.1016/j.neulet.2009.04.048	*NCSTN*	rs10752637
Ma 2012	https://doi.org/10.1016/j.neurobiolaging.2010.05.018	*PIN1*	rs2287839
Marioni 2018	https://doi.org/10.1038/s41398-018-0150-6	*BCKDK*	rs889555
Marioni 2018	https://doi.org/10.1038/s41398-018-0150-6	*PILRA*	rs1859788
Marioni 2018	https://doi.org/10.1038/s41398-018-0150-6	*TOMM40*	rs157580
Marioni 2018	https://doi.org/10.1038/s41398-018-0150-6	*PICALM*	rs10792832
Marioni 2018	https://doi.org/10.1038/s41398-018-0150-6	*CLU*	rs4236673
Marioni 2018	https://doi.org/10.1038/s41398-018-0150-6	*SORL1*	rs11218343

Study	DOI/PMID	Gene	rsID
Marioni 2018	https://doi.org/10.1038/s41398-018-0150-6	*MS4A*	rs11605427
Marioni 2018	https://doi.org/10.1038/s41398-018-0150-6	*ADAM10*	rs593742
Marioni 2018	https://doi.org/10.1038/s41398-018-0150-6	*CASS4*	rs6069736
Marioni 2018	https://doi.org/10.1038/s41398-018-0150-6	*ACE*	rs6504163
Martinez-Mir 2013	https://doi.org/10.3233/JAD-122257	*NRXN3*	rs17757879
Martiskainen 2017	https://doi.org/10.1002/ana.24969	*APP*	rs63750847
Milind 2020	https://doi.org/10.1371/journal.pgen.1008775	*TMEM106B*	rs1990620
Minoretti 2006	https://doi.org/10.1016/j.neulet.2005.08.047	*TLR4*	rs4986790
Miron 2018	https://doi.org/10.1016/j.jalz.2017.12.004	*CDK5RAP2/TLR4/DBC1*	rs4837766
Montesanto 2016	https://doi.org/10.3233/JAD-150993	*UCP5*	rs9472817
Moraes 2013	https://doi.org/10.1159/000350368	*IL6*	rs1800795
Moraes 2013	https://doi.org/10.1159/000350368	*IL10*	rs1800896
Mukherjee 2012	https://dx.doi.org/10.1007%2Fs11682-012-9184-1	*RNASE13*	rs3748348
Nho 2015	https://doi.org/10.1002/ana.24349	*REST*	rs3796529
Olgiati 2011	https://doi.org/10.4061/2011/832379	*CLU*	rs11136000
Olgiati 2011	https://doi.org/10.4061/2011/832379	*PICALM*	rs3851179
Olgiati 2011	https://doi.org/10.4061/2011/832379	*TNK1*	rs1554498
Olgiati 2011	https://doi.org/10.4061/2011/832379	*LDLR*	rs5930
Olgiati 2011	https://doi.org/10.4061/2011/832379	*CHRNB2*	rs4845378
Olgiati 2011	https://doi.org/10.4061/2011/832379	*CCR2*	rs1799864
Pan 2014	https://doi.org/10.1177/1533317514534760	*ESR1*	rs9340799
Pan 2014	https://doi.org/10.1177/1533317514534760	*ESR1*	rs2234693

Study	DOI/PMID	Gene	rsID
Perry 2008	https://doi.org/10.1016/j.neurobiolaging.2006.10.017	*HBG2*	rs7482144
Poduslo 2010	https://doi.org/10.1002/ajmg.b.30963	*LRP1B*	rs6732847
Ren 2016	https://doi.org/10.1016/j.neulet.2016.03.021	*LPL*	rs328
Ridge 2017	https://doi.org/10.1186/s13073-017-0486-1	*SAR1A*	rs7653
Ridge 2017	https://doi.org/10.1186/s13073-017-0486-1	*RAB10*	rs142787485
Santos-Reboucas 2017	https://doi.org/10.1007/s12017-017-8444-z	*PICALM*	rs3851179
Sanz 2014	https://doi.org/10.1016/j.exger.2014.10.009	*P2X7R*	rs208294
Sarajarvi 2010	https://doi.org/10.3233/JAD-2010-100597	*TNFa*	rs1800629
Sassi 2016	https://doi.org/10.1016/j.neurobiolaging.2016.04.004	*ABCA7*	rs72973581
Scacchi 2003	https://www.ncbi.nlm.nih.gov/pubmed/12618290	*PON1*	rs662
Scacchi 2013	https://doi.org/10.1159/000345788	*P21*	rs1059234
Scelsi 2018	https://doi.org/10.1093/brain/awy141	*LCORL*	rs6850306
Sevlever 2015	https://doi.org/10.1186/s13024-015-0015-x	*VAMP1*	rs2072376
Sims 2017	https://doi.org/10.1038/ng.3916	*PLCG2*	rs72824905
Song 2010	https://doi.org/10.1016/j.neulet.2010.05.049	*A2M*	rs226380
Spisak 2014	https://doi.org/10.1016/j.pjnns.2014.09.002	*SOD1*	rs2070424
Stamati 2019	https://doi.org/10.1007/s12031-019-01363-3	*SCFD1*	rs10139154
Su 2016	https://doi.org/10.1016/j.jocn.2015.11.032	*PTSG2*	rs20417
Tan 2013	https://doi.org/10.1016/j.jneuroim.2013.10.002	*NLRP3*	rs35829419
Tang 2013	https://doi.org/10.1007/s10072-012-1115-9	*PTSG2*	rs689466
Tian 2015	https://doi.org/10.1016/j.brainres.2014.11.019	*IL-33*	rs11792633
Uchida 2005	https://doi.org/10.1097/00019442-200512000-00005	*SIGMAR1*	rs1799729, rs1800866

Study	DOI/PMID	Gene	rsID
Van Deerlin 2010	https://dx.doi.org/10.1038%2Fng.536	*TMEM106B*	rs1990622
Vargas-Alarcon 2016	https://doi.org/10.1016/j.imlet.2016.07.011	*IL-10*	rs1800896
Vargas-Alarcon 2016	https://doi.org/10.1016/j.imlet.2016.07.011	*IL-10*	rs1800871
Vargas-Alarcon 2016	https://doi.org/10.1016/j.imlet.2016.07.011	*IL-10*	rs1800872
Vitali 2009	https://doi.org/10.1007/s00702-009-0324-8	*COX10*	rs11870213
Vitali 2009	https://doi.org/10.1007/s00702-009-0324-8	*COX15*	rs2231687
Wang 2002	https://doi.org/10.1007/s00439-002-0697-3	*SERPINA3*	rs11538071
Wang 2007	https://doi.org/10.1016/j.brainres.2007.02.005	*ABCA1*	rs2230806
Wang 2012	https://doi.org/10.1016/j.neulet.2012.08.044	*NEDD9*	rs760678
Wang 2015a	https://doi.org/10.3233/JAD-140729	*NOCT*	rs13116075
Wang 2015b	https://doi.org/10.1177/0891988714554707	*IDE*	rs1999764
Wang 2017	https://doi.org/10.1007/s40520-016-0539-0	*BACE1*	rs638405
Wu 2011	https://doi.org/10.1016/j.brainres.2010.12.036	*DAPK1*	rs4878104
Wu 2017	https://doi.org/10.18632/oncotarget.15380	*EXOC3L2*	rs597668
Yang 2015	https://doi.org/10.2174/1567205012030150317151426	*CUGBP2*	rs2242451
Yu 2012	https://doi.org/10.2174/156720512800492495	*TLR4*	rs10759930
Yu 2012	https://doi.org/10.2174/156720512800492495	*TLR4*	rs1927914
Yu 2012	https://doi.org/10.2174/156720512800492495	*TLR4*	rs1927911
Yu 2012	https://doi.org/10.2174/156720512800492495	*TLR4*	rs12377632
Yu 2012	https://doi.org/10.2174/156720512800492495	*TLR4*	rs2149356
Yu 2012	https://doi.org/10.2174/156720512800492495	*TLR4*	rs7037117
Yu 2012	https://doi.org/10.2174/156720512800492495	*TLR4*	rs7045953

Study	DOI/PMID	Gene	rsID
Zhang 2011	https://doi.org/10.1016/j.brainres.2010.10.074	*TFAM*	rs1937
Zhang 2017	https://doi.org/10.1007/s12035-016-9780-y	*SORL1*	rs11218343
Zhou 2008	https://doi.org/10.1016/j.neulet.2008.07.093	*LRP*	rs1799986
Zhou 2017	https://doi.org/10.1016/j.cca.2017.03.013	*BIN1*	rs242557
Zhou 2018	https://doi.org/10.1097/MD.0000000000012470	*CD36*	rs3211956
Zuo 2009	https://doi.org/10.1016/j.brainres.2008.10.034	*IDE*	rs4646954
Zuo 2009	https://doi.org/10.1016/j.brainres.2008.10.034	*IDE*	rs3758505

APPENDIX B

This serves as the Appendix for CHAPTER 2:

IDENTIFICATION OF COMMON GENETIC VARIANTS THAT MODIFY THE ASSOCIATION BETWEEN ALZHEIMER'S DISEASE BIOMARKERS AND HIPPOCAMPAL VOLUME

B.1 ACKNOWLEDGEMENTS

The results published here are in whole or in part based on data obtained from Agora, a platform initially developed by the National Institute on Aging-funded AMP-AD consortium that shares evidence in support of Alzheimer's disease target discovery. We also want to acknowledge the participants and investigators of the FinnGen study. In addition, data collection and sharing for this project was funded by the Alzheimer's Disease Neuroimaging Initiative and the Vanderbilt Memory & Alzheimer's Center. Funding details are provided in the Funding section below.

B.2 FUNDING SOURCES

This research was supported in part by grants K01-AG049164, K24-AG046373, R01-AG059716, R01-AG034962, R01-HL111516, R01-NS100980, R01-AG056534, R01-AG027161, R01-AG054047, R01-AG021155, R01-AG037639, U01-AG46152, U01-AG006781, U01-AG032984, U01-HG004610, U01-HG006375, U19-AG033655, U24-AG021886, and U24-AG041689 from the Intramural Research Program, the National Institute on Aging, the National Institutes of Health, the Vanderbilt University Advanced Computing Center for Research and

Education (ACCRE) instrumentation grant (S10-OD023680), the Vanderbilt Institute for Clinical and Translational Research (VICTR) grant (UL1-TR000445, UL1-TR002243), and the Vanderbilt Memory & Alzheimer's Center. Dr. Deming is supported by the National Institute on Aging T32AG000213 Biology of Aging and Age-Related Disease training grant. Dr. Zetterberg is a Wallenberg Scholar supported by grants from the Swedish Research Council (#2018-02532), the European Research Council (#681712), Swedish State Support for Clinical Research (#ALFGBG-720931), the Alzheimer's Drug Discovery Foundation, USA (#201809-2016862), and the UK Dementia Research Institute at UCL. Dr. Blennow is supported by the Swedish Research Council (#2017-00915), the Alzheimer Drug Discovery Foundation, USA (#RDAPB-201809-2016615), the Swedish Alzheimer Foundation (#AF-742881), Hjärnfonden, Sweden (#FO2017-0243), the Swedish state under the agreement between the Swedish government and the County Councils, the ALF-agreement (#ALFGBG-715986), and European Union Joint Program for Neurodegenerative Disorders (JPND2019-466-236). Work with the MCSA data was supported by National Institutes of Health grants U01-AG006786, R01-NS097495, R01-AG56366, P50-AG016574, P30-AG062677, R37-AG011378, R01-AG041851, R01-AG034676 and the GHR Foundation. Data collection and sharing for ADNI were supported by National Institutes of Health Grant U01-AG024904 and Department of Defense (award number W81XWH-12-2-0012). ADNI is also funded by the National Institute on Aging, the National Institute of Biomedical Imaging and Bioengineering, and through generous contributions from the following: AbbVie, Alzheimer's Association; Alzheimer's Drug Discovery Foundation; Araclon Biotech; BioClinica, Inc.; Biogen; Bristol-Myers Squibb Company; CereSpir, Inc.; Cogstate; Eisai Inc.; Elan Pharmaceuticals, Inc.; Eli Lilly and Company; EuroImmun; F. Hoffmann-La Roche Ltd and its affiliated company Genentech, Inc.; Fujirebio; GE Healthcare; IXICO Ltd.; Janssen Alzheimer Immunotherapy

Research & Development, LLC.; Johnson & Johnson Pharmaceutical Research & Development LLC.; Lumosity; Lundbeck; Merck & Co., Inc.; Meso Scale Diagnostics, LLC.; NeuroRx Research; Neurotrack Technologies; Novartis Pharmaceuticals Corporation; Pfizer Inc.; Piramal Imaging; Servier; Takeda Pharmaceutical Company; and Transition Therapeutics. The Canadian Institutes of Health Research is providing funds to support ADNI clinical sites in Canada. Private sector contributions are facilitated by the Foundation for the National Institutes of Health (www.fnih.org). The grantee organization is the Northern California Institute for Research and Education, and the study is coordinated by the Alzheimer's Therapeutic Research Institute at the University of Southern California. ADNI data are disseminated by the Laboratory for Neuro Imaging at the University of Southern California.

B.3 APPENDIX TABLES

Due to size, some tables within the Appendix will be abridged. Full tables will be available at *Brain Communications* and are also available by request.

Table B.1: Top 20 suggestively significant ($p < 1x10^{-5}$) SNPs in the SNP x CSF Aβ42 GWAS on baseline hippocampal volume.

Abbreviations: CHR, chromosome; A1, minor allele; SE, standard error; L95, lower 95% confidence interval, U95, upper 95% CI.

CHR	SNP	A1	N	Beta	SE	L95	U95	P
8	rs11135840	A	1065	0.1549	0.03111	0.09396	0.2159	7.42E-07
8	rs7017203	C	1065	0.1549	0.03111	0.09396	0.2159	7.42E-07
6	rs2185921	A	1065	-0.3096	0.06242	-0.432	-0.1873	8.21E-07
8	rs9314297	G	1065	0.1539	0.03114	0.09289	0.215	8.96E-07
6	rs77207148	A	1065	-0.3101	0.06289	-0.4333	-0.1868	9.52E-07
6	rs74419807	C	1065	-0.3101	0.06289	-0.4333	-0.1868	9.52E-07
6	rs79140486	A	1065	-0.3101	0.06289	-0.4333	-0.1868	9.52E-07
20	rs768875	G	1065	-0.2005	0.04102	-0.2809	-0.1201	1.18E-06
20	rs1624243	T	1065	-0.2005	0.04102	-0.2809	-0.1201	1.18E-06
20	rs562596	C	1065	-0.2005	0.04102	-0.2809	-0.1201	1.18E-06
20	rs845710	G	1065	-0.2005	0.04102	-0.2809	-0.1201	1.18E-06
20	rs439580	C	1065	-0.2005	0.04102	-0.2809	-0.1201	1.18E-06
20	rs550630	T	1065	-0.1992	0.04102	-0.2796	-0.1188	1.38E-06
20	rs552504	T	1065	-0.1988	0.04102	-0.2792	-0.1184	1.45E-06
5	rs1564800	A	1065	0.1775	0.03717	0.1046	0.2504	2.05E-06
20	rs1884197	T	1065	-0.1924	0.041	-0.2728	-0.112	3.06E-06
19	rs283815	G	1065	0.157	0.03382	0.09068	0.2233	3.90E-06
6	rs116083533	A	1065	-0.2904	0.06259	-0.413	-0.1677	3.94E-06
8	rs2320782	T	1065	0.1455	0.03146	0.08381	0.2071	4.23E-06
17	rs7220473	T	1065	-0.1558	0.03383	-0.2221	-0.08953	4.60E-06

Table B.2: Top 20 suggestively significant ($p < 1x10^{-5}$) SNPs in the SNP x CSF Aβ42 GWAS on annual change in hippocampal volume.

Abbreviations: CHR, chromosome; A1, minor allele; SE, standard error; L95, lower 95% confidence interval, U95, upper 95% CI.

CHR	SNP	A1	N	Beta	SE	L95	U95	P
3	rs4677869	T	1065	0.01559	0.00283	0.01005	0.02114	4.50E-08
3	rs2288678	G	1065	0.01602	0.002949	0.01024	0.0218	6.90E-08
3	rs11706210	C	1065	0.01546	0.002938	0.009697	0.02122	1.74E-07
3	rs11707039	A	1065	0.01546	0.002938	0.009697	0.02122	1.74E-07
3	rs4677982	C	1065	0.01507	0.002929	0.009331	0.02081	3.17E-07
3	rs4677983	A	1065	0.01494	0.002923	0.009213	0.02067	3.79E-07
3	rs4677984	T	1065	0.01494	0.002923	0.009213	0.02067	3.79E-07
3	rs4677870	C	1065	0.01494	0.002923	0.009213	0.02067	3.79E-07
3	rs35989119	C	1065	0.01484	0.002925	0.009106	0.02057	4.62E-07
3	rs10934625	C	1065	0.01483	0.002925	0.0091	0.02057	4.67E-07
1	rs113393658	A	1065	-0.02517	0.005098	-0.03517	-0.01518	9.18E-07
1	rs146752822	A	1065	-0.02517	0.005098	-0.03517	-0.01518	9.18E-07
1	rs12132798	G	1065	-0.02517	0.005098	-0.03517	-0.01518	9.18E-07
1	rs12123296	T	1065	-0.02508	0.005099	-0.03507	-0.01508	1.01E-06
1	rs12126534	A	1065	-0.02508	0.005099	-0.03507	-0.01508	1.01E-06
1	rs112735413	A	1065	-0.02508	0.005099	-0.03507	-0.01508	1.01E-06
1	rs75410548	C	1065	-0.02508	0.005099	-0.03507	-0.01508	1.01E-06
1	rs76992333	T	1065	-0.02508	0.005099	-0.03507	-0.01508	1.01E-06
1	rs77107095	A	1065	-0.02476	0.00504	-0.03464	-0.01488	1.04E-06
1	rs112636864	A	1065	-0.02476	0.00504	-0.03464	-0.01488	1.04E-06

Table B.3: Top 20 suggestively significant ($p < 1x10^{-5}$) SNPs in the SNP x CSF p-tau GWAS on baseline hippocampal volume.

Abbreviations: CHR, chromosome; A1, minor allele; SE, standard error; L95, lower 95% confidence interval, U95, upper 95% CI.

CHR	SNP	A1	N	Beta	SE	L95	U95	P
7	rs2005751	T	1065	0.2868	0.05847	0.1722	0.4014	1.08E-06
4	rs2732177	A	1065	-0.2672	0.05579	-0.3765	-0.1578	1.91E-06
4	rs2732176	G	1065	-0.2672	0.05579	-0.3765	-0.1578	1.91E-06
4	rs2627722	T	1065	-0.2659	0.05581	-0.3753	-0.1565	2.15E-06
4	rs2627679	T	1065	-0.2665	0.05602	-0.3763	-0.1568	2.22E-06
4	rs2732200	G	1065	-0.2665	0.05602	-0.3763	-0.1568	2.22E-06
4	rs2627678	A	1065	-0.2665	0.05602	-0.3763	-0.1568	2.22E-06
7	rs2008810	C	1065	0.2841	0.05976	0.167	0.4012	2.27E-06
4	rs2627677	G	1065	-0.2662	0.05601	-0.376	-0.1564	2.29E-06
4	rs2627676	G	1065	-0.2662	0.05601	-0.376	-0.1564	2.29E-06
4	rs2627675	C	1065	-0.2662	0.05601	-0.376	-0.1564	2.29E-06
4	rs2732199	A	1065	-0.2662	0.05601	-0.376	-0.1564	2.29E-06
4	rs2627672	G	1065	-0.2662	0.05601	-0.376	-0.1564	2.29E-06
4	rs2732198	T	1065	-0.2662	0.05601	-0.376	-0.1564	2.29E-06
4	rs2732197	C	1065	-0.2662	0.05601	-0.376	-0.1564	2.29E-06
4	rs2732195	T	1065	-0.2662	0.05601	-0.376	-0.1564	2.29E-06
4	rs2732194	T	1065	-0.2662	0.05601	-0.376	-0.1564	2.29E-06
4	rs17013031	A	1065	-0.2662	0.05601	-0.376	-0.1564	2.29E-06
4	rs17013033	G	1065	-0.2662	0.05601	-0.376	-0.1564	2.29E-06
4	rs17013036	C	1065	-0.2662	0.05601	-0.376	-0.1564	2.29E-06

Table B.4: Top 20 suggestively significant ($p < 1x10^{-5}$) SNPs in the SNP x CSF p-tau GWAS on annual change in hippocampal volume.

CHR	SNP	A1	N	Beta	SE	L95	U95	P
3	rs114106809	T	1065	0.05861	0.01085	0.03735	0.07988	8.14E-08
3	rs75600480	A	1065	0.058	0.01079	0.03685	0.07915	9.46E-08
3	rs78673878	C	1065	0.05904	0.01108	0.03733	0.08075	1.20E-07
3	rs79531054	G	1065	0.06429	0.01208	0.04062	0.08797	1.25E-07
3	rs73173513	C	1065	0.05882	0.01107	0.03712	0.08053	1.33E-07
19	rs77655458	T	1065	0.02202	0.004593	0.01302	0.03102	1.86E-06
19	rs79317238	A	1065	0.02202	0.004593	0.01302	0.03102	1.87E-06
19	rs77643967	T	1065	0.02202	0.004593	0.01302	0.03102	1.87E-06
19	rs16992410	G	1065	0.02202	0.004593	0.01302	0.03102	1.87E-06
19	rs75916762	A	1065	0.02202	0.004593	0.01302	0.03102	1.87E-06
19	rs79980542	C	1065	0.02202	0.004593	0.01302	0.03102	1.87E-06
19	rs74715939	A	1065	0.02191	0.0046	0.01289	0.03092	2.17E-06
19	rs141742577	C	1065	0.02204	0.004631	0.01296	0.03112	2.21E-06
3	rs62238463	G	1065	0.03176	0.006679	0.01867	0.04485	2.25E-06
19	rs11672696	T	1065	0.02184	0.004595	0.01283	0.03084	2.30E-06
19	rs77753384	G	1065	0.02185	0.004599	0.01283	0.03086	2.31E-06
19	rs78879389	A	1065	0.02184	0.004598	0.01283	0.03085	2.31E-06
19	rs75856878	T	1065	0.02184	0.004598	0.01283	0.03085	2.31E-06
19	rs76243172	A	1065	0.02184	0.004598	0.01283	0.03085	2.31E-06
19	rs76614870	T	1065	0.02184	0.004598	0.01283	0.03085	2.31E-06

Table B.5: All suggestively significant ($p < 1x10^{-5}$) SNPs in the SNP x CSF tau GWAS on baseline hippocampal volume.

CHR	SNP	A1	N	Beta	SE	L95	U95	P
2	rs6435166	T	1065	-0.1996	0.04198	-0.2818	-0.1173	2.27E-06
5	rs254028	C	1065	-0.2035	0.0431	-0.288	-0.119	2.65E-06
19	rs4806251	T	1065	-0.3142	0.06663	-0.4447	-0.1836	2.74E-06
5	rs254026	C	1065	-0.1983	0.04227	-0.2812	-0.1155	3.06E-06
19	rs8105294	A	1065	-0.3099	0.06632	-0.4399	-0.18	3.34E-06
5	rs173825	C	1065	-0.1974	0.0423	-0.2803	-0.1145	3.45E-06
5	rs453632	T	1065	-0.2018	0.0434	-0.2869	-0.1168	3.73E-06
19	rs10405023	C	1065	-0.3082	0.06638	-0.4383	-0.1781	3.87E-06
16	rs9927279	G	1065	-0.1717	0.03702	-0.2443	-0.09919	3.94E-06
10	rs10786273	A	1065	-0.323	0.06965	-0.4595	-0.1865	3.96E-06
6	rs13437308	T	1065	-0.2283	0.04931	-0.325	-0.1317	4.10E-06
5	rs33820	A	1065	-0.1959	0.04276	-0.2797	-0.112	5.20E-06
13	rs4377014	T	1065	-0.1565	0.03432	-0.2237	-0.0892	5.73E-06
13	rs2475538	T	1065	-0.1563	0.03433	-0.2236	-0.08902	5.91E-06
13	rs3011022	C	1065	-0.1563	0.03433	-0.2236	-0.08902	5.91E-06
13	rs61946436	G	1065	-0.1572	0.03463	-0.2251	-0.08933	6.28E-06
13	rs326508	A	1065	-0.1552	0.03427	-0.2223	-0.08799	6.64E-06
13	rs326507	T	1065	-0.1552	0.03427	-0.2223	-0.08799	6.64E-06
6	rs11967828	T	1065	-0.2196	0.04872	-0.3151	-0.1241	7.31E-06
6	rs7762227	C	1065	-0.2194	0.0487	-0.3148	-0.1239	7.38E-06
6	rs6925949	A	1065	-0.22	0.04886	-0.3157	-0.1242	7.47E-06
6	rs9501991	A	1065	-0.2175	0.04859	-0.3127	-0.1223	8.43E-06

Table B.6: Top 20 suggestively significant ($p < 1x10^{-5}$) SNPs in the SNP x CSF tau GWAS on annual change in hippocampal volume.

CHR	BP	A1	N	Beta	SE	L95	U95	P
9	130164818	T	1065	0.01505	0.002898	0.009374	0.02073	2.45E-07
9	130242166	A	1065	0.0152	0.002951	0.009412	0.02098	3.12E-07
9	130248885	T	1065	0.013	0.002542	0.008016	0.01798	3.76E-07
9	130238024	T	1065	0.01312	0.002578	0.008073	0.01818	4.20E-07
9	130238540	A	1065	0.01312	0.002578	0.008073	0.01818	4.20E-07
9	130249144	C	1065	0.01312	0.002578	0.008073	0.01818	4.20E-07
9	130257205	G	1065	0.01312	0.002578	0.008071	0.01818	4.21E-07
9	130240980	A	1065	0.01495	0.002948	0.009174	0.02073	4.65E-07
9	130241822	T	1065	0.01495	0.002948	0.009174	0.02073	4.65E-07
9	130246660	T	1065	0.01495	0.002948	0.009174	0.02073	4.65E-07
9	130255810	C	1065	0.01495	0.002948	0.009171	0.02073	4.67E-07
9	130266566	A	1065	0.01314	0.002592	0.008059	0.01822	4.71E-07
1	221831337	C	1065	-0.01629	0.003255	-0.02267	-0.009909	6.58E-07
1	221854085	T	1065	-0.01618	0.003247	-0.02255	-0.009819	7.27E-07
1	221854205	A	1065	-0.01618	0.003247	-0.02255	-0.009819	7.27E-07
1	221855326	C	1065	-0.0162	0.003255	-0.02258	-0.009824	7.48E-07
1	221833258	C	1065	-0.01616	0.003247	-0.02253	-0.0098	7.50E-07
1	221833607	C	1065	-0.01616	0.003247	-0.02253	-0.0098	7.50E-07
1	221833685	C	1065	-0.01616	0.003247	-0.02253	-0.0098	7.50E-07
1	221833729	C	1065	-0.01616	0.003247	-0.02253	-0.0098	7.50E-07

Table B.7: Top 20 MAGMA gene associations using summary statistics from SNP x CSF Aβ42 GWAS on annual change in hippocampal volume.

GENE	CHR	START	STOP	NSNPS	NPARAM	N	ZSTAT	P	p.fdr
TOMM40	19	45394477	45406946	27	4	1065	4.1584	1.60E-05	0.27952691
LOC101060400	17	46712166	46724875	37	7	1065	3.8579	5.72E-05	0.49866435
USH2A	1	215796236	216596738	1692	156	1065	3.6109	0.00015256	0.56229784
DPYD	1	97543299	98386615	1574	127	1065	3.5775	0.00017343	0.56229784
HOXB9	17	46698518	46703835	14	3	1065	3.5736	0.00017605	0.56229784
PACS1	11	65837747	66012218	225	13	1065	3.5489	0.00019344	0.56229784
APOE	19	45409039	45412650	4	2	1065	3.4169	0.00031675	0.78920525
CDK5RAP3	17	46047894	46059152	28	4	1065	3.2917	0.00049798	0.82081371
MBTPS1	16	84087368	84150517	225	24	1065	3.2829	0.0005138	0.82081371
NRL	14	24547902	24584223	27	6	1065	3.2798	0.00051942	0.82081371
COBL	7	51083909	51384515	480	38	1065	3.278	0.00052272	0.82081371
ISM1	20	13202418	13281297	202	24	1065	3.2419	0.00059376	0.82081371
HOXB3	17	46626232	46667634	79	14	1065	3.2333	0.00061181	0.82081371
HOXB13	17	46802125	46806111	7	4	1065	3.1058	0.0009488	0.84276115
CAPN10	2	241526133	241538526	49	5	1065	3.1003	0.00096669	0.84276115
PPA1	10	71962586	71993667	97	12	1065	3.0624	0.0010979	0.84276115
IL12RB2	1	67773047	67862583	199	14	1065	3.0573	0.0011165	0.84276115
LTBR	12	6484534	6500737	6	2	1065	3.0522	0.0011358	0.84276115
DCAF11	14	24583906	24594451	14	2	1065	2.9967	0.0013644	0.84276115
YIF1A	11	66052051	66056638	5	2	1065	2.9663	0.001507	0.84276115

Table B.8. Top 20 MAGMA gene associations using summary statistics from SNP x CSF Aβ42 GWAS on annual change in hippocampal volume when including *APOE4* status as a covariate in the GWAS.

GENE	CHR	START	STOP	NSNPS	NPARAM	N	ZSTAT	P	p.fdr
DPYD	1	97543299	98386615	1574	127	1058	3.919	4.45E-05	0.7432733
LOC101060400	17	46712166	46724875	37	7	1058	3.5103	0.00022376	0.7432733
MICU3	8	16884747	16980148	234	23	1058	3.4812	0.00024961	0.7432733
PACS1	11	65837747	66012218	225	13	1058	3.4777	0.00025283	0.7432733
COBL	7	51083909	51384515	480	38	1058	3.431	0.00030067	0.7432733
OR10H2	19	15838834	15839862	5	2	1058	3.4288	0.0003031	0.7432733
USH2A	1	215796236	216596738	1692	156	1058	3.3874	0.00035276	0.7432733
HOXB9	17	46698518	46703835	14	3	1058	3.331	0.00043267	0.7432733
ISM1	20	13202418	13281297	202	24	1058	3.3236	0.00044424	0.7432733
TLDC1	16	84509966	84538366	151	21	1058	3.3122	0.00046289	0.7432733
ACD	16	67691415	67694718	4	2	1058	3.2379	0.00060204	0.7432733
HOXB3	17	46626232	46667634	79	14	1058	3.1576	0.00079542	0.7432733
FIZ1	19	56102737	56110893	10	3	1058	3.1311	0.00087088	0.7432733
NRL	14	24547902	24584223	27	6	1058	3.1308	0.00087153	0.7432733
CAPN10	2	241526133	241538526	49	5	1058	3.1189	0.00090762	0.7432733
TOMM40	19	45394477	45406946	27	4	1058	3.1069	0.00094531	0.7432733
DCAF11	14	24583906	24594451	14	2	1058	3.0864	0.0010129	0.7432733
IL12RB2	1	67773047	67862583	199	14	1058	3.0697	0.0010714	0.7432733
SPNS2	17	4402129	4443228	54	7	1058	3.0502	0.0011433	0.7432733
VILL	3	38032217	38048676	41	5	1058	3.0365	0.0011967	0.7432733

Table B.9: Top 20 MAGMA pathway associations using summary statistics from SNP x CSF Aβ42 GWAS on annual change in hippocampal volume.

FULL_NAME	BETA	BETA_STD	SE	P	p.fdr
GO_REGULATION_OF_DOUBLE_STRAND_BREAK_REPAIR	0.35356	0.020355	0.1033	0.00031104	0.4851339
GO_NEGATIVE_REGULATION_OF_CELL_CYCLE_PHASE_TRANSITION	0.19246	0.02148	0.05654	0.00033282	0.4851339
GO_TUBE_CLOSURE	0.31393	0.021863	0.093128	0.00037544	0.4851339
GO_HEMATOPOIETIC_PROGENITOR_CELL_DIFFERENTIATION	0.23309	0.021665	0.069213	0.00037995	0.4851339
GO_SCF_DEPENDENT_PROTEASOMAL_UBIQUITIN_ DEPENDENT_PROTEIN_CATABOLIC_PROCESS	0.3073	0.021149	0.091365	0.00038574	0.4851339
GO_CELLULAR_RESPONSE_TO_PROSTAGLANDIN_STIMULUS	0.70559	0.024469	0.21046	0.0004012	0.4851339
REACTOME_DEGRADATION_OF_BETA_CATENIN_ BY_THE_DESTRUCTION_COMPLEX	0.32417	0.021493	0.0981	0.00047676	0.4851339
GO_POSITIVE_REGULATION_OF_MICROGLIAL_CELL_MIGRATION	1.0484	0.017749	0.31811	0.00049201	0.4851339
GO_STAT_FAMILY_PROTEIN_BINDING	0.84409	0.016908	0.25622	0.00049422	0.4851339
GO_POSITIVE_REGULATION_OF_VIRAL_ENTRY_INTO_HOST_CELL	0.78362	0.017797	0.23979	0.00054289	0.4851339
GO_NEURON_PROJECTION_MAINTENANCE	0.78012	0.017717	0.23934	0.00055924	0.4851339
GO_CELLULAR_RESPONSE_TO_PROSTAGLANDIN_E_STIMULUS	0.80314	0.023544	0.24691	0.00057275	0.4851339
GO_MITOTIC_DNA_INTEGRITY_CHECKPOINT	0.25977	0.019418	0.080063	0.00058948	0.4851339
BIOCARTA_FBW7_PATHWAY	0.80906	0.018375	0.25093	0.00063294	0.4851339
GO_CENTRAL_ELEMENT	1.0939	0.021911	0.34042	0.00065733	0.4851339
GO_PROTEIN_KINASE_ACTIVITY	0.11181	0.019297	0.03513	0.00073108	0.4851339
BIOCARTA_SKP2E2F_PATHWAY	0.76947	0.01842	0.24196	0.00073737	0.4851339
REACTOME_SCF_SKP2_MEDIATED_DEGRADATION_OF_P27_P21	0.34028	0.019251	0.1075	0.00077573	0.4851339
GO_RESPONSE_TO_PROSTAGLANDIN_E	0.65028	0.022009	0.2059	0.00079532	0.4851339
GO_ASTROCYTE_CELL_MIGRATION	0.90855	0.019455	0.28803	0.00080588	0.4851339

Table B.10: Top 20 MAGMA pathway associations using summary statistics from SNP x CSF Aβ42 GWAS on annual change in hippocampal volume when including *APOE4* status as a covariate in the GWAS.

FULL_NAME	BETA	BETA_STD	SE	P	p.fdr
BIOCARTA_FBW7_PATHWAY	0.93096	0.021143	0.25383	0.00012279	0.46831349
BIOCARTA_SKP2E2F_PATHWAY	0.89436	0.02141	0.24475	0.0001294	0.46831349
GO_PROTEIN_KINASE_ACTIVITY	0.1268	0.021884	0.035536	0.00018032	0.46831349
GO_NEGATIVE_REGULATION_OF_ CELL_CYCLE_PHASE_TRANSITION	0.20093	0.022425	0.057196	0.00022213	0.46831349
GO_HEMATOPOIETIC_PROGENITOR_CELL_DIFFERENTIATION	0.24015	0.022322	0.070017	0.00030274	0.46831349
GO_REGULATION_OF_STEM_CELL_DIFFERENTIATION	0.27861	0.021553	0.081473	0.00031438	0.46831349
REACTOME_G2_PHASE	0.88217	0.014935	0.25969	0.00034151	0.46831349
GO_POSITIVE_REGULATION_OF_MICROGLIAL_CELL_MIGRATION	1.0915	0.018479	0.3218	0.00034792	0.46831349
GO_POSITIVE_REGULATION_OF_VIRAL_ENTRY_INTO_HOST_CELL	0.81558	0.018523	0.24258	0.0003876	0.46831349
GO_NEGATIVE_REGULATION_OF_PROTEIN_ LOCALIZATION_TO_CELL_PERIPHERY	0.49089	0.018198	0.14605	0.00038915	0.46831349
GO_G1_DNA_DAMAGE_CHECKPOINT	0.35066	0.020702	0.10553	0.00044638	0.46831349
GO_MITOTIC_DNA_INTEGRITY_CHECKPOINT	0.26838	0.020061	0.080993	0.00046162	0.46831349
REACTOME_SYNDECAN_INTERACTIONS	0.53621	0.020688	0.16497	0.00057743	0.50657753
GO_ASTROCYTE_CELL_MIGRATION	0.94636	0.020264	0.29138	0.00058256	0.50657753
GO_NEGATIVE_REGULATION_OF_MITOTIC_CELL_CYCLE	0.1574	0.019956	0.049514	0.00074088	0.53250858
GO_KINASE_ACTIVITY	0.1007	0.019534	0.031702	0.00074698	0.53250858
REACTOME_HEME_BIOSYNTHESIS	0.76593	0.018335	0.24331	0.00082359	0.53250858
REACTOME_CYCLIN_A:CDK2_ASSOCIATED_EVENTS_AT_S_PHASE_ENTRY	0.2707	0.018406	0.086344	0.00086033	0.53250858
GO_NEGATIVE_REGULATION_OF_PROTEIN_ LOCALIZATION_TO_MEMBRANE	0.41975	0.016805	0.13744	0.0011303	0.53250858
REACTOME_TRANSCRIPTIONAL_REGULATION_BY_RUNX2	0.2563	0.020107	0.083963	0.0011365	0.53250858

Table B.11. Top 20 MAGMA gene associations using summary statistics from SNP x CSF p-tau GWAS on annual change in hippocampal volume.

GENE	CHR	START	STOP	NSNPS	NPARAM	N	ZSTAT	P	p.fdr
PLCB4	20	9049357	9461463	666	63	1065	4.0521	2.54E-05	0.44258282
LRSAM1	9	130213765	130265780	104	12	1065	3.8749	5.33E-05	0.4508096
HDGFRP2	19	4472255	4502223	84	8	1065	3.7809	7.81E-05	0.4508096
HEATR3	16	50099881	50139392	92	6	1065	3.6975	0.00010888	0.4508096
MIPEP	13	24304328	24463587	356	22	1065	3.5303	0.00020753	0.4508096
SEC61B	9	101984570	101992901	14	1	1065	3.5058	0.00022765	0.4508096
ANTXR1	2	69240276	69476459	473	61	1065	3.4694	0.00026083	0.4508096
OR8B2	11	124252298	124276648	46	3	1065	3.4654	0.00026467	0.4508096
EPB41L4B	9	111934254	112083021	249	35	1065	3.4487	0.00028163	0.4508096
TRAPPC4	11	118889241	118894384	17	2	1065	3.4354	0.00029583	0.4508096
PABPC1	8	101715144	101734969	20	3	1065	3.3614	0.00038772	0.4508096
EPB41L5	2	120770604	120936697	225	9	1065	3.3598	0.00039004	0.4508096
NCLN	19	3185875	3209573	72	6	1065	3.3587	0.00039153	0.4508096
CDKN1C	11	2904448	2907063	1	1	1065	3.3295	0.000435	0.4508096
PIGG	4	492989	533320	113	5	1065	3.3136	0.00046058	0.4508096
TOX	8	59717977	60031767	608	61	1065	3.3012	0.00048144	0.4508096
EBF3	10	131633496	131762546	76	18	1065	3.2988	0.00048554	0.4508096
SLC37A4	11	118895061	118901616	9	2	1065	3.2739	0.00053032	0.4508096
AOAH	7	36552549	36764154	489	57	1065	3.2617	0.00055381	0.4508096
VGLL2	6	117586721	117594728	17	2	1065	3.2535	0.00056988	0.4508096

Table B.12. Top 20 MAGMA pathway associations using summary statistics from SNP x CSF p-tau GWAS on annual change in hippocampal volume.

FULL_NAME	BETA	BETA_STD	SE	P	p.fdr
GO_ENDOLYSOSOME_LUMEN	1.302	0.022042	0.3531	0.00011375	0.77298813
REACTOME_EXTRACELLULAR_MATRIX_ORGANIZATION	0.19631	0.02476	0.05365	0.00012699	0.77298813
GO_GLUTAMINE_TRANSPORT	1.0037	0.018613	0.28924	0.00026084	0.84970462
GO_REGULATION_OF_CARTILAGE_DEVELOPMENT	0.40241	0.023366	0.11777	0.00031737	0.84970462
GO_L_GLUTAMINE_TRANSMEMBRANE_TRANSPORTER_ACTIVITY	1.0217	0.017298	0.30174	0.00035526	0.84970462
REACTOME_GLUCAGON_TYPE_LIGAND_RECEPTORS	0.51322	0.020178	0.15363	0.00041878	0.84970462
GO_VESICLE_TARGETING	0.28065	0.019545	0.086155	0.00056308	0.8708044
REACTOME_TRANSPORT_OF_BILE_SALTS_AND_ ORGANIC_ACIDS_METAL_IONS_AND_AMINE_COMPOUNDS	0.30527	0.021009	0.096323	0.0007658	0.8708044
GO_DRUG_TRANSMEMBRANE_TRANSPORT	0.31868	0.020854	0.1014	0.00083845	0.8708044
REACTOME_METABOLISM_OF_ANGIOTENSINOGEN_TO_ANGIOTENSINS	0.73571	0.021567	0.23537	0.00088847	0.8708044
GO_GLIAL_CELL_FATE_SPECIFICATION	1.3925	0.023575	0.44934	0.00097265	0.8708044
GO_ALANINE_TRANSPORT	0.84677	0.020271	0.2738	0.00099367	0.8708044
GO_SPLICEOSOMAL_CONFORMATIONAL_CHANGES_TO_ GENERATE_CATALYTIC_CONFORMATION	1.0782	0.018253	0.34885	0.0010003	0.8708044
GO_INTRINSIC_COMPONENT_OF_PLASMA_MEMBRANE	0.07221	0.020453	0.023676	0.0011463	0.8708044
GO_REGULATION_OF_SYSTEMIC_ARTERIAL_ BLOOD_PRESSURE_BY_HORMONE	0.48269	0.021292	0.15862	0.0011731	0.8708044
GO_METHYLTRANSFERASE_COMPLEX	0.23789	0.018403	0.078979	0.0012994	0.8708044
GO_ADAPTATION_OF_SIGNALING_PATHWAY	0.65069	0.019075	0.21696	0.0013558	0.8708044
GO_GOLGI_VESICLE_BUDDING	0.28021	0.018091	0.09346	0.0013601	0.8708044
GO_REGULATION_OF_PROTEIN_KINASE_C_ACTIVITY	1.4651	0.022186	0.49138	0.0014361	0.8708044
REACTOME_ADP_SIGNALLING_THROUGH_P2Y_PURINOCEPTOR_12	0.52123	0.017641	0.17548	0.0014899	0.8708044

APPENDIX C

This serves as the Appendix for CHAPTER 3:

EXAMINING TRANSCRIPTOMIC MODIFIERS OF THE *APOE*-ε4 EFFECTS ON COGNITION

C.1 ACKNOWLEDGEMENTS

The results published here are in whole or in part based on data obtained from Agora and the AD Knowledge Portal (https://adknowledgeportal.org), which are supported by the NIA-funded AMP-AD consortium that shares evidence in support of AD target discovery.

C.2 FUNDING SOURCES

This research was supported in part by grants K01AG049164, K24AG046373, R21AG059941, R01AG059716, R01AG034962, R01HL111516, R01NS100980, R01AG056534, RF1AG15819 from the Intramural Research Program, the National Institute on Aging, the National Institutes of Health, the Vanderbilt University Advanced Computing Center for Research and Education (ACCRE) instrumentation grant (S10OD023680), the Vanderbilt Institute for Clinical and Translational Research (VICTR) grant (UL1TR000445, UL1TR002243), and the Vanderbilt Memory & Alzheimer's Center.

Additional study data were provided by the Rush Alzheimer's Disease Center, Rush University Medical Center, Chicago. Data collection was supported through funding by NIA grants P30AG010161 (ROS), R01AG015819 (ROSMAP; genomics and RNAseq), R01AG017917 (MAP), R01AG030146, R01AG036042 (5hC methylation, ATACseq), RC2AG036547 (H3K9Ac), R01AG036836 (RNAseq), R01AG408015 (monocyte RNAseq) RF1AG057473 (single nucleus RNAseq), U01AG032984 (genomic and whole exome sequencing), U01AG046152 (ROSMAP AMP-AD, targeted proteomics), U01AG046161(TMT proteomics), U01AG61356 (whole genome sequencing, targeted proteomics, ROSMAP AMP-AD), the Illinois Department of Public Health (ROSMAP), and the Translational Genomics Research Institute (genomic). Additional phenotypic data can be requested at www.radc.rush.edu.

APPENDIX D

This serves as the Appendix for CHAPTER 4:

LEVERAGING WEIGHTED GENE CO-EXPRESSION NETWORK ANALYSIS (WGCNA) AS A TOOL FOR AD DRUG DISCOVERY

D.1 ACKNOWLEDGEMENTS

The results published here are in whole or in part based on data obtained from Agora, a platform initially developed by the National Institute on Aging-funded AMP-AD consortium that shares evidence in support of Alzheimer's disease target discovery.

D.2 FUNDING SOURCES

This research was supported in part by grants K01AG049164, K24AG046373, R21AG059941, R01AG059716, R01AG034962, R01HL111516, R01NS100980, R01AG056534, RF1AG15819 from the Intramural Research Program, the National Institute on Aging, the National Institutes of Health, the Vanderbilt University Advanced Computing Center for Research and Education (ACCRE) instrumentation grant (S10OD023680), the Vanderbilt Institute for Clinical and Translational Research (VICTR) grant (UL1TR000445, UL1TR002243), and the Vanderbilt Memory & Alzheimer's Center.

Additional study data were provided by the Rush Alzheimer's Disease Center, Rush University Medical Center, Chicago. Data collection was supported through funding by NIA

grants P30AG010161 (ROS), R01AG015819 (ROSMAP; genomics and RNAseq), R01AG017917 (MAP), R01AG030146, R01AG036042 (5hC methylation, ATACseq), RC2AG036547 (H3K9Ac), R01AG036836 (RNAseq), R01AG408015 (monocyte RNAseq) RF1AG057473 (single nucleus RNAseq), U01AG032984 (genomic and whole exome sequencing), U01AG046152 (ROSMAP AMP-AD, targeted proteomics), U01AG046161(TMT proteomics), U01AG61356 (whole genome sequencing, targeted proteomics, ROSMAP AMP-AD), the Illinois Department of Public Health (ROSMAP), and the Translational Genomics Research Institute (genomic). Additional phenotypic data can be requested at www.radc.rush.edu.

Reference transcriptome data were generated as part of the CommonMind Consortium supported by funding from Takeda Pharmaceuticals Company Limited, F. Hoffman-La Roche Ltd and NIH grants R01MH085542, R01MH093725, P50MH066392, P50MH080405, R01MH097276, RO1-MH-075916, P50M096891, P50MH084053S1, R37MH057881, AG02219, AG05138, MH06692, R01MH110921, R01MH109677, R01MH109897, U01MH103392, and contract HHSN271201300031C through IRP NIMH. Brain tissue for the study was obtained from the following brain bank collections: the Mount Sinai NIH Brain and Tissue Repository, the University of Pennsylvania Alzheimer's Disease Core Center, the University of Pittsburgh NeuroBioBank and Brain and Tissue Repositories, and the NIMH Human Brain Collection Core. CMC Leadership: Panos Roussos, Joseph Buxbaum, Andrew Chess, Schahram Akbarian, Vahram Haroutunian (Icahn School of Medicine at Mount Sinai), Bernie Devlin, David Lewis (University of Pittsburgh), Raquel Gur, Chang-Gyu Hahn (University of Pennsylvania), Enrico Domenici (University of Trento), Mette A. Peters, Solveig Sieberts (Sage Bionetworks), Thomas Lehner, Stefano Marenco, Barbara K. Lipska (NIMH).

D.3 SUPPLEMENTAL METHODS

D.3.1 Generation of the gene co-expression network published by Logsdon et al., 2019.[277]

The main goal of this analysis was to determine whether or not we could recreate a previously generated gene network prior to using WGCNA for alternate analyses. Processing and quality control (QC) of bulk RNA sequencing (RNAseq) from the dorsolateral prefrontal cortex (DLPFC) followed the procedure described within the publication. Logsdon et al., leveraged the weighted gene co-expression network (WGCNA) R package.[439, 442, 534, 535] Though not specified, the authors appeared to have used the method published by Parikshak et al., in 2013.[536] Code for the method can be obtained online at: https://horvath.genetics.ucla.edu/html/CoexpressionNetwork/developingcortex/. Using the follow parameters: soft power = 13, deepsplit = 2, and mergeCutHeight = 0.15, with a minimum module size of 100, we were able to obtain nearly an identical network to Logsdon et al (See **Figures D.1 and D.2**). Though it is not 100% identical, we believe that WGCNA is able to yield robust and reproducible results.

Figure D.1. Heatmap demonstrating correspondence of our network modules and the previously published Logsdon modules.

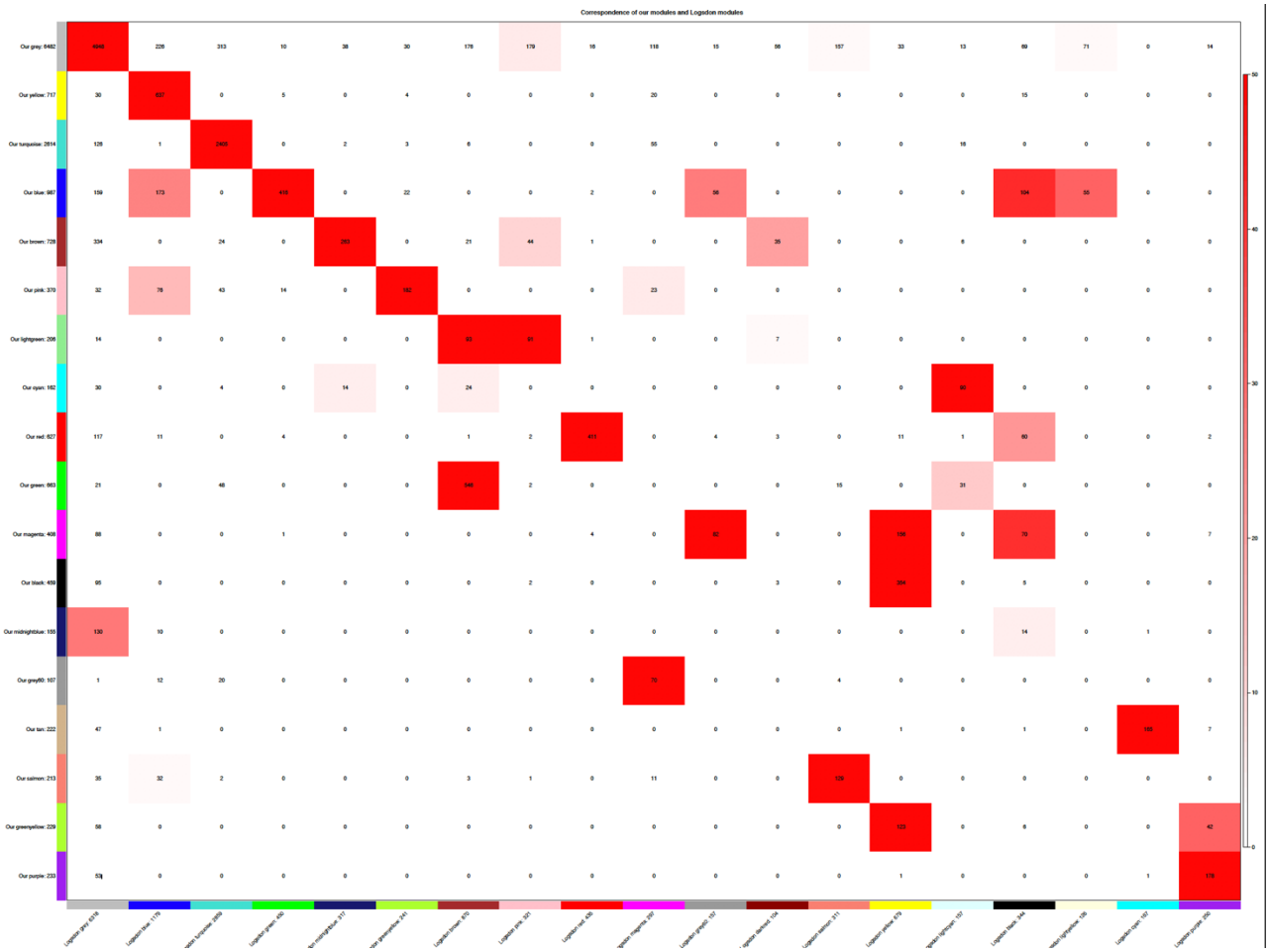

The modules we generated are listed on the y-axis, and the previously published modules are on the x-axis. Coloration of the heatmap is indicative of percentage overlap between the two networks such that a darker red color means more overlap. As demonstrated, we have a significant amount of overlap between both networks.

Figure D.2. Histogram demonstrating the highest % of gene overlap in each module between our network and the Logsdon network.

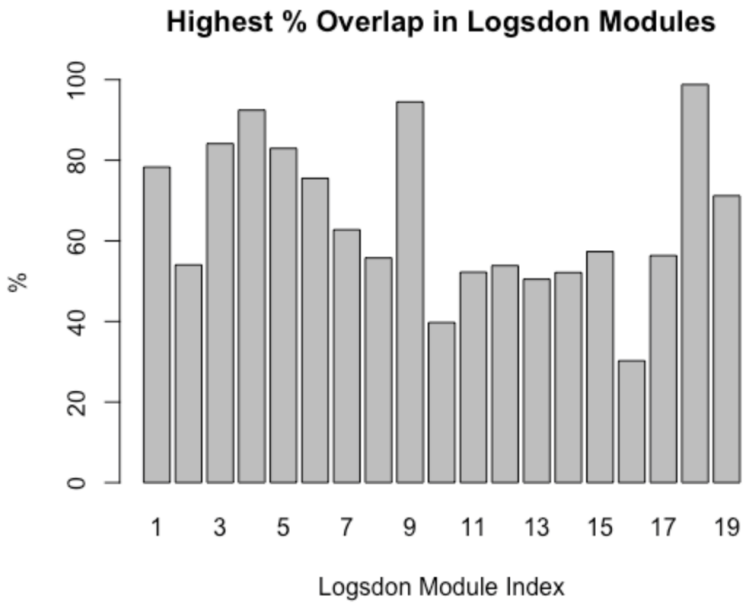

REFERENCES

1. Jack CR, Knopman DS, Jagust WJ, et al. Hypothetical model of dynamic biomarkers of the Alzheimer's pathological cascade. *The Lancet Neurology*. 2010;9(1):119.
2. Jack CR, Knopman DS, Jagust WJ, et al. Tracking pathophysiological processes in Alzheimer's disease: an updated hypothetical model of dynamic biomarkers. *The Lancet Neurology*. 2013;12(2):207-216.
3. Jack CR, Jr., Bennett DA, Blennow K, et al. NIA-AA Research Framework: Toward a biological definition of Alzheimer's disease. *Alzheimers Dement*. Apr 2018;14(4):535-562. doi:10.1016/j.jalz.2018.02.018
4. Association As. 2019 Alzheimer's Disease Facts and Figures. *Alzheimer's & Dementia*. 2019;15(3):321-387.
5. Wong W. Economic Burden of Alzheimer Disease and Managed Care Considerations. *Supplements and Featured Publications*. 2020;26(8)Addressing Unmet Needs in Alzheimer Disease: Implications of Delayed Diagnosis and Examining New and Emerging Therapies.
6. 2021 Alzheimer's disease facts and figures. *Alzheimers Dement*. Mar 2021;17(3):327-406. doi:10.1002/alz.12328
7. Bekris LM, Yu C-E, Bird TD, Tsuang DW. Genetics of Alzheimer disease. *J Geriatr Psychiatry Neurol*. 2010;23(4):213-227. doi:10.1177/0891988710383571
8. Reitz C, Rogaeva E, Beecham GW. Late-onset vs nonmendelian early-onset Alzheimer disease. *Neurology Genetics*. 2020;6(5):e512. doi:10.1212/NXG.0000000000000512
9. Rabinovici GD. Late-onset Alzheimer Disease. *Continuum (Minneap Minn)*. 2019;25(1):14-33. doi:10.1212/CON.0000000000000700
10. Cruchaga C, Chakraverty S, Mayo K, et al. Rare Variants in APP, PSEN1 and PSEN2 Increase Risk for AD in Late-Onset Alzheimer's Disease Families. *PLOS ONE*. 2012;7(2):e31039. doi:10.1371/journal.pone.0031039
11. Pottier C, Hannequin D, Coutant S, et al. High frequency of potentially pathogenic SORL1 mutations in autosomal dominant early-onset Alzheimer disease. *Mol Psychiatry*. Sep 2012;17(9):875-9. doi:10.1038/mp.2012.15
12. Cruchaga C, Del-Aguila JL, Saef B, et al. Polygenic risk score of sporadic late-onset Alzheimer's disease reveals a shared architecture with the familial and early-onset forms. *Alzheimers Dement*. Feb 2018;14(2):205-214. doi:10.1016/j.jalz.2017.08.013
13. Baker E, Escott-Price V. Polygenic Risk Scores in Alzheimer's Disease: Current Applications and Future Directions. Mini Review. *Frontiers in Digital Health*. 2020-August-11 2020;2:14. doi:10.3389/fdgth.2020.00014
14. Escott-Price V, Myers AJ, Huentelman M, Hardy J. Polygenic risk score analysis of pathologically confirmed Alzheimer disease. *Ann Neurol*. Aug 2017;82(2):311-314. doi:10.1002/ana.24999
15. Escott-Price V, Sims R, Bannister C, et al. Common polygenic variation enhances risk prediction for Alzheimer's disease. *Brain*. Dec 2015;138(Pt 12):3673-84. doi:10.1093/brain/awv268
16. Desikan RS, Fan CC, Wang Y, et al. Genetic assessment of age-associated Alzheimer disease risk: Development and validation of a polygenic hazard score. *PLoS Med*. Mar 2017;14(3):e1002258. doi:10.1371/journal.pmed.1002258
17. Chouraki V, Reitz C, Maury F, et al. Evaluation of a Genetic Risk Score to Improve Risk Prediction for Alzheimer's Disease. *J Alzheimers Dis*. Jun 18 2016;53(3):921-32. doi:10.3233/jad-150749
18. Hippius H, Neundörfer G. The discovery of Alzheimer's disease. *Dialogues Clin Neurosci*. 2003;5(1):101-108. doi:10.31887/DCNS.2003.5.1/hhippius
19. O'Brien RJ, Wong PC. Amyloid precursor protein processing and Alzheimer's disease. *Annu Rev Neurosci*. 2011;34:185-204. doi:10.1146/annurev-neuro-061010-113613
20. Iqbal K, Liu F, Gong C-X. Tau and neurodegenerative disease: the story so far. *Nature Reviews Neurology*. 2016/01/01 2016;12(1):15-27. doi:10.1038/nrneurol.2015.225
21. Bloom GS. Amyloid-β and Tau: The Trigger and Bullet in Alzheimer Disease Pathogenesis. *JAMA Neurology*. 2014;71(4):505-508. doi:10.1001/jamaneurol.2013.5847
22. Silbert LC. Does statin use decrease the amount of Alzheimer disease pathology in the brain? *Neurology*. 2007;69(9):E8. doi:10.1212/01.wnl.0000280585.95661.1b
23. Chen X-Q, Mobley WC. Alzheimer Disease Pathogenesis: Insights From Molecular and Cellular Biology Studies of Oligomeric Aβ and Tau Species. *Front Neurosci*. 2019;13:659-659. doi:10.3389/fnins.2019.00659
24. Kimberly WT, Esler WP, Ye W, et al. Notch and the Amyloid Precursor Protein Are Cleaved by Similar γ-Secretase(s). *Biochemistry*. 2003/01/01 2003;42(1):137-144. doi:10.1021/bi026888g

25. Ethell DW. An amyloid-notch hypothesis for Alzheimer's disease. *Neuroscientist*. Dec 2010;16(6):614-7. doi:10.1177/1073858410366162
26. Gu L, Guo Z. Alzheimer's Aβ42 and Aβ40 peptides form interlaced amyloid fibrils. *J Neurochem*. 2013;126(3):305-311. doi:10.1111/jnc.12202
27. DeTure MA, Dickson DW. The neuropathological diagnosis of Alzheimer's disease. *Molecular Neurodegeneration*. 2019/08/02 2019;14(1):32. doi:10.1186/s13024-019-0333-5
28. D'Andrea MR, Nagele RG. Morphologically distinct types of amyloid plaques point the way to a better understanding of Alzheimer's disease pathogenesis. *Biotech Histochem*. Apr 2010;85(2):133-47. doi:10.3109/10520290903389445
29. Ismail R, Parbo P, Madsen LS, et al. The relationships between neuroinflammation, beta-amyloid and tau deposition in Alzheimer's disease: a longitudinal PET study. *Journal of Neuroinflammation*. 2020/05/06 2020;17(1):151. doi:10.1186/s12974-020-01820-6
30. Svenningsson AL, Stomrud E, Insel PS, Mattsson N, Palmqvist S, Hansson O. β-amyloid pathology and hippocampal atrophy are independently associated with memory function in cognitively healthy elderly. *Scientific Reports*. 2019/08/01 2019;9(1):11180. doi:10.1038/s41598-019-47638-y
31. Bilgel M, An Y, Helphrey J, et al. Effects of amyloid pathology and neurodegeneration on cognitive change in cognitively normal adults. *Brain : a journal of neurology*. 2018;141(8):2475-2485. doi:10.1093/brain/awy150
32. Gupta A, Goyal R. Amyloid beta plaque: a culprit for neurodegeneration. *Acta Neurologica Belgica*. 2016/12/01 2016;116(4):445-450. doi:10.1007/s13760-016-0639-9
33. Chen G-f, Xu T-h, Yan Y, et al. Amyloid beta: structure, biology and structure-based therapeutic development. *Acta Pharmacologica Sinica*. 2017/09/01 2017;38(9):1205-1235. doi:10.1038/aps.2017.28
34. Krishnadas N, Villemagne VL, Doré V, Rowe CC. Advances in Brain Amyloid Imaging. *Seminars in Nuclear Medicine*. 2021/05/01/ 2021;51(3):241-252. doi:https://doi.org/10.1053/j.semnuclmed.2020.12.005
35. Iino T, Watanabe S, Yamashita K, et al. Quantification of Amyloid-β in Plasma by Simple and Highly Sensitive Immunoaffinity Enrichment and LC-MS/MS Assay. *The Journal of Applied Laboratory Medicine*. 2021;6(4):834-845. doi:10.1093/jalm/jfaa225
36. Ben Bouallègue F, Mariano-Goulart D, Payoux P, the Alzheimer's Disease Neuroimaging I. Comparison of CSF markers and semi-quantitative amyloid PET in Alzheimer's disease diagnosis and in cognitive impairment prognosis using the ADNI-2 database. *Alzheimer's Research & Therapy*. 2017/04/26 2017;9(1):32. doi:10.1186/s13195-017-0260-z
37. Landau SM, Lu M, Joshi AD, et al. Comparing positron emission tomography imaging and cerebrospinal fluid measurements of β-amyloid. *Ann Neurol*. Dec 2013;74(6):826-36. doi:10.1002/ana.23908
38. Toledo JB, Bjerke M, Da X, et al. Nonlinear Association Between Cerebrospinal Fluid and Florbetapir F-18 β-Amyloid Measures Across the Spectrum of Alzheimer Disease. *JAMA Neurol*. May 2015;72(5):571-81. doi:10.1001/jamaneurol.2014.4829
39. Barbier P, Zejneli O, Martinho M, et al. Role of Tau as a Microtubule-Associated Protein: Structural and Functional Aspects. Review. *Frontiers in Aging Neuroscience*. 2019-August-07 2019;11doi:10.3389/fnagi.2019.00204
40. Alonso AD, Cohen LS, Corbo C, et al. Hyperphosphorylation of Tau Associates With Changes in Its Function Beyond Microtubule Stability. Review. *Frontiers in Cellular Neuroscience*. 2018-October-09 2018;12doi:10.3389/fncel.2018.00338
41. Goedert M, Eisenberg DS, Crowther RA. Propagation of Tau Aggregates and Neurodegeneration. *Annu Rev Neurosci*. 2017/07/25 2017;40(1):189-210. doi:10.1146/annurev-neuro-072116-031153
42. Braak H, Braak E. Neuropathological stageing of Alzheimer-related changes. *Acta neuropathologica*. 1991;82(4):239-259.
43. Medeiros R, Baglietto-Vargas D, LaFerla FM. The role of tau in Alzheimer's disease and related disorders. *CNS Neurosci Ther*. 2011;17(5):514-524. doi:10.1111/j.1755-5949.2010.00177.x
44. Dixit R, Ross JL, Goldman YE, Holzbaur ELF. Differential regulation of dynein and kinesin motor proteins by tau. *Science*. 2008;319(5866):1086-1089. doi:10.1126/science.1152993
45. Beharry C, Cohen LS, Di J, Ibrahim K, Briffa-Mirabella S, Alonso AdC. Tau-induced neurodegeneration: mechanisms and targets. *Neuroscience Bulletin*. 2014/04/01 2014;30(2):346-358. doi:10.1007/s12264-013-1414-z
46. Grundke-Iqbal I, Iqbal K, Tung YC, Quinlan M, Wisniewski HM, Binder LI. Abnormal phosphorylation of the microtubule-associated protein tau (tau) in Alzheimer cytoskeletal pathology. *Proc Natl Acad Sci U S A*. Jul 1986;83(13):4913-7. doi:10.1073/pnas.83.13.4913

47. Takeda S. Tau Propagation as a Diagnostic and Therapeutic Target for Dementia: Potentials and Unanswered Questions. Review. *Front Neurosci*. 2019-December-13 2019;13doi:10.3389/fnins.2019.01274
48. Bejanin A, Schonhaut DR, La Joie R, et al. Tau pathology and neurodegeneration contribute to cognitive impairment in Alzheimer's disease. *Brain*. 2017;140(12):3286-3300. doi:10.1093/brain/awx243
49. Giannakopoulos P, Herrmann FR, Bussière T, et al. Tangle and neuron numbers, but not amyloid load, predict cognitive status in Alzheimer's disease. *Neurology*. May 13 2003;60(9):1495-500. doi:10.1212/01.wnl.0000063311.58879.01
50. Gómez-Isla T, Hollister R, West H, et al. Neuronal loss correlates with but exceeds neurofibrillary tangles in Alzheimer's disease. *Ann Neurol*. Jan 1997;41(1):17-24. doi:10.1002/ana.410410106
51. Lachno DR, Romeo MJ, Siemers ER, et al. Validation of ELISA methods for quantification of total tau and phosporylated-tau181 in human cerebrospinal fluid with measurement in specimens from two Alzheimer's disease studies. *J Alzheimers Dis*. 2011;26(3):531-41. doi:10.3233/jad-2011-110296
52. Leuzy A, Chiotis K, Lemoine L, et al. Tau PET imaging in neurodegenerative tauopathies—still a challenge. *Molecular Psychiatry*. 2019/08/01 2019;24(8):1112-1134. doi:10.1038/s41380-018-0342-8
53. Hardy J, Selkoe DJ. The amyloid hypothesis of Alzheimer's disease: progress and problems on the road to therapeutics. *Science*. 2002;297(5580):353-356.
54. Hardy John A, Higgins Gerald A. Alzheimer's Disease: The Amyloid Cascade Hypothesis. *Science*. 1992/04/10 1992;256(5054):184-185. doi:10.1126/science.1566067
55. Barage SH, Sonawane KD. Amyloid cascade hypothesis: Pathogenesis and therapeutic strategies in Alzheimer's disease. *Neuropeptides*. 2015/08/01/ 2015;52:1-18. doi:https://doi.org/10.1016/j.npep.2015.06.008
56. Selkoe DJ, Hardy J. The amyloid hypothesis of Alzheimer's disease at 25 years. *EMBO Mol Med*. 2016;8(6):595-608. doi:10.15252/emmm.201606210
57. Götz J, Chen F, van Dorpe J, Nitsch RM. Formation of neurofibrillary tangles in P301l tau transgenic mice induced by Abeta 42 fibrils. *Science*. Aug 24 2001;293(5534):1491-5. doi:10.1126/science.1062097
58. Oddo S, Caccamo A, Kitazawa M, Tseng BP, LaFerla FM. Amyloid deposition precedes tangle formation in a triple transgenic model of Alzheimer's disease. *Neurobiol Aging*. Dec 2003;24(8):1063-70. doi:10.1016/j.neurobiolaging.2003.08.012
59. Walls KC, Ager RR, Vasilevko V, Cheng D, Medeiros R, LaFerla FM. p-Tau immunotherapy reduces soluble and insoluble tau in aged 3xTg-AD mice. *Neurosci Lett*. Jul 11 2014;575:96-100. doi:10.1016/j.neulet.2014.05.047
60. Villemagne VL, Burnham S, Bourgeat P, et al. Amyloid β deposition, neurodegeneration, and cognitive decline in sporadic Alzheimer's disease: a prospective cohort study. *Lancet Neurol*. Apr 2013;12(4):357-67. doi:10.1016/s1474-4422(13)70044-9
61. Koscik RL, Betthauser TJ, Jonaitis EM, et al. Amyloid duration is associated with preclinical cognitive decline and tau PET. *Alzheimer's & Dementia: Diagnosis, Assessment & Disease Monitoring*. 2020/01/01 2020;12(1):e12007. doi:10.1002/dad2.12007
62. Guillozet AL, Weintraub S, Mash DC, Mesulam MM. Neurofibrillary Tangles, Amyloid, and Memory in Aging and Mild Cognitive Impairment. *Archives of Neurology*. 2003;60(5):729-736. doi:10.1001/archneur.60.5.729
63. Cummings J. Lessons learned from Alzheimer disease: clinical trials with negative outcomes. *Clinical Translational Science*. 2018;11(2):147-152.
64. Cummings J, Lee G, Ritter A, Sabbagh M, Zhong K. Alzheimer's disease drug development pipeline: 2020. *Alzheimer's & Dementia: Translational Research & Clinical Interventions*. 2020;6(1):e12050. doi:10.1002/trc2.12050
65. Cummings JL, Morstorf T, Zhong K. Alzheimer's disease drug-development pipeline: few candidates, frequent failures. *Alzheimer's Research & Therapy*. 2014/07/03 2014;6(4):37. doi:10.1186/alzrt269
66. Oxford AE, Stewart ES, Rohn TT. Clinical Trials in Alzheimer's Disease: A Hurdle in the Path of Remedy. *Int J Alzheimers Dis*. 2020;2020:5380346-5380346. doi:10.1155/2020/5380346
67. Mehta D, Jackson R, Paul G, Shi J, Sabbagh M. Why do trials for Alzheimer's disease drugs keep failing? A discontinued drug perspective for 2010-2015. *Expert Opin Investig Drugs*. 2017;26(6):735-739. doi:10.1080/13543784.2017.1323868
68. Association As. Treatments and Research. Alzheimer's Association. Accessed February 24, 2022, https://www.alz.org/help-support/i-have-alz/treatments-research
69. Budd Haeberlein S, O'Gorman J, Chiao P, et al. Clinical Development of Aducanumab, an Anti-Aβ Human Monoclonal Antibody Being Investigated for the Treatment of Early Alzheimer's Disease. *J Prev Alzheimers Dis*. 2017;4(4):255-263. doi:10.14283/jpad.2017.39

70. Knopman DS, Jones DT, Greicius MD. Failure to demonstrate efficacy of aducanumab: An analysis of the EMERGE and ENGAGE trials as reported by Biogen, December 2019. https://doi.org/10.1002/alz.12213. *Alzheimer's & Dementia*. 2021/04/01 2021;17(4):696-701. doi:https://doi.org/10.1002/alz.12213
71. Mullard A. Controversial Alzheimer's drug approval could affect other diseases. *Science*. 2021;595. doi:https://doi.org/10.1038/d41586-021-01763-9 Accessed February 24, 2022.
72. Knopman DS, Perlmutter JS. Prescribing Aducanumab in the Face of Meager Efficacy and Real Risks. *Neurology*. 2021;97(11):545. doi:10.1212/WNL.0000000000012452
73. Musiek ES, Gomez-Isla T, Holtzman DM. Aducanumab for Alzheimer disease: the amyloid hypothesis moves from bench to bedside. *The Journal of Clinical Investigation*. 10/15/ 2021;131(20)doi:10.1172/JCI154889
74. Luchicchi A, Bloem B, Viaña JNM, Mansvelder HD, Role LW. Illuminating the role of cholinergic signaling in circuits of attention and emotionally salient behaviors. Review. *Frontiers in Synaptic Neuroscience*. 2014-October-27 2014;6doi:10.3389/fnsyn.2014.00024
75. Perry E, Walker M, Grace J, Perry R. Acetylcholine in mind: a neurotransmitter correlate of consciousness? *Trends in Neurosciences*. 1999/06/01/ 1999;22(6):273-280. doi:https://doi.org/10.1016/S0166-2236(98)01361-7
76. Terry AV, Buccafusco JJ. The Cholinergic Hypothesis of Age and Alzheimer's Disease-Related Cognitive Deficits: Recent Challenges and Their Implications for Novel Drug Development. *Journal of Pharmacology and Experimental Therapeutics*. 2003;306(3):821. doi:10.1124/jpet.102.041616
77. Francis PT, Palmer AM, Snape M, Wilcock GK. The cholinergic hypothesis of Alzheimer's disease: a review of progress. *Journal of Neurology, Neurosurgery & Psychiatry*. 1999;66(2):137. doi:10.1136/jnnp.66.2.137
78. Marucci G, Buccioni M, Ben DD, Lambertucci C, Volpini R, Amenta F. Efficacy of acetylcholinesterase inhibitors in Alzheimer's disease. *Neuropharmacology*. 2021/06/01/ 2021;190:108352. doi:https://doi.org/10.1016/j.neuropharm.2020.108352
79. Johnson JW, Kotermanski SE. Mechanism of action of memantine. *Current Opinion in Pharmacology*. 2006/02/01/ 2006;6(1):61-67. doi:https://doi.org/10.1016/j.coph.2005.09.007
80. Wang R, Reddy PH. Role of Glutamate and NMDA Receptors in Alzheimer's Disease. *Journal of Alzheimer's disease : JAD*. 2017;57(4):1041-1048. doi:10.3233/JAD-160763
81. Thomas SJ, Grossberg GT. Memantine: a review of studies into its safety and efficacy in treating Alzheimer's disease and other dementias. *Clin Interv Aging*. 2009;4:367-377. doi:10.2147/cia.s6666
82. Neves G, Cooke SF, Bliss TVP. Synaptic plasticity, memory and the hippocampus: a neural network approach to causality. *Nature Reviews Neuroscience*. 2008/01/01 2008;9(1):65-75. doi:10.1038/nrn2303
83. Takeuchi T, Duszkiewicz AJ, Morris RGM. The synaptic plasticity and memory hypothesis: encoding, storage and persistence. *Philos Trans R Soc Lond B Biol Sci*. 2013;369(1633):20130288-20130288. doi:10.1098/rstb.2013.0288
84. Liu J, Chang L, Song Y, Li H, Wu Y. The Role of NMDA Receptors in Alzheimer's Disease. Review. *Front Neurosci*. 2019-February-08 2019;13doi:10.3389/fnins.2019.00043
85. Zhu M, Zhao S. Candidate gene identification approach: progress and challenges. *Int J Biol Sci*. 2007;3(7):420-427. doi:10.7150/ijbs.3.420
86. Kwon JM, Goate AM. The candidate gene approach. *Alcohol Res Health*. 2000;24(3):164-168.
87. Cummings J, Lee G, Ritter A, Sabbagh M, Zhong K. Alzheimer's disease drug development pipeline: 2019. *Alzheimers Dement (N Y)*. 2019;5:272-293. doi:10.1016/j.trci.2019.05.008
88. Drummond E, Wisniewski T. Alzheimer's disease: experimental models and reality. *Acta neuropathologica*. 2017;133(2):155-175. doi:10.1007/s00401-016-1662-x
89. Castrillo JI, Lista S, Hampel H, Ritchie CW. Systems Biology Methods for Alzheimer's Disease Research Toward Molecular Signatures, Subtypes, and Stages and Precision Medicine: Application in Cohort Studies and Trials. In: Perneczky R, ed. *Biomarkers for Alzheimer's Disease Drug Development*. Springer New York; 2018:31-66.
90. Gatz M, Reynolds CA, Fratiglioni L. Role of genes and environments for explaining alzheimer disease. *Archives of General Psychiatry*. 2006;63(2):168-174.
91. Kunkle BW, Grenier-Boley B, Sims R, et al. Genetic meta-analysis of diagnosed Alzheimer's disease identifies new risk loci and implicates Aβ, tau, immunity and lipid processing. *Nature Genetics*. 2019/03/01 2019;51(3):414-430. doi:10.1038/s41588-019-0358-2
92. Lambert JC, Ibrahim-Verbaas CA, Harold D, et al. Meta-analysis of 74,046 individuals identifies 11 new susceptibility loci for Alzheimer's disease. *Nat Genet*. Dec 2013;45(12):1452-8. doi:10.1038/ng.2802

93. Jansen IE, Savage JE, Watanabe K, et al. Genome-wide meta-analysis identifies new loci and functional pathways influencing Alzheimer's disease risk. *Nature Genetics*. 2019/03/01 2019;51(3):404-413. doi:10.1038/s41588-018-0311-9
94. Harper AR, Nayee S, Topol EJ. Protective alleles and modifier variants in human health and disease. *Nature Reviews Genetics*. 2015/12/01 2015;16(12):689-701. doi:10.1038/nrg4017
95. Karch CM, Goate AM. Alzheimer's Disease Risk Genes and Mechanisms of Disease Pathogenesis. *Biological Psychiatry*. 2015/01/01/ 2015;77(1):43-51. doi:https://doi.org/10.1016/j.biopsych.2014.05.006
96. Montine TJ, Cholerton BA, Corrada MM, et al. Concepts for brain aging: resistance, resilience, reserve, and compensation. *Alzheimer's Research & Therapy*. 2019/03/11 2019;11(1):22. doi:10.1186/s13195-019-0479-y
97. Andrews SJ, Fulton-Howard B, Goate A. Protective Variants in Alzheimer's Disease. *Current Genetic Medicine Reports*. 2019/03/01 2019;7(1):1-12. doi:10.1007/s40142-019-0156-2
98. Silva MVF, Loures CdMG, Alves LCV, de Souza LC, Borges KBG, Carvalho MdG. Alzheimer's disease: risk factors and potentially protective measures. *Journal of Biomedical Science*. 2019/05/09 2019;26(1):33. doi:10.1186/s12929-019-0524-y
99. Hohman TJ, McLaren DG, Mormino EC, Gifford KA, Libon DJ, Jefferson AL. Asymptomatic Alzheimer disease: Defining resilience. *Neurology*. 2016;87(23):2443-2450.
100. Driscoll I, Troncoso J. Asymptomatic Alzheimers Disease: A Prodrome or a State of Resilience? *Current Alzheimer Research*. 2011;8(4):330-335.
101. Rahimi J, Kovacs GG. Prevalence of mixed pathologies in the aging brain. *Alzheimers Research & Therapy*. 2014;6(9):82.
102. Sonnen JA, Santa Cruz K, Hemmy LS, et al. Ecology of the aging human brain. *Archives of Neurology*. 2011;68(8):1049-1056.
103. Kotowski IK, Pertsemlidis A, Luke A, et al. A spectrum of PCSK9 alleles contributes to plasma levels of low-density lipoprotein cholesterol. *Am J Hum Genet*. 2006;78(3):410-422. doi:10.1086/500615
104. Center USM. PCSK9-inhibitor drug class that grew out of UTSW research becomes a game-changer for patient with extremely high cholesterol. Accessed September 1, 2020. https://www.utsouthwestern.edu/newsroom/articles/year-2016/pcsk9-patient-khera.html
105. Benitez BA, Jin SC, Guerreiro R, et al. Missense variant in TREML2 protects against Alzheimer's disease. *Neurobiology of aging*. 2014;35(6):1510.e19-1510.e1.51000000000000001E26. doi:10.1016/j.neurobiolaging.2013.12.010
106. Sims R, van der Lee SJ, Naj AC, et al. Rare coding variants in PLCG2, ABI3, and TREM2 implicate microglial-mediated innate immunity in Alzheimer's disease. *Nature Genetics*. 2017/09/01 2017;49(9):1373-1384. doi:10.1038/ng.3916
107. Arboleda-Velasquez JF, Lopera F, O'Hare M, et al. Resistance to autosomal dominant Alzheimer's disease in an APOE3 Christchurch homozygote: a case report. *Nature Medicine*. 2019/11/01 2019;25(11):1680-1683. doi:10.1038/s41591-019-0611-3
108. Wollmer MA, Streffer JR, Lütjohann D, et al. ABCA1 modulates CSF cholesterol levels and influences the age at onset of Alzheimer's disease. *Neurobiology of Aging*. 2003/05/01/ 2003;24(3):421-426. doi:https://doi.org/10.1016/S0197-4580(02)00094-5
109. Arenaza-Urquijo EM, Vemuri P. Resistance vs resilience to Alzheimer disease: Clarifying terminology for preclinical studies. *Neurology*. Apr 10 2018;90(15):695-703. doi:10.1212/wnl.0000000000005303
110. Andersen SL. Centenarians as Models of Resistance and Resilience to Alzheimer's Disease and Related Dementias. *Advances in Geriatric Medicine and Research*. 2020;2(3):e200018. e200018. doi:10.20900/agmr20200018
111. Stern Y. Cognitive reserve in ageing and Alzheimer's disease. *The Lancet Neurology*. 2012;11(11):1006-1012. doi:10.1016/S1474-4422(12)70191-6
112. Sharp ES, Gatz M. Relationship between education and dementia: an updated systematic review. *Alzheimer Dis Assoc Disord*. Oct-Dec 2011;25(4):289-304. doi:10.1097/WAD.0b013e318211c83c
113. Stern Y. What is cognitive reserve? Theory and research application of the reserve concept. *J Int Neuropsychol Soc*. Mar 2002;8(3):448-60.
114. Stern Y, Arenaza-Urquijo EM, Bartrés-Faz D, et al. Whitepaper: Defining and investigating cognitive reserve, brain reserve, and brain maintenance. https://doi.org/10.1016/j.jalz.2018.07.219. *Alzheimer's & Dementia*. 2020/09/01 2020;16(9):1305-1311. doi:https://doi.org/10.1016/j.jalz.2018.07.219
115. Ouellette AR, Neuner SM, Dumitrescu L, et al. Cross-Species Analyses Identify Dlgap2 as a Regulator of Age-Related Cognitive Decline and Alzheimer's Dementia. *Cell Rep*. Sep 1 2020;32(9):108091. doi:10.1016/j.celrep.2020.108091

116. Jonsson T, Atwal JK, Steinberg S, et al. A mutation in APP protects against Alzheimer's disease and age-related cognitive decline. *Nature*. Aug 02 2012;488(7409):96-9. doi:10.1038/nature11283
117. Corder EH, Saunders AM, Risch NJ, et al. Protective effect of apolipoprotein E type 2 allele for late onset Alzheimer disease. *Nature Genetics*. 1994/06/01 1994;7(2):180-184. doi:10.1038/ng0694-180
118. Belloy ME, Napolioni V, Han SS, Le Guen Y, Greicius MD, Initiative ftAsDN. Association of Klotho-VS Heterozygosity With Risk of Alzheimer Disease in Individuals Who Carry APOE4. *JAMA Neurology*. 2020;77(7):849-862. doi:10.1001/jamaneurol.2020.0414
119. Ayers KL, Mirshahi UL, Wardeh AH, et al. A loss of function variant in CASP7 protects against Alzheimer's disease in homozygous APOE ε4 allele carriers. *BMC Genomics*. 2016/06/23 2016;17(2):445. doi:10.1186/s12864-016-2725-z
120. Fehér Á, Giricz Z, Juhász A, Pákáski M, Janka Z, Kálmán J. ABCA1 rs2230805 and rs2230806 common gene variants are associated with Alzheimer's disease. *Neurosci Lett*. Jan 18 2018;664:79-83. doi:10.1016/j.neulet.2017.11.027
121. Sassi C, Nalls MA, Ridge PG, et al. ABCA7 p.G215S as potential protective factor for Alzheimer's disease. *Neurobiology of aging*. 2016;46:235.e1-235.e2359. doi:10.1016/j.neurobiolaging.2016.04.004
122. Zhang C-C, Wang H-F, Tan M-S, et al. SORL1 Is Associated with the Risk of Late-Onset Alzheimer's Disease: a Replication Study and Meta-Analyses. *Molecular Neurobiology*. 2017/04/01 2017;54(3):1725-1732. doi:10.1007/s12035-016-9780-y
123. Ridge PG, Karch CM, Hsu S, et al. Linkage, whole genome sequence, and biological data implicate variants in RAB10 in Alzheimer's disease resilience. *Genome Med*. 2017;9(1):100-100. doi:10.1186/s13073-017-0486-1
124. Santos-Rebouças CB, Gonçalves AP, dos Santos JM, et al. rs3851179 Polymorphism at 5′ to the PICALM Gene is Associated with Alzheimer and Parkinson Diseases in Brazilian Population. *NeuroMolecular Medicine*. 2017/09/01 2017;19(2):293-299. doi:10.1007/s12017-017-8444-z
125. Nho K, Kim S, Risacher SL, et al. Protective variant for hippocampal atrophy identified by whole exome sequencing. *Annals of Neurology*. 2015/03/01 2015;77(3):547-552. doi:10.1002/ana.24349
126. Ghani M, Sato C, Kakhki EG, et al. Mutation analysis of the MS4A and TREM gene clusters in a case-control Alzheimer's disease data set. *Neurobiology of Aging*. 2016/06/01/ 2016;42:217.e7-217.e13. doi:https://doi.org/10.1016/j.neurobiolaging.2016.03.009
127. Weinstein G, Beiser AS, Choi SH, et al. Serum brain-derived neurotrophic factor and the risk for dementia: the Framingham Heart Study. *JAMA Neurol*. Jan 2014;71(1):55-61. doi:10.1001/jamaneurol.2013.4781
128. Ouellette AR, Neuner SM, Dumitrescu L, et al. Cross-Species Analyses Identify Dlgap2 as a Regulator of Age-Related Cognitive Decline and Alzheimer's Dementia. *Cell Reports*. 2020;32(9)doi:10.1016/j.celrep.2020.108091
129. Alzforum. APP. February 18, 2021. Accessed February 21, 2021. https://www.alzforum.org/mutations/app
130. Benilova I, Gallardo R, Ungureanu AA, et al. The Alzheimer disease protective mutation A2T modulates kinetic and thermodynamic properties of amyloid-β (Aβ) aggregation. *J Biol Chem*. Nov 7 2014;289(45):30977-89. doi:10.1074/jbc.M114.599027
131. Maloney JA, Bainbridge T, Gustafson A, et al. Molecular mechanisms of Alzheimer disease protection by the A673T allele of amyloid precursor protein. *J Biol Chem*. Nov 7 2014;289(45):30990-1000. doi:10.1074/jbc.M114.589069
132. Martiskainen H, Herukka S-K, Stančáková A, et al. Decreased plasma β-amyloid in the Alzheimer's disease APP A673T variant carriers. https://doi.org/10.1002/ana.24969. *Annals of Neurology*. 2017/07/01 2017;82(1):128-132. doi:https://doi.org/10.1002/ana.24969
133. Mengel-From J, Jeune B, Pentti T, McGue M, Christensen K, Christiansen L. The APP A673T frequency differs between Nordic countries. *Neurobiol Aging*. Oct 2015;36(10):2909.e1-4. doi:10.1016/j.neurobiolaging.2015.07.011
134. Wang L-S, Naj AC, Graham RR, et al. Rarity of the Alzheimer disease-protective APP A673T variant in the United States. *JAMA neurology*. 2015;72(2):209-216. doi:10.1001/jamaneurol.2014.2157
135. Bamne MN, Demirci FY, Berman S, et al. Investigation of an amyloid precursor protein protective mutation (A673T) in a North American case-control sample of late-onset Alzheimer's disease. *Neurobiol Aging*. Jul 2014;35(7):1779.e15-6. doi:10.1016/j.neurobiolaging.2014.01.020
136. Liu YW, He YH, Zhang YX, et al. Absence of A673T variant in APP gene indicates an alternative protective mechanism contributing to longevity in Chinese individuals. *Neurobiol Aging*. Apr 2014;35(4):935.e11-2. doi:10.1016/j.neurobiolaging.2013.09.023

137. Liu C-C, Liu C-C, Kanekiyo T, Xu H, Bu G. Apolipoprotein E and Alzheimer disease: risk, mechanisms and therapy. *Nat Rev Neurol*. 2013;9(2):106-118. doi:10.1038/nrneurol.2012.263
138. Corder EH, Saunders AM, Strittmatter WJ, et al. Gene dose of apolipoprotein E type 4 allele and the risk of Alzheimer's disease in late onset families. *Science*. 1993;261(5123):921-923.
139. Saunders AM, Strittmatter WJ, Schmechel D, et al. Association of apolipoprotein E allele epsilon 4 with late-onset familial and sporadic Alzheimer's disease. *Neurology*. 1993;43(8):1467-1472. doi:10.1212/wnl.43.8.1467
140. Strittmatter WJ, Saunders AM, Schmechel D, et al. Apolipoprotein E: high-avidity binding to beta-amyloid and increased frequency of type 4 allele in late-onset familial Alzheimer disease. *Proc Natl Acad Sci U S A*. 1993;90(5):1977-1981. doi:10.1073/pnas.90.5.1977
141. Safieh M, Korczyn AD, Michaelson DM. ApoE4: an emerging therapeutic target for Alzheimer's disease. *BMC Medicine*. 2019/03/20 2019;17(1):64. doi:10.1186/s12916-019-1299-4
142. Reiman EM, Arboleda-Velasquez JF, Quiroz YT, et al. Exceptionally low likelihood of Alzheimer's dementia in APOE2 homozygotes from a 5,000-person neuropathological study. *Nature Communications*. 2020/02/03 2020;11(1):667. doi:10.1038/s41467-019-14279-8
143. Wu L, Zhao L. ApoE2 and Alzheimer's disease: time to take a closer look. *Neural Regen Res*. 2016;11(3):412-413. doi:10.4103/1673-5374.179044
144. Li Z, Shue F, Zhao N, Shinohara M, Bu G. APOE2: protective mechanism and therapeutic implications for Alzheimer's disease. *Molecular Neurodegeneration*. 2020/11/04 2020;15(1):63. doi:10.1186/s13024-020-00413-4
145. Zhao N, Liu C-C, Qiao W, Bu G. Apolipoprotein E, Receptors, and Modulation of Alzheimer's Disease. *Biological psychiatry*. 2018;83(4):347-357. doi:10.1016/j.biopsych.2017.03.003
146. Fu Y, Zhao J, Atagi Y, et al. Apolipoprotein E lipoprotein particles inhibit amyloid-β uptake through cell surface heparan sulphate proteoglycan. *Molecular Neurodegeneration*. 2016/05/05 2016;11(1):37. doi:10.1186/s13024-016-0099-y
147. Therriault J, Benedet AL, Pascoal TA, et al. Association of Apolipoprotein E ε4 With Medial Temporal Tau Independent of Amyloid-β. *JAMA Neurology*. 2020;77(4):470-479. doi:10.1001/jamaneurol.2019.4421
148. Therriault J, Benedet AL, Pascoal TA, et al. APOEε4 potentiates the relationship between amyloid-β and tau pathologies. *Molecular Psychiatry*. 2020/03/11 2020;doi:10.1038/s41380-020-0688-6
149. Shi Y, Yamada K, Liddelow SA, et al. ApoE4 markedly exacerbates tau-mediated neurodegeneration in a mouse model of tauopathy. *Nature*. 2017;549(7673):523-527.
150. Yamazaki Y, Painter MM, Bu G, Kanekiyo T. Apolipoprotein E as a Therapeutic Target in Alzheimer's Disease: A Review of Basic Research and Clinical Evidence. *CNS Drugs*. 2016;30(9):773-789. doi:10.1007/s40263-016-0361-4
151. Yamazaki Y, Zhao N, Caulfield TR, Liu C-C, Bu G. Apolipoprotein E and Alzheimer disease: pathobiology and targeting strategies. *Nat Rev Neurol*. 2019/09// 2019;15(9):501-518. doi:10.1038/s41582-019-0228-7
152. Henneman P, van der Sman-de Beer F, Moghaddam PH, et al. The expression of type III hyperlipoproteinemia: involvement of lipolysis genes. *Eur J Hum Genet*. 2009;17(5):620-628. doi:10.1038/ejhg.2008.202
153. Martínez-Martínez AB, Torres-Perez E, Devanney N, Del Moral R, Johnson LA, Arbones-Mainar JM. Beyond the CNS: The many peripheral roles of APOE. *Neurobiology of Disease*. 2020/05/01/ 2020;138:104809. doi:https://doi.org/10.1016/j.nbd.2020.104809
154. Chernick D, Ortiz-Valle S, Jeong A, Qu W, Li L. Peripheral versus central nervous system APOE in Alzheimer's disease: Interplay across the blood-brain barrier. *Neuroscience letters*. 2019;708:134306-134306. doi:10.1016/j.neulet.2019.134306
155. Williams T, Borchelt DR, Chakrabarty P. Therapeutic approaches targeting Apolipoprotein E function in Alzheimer's disease. *Molecular Neurodegeneration*. 2020/01/31 2020;15(1):8. doi:10.1186/s13024-020-0358-9
156. Ewbank DC. Mortality differences by APOE genotype estimated from demographic synthesis. *Genetic epidemiology*. Feb 2002;22(2):146-55. doi:10.1002/gepi.0164
157. Huq AJ, Fransquet P, Laws SM, et al. Genetic resilience to Alzheimer's disease in APOE ε4 homozygotes: A systematic review. *Alzheimers Dement*. Dec 2019;15(12):1612-1623. doi:10.1016/j.jalz.2019.05.011
158. Arking DE, Krebsova A, Macek M, Sr., et al. Association of human aging with a functional variant of klotho. *Proc Natl Acad Sci U S A*. Jan 22 2002;99(2):856-61. doi:10.1073/pnas.022484299
159. Porter T, Burnham SC, Milicic L, et al. Klotho allele status is not associated with Aβ and APOE ε4-related cognitive decline in preclinical Alzheimer's disease. *Neurobiol Aging*. Apr 2019;76:162-165. doi:10.1016/j.neurobiolaging.2018.12.014

160. de Vries CF, Staff RT, Harris SE, et al. Klotho, APOEε4, cognitive ability, brain size, atrophy, and survival: a study in the Aberdeen Birth Cohort of 1936. *Neurobiol Aging*. Jul 2017;55:91-98. doi:10.1016/j.neurobiolaging.2017.02.019
161. Dubal DB, Yokoyama JS, Zhu L, et al. Life extension factor klotho enhances cognition. *Cell Rep*. May 22 2014;7(4):1065-76. doi:10.1016/j.celrep.2014.03.076
162. Yokoyama JS, Sturm VE, Bonham LW, et al. Variation in longevity gene KLOTHO is associated with greater cortical volumes. *Ann Clin Transl Neurol*. Mar 2015;2(3):215-30. doi:10.1002/acn3.161
163. Erickson CM, Schultz SA, Oh JM, et al. KLOTHO heterozygosity attenuates APOE4-related amyloid burden in preclinical AD. *Neurology*. Apr 16 2019;92(16):e1878-e1889. doi:10.1212/wnl.0000000000007323
164. Dubal DB, Yokoyama JS. Longevity Gene KLOTHO and Alzheimer Disease—A Better Fate for Individuals Who Carry APOE ε4. *JAMA Neurology*. 2020;77(7):798-800. doi:10.1001/jamaneurol.2020.0112
165. Dërmaku-Sopjani M, Kolgeci S, Abazi S, Sopjani M. Significance of the anti-aging protein Klotho. *Molecular Membrane Biology*. 2013/12/01 2013;30(8):369-385. doi:10.3109/09687688.2013.837518
166. Kurosu H, Yamamoto M, Clark JD, et al. Suppression of aging in mice by the hormone Klotho. *Science*. Sep 16 2005;309(5742):1829-33. doi:10.1126/science.1112766
167. Wolf EJ, Morrison FG, Sullivan DR, et al. The goddess who spins the thread of life: Klotho, psychiatric stress, and accelerated aging. *Brain Behav Immun*. Aug 2019;80:193-203. doi:10.1016/j.bbi.2019.03.007
168. Ullah M, Sun Z. Klotho Deficiency Accelerates Stem Cells Aging by Impairing Telomerase Activity. *J Gerontol A Biol Sci Med Sci*. Aug 16 2019;74(9):1396-1407. doi:10.1093/gerona/gly261
169. Kuang X, Zhou HJ, Thorne AH, Chen XN, Li LJ, Du JR. Neuroprotective Effect of Ligustilide through Induction of α-Secretase Processing of Both APP and Klotho in a Mouse Model of Alzheimer's Disease. *Front Aging Neurosci*. 2017;9:353. doi:10.3389/fnagi.2017.00353
170. Zeng CY, Yang TT, Zhou HJ, et al. Lentiviral vector-mediated overexpression of Klotho in the brain improves Alzheimer's disease-like pathology and cognitive deficits in mice. *Neurobiol Aging*. Jun 2019;78:18-28. doi:10.1016/j.neurobiolaging.2019.02.003
171. Simonovitch S, Schmukler E, Bespalko A, et al. Impaired Autophagy in APOE4 Astrocytes. *J Alzheimers Dis*. 2016;51(3):915-27. doi:10.3233/jad-151101
172. Parcon PA, Balasubramaniam M, Ayyadevara S, et al. Apolipoprotein E4 inhibits autophagy gene products through direct, specific binding to CLEAR motifs. *Alzheimer's & Dementia*. 2018/02/01/ 2018;14(2):230-242. doi:https://doi.org/10.1016/j.jalz.2017.07.754
173. Zhao Y, Zeng C-Y, Li X-H, Yang T-T, Kuang X, Du J-R. Klotho overexpression improves amyloid-β clearance and cognition in the APP/PS1 mouse model of Alzheimer's disease. *Aging Cell*. 2020/10/01 2020;19(10):e13239. doi:10.1111/acel.13239
174. Burguillos MA, Deierborg T, Kavanagh E, et al. Caspase signalling controls microglia activation and neurotoxicity. *Nature*. Apr 21 2011;472(7343):319-24. doi:10.1038/nature09788
175. Roth KA. Caspases, Apoptosis, and Alzheimer Disease: Causation, Correlation, and Confusion. *Journal of Neuropathology & Experimental Neurology*. 2001;60(9):829-838. doi:10.1093/jnen/60.9.829
176. McKenzie BA, Fernandes JP, Doan MAL, Schmitt LM, Branton WG, Power C. Activation of the executioner caspases-3 and -7 promotes microglial pyroptosis in models of multiple sclerosis. *Journal of Neuroinflammation*. 2020/08/29 2020;17(1):253. doi:10.1186/s12974-020-01902-5
177. Rohn TT, Head E. Caspases as therapeutic targets in Alzheimer's disease: is it time to "cut" to the chase? *Int J Clin Exp Pathol*. 2009;2(2):108-118.
178. Yamamoto M, Clark JD, Pastor JV, et al. Regulation of oxidative stress by the anti-aging hormone klotho. *J Biol Chem*. Nov 11 2005;280(45):38029-34. doi:10.1074/jbc.M509039200
179. Chew H, Solomon VA, Fonteh AN. Involvement of Lipids in Alzheimer's Disease Pathology and Potential Therapies. Review. *Frontiers in Physiology*. 2020-June-09 2020;11:598. doi:10.3389/fphys.2020.00598
180. Nordestgaard LT, Tybjærg-Hansen A, Nordestgaard BG, Frikke-Schmidt R. Loss-of-function mutation in ABCA1 and risk of Alzheimer's disease and cerebrovascular disease. *Alzheimers Dement*. Dec 2015;11(12):1430-1438. doi:10.1016/j.jalz.2015.04.006
181. Koldamova R, Fitz NF, Lefterov I. The role of ATP-binding cassette transporter A1 in Alzheimer's disease and neurodegeneration. *Biochim Biophys Acta*. Aug 2010;1801(8):824-30. doi:10.1016/j.bbalip.2010.02.010
182. De Roeck A, Van Broeckhoven C, Sleegers K. The role of ABCA7 in Alzheimer's disease: evidence from genomics, transcriptomics and methylomics. *Acta neuropathologica*. 2019;138(2):201-220. doi:10.1007/s00401-019-01994-1
183. Andersen OM, Rudolph I-M, Willnow TE. Risk factor SORL1: from genetic association to functional validation in Alzheimer's disease. *Acta neuropathologica*. 2016;132(5):653-665. doi:10.1007/s00401-016-1615-4

184. Elali A, Rivest S. The role of ABCB1 and ABCA1 in beta-amyloid clearance at the neurovascular unit in Alzheimer's disease. *Frontiers in physiology*. 2013;4:45-45. doi:10.3389/fphys.2013.00045
185. Fitz NF, Cronican AA, Saleem M, et al. Abca1 deficiency affects Alzheimer's disease-like phenotype in human ApoE4 but not in ApoE3-targeted replacement mice. *J Neurosci*. 2012;32(38):13125-13136. doi:10.1523/JNEUROSCI.1937-12.2012
186. Aikawa T, Holm M-L, Kanekiyo T. ABCA7 and Pathogenic Pathways of Alzheimer's Disease. *Brain Sci*. 2018;8(2):27. doi:10.3390/brainsci8020027
187. Fu Y, Hsiao JH, Paxinos G, Halliday GM, Kim WS. ABCA7 Mediates Phagocytic Clearance of Amyloid-β in the Brain. *J Alzheimers Dis*. Sep 6 2016;54(2):569-84. doi:10.3233/jad-160456
188. Sakae N, Liu CC, Shinohara M, et al. ABCA7 Deficiency Accelerates Amyloid-β Generation and Alzheimer's Neuronal Pathology. *J Neurosci*. Mar 30 2016;36(13):3848-59. doi:10.1523/jneurosci.3757-15.2016
189. Kim WS, Li H, Ruberu K, et al. Deletion of Abca7 increases cerebral amyloid-β accumulation in the J20 mouse model of Alzheimer's disease. *J Neurosci*. Mar 6 2013;33(10):4387-94. doi:10.1523/jneurosci.4165-12.2013
190. Taira K, Bujo H, Hirayama S, et al. LR11, a mosaic LDL receptor family member, mediates the uptake of ApoE-rich lipoproteins in vitro. *Arterioscler Thromb Vasc Biol*. Sep 2001;21(9):1501-6. doi:10.1161/hq0901.094500
191. Yin RH, Yu JT, Tan L. The Role of SORL1 in Alzheimer's Disease. *Mol Neurobiol*. 2015;51(3):909-18. doi:10.1007/s12035-014-8742-5
192. Verheijen J, Van den Bossche T, van der Zee J, et al. A comprehensive study of the genetic impact of rare variants in SORL1 in European early-onset Alzheimer's disease. *Acta Neuropathologica*. 2016/08/01 2016;132(2):213-224. doi:10.1007/s00401-016-1566-9
193. Holstege H, van der Lee SJ, Hulsman M, et al. Characterization of pathogenic SORL1 genetic variants for association with Alzheimer's disease: a clinical interpretation strategy. *European Journal of Human Genetics*. 2017/08/01 2017;25(8):973-981. doi:10.1038/ejhg.2017.87
194. Vardarajan BN, Zhang Y, Lee JH, et al. Coding mutations in SORL1 and Alzheimer disease. *Ann Neurol*. Feb 2015;77(2):215-27. doi:10.1002/ana.24305
195. Kölsch H, Jessen F, Wiltfang J, et al. Influence of SORL1 gene variants: association with CSF amyloid-beta products in probable Alzheimer's disease. *Neurosci Lett*. Jul 25 2008;440(1):68-71. doi:10.1016/j.neulet.2008.05.049
196. Alexopoulos P, Guo L-H, Kratzer M, Westerteicher C, Kurz A, Perneczky R. Impact of SORL1 single nucleotide polymorphisms on Alzheimer's disease cerebrospinal fluid markers. *Dement Geriatr Cogn Disord*. 2011;32(3):164-170. doi:10.1159/000332017
197. Riddell DR, Zhou H, Comery TA, et al. The LXR agonist TO901317 selectively lowers hippocampal Abeta42 and improves memory in the Tg2576 mouse model of Alzheimer's disease. *Mol Cell Neurosci*. Apr 2007;34(4):621-8. doi:10.1016/j.mcn.2007.01.011
198. Donkin JJ, Stukas S, Hirsch-Reinshagen V, et al. ATP-binding cassette transporter A1 mediates the beneficial effects of the liver X receptor agonist GW3965 on object recognition memory and amyloid burden in amyloid precursor protein/presenilin 1 mice. *The Journal of biological chemistry*. 2010;285(44):34144-34154. doi:10.1074/jbc.M110.108100
199. Stefan CJ, Trimble WS, Grinstein S, et al. Membrane dynamics and organelle biogenesis—lipid pipelines and vesicular carriers. *BMC Biology*. 2017/10/31 2017;15(1):102. doi:10.1186/s12915-017-0432-0
200. Marsh J, Alifragis P. Synaptic dysfunction in Alzheimer's disease: the effects of amyloid beta on synaptic vesicle dynamics as a novel target for therapeutic intervention. *Neural Regen Res*. 2018;13(4):616-623. doi:10.4103/1673-5374.230276
201. Van Acker ZP, Bretou M, Annaert W. Endo-lysosomal dysregulations and late-onset Alzheimer's disease: impact of genetic risk factors. *Molecular Neurodegeneration*. 2019/06/03 2019;14(1):20. doi:10.1186/s13024-019-0323-7
202. Mañucat-Tan NB, Saadipour K, Wang YJ, Bobrovskaya L, Zhou XF. Cellular Trafficking of Amyloid Precursor Protein in Amyloidogenesis Physiological and Pathological Significance. *Mol Neurobiol*. Feb 2019;56(2):812-830. doi:10.1007/s12035-018-1106-9
203. Baranello RJ, Bharani KL, Padmaraju V, et al. Amyloid-beta protein clearance and degradation (ABCD) pathways and their role in Alzheimer's disease. *Current Alzheimer research*. 2015;12(1):32-46. doi:10.2174/1567205012666141218140953
204. Horak M, Petralia RS, Kaniakova M, Sans N. ER to synapse trafficking of NMDA receptors. Review. *Frontiers in Cellular Neuroscience*. 2014-November-27 2014;8:394. doi:10.3389/fncel.2014.00394

205. Barr F, Lambright DG. Rab GEFs and GAPs. *Curr Opin Cell Biol*. 2010;22(4):461-470. doi:10.1016/j.ceb.2010.04.007
206. Tavana JP, Rosene M, Jensen NO, Ridge PG, Kauwe JS, Karch CM. RAB10: an Alzheimer's disease resilience locus and potential drug target. *Clin Interv Aging*. 2018;14:73-79. doi:10.2147/CIA.S159148
207. Mignogna ML, D'Adamo P. Critical importance of RAB proteins for synaptic function. *Small GTPases*. 2018;9(1-2):145-157. doi:10.1080/21541248.2016.1277001
208. Zeng FF, Liu J, He H, et al. Association of PICALM Gene Polymorphisms with Alzheimer's Disease: Evidence from an Updated Meta-Analysis. *Curr Alzheimer Res*. 2019;16(13):1196-1205. doi:10.2174/1567205016666190805165607
209. Masri I, Salami A, El Shamieh S, Bissar-Tadmouri N. rs3851179G>A in PICALM is protective against Alzheimer's disease in five different countries surrounding the Mediterranean. *Curr Aging Sci*. Oct 19 2019;13(2):162-168
. doi:10.2174/1874609812666191019143237
210. Baig S, Joseph SA, Tayler H, et al. Distribution and expression of picalm in Alzheimer disease. *J Neuropathol Exp Neurol*. 2010;69(10):1071-1077. doi:10.1097/NEN.0b013e3181f52e01
211. Xu W, Tan L, Yu J-T. The Role of PICALM in Alzheimer's Disease. *Molecular Neurobiology*. 2015/08/01 2015;52(1):399-413. doi:10.1007/s12035-014-8878-3
212. Lambert JC, Heath S, Even G, et al. Genome-wide association study identifies variants at CLU and CR1 associated with Alzheimer's disease. *Nat Genet*. Oct 2009;41(10):1094-9. doi:10.1038/ng.439
213. Harold D, Abraham R, Hollingworth P, et al. Genome-wide association study identifies variants at CLU and PICALM associated with Alzheimer's disease. *Nature genetics*. 2009;41(10):1088-1093.
214. Ando K, Brion JP, Stygelbout V, et al. Clathrin adaptor CALM/PICALM is associated with neurofibrillary tangles and is cleaved in Alzheimer's brains. *Acta Neuropathol*. Jun 2013;125(6):861-78. doi:10.1007/s00401-013-1111-z
215. Zhao Z, Sagare AP, Ma Q, et al. Central role for PICALM in amyloid-β blood-brain barrier transcytosis and clearance. *Nat Neurosci*. 2015;18(7):978-987. doi:10.1038/nn.4025
216. Parikh I, Fardo DW, Estus S. Genetics of PICALM expression and Alzheimer's disease. *PloS one*. 2014;9(3):e91242-e91242. doi:10.1371/journal.pone.0091242
217. Jackson J, Jambrina E, Li J, et al. Targeting the Synapse in Alzheimer's Disease. Mini Review. *Front Neurosci*. 2019-July-23 2019;13:735. doi:10.3389/fnins.2019.00735
218. Abraham WC, Jones OD, Glanzman DL. Is plasticity of synapses the mechanism of long-term memory storage? *npj Science of Learning*. 2019/07/02 2019;4(1):9. doi:10.1038/s41539-019-0048-y
219. Lu T, Aron L, Zullo J, et al. REST and stress resistance in ageing and Alzheimer's disease. *Nature*. 2014;507(7493):448-454. doi:10.1038/nature13163
220. Nho K, Kim S, Risacher SL, et al. Protective variant for hippocampal atrophy identified by whole exome sequencing. *Annals of Neurology*. 2015;77(3):547-552. doi:10.1002/ana.24349
221. Meyer K, Feldman HM, Lu T, et al. REST and Neural Gene Network Dysregulation in iPSC Models of Alzheimer's Disease. *Cell Rep*. Jan 29 2019;26(5):1112-1127.e9. doi:10.1016/j.celrep.2019.01.023
222. Gao Z, Ure K, Ding P, et al. The Master Negative Regulator REST/NRSF Controls Adult Neurogenesis by Restraining the Neurogenic Program in Quiescent Stem Cells. *The Journal of Neuroscience*. 2011;31(26):9772. doi:10.1523/JNEUROSCI.1604-11.2011
223. Song M, Martinowich K, Lee FS. BDNF at the synapse: why location matters. *Molecular psychiatry*. 2017;22(10):1370-1375. doi:10.1038/mp.2017.144
224. Bruce AW, Donaldson IJ, Wood IC, et al. Genome-wide analysis of repressor element 1 silencing transcription factor/neuron-restrictive silencing factor (REST/NRSF) target genes. *Proceedings of the National Academy of Sciences of the United States of America*. 2004;101(28):10458. doi:10.1073/pnas.0401827101
225. Cunha C, Brambilla R, Thomas K. A simple role for BDNF in learning and memory? Review. *Frontiers in Molecular Neuroscience*. 2010-February-09 2010;3:1. doi:10.3389/neuro.02.001.2010
226. Ng TKS, Ho CSH, Tam WWS, Kua EH, Ho RC-M. Decreased Serum Brain-Derived Neurotrophic Factor (BDNF) Levels in Patients with Alzheimer's Disease (AD): A Systematic Review and Meta-Analysis. *Int J Mol Sci*. 2019;20(2):257. doi:10.3390/ijms20020257
227. de Pins B, Cifuentes-Díaz C, Farah AT, et al. Conditional BDNF Delivery from Astrocytes Rescues Memory Deficits, Spine Density, and Synaptic Properties in the 5xFAD Mouse Model of Alzheimer Disease. *The Journal of Neuroscience*. 2019;39(13):2441. doi:10.1523/JNEUROSCI.2121-18.2019
228. Wu CC, Lien CC, Hou WH, Chiang PM, Tsai KJ. Gain of BDNF Function in Engrafted Neural Stem Cells Promotes the Therapeutic Potential for Alzheimer's Disease. *Sci Rep*. Jun 6 2016;6:27358. doi:10.1038/srep27358

229. Xie Y, Hayden MR, Xu B. BDNF overexpression in the forebrain rescues Huntington's disease phenotypes in YAC128 mice. *J Neurosci*. Nov 3 2010;30(44):14708-18. doi:10.1523/jneurosci.1637-10.2010
230. Ventriglia M, Bocchio Chiavetto L, Benussi L, et al. Association between the BDNF 196 A/G polymorphism and sporadic Alzheimer's disease. *Molecular Psychiatry*. 2002/02/01 2002;7(2):136-137. doi:10.1038/sj.mp.4000952
231. Rogaeva E, Schmitt-Ulms G. Does BDNF Val66Met contribute to preclinical Alzheimer's disease? *Brain*. 2016;139(10):2586-2589. doi:10.1093/brain/aww201
232. Lim YY, Hassenstab J, Cruchaga C, et al. BDNF Val66Met moderates memory impairment, hippocampal function and tau in preclinical autosomal dominant Alzheimer's disease. *Brain : a journal of neurology*. 2016;139(Pt 10):2766-2777. doi:10.1093/brain/aww200
233. Lim YY, Hassenstab J, Goate A, et al. Effect of BDNFVal66Met on disease markers in dominantly inherited Alzheimer's disease. *Annals of neurology*. 2018;84(3):424-435. doi:10.1002/ana.25299
234. Lim YY, Villemagne VL, Laws SM, et al. Effect of BDNF Val66Met on memory decline and hippocampal atrophy in prodromal Alzheimer's disease: a preliminary study. *PloS one*. 2014;9(1):e86498-e86498. doi:10.1371/journal.pone.0086498
235. Egan MF, Kojima M, Callicott JH, et al. The BDNF val66met Polymorphism Affects Activity-Dependent Secretion of BDNF and Human Memory and Hippocampal Function. *Cell*. 2003;112(2):257-269. doi:10.1016/S0092-8674(03)00035-7
236. Rasmussen AH, Rasmussen HB, Silahtaroglu A. The DLGAP family: neuronal expression, function and role in brain disorders. *Mol Brain*. 2017;10(1):43-43. doi:10.1186/s13041-017-0324-9
237. Chaudhry M, Wang X, Bamne MN, et al. Genetic variation in imprinted genes is associated with risk of late-onset Alzheimer's disease. *Journal of Alzheimer's disease : JAD*. 2015;44(3):989-994. doi:10.3233/JAD-142106
238. DLGAP1. Accessed October 30, 2020, https://agora.ampadportal.org/genes/(genes-router:gene-details/ENSG00000170579)
239. Roselli F, Livrea P, Almeida OFX. CDK5 is essential for soluble amyloid β-induced degradation of GKAP and remodeling of the synaptic actin cytoskeleton. *PloS one*. 2011;6(7):e23097-e23097. doi:10.1371/journal.pone.0023097
240. Kinney JW, Bemiller SM, Murtishaw AS, Leisgang AM, Salazar AM, Lamb BT. Inflammation as a central mechanism in Alzheimer's disease. *Alzheimers Dement (N Y)*. 2018;4:575-590. doi:10.1016/j.trci.2018.06.014
241. Tsai AP, Dong C, Preuss C, et al. PLCG2 as a Risk Factor for Alzheimer's Disease. *bioRxiv*. 2020:2020.05.19.104216. doi:10.1101/2020.05.19.104216
242. Efthymiou AG, Goate AM. Late onset Alzheimer's disease genetics implicates microglial pathways in disease risk. *Molecular Neurodegeneration*. 2017/05/26 2017;12(1):43. doi:10.1186/s13024-017-0184-x
243. Hollingworth P, Harold D, Sims R, et al. Common variants at ABCA7, MS4A6A/MS4A4E, EPHA1, CD33 and CD2AP are associated with Alzheimer's disease. *Nature genetics*. 2011;43(5):429-435. doi:10.1038/ng.803
244. Magno L, Lessard CB, Martins M, et al. Alzheimer's disease phospholipase C-gamma-2 (PLCG2) protective variant is a functional hypermorph. *Alzheimer's Research & Therapy*. 2019/02/02 2019;11(1):16. doi:10.1186/s13195-019-0469-0
245. van der Lee SJ, Conway OJ, Jansen I, et al. A nonsynonymous mutation in PLCG2 reduces the risk of Alzheimer's disease, dementia with Lewy bodies and frontotemporal dementia, and increases the likelihood of longevity. *Acta Neuropathologica*. 2019/08/01 2019;138(2):237-250. doi:10.1007/s00401-019-02026-8
246. Koss H, Bunney TD, Behjati S, Katan M. Dysfunction of phospholipase Cγ in immune disorders and cancer. *Trends Biochem Sci*. Dec 2014;39(12):603-11. doi:10.1016/j.tibs.2014.09.004
247. Guerreiro R, Wojtas A, Bras J, et al. TREM2 Variants in Alzheimer's Disease. *New England Journal of Medicine*. 2013/01/10 2012;368(2):117-127. doi:10.1056/NEJMoa1211851
248. Yu P, Constien R, Dear N, et al. Autoimmunity and Inflammation Due to a Gain-of-Function Mutation in Phospholipase Cγ2 that Specifically Increases External Ca²⁺ Entry. *Immunity*. 2005;22(4):451-465. doi:10.1016/j.immuni.2005.01.018
249. Zheng H, Liu C-C, Atagi Y, et al. Opposing roles of the triggering receptor expressed on myeloid cells 2 and triggering receptor expressed on myeloid cells-like transcript 2 in microglia activation. *Neurobiology of aging*. 2016;42:132-141. doi:10.1016/j.neurobiolaging.2016.03.004
250. Ford JW, McVicar DW. TREM and TREM-like receptors in inflammation and disease. *Curr Opin Immunol*. Feb 2009;21(1):38-46. doi:10.1016/j.coi.2009.01.009
251. Song Y-N, Li J-Q, Tan C-C, et al. TREML2 Mutation Mediate Alzheimer's Disease Risk by Altering Neuronal Degeneration. Original Research. *Front Neurosci*. 2019-May-15 2019;13:455. doi:10.3389/fnins.2019.00455

252. Laurent C, Buée L, Blum D. Tau and neuroinflammation: What impact for Alzheimer's Disease and Tauopathies? *Biomed J*. Feb 2018;41(1):21-33. doi:10.1016/j.bj.2018.01.003
253. Karch CM, Jeng AT, Nowotny P, Cady J, Cruchaga C, Goate AM. Expression of novel Alzheimer's disease risk genes in control and Alzheimer's disease brains. *PLoS One*. 2012;7(11):e50976. doi:10.1371/journal.pone.0050976
254. Deming Y, Filipello F, Cignarella F, et al. The MS4A gene cluster is a key modulator of soluble TREM2 and Alzheimer's disease risk. *Sci Transl Med*. 2019;11(505):eaau2291. doi:10.1126/scitranslmed.aau2291
255. Li Z, Farias FHG, Dube U, et al. The TMEM106B FTLD-protective variant, rs1990621, is also associated with increased neuronal proportion. *Acta Neuropathol*. Jan 2020;139(1):45-61. doi:10.1007/s00401-019-02066-0
256. Satoh J-i, Kino Y, Kawana N, et al. TMEM106B expression is reduced in Alzheimer's disease brains. *Alzheimer's Research & Therapy*. 2014/03/31 2014;6(2):17. doi:10.1186/alzrt247
257. Finch N, Carrasquillo MM, Baker M, et al. TMEM106B regulates progranulin levels and the penetrance of FTLD in GRN mutation carriers. *Neurology*. Feb 1 2011;76(5):467-74. doi:10.1212/WNL.0b013e31820a0e3b
258. Rhinn H, Abeliovich A. Differential Aging Analysis in Human Cerebral Cortex Identifies Variants in TMEM106B and GRN that Regulate Aging Phenotypes. *Cell Syst*. Apr 26 2017;4(4):404-415.e5. doi:10.1016/j.cels.2017.02.009
259. Klein ZA, Takahashi H, Ma M, et al. Loss of TMEM106B Ameliorates Lysosomal and Frontotemporal Dementia-Related Phenotypes in Progranulin-Deficient Mice. *Neuron*. 2017;95(2):281-296.e6. doi:10.1016/j.neuron.2017.06.026
260. Ren Y, van Blitterswijk M, Allen M, et al. TMEM106B haplotypes have distinct gene expression patterns in aged brain. *Molecular Neurodegeneration*. 2018/07/03 2018;13(1):35. doi:10.1186/s13024-018-0268-2
261. Bettcher BM, Kramer JH. Longitudinal inflammation, cognitive decline, and Alzheimer's disease: a mini-review. *Clin Pharmacol Ther*. 2014;96(4):464-469. doi:10.1038/clpt.2014.147
262. Heneka MT, Carson MJ, El Khoury J, et al. Neuroinflammation in Alzheimer's disease. *The Lancet Neurology*. 2015;14(4):388-405. doi:10.1016/S1474-4422(15)70016-5
263. Driscoll I, Troncoso J. Asymptomatic Alzheimer's disease: a prodrome or a state of resilience? *Current Alzheimer research*. 2011;8(4):330-335. doi:10.2174/156720511795745348
264. Mukherjee S, Kim S, Ramanan VK, et al. Gene-based GWAS and biological pathway analysis of the resilience of executive functioning. *Brain Imaging and Behavior*. 2013;8(1):110-118.
265. Teipel SJ. Risk and resilience: a new perspective on Alzheimer's Disease. *Geriatric Mental Health Care*. 2013;1(3):47-55.
266. Hohman TJ, Bell SP, Jefferson AL. The Role of Vascular Endothelial Growth Factor in Neurodegeneration and Cognitive Decline: Exploring Interactions With Biomarkers of Alzheimer Disease. *JAMA Neurology*. 2015;72(5):520-529.
267. Hohman TJ, Dumitrescu L, Cox NJ, Jefferson AL. Genetic resilience to amyloid related cognitive decline. *Brain Imaging and Behavior*. 2016:1-9.
268. Kang MS, Aliaga AA, Shin M, et al. Amyloid-beta modulates the association between neurofilament light chain and brain atrophy in Alzheimer's disease. *Molecular Psychiatry*. 2021/10/01 2021;26(10):5989-6001. doi:10.1038/s41380-020-0818-1
269. Iqbal K, Liu F, Gong C-X, Alonso ADC, Grundke-Iqbal I. Mechanisms of tau-induced neurodegeneration. *Acta neuropathologica*. 2009;118(1):53-69. doi:10.1007/s00401-009-0486-3
270. Nosheny RL, Insel PS, Mattsson N, et al. Associations among amyloid status, age, and longitudinal regional brain atrophy in cognitively unimpaired older adults. *Neurobiology of Aging*. 2019/10/01/ 2019;82:110-119. doi:https://doi.org/10.1016/j.neurobiolaging.2019.07.005
271. Solé-Padullés C, Lladó A, Bartrés-Faz D, et al. Association between cerebrospinal fluid tau and brain atrophy is not related to clinical severity in the Alzheimer's disease continuum. *Psychiatry Research: Neuroimaging*. 2011/06/30/ 2011;192(3):140-146. doi:https://doi.org/10.1016/j.pscychresns.2010.12.001
272. Jefferson AL, Gifford KA, Acosta LMY, et al. The Vanderbilt Memory & Aging Project: Study Design and Baseline Cohort Overview. *Journal of Alzheimer's Disease*. 2016;(Preprint):1-20.
273. Sager MA, Hermann B, La Rue A. Middle-aged children of persons with Alzheimer's disease: APOE genotypes and cognitive function in the Wisconsin Registry for Alzheimer's Prevention. *J Geriatr Psychiatry Neurol*. 2005;18(4):245-249.
274. Johnson SC, Koscik RL, Jonaitis EM, et al. The Wisconsin Registry for Alzheimer's Prevention: A review of findings and current directions. *Alzheimer's & dementia (Amsterdam, Netherlands)*. 2018;10:130-142. doi:10.1016/j.dadm.2017.11.007

275. Albert M, Soldan A, Gottesman R, et al. Cognitive changes preceding clinical symptom onset of mild cognitive impairment and relationship to ApoE genotype. *Current Alzheimer Research*. 2014;11(8):773-784.
276. Emrani S, Arain HA, DeMarshall C, Nuriel T. APOE4 is associated with cognitive and pathological heterogeneity in patients with Alzheimer's disease: a systematic review. *Alzheimer's Research & Therapy*. 2020/11/04 2020;12(1):141. doi:10.1186/s13195-020-00712-4
277. Logsdon BA, Perumal TM, Swarup V, et al. Meta-analysis of the human brain transcriptome identifies heterogeneity across human AD coexpression modules robust to sample collection and methodological approach. *bioRxiv*. 2019:510420. doi:10.1101/510420
278. Jack CR, Jr., Bennett DA, Blennow K, et al. A/T/N: An unbiased descriptive classification scheme for Alzheimer disease biomarkers. *Neurology*. 2016;87(5):539-547. doi:10.1212/WNL.0000000000002923
279. Snowdon DA, Kemper SJ, Mortimer JA, Greiner LH, Wekstein DR, Markesbery WR. Linguistic Ability in Early Life and Cognitive Function and Alzheimer's Disease in Late Life: Findings From the Nun Study. *JAMA*. 1996;275(7):528-532. doi:10.1001/jama.1996.03530310034029
280. Snowdon DA. Aging and Alzheimer's disease: lessons from the Nun Study. *Gerontologist*. Apr 1997;37(2):150-6. doi:10.1093/geront/37.2.150
281. Chiang GC, Insel PS, Tosun D, et al. Hippocampal atrophy rates and CSF biomarkers in elderly APOE2 normal subjects. *Neurology*. 2010;75(22):1976-1981. doi:10.1212/WNL.0b013e3181ffe4d1
282. Dumitrescu L, Mahoney ER, Mukherjee S, et al. Genetic variants and functional pathways associated with resilience to Alzheimer's disease. *Brain*. Aug 1 2020;143(8):2561-2575. doi:10.1093/brain/awaa209
283. Stricker NH, Dodge HH, Dowling NM, Han SD, Erosheva EA, Jagust WJ. CSF biomarker associations with change in hippocampal volume and precuneus thickness: implications for the Alzheimer's pathological cascade. *Brain Imaging and Behavior*. 2012;6(4):599-609.
284. Fletcher E, Villeneuve S, Maillard P, et al. β-amyloid, hippocampal atrophy and their relation to longitudinal brain change in cognitively normal individuals. *Neurobiology of aging*. 2016;40:173-180. doi:10.1016/j.neurobiolaging.2016.01.133
285. Frankó E, Joly O, for the Alzheimer's Disease Neuroimaging I. Evaluating Alzheimer's Disease Progression Using Rate of Regional Hippocampal Atrophy. *PLOS ONE*. 2013;8(8):e71354. doi:10.1371/journal.pone.0071354
286. Andrews KA, Frost C, Modat M, et al. Acceleration of hippocampal atrophy rates in asymptomatic amyloidosis. *Neurobiology of Aging*. 2016/03/01/ 2016;39:99-107. doi:https://doi.org/10.1016/j.neurobiolaging.2015.10.013
287. Moghekar A, Li S, Lu Y, et al. CSF biomarker changes precede symptom onset of mild cognitive impairment. *Neurology*. November 12, 2013 2013;81(20):1753-1758. doi:10.1212/01.wnl.0000435558.98447.17
288. Roberts RO, Geda YE, Knopman DS, et al. The Mayo Clinic Study of Aging: design and sampling, participation, baseline measures and sample characteristics. *Neuroepidemiology*. 2008;30(1):58-69. doi:10.1159/000115751
289. Ramanan VK, Wang X, Przybelski SA, et al. Variants in PPP2R2B and IGF2BP3 are associated with higher tau deposition. *Brain Communications*. 2020;2(2)doi:10.1093/braincomms/fcaa159
290. Purcell S, Neale B, Todd-Brown K, et al. PLINK: a tool set for whole-genome association and population-based linkage analyses. *The American Journal of Human Genetics*. 2007;81(3):559-575.
291. Price AL, Patterson NJ, Plenge RM, Weinblatt ME, Shadick NA, Reich D. Principal components analysis corrects for stratification in genome-wide association studies. *Nature genetics*. 2006;38(8):904-909.
292. Das S, Forer L, Schonherr S, et al. Next-generation genotype imputation service and methods. *Nat Genet*. Oct 2016;48(10):1284-1287. doi:10.1038/ng.3656
293. Ramanan VK, Lesnick TG, Przybelski SA, et al. Coping with brain amyloid: genetic heterogeneity and cognitive resilience to Alzheimer's pathophysiology. *Acta Neuropathol Commun*. Mar 23 2021;9(1):48. doi:10.1186/s40478-021-01154-1
294. Pettigrew C, Soldan A, Zhu Y, et al. Cognitive reserve and cortical thickness in preclinical Alzheimer's disease. *Brain imaging and behavior*. 2017;11(2):357-367. doi:10.1007/s11682-016-9581-y
295. About ADNI. 2008. http://www.adni-info.org/Scientists/AboutADNI.aspx
296. Ruigrok ANV, Salimi-Khorshidi G, Lai M-C, et al. A meta-analysis of sex differences in human brain structure. *Neuroscience & Biobehavioral Reviews*. 2014/02/01/ 2014;39:34-50. doi:https://doi.org/10.1016/j.neubiorev.2013.12.004
297. Whitwell JL, Wiste HJ, Weigand SD, et al. Comparison of imaging biomarkers in the Alzheimer Disease Neuroimaging Initiative and the Mayo Clinic Study of Aging. *Archives of neurology*. 2012;69(5):614-622. doi:10.1001/archneurol.2011.3029

298. Varatharajah Y, Ramanan VK, Iyer R, Vemuri P. Predicting Short-term MCI-to-AD Progression Using Imaging, CSF, Genetic Factors, Cognitive Resilience, and Demographics. *Sci Rep*. Feb 19 2019;9(1):2235. doi:10.1038/s41598-019-38793-3
299. Jack CR, Jr., Bernstein MA, Fox NC, et al. The Alzheimer's Disease Neuroimaging Initiative (ADNI): MRI methods. *J Magn Reson Imaging*. Apr 2008;27(4):685-91. doi:10.1002/jmri.21049
300. Wennberg AMV, Lesnick TG, Schwarz CG, et al. Longitudinal Association Between Brain Amyloid-Beta and Gait in the Mayo Clinic Study of Aging. *The Journals of Gerontology: Series A*. 2018;73(9):1244-1250. doi:10.1093/gerona/glx240
301. Mormino EC, Betensky RA, Hedden T, et al. Amyloid and APOE ε4 interact to influence short-term decline in preclinical Alzheimer disease. *Neurology*. 2014;82(20):1760-1767.
302. Raghavan NS, Dumitrescu L, Mormino E, et al. Common Variants in RBFOX1 are Associated with Brain Amyloidosis. *In Review*. 2020;
303. Deming Y, Li Z, Kapoor M, et al. Genome-wide association study identifies four novel loci associated with Alzheimer's endophenotypes and disease modifiers. *Acta Neuropathologica*. May 2017;133(5):839-856. doi:10.1007/s00401-017-1685-y
304. Jack CR, Jr., Wiste HJ, Weigand SD, et al. Defining imaging biomarker cut points for brain aging and Alzheimer's disease. *Alzheimers Dement*. Mar 2017;13(3):205-216. doi:10.1016/j.jalz.2016.08.005
305. Properzi MJ, Buckley RF, Chhatwal JP, et al. Nonlinear Distributional Mapping (NoDiM) for harmonization across amyloid-PET radiotracers. *NeuroImage*. Feb 1 2019;186:446-454. doi:10.1016/j.neuroimage.2018.11.019
306. Roostaei T, Nazeri A, Felsky D, et al. Genome-wide interaction study of brain beta-amyloid burden and cognitive impairment in Alzheimer's disease. *Mol Psychiatry*. Feb 2017;22(2):287-295. doi:10.1038/mp.2016.35
307. Raghavan NS, Dumitrescu L, Mormino E, et al. Association Between Common Variants in RBFOX1, an RNA-Binding Protein, and Brain Amyloidosis in Early and Preclinical Alzheimer Disease. *JAMA Neurol*. Jun 22 2020;doi:10.1001/jamaneurol.2020.1760
308. Lonsdale J, Thomas J, Salvatore M, et al. The Genotype-Tissue Expression (GTEx) project. Commentary. *Nature Genetics*. 06//print 2013;45(6):580-585. doi:10.1038/ng.2653 http://www.nature.com/ng/journal/v45/n6/abs/ng.2653.html#supplementary-information
309. Sieberts SK, Perumal TM, Carrasquillo MM, et al. Large eQTL meta-analysis reveals differing patterns between cerebral cortical and cerebellar brain regions. *Scientific Data*. 2020/10/12 2020;7(1):340. doi:10.1038/s41597-020-00642-8
310. Wallace C. Eliciting priors and relaxing the single causal variant assumption in colocalisation analyses. *PLOS Genetics*. 2020;16(4):e1008720. doi:10.1371/journal.pgen.1008720
311. Giambartolomei C, Vukcevic D, Schadt EE, et al. Bayesian Test for Colocalisation between Pairs of Genetic Association Studies Using Summary Statistics. *PLOS Genetics*. 2014;10(5):e1004383. doi:10.1371/journal.pgen.1004383
312. Liang WS, Dunckley T, Beach TG, et al. Gene expression profiles in anatomically and functionally distinct regions of the normal aged human brain. *Physiol Genomics*. 2007;28(3):311-322. doi:10.1152/physiolgenomics.00208.2006
313. Readhead B, Haure-Mirande JV, Funk CC, et al. Multiscale Analysis of Independent Alzheimer's Cohorts Finds Disruption of Molecular, Genetic, and Clinical Networks by Human Herpesvirus. *Neuron*. Jul 11 2018;99(1):64-82.e7. doi:10.1016/j.neuron.2018.05.023
314. Liang WS, Dunckley T, Beach TG, et al. Altered neuronal gene expression in brain regions differentially affected by Alzheimer's disease: a reference data set. *Physiol Genomics*. Apr 22 2008;33(2):240-56. doi:10.1152/physiolgenomics.00242.2007
315. Liang WS, Reiman EM, Valla J, et al. Alzheimer's disease is associated with reduced expression of energy metabolism genes in posterior cingulate neurons. *Proc Natl Acad Sci U S A*. Mar 18 2008;105(11):4441-6. doi:10.1073/pnas.0709259105
316. de Leeuw CA, Mooij JM, Heskes T, Posthuma D. MAGMA: generalized gene-set analysis of GWAS data. *PLoS Comput Biol*. 2015;11(4):e1004219-e1004219. doi:10.1371/journal.pcbi.1004219
317. Ashburner M, Ball CA, Blake JA, et al. Gene ontology: tool for the unification of biology. The Gene Ontology Consortium. *Nature genetics*. 2000;25(1):25-29. doi:10.1038/75556
318. Kanehisa M, Furumichi M, Tanabe M, Sato Y, Morishima K. KEGG: new perspectives on genomes, pathways, diseases and drugs. *Nucleic Acids Research*. 2017;45(D1):D353-D361.
319. Kanehisa M, Sato Y, Kawashima M, Furumichi M, Tanabe M. KEGG as a reference resource for gene and protein annotation. *Nucleic acids research*. 2016;44(D1):D457-D462. doi:10.1093/nar/gkv1070

320. Ogata H, Goto S, Sato K, Fujibuchi W, Bono H, Kanehisa M. KEGG: Kyoto Encyclopedia of Genes and Genomes. *Nucleic acids research*. 1999;27(1):29-34. doi:10.1093/nar/27.1.29
321. Croft D, O'Kelly G, Wu G, et al. Reactome: a database of reactions, pathways and biological processes. *Nucleic acids research*. 2011;39(Database issue):D691-D697. doi:10.1093/nar/gkq1018
322. Fabregat A, Sidiropoulos K, Garapati P, et al. The Reactome pathway Knowledgebase. *Nucleic acids research*. 2016;44(D1):D481-D487. doi:10.1093/nar/gkv1351
323. Nishimura D. BioCarta. *Biotech Software & Internet Report*. 2001/06/01 2001;2(3):117-120. doi:10.1089/152791601750294344
324. Schaefer CF, Anthony K, Krupa S, et al. PID: the Pathway Interaction Database. *Nucleic acids research*. 2009;37(Database issue):D674-D679. doi:10.1093/nar/gkn653
325. Chiang GC, Insel PS, Tosun D, et al. Impact of apolipoprotein E4-cerebrospinal fluid β-amyloid interaction on hippocampal volume loss over 1 year in mild cognitive impairment. *Alzheimer's & dementia : the journal of the Alzheimer's Association*. 2011;7(5):514-520. doi:10.1016/j.jalz.2010.12.010
326. Yu C-E, Seltman H, Peskind ER, et al. Comprehensive analysis of APOE and selected proximate markers for late-onset Alzheimer's disease: patterns of linkage disequilibrium and disease/marker association. *Genomics*. 2007;89(6):655-665. doi:10.1016/j.ygeno.2007.02.002
327. Heinz S, Benner C, Spann N, et al. Simple combinations of lineage-determining transcription factors prime cis-regulatory elements required for macrophage and B cell identities. *Mol Cell*. 2010;38(4):576-589. doi:10.1016/j.molcel.2010.05.004
328. World Health O. ICD-10 : international statistical classification of diseases and related health problems : tenth revision. 2nd ed ed. Geneva: World Health Organization; 2004.
329. Cruchaga C, Kauwe JSK, Mayo K, et al. SNPs associated with cerebrospinal fluid phospho-tau levels influence rate of decline in Alzheimer's disease. *PLoS Genetics*. 2010;6(9):e1001101.
330. Bahcall OG. GTEx pilot quantifies eQTL variation across tissues and individuals. *Nature Reviews Genetics*. 2015/07/01 2015;16(7):375-375. doi:10.1038/nrg3969
331. Aguet F, Brown AA, Castel SE, et al. Genetic effects on gene expression across human tissues. *Nature*. 2017/10/01 2017;550(7675):204-213. doi:10.1038/nature24277
332. O'Connor TP, Cockburn K, Wang W, Tapia L, Currie E, Bamji SX. Semaphorin 5B mediates synapse elimination in hippocampal neurons. *Neural Development*. 2009/05/23 2009;4(1):18. doi:10.1186/1749-8104-4-18
333. Zhang Y, Chen K, Sloan SA, et al. An RNA-Sequencing Transcriptome and Splicing Database of Glia, Neurons, and Vascular Cells of the Cerebral Cortex. *The Journal of Neuroscience*. 2014;34(36):11929. doi:10.1523/JNEUROSCI.1860-14.2014
334. Zhang Y, Sloan Steven A, Clarke Laura E, et al. Purification and Characterization of Progenitor and Mature Human Astrocytes Reveals Transcriptional and Functional Differences with Mouse. *Neuron*. 2016;89(1):37-53. doi:10.1016/j.neuron.2015.11.013
335. Alto LT, Terman JR. Semaphorins and their Signaling Mechanisms. *Methods Mol Biol*. 2017;1493:1-25. doi:10.1007/978-1-4939-6448-2_1
336. Jung JS, Zhang KD, Wang Z, et al. Semaphorin-5B Controls Spiral Ganglion Neuron Branch Refinement during Development. *The Journal of Neuroscience*. 2019;39(33):6425. doi:10.1523/JNEUROSCI.0113-19.2019
337. Lett RLM, Wang W, O'Connor TP. Semaphorin 5B Is a Novel Inhibitory Cue for Corticofugal Axons. *Cerebral Cortex*. 2008;19(6):1408-1421. doi:10.1093/cercor/bhn179
338. Liu RQ, Wang W, Legg A, Abramyan J, Connor TP. Semaphorin 5B is a repellent cue for sensory afferents projecting into the developing spinal cord. *Development*. 2014;141(9):1940. doi:10.1242/dev.103630
339. Matsuoka RL, Chivatakarn O, Badea TC, et al. Class 5 transmembrane semaphorins control selective Mammalian retinal lamination and function. *Neuron*. 2011;71(3):460-473. doi:10.1016/j.neuron.2011.06.009
340. Hong CH, Falvey C, Harris TB, et al. Anemia and risk of dementia in older adults: findings from the Health ABC study. *Neurology*. 2013;81(6):528-533. doi:10.1212/WNL.0b013e31829e701d
341. Jeong S-M, Shin DW, Lee JE, Hyeon JH, Lee J, Kim S. Anemia is associated with incidence of dementia: a national health screening study in Korea involving 37,900 persons. *Alzheimer's Research & Therapy*. 2017/12/06 2017;9(1):94. doi:10.1186/s13195-017-0322-2
342. Wolters FJ, Zonneveld HI, Licher S, et al. Hemoglobin and anemia in relation to dementia risk and accompanying changes on brain MRI. *Neurology*. 2019;93(9):e917. doi:10.1212/WNL.0000000000008003
343. Bianchi VE. Role of nutrition on anemia in elderly. *Clinical Nutrition ESPEN*. 2016;11:e1-e11. doi:10.1016/j.clnesp.2015.09.003

344. Wang HX, Wahlin Å, Basun H, Fastbom J, Winblad B, Fratiglioni L. Vitamin B₁₂ and folate in relation to the development of Alzheimer's disease. *Neurology*. 2001;56(9):1188. doi:10.1212/WNL.56.9.1188
345. Petr MA, Tulika T, Carmona-Marin LM, Scheibye-Knudsen M. Protecting the Aging Genome. *Trends in Cell Biology*. 2020/02/01/ 2020;30(2):117-132. doi:https://doi.org/10.1016/j.tcb.2019.12.001
346. Maynard S, Fang EF, Scheibye-Knudsen M, Croteau DL, Bohr VA. DNA Damage, DNA Repair, Aging, and Neurodegeneration. *Cold Spring Harb Perspect Med*. 2015;5(10):a025130. doi:10.1101/cshperspect.a025130
347. Lin X, Kapoor A, Gu Y, et al. Contributions of DNA Damage to Alzheimer's Disease. *Int J Mol Sci*. 2020;21(5):1666. doi:10.3390/ijms21051666
348. Suberbielle E, Djukic B, Evans M, et al. DNA repair factor BRCA1 depletion occurs in Alzheimer brains and impairs cognitive function in mice. *Nature Communications*. 2015/11/30 2015;6(1):8897. doi:10.1038/ncomms9897
349. Hu Y-B, Dammer EB, Ren R-J, Wang G. The endosomal-lysosomal system: from acidification and cargo sorting to neurodegeneration. *Translational Neurodegeneration*. 2015/09/30 2015;4(1):18. doi:10.1186/s40035-015-0041-1
350. van Weering JRT, Scheper W. Endolysosome and Autolysosome Dysfunction in Alzheimer's Disease: Where Intracellular and Extracellular Meet. *CNS Drugs*. 2019/07/01 2019;33(7):639-648. doi:10.1007/s40263-019-00643-1
351. Vaz-Silva J, Gomes P, Jin Q, et al. Endolysosomal degradation of Tau and its role in glucocorticoid-driven hippocampal malfunction. *EMBO J*. 2018;37(20):e99084. doi:10.15252/embj.201899084
352. Liu C-C, Kanekiyo T, Xu H, Bu G. Apolipoprotein E and Alzheimer disease: risk, mechanisms and therapy. 10.1038/nrneurol.2012.263. *Nature Reviews Neurology*. 02//print 2013;9(2):106-118.
353. Yip AG, McKee AC, Green RC, et al. APOE, vascular pathology, and the AD brain. *Neurology*. Jul 26 2005;65(2):259-65. doi:10.1212/01.wnl.0000168863.49053.4d
354. Yamazaki Y, Zhao N, Caulfield TR, Liu C-C, Bu G. Apolipoprotein E and Alzheimer disease: pathobiology and targeting strategies. *Nature Reviews Neurology*. 2019/09/01 2019;15(9):501-518. doi:10.1038/s41582-019-0228-7
355. Lautner R, Insel PS, Skillbäck T, et al. Preclinical effects of APOE ε4 on cerebrospinal fluid Aβ42 concentrations. *Alzheimers Res Ther*. Oct 23 2017;9(1):87. doi:10.1186/s13195-017-0313-3
356. Reitz C, Rogaeva E, Beecham GW. Late-onset vs nonmendelian early-onset Alzheimer disease: A distinction without a difference? *Neurol Genet*. Oct 2020;6(5):e512. doi:10.1212/nxg.0000000000000512
357. Kunkle BW, Grenier-Boley B, Sims R, et al. Genetic meta-analysis of diagnosed Alzheimer's disease identifies new risk loci and implicates Aβ, tau, immunity and lipid processing. *Nature genetics*. 2019;51(3):414-430. doi:10.1038/s41588-019-0358-2
358. Wightman DP, Jansen IE, Savage JE, et al. A genome-wide association study with 1,126,563 individuals identifies new risk loci for Alzheimer's disease. *Nature Genetics*. 2021/09/01 2021;53(9):1276-1282. doi:10.1038/s41588-021-00921-z
359. Corder EH, Saunders AM, Strittmatter WJ, et al. Gene dose of apolipoprotein E type 4 allele and the risk of Alzheimer's disease in late onset families. *Science*. Aug 13 1993;261(5123):921-3. doi:10.1126/science.8346443
360. Saunders AM, Strittmatter WJ, Schmechel D, et al. Association of apolipoprotein E allele epsilon 4 with late-onset familial and sporadic Alzheimer's disease. *Neurology*. Aug 1993;43(8):1467-72. doi:10.1212/wnl.43.8.1467
361. Wu L, Zhao L. ApoE2 and Alzheimer's disease: time to take a closer look. *Neural Regen Res*. Mar 2016;11(3):412-3. doi:10.4103/1673-5374.179044
362. Baek MS, Cho H, Lee HS, Lee JH, Ryu YH, Lyoo CH. Effect of APOE ε4 genotype on amyloid-β and tau accumulation in Alzheimer's disease. *Alzheimer's Research & Therapy*. 2020/10/31 2020;12(1):140. doi:10.1186/s13195-020-00710-6
363. Jack CR, Jr., Knopman DS, Jagust WJ, et al. Tracking pathophysiological processes in Alzheimer's disease: an updated hypothetical model of dynamic biomarkers. *Lancet Neurol*. Feb 2013;12(2):207-16. doi:10.1016/s1474-4422(12)70291-0
364. Jack CR, Jr., Knopman DS, Jagust WJ, et al. Hypothetical model of dynamic biomarkers of the Alzheimer's pathological cascade. *Lancet Neurol*. Jan 2010;9(1):119-28. doi:10.1016/s1474-4422(09)70299-6
365. Seto M, Weiner RL, Dumitrescu L, Hohman TJ. Protective genes and pathways in Alzheimer's disease: moving towards precision interventions. *Molecular Neurodegeneration*. 2021/04/29 2021;16(1):29. doi:10.1186/s13024-021-00452-5

366. Ma Y, Yu L, Olah M, et al. Epigenomic features related to microglia are associated with attenuated effect of APOE ε4 on Alzheimer's disease risk in humans. https://doi.org/10.1002/alz.12425. *Alzheimer's & Dementia*. 2021/09/05 2021;n/a(n/a)doi:https://doi.org/10.1002/alz.12425
367. Husain MA, Laurent B, Plourde M. APOE and Alzheimer's Disease: From Lipid Transport to Physiopathology and Therapeutics. Review. *Front Neurosci*. 2021-February-17 2021;15(85)doi:10.3389/fnins.2021.630502
368. Sullivan PF, Fan C, Perou CM. Evaluating the comparability of gene expression in blood and brain. *Am J Med Genet B Neuropsychiatr Genet*. Apr 5 2006;141b(3):261-8. doi:10.1002/ajmg.b.30272
369. Tylee DS, Kawaguchi DM, Glatt SJ. On the outside, looking in: a review and evaluation of the comparability of blood and brain "-omes". *Am J Med Genet B Neuropsychiatr Genet*. Oct 2013;162b(7):595-603. doi:10.1002/ajmg.b.32150
370. Cullen NC, Mälarstig An, Stomrud E, Hansson O, Mattsson-Carlgren N. Accelerated inflammatory aging in Alzheimer's disease and its relation to amyloid, tau, and cognition. *Scientific Reports*. 2021/01/21 2021;11(1):1965. doi:10.1038/s41598-021-81705-7
371. King E, O'Brien JT, Donaghy P, et al. Peripheral inflammation in prodromal Alzheimer's and Lewy body dementias. *Journal of Neurology, Neurosurgery & Psychiatry*. 2018;89(4):339. doi:10.1136/jnnp-2017-317134
372. Tao Q, Ang TFA, DeCarli C, et al. Association of Chronic Low-grade Inflammation With Risk of Alzheimer Disease in ApoE4 Carriers. *JAMA Netw Open*. Oct 5 2018;1(6):e183597. doi:10.1001/jamanetworkopen.2018.3597
373. Kloske CM, Wilcock DM. The Important Interface Between Apolipoprotein E and Neuroinflammation in Alzheimer's Disease. Review. *Frontiers in Immunology*. 2020-April-30 2020;11(754)doi:10.3389/fimmu.2020.00754
374. Krasemann S, Madore C, Cialic R, et al. The TREM2-APOE Pathway Drives the Transcriptional Phenotype of Dysfunctional Microglia in Neurodegenerative Diseases. *Immunity*. 2017/09/19/ 2017;47(3):566-581.e9. doi:https://doi.org/10.1016/j.immuni.2017.08.008
375. Jefferson AL, Gifford KA, Acosta LMY, et al. The Vanderbilt Memory & Aging Project: Study Design and Baseline Cohort Overview. *Journal of Alzheimer's disease : JAD*. 2016;52(2):539-559. doi:10.3233/JAD-150914
376. Bennett DA, Buchman AS, Boyle PA, Barnes LL, Wilson RS, Schneider JA. Religious Orders Study and Rush Memory and Aging Project. *Journal of Alzheimer's disease : JAD*. 2018;64(s1):S161-S189. doi:10.3233/JAD-179939
377. Kresge HA, Khan OA, Wagener MA, et al. Subclinical Compromise in Cardiac Strain Relates to Lower Cognitive Performances in Older Adults. *Journal of the American Heart Association*. 2018;7(4):e007562. doi:doi:10.1161/JAHA.117.007562
378. Crane PK, Carle A, Gibbons LE, et al. Development and assessment of a composite score for memory in the Alzheimer's Disease Neuroimaging Initiative (ADNI). *Brain Imaging Behav*. Dec 2012;6(4):502-16. doi:10.1007/s11682-012-9186-z
379. Wilson RS, Boyle PA, Yu L, et al. Temporal course and pathologic basis of unawareness of memory loss in dementia. *Neurology*. 2015;85(11):984-991.
380. De Jager PL, Ma Y, McCabe C, et al. A multi-omic atlas of the human frontal cortex for aging and Alzheimer's disease research. *Sci Data*. Aug 7 2018;5:180142. doi:10.1038/sdata.2018.142
381. Mostafavi S, Gaiteri C, Sullivan SE, et al. A molecular network of the aging human brain provides insights into the pathology and cognitive decline of Alzheimer's disease. *Nat Neurosci*. Jun 2018;21(6):811-819. doi:10.1038/s41593-018-0154-9
382. Lee AJ, Ma Y, Yu L, et al. Multi-region brain transcriptomes uncover two subtypes of aging individuals with differences in Alzheimer's disease risk and the impact of APOEε4. *bioRxiv*. 2021;
383. Logsdon BA, Perumal TM, Swarup V, et al. Meta-analysis of the human brain transcriptome identifies heterogeneity across human AD coexpression modules robust to sample collection and methodological approach. *bioRxiv*. 2019:510420. doi:10.1101/510420
384. Dobin A, Davis CA, Schlesinger F, et al. STAR: ultrafast universal RNA-seq aligner. *Bioinformatics*. 2013;29(1):15-21. doi:10.1093/bioinformatics/bts635
385. Howe KL, Achuthan P, Allen J, et al. Ensembl 2021. *Nucleic Acids Research*. 2021;49(D1):D884-D891. doi:10.1093/nar/gkaa942
386. Liao Y, Smyth GK, Shi W. featureCounts: an efficient general purpose program for assigning sequence reads to genomic features. *Bioinformatics*. Apr 1 2014;30(7):923-30. doi:10.1093/bioinformatics/btt656
387. Institute B. Picard Toolkit. *Broad Institute, GitHub Repository*. 2019;

388. Hansen KD, Irizarry RA, Wu Z. Removing technical variability in RNA-seq data using conditional quantile normalization. *Biostatistics*. 2012;13(2):204-216. doi:10.1093/biostatistics/kxr054
389. Law CW, Chen Y, Shi W, Smyth GK. voom: precision weights unlock linear model analysis tools for RNA-seq read counts. *Genome Biology*. 2014/02/03 2014;15(2):R29. doi:10.1186/gb-2014-15-2-r29
390. Ritchie ME, Phipson B, Wu D, et al. limma powers differential expression analyses for RNA-sequencing and microarray studies. *Nucleic acids research*. 2015;43(7):e47-e47.
391. Skillbäck T, Farahmand BY, Rosén C, et al. Cerebrospinal fluid tau and amyloid-β1-42 in patients with dementia. *Brain*. 2015;138(9):2716-2731. doi:10.1093/brain/awv181
392. Dorey A, Perret-Liaudet A, Tholance Y, Fourier A, Quadrio I. Cerebrospinal Fluid Aβ40 Improves the Interpretation of Aβ42 Concentration for Diagnosing Alzheimer's Disease. *Front Neurol*. 2015;6:247-247. doi:10.3389/fneur.2015.00247
393. Mirra SS, Heyman A, McKeel D, et al. The Consortium to Establish a Registry for Alzheimer's Disease (CERAD) Part II. Standardization of the neuropathologic assessment of Alzheimer's disease. *Neurology*. 1991;41(4):479-479.
394. Bennett DA, Schneider JA, Arvanitakis Z, et al. Neuropathology of older persons without cognitive impairment from two community-based studies. *Neurology*. 2006;66(12):1837-1844.
395. Benjamini Y, Hochberg Y. Controlling the False Discovery Rate: A Practical and Powerful Approach to Multiple Testing. https://doi.org/10.1111/j.2517-6161.1995.tb02031.x. *Journal of the Royal Statistical Society: Series B (Methodological)*. 1995/01/01 1995;57(1):289-300. doi:https://doi.org/10.1111/j.2517-6161.1995.tb02031.x
396. Becknell B, Eichler TE, Beceiro S, et al. Ribonucleases 6 and 7 have antimicrobial function in the human and murine urinary tract. *Kidney Int*. 2015;87(1):151-161. doi:10.1038/ki.2014.268
397. Fang Y, Li J, Niu X, Ma N, Zhao J. Hypomethylation of Rnase6 Promoter Enhances Proliferation and Migration of Murine Aortic Vascular Smooth Muscle Cells and Aggravates Atherosclerosis in Mice. *Front Bioeng Biotechnol*. 2021;9:695461-695461. doi:10.3389/fbioe.2021.695461
398. Shen X-N, Niu L-D, Wang Y-J, et al. Inflammatory markers in Alzheimer's disease and mild cognitive impairment: a meta-analysis and systematic review of 170 studies. *Journal of Neurology, Neurosurgery & Psychiatry*. 2019;90(5):590. doi:10.1136/jnnp-2018-319148
399. Pascoal TA, Benedet AL, Ashton NJ, et al. Microglial activation and tau propagate jointly across Braak stages. *Nature Medicine*. 2021/08/26 2021;doi:10.1038/s41591-021-01456-w
400. Patrick E, Olah M, Taga M, et al. A cortical immune network map identifies distinct microglial transcriptional programs associated with β-amyloid and Tau pathologies. *Transl Psychiatry*. Jan 14 2021;11(1):50. doi:10.1038/s41398-020-01175-9
401. Hickman SE, El Khoury J. TREM2 and the neuroimmunology of Alzheimer's disease. *Biochem Pharmacol*. 2014;88(4):495-498. doi:10.1016/j.bcp.2013.11.021
402. Olah M, Menon V, Habib N, et al. Single cell RNA sequencing of human microglia uncovers a subset associated with Alzheimer's disease. *Nature Communications*. 2020/11/30 2020;11(1):6129. doi:10.1038/s41467-020-19737-2
403. Miller JA, Woltjer RL, Goodenbour JM, Horvath S, Geschwind DH. Genes and pathways underlying regional and cell type changes in Alzheimer's disease. *Genome Med*. 2013/05/25 2013;5(5):48. doi:10.1186/gm452
404. Fernandez CG, Hamby ME, McReynolds ML, Ray WJ. The Role of APOE4 in Disrupting the Homeostatic Functions of Astrocytes and Microglia in Aging and Alzheimer's Disease. Review. *Frontiers in Aging Neuroscience*. 2019-February-11 2019;11doi:10.3389/fnagi.2019.00014
405. Qiao X, Cummins DJ, Paul SM. Neuroinflammation-induced acceleration of amyloid deposition in the APPV717F transgenic mouse. *Eur J Neurosci*. Aug 2001;14(3):474-82. doi:10.1046/j.0953-816x.2001.01666.x
406. Egensperger R, Kösel S, von Eitzen U, Graeber MB. Microglial activation in Alzheimer disease: Association with APOE genotype. *Brain Pathol*. Jul 1998;8(3):439-47. doi:10.1111/j.1750-3639.1998.tb00166.x
407. Lynch JR, Tang W, Wang H, et al. APOE genotype and an ApoE-mimetic peptide modify the systemic and central nervous system inflammatory response. *J Biol Chem*. Dec 5 2003;278(49):48529-33. doi:10.1074/jbc.M306923200
408. Mukherjee S, Kim S, Ramanan VK, et al. Gene-based GWAS and biological pathway analysis of the resilience of executive functioning. *Brain imaging and behavior*. 2014;8(1):110-118. doi:10.1007/s11682-013-9259-7
409. Park KHJ, Barrett T. Gliosis Precedes Amyloid-β Deposition and Pathological Tau Accumulation in the Neuronal Cell Cycle Re-Entry Mouse Model of Alzheimer's Disease. *J Alzheimers Dis Rep*. 2020;4(1):243-253. doi:10.3233/ADR-200170

410. Walker KA, Gottesman RF, Wu A, et al. Systemic inflammation during midlife and cognitive change over 20 years. *Neurology*. 2019;92(11):e1256. doi:10.1212/WNL.0000000000007094
411. Walker KA, Windham BG, Brown CH, et al. The Association of Mid- and Late-Life Systemic Inflammation with Brain Amyloid Deposition: The ARIC-PET Study. *Journal of Alzheimer's disease : JAD*. 2018;66(3):1041-1052. doi:10.3233/JAD-180469
412. Zhong L, Chen X-F. The Emerging Roles and Therapeutic Potential of Soluble TREM2 in Alzheimer's Disease. Review. *Frontiers in Aging Neuroscience*. 2019-November-26 2019;11doi:10.3389/fnagi.2019.00328
413. Suárez-Calvet M, Kleinberger G, Araque Caballero M, et al. sTREM2 cerebrospinal fluid levels are a potential biomarker for microglia activity in early-stage Alzheimer's disease and associate with neuronal injury markers. *EMBO Mol Med*. May 2016;8(5):466-76. doi:10.15252/emmm.201506123
414. Ma L-Z, Tan L, Bi Y-L, et al. Dynamic changes of CSF sTREM2 in preclinical Alzheimer's disease: the CABLE study. *Molecular Neurodegeneration*. 2020/04/10 2020;15(1):25. doi:10.1186/s13024-020-00374-8
415. Suarez-Calvet M, Morenas-Rodriguez E, Kleinberger G, et al. Early increase of CSF sTREM2 in Alzheimer's disease is associated with tau related-neurodegeneration but not with amyloid-beta pathology. *Mol Neurodegener*. Jan 10 2019;14(1):1. doi:10.1186/s13024-018-0301-5
416. Ewers M, Biechele G, Suárez-Calvet M, et al. Higher CSF sTREM2 and microglia activation are associated with slower rates of beta-amyloid accumulation. https://doi.org/10.15252/emmm.202012308. *EMBO Mol Med*. 2020/09/07 2020;12(9):e12308. doi:https://doi.org/10.15252/emmm.202012308
417. Ewers M, Franzmeier N, Suárez-Calvet M, et al. Increased soluble TREM2 in cerebrospinal fluid is associated with reduced cognitive and clinical decline in Alzheimer's disease. *Sci Transl Med*. Aug 28 2019;11(507)doi:10.1126/scitranslmed.aav6221
418. Wang L, Gao T, Cai T, Li K, Zheng P, Liu J. Cerebrospinal fluid levels of YKL-40 in prodromal Alzheimer's disease. *Neurosci Lett*. Jan 10 2020;715:134658. doi:10.1016/j.neulet.2019.134658
419. Ng A, Tam WW, Zhang MW, et al. IL-1β, IL-6, TNF- α and CRP in Elderly Patients with Depression or Alzheimer's disease: Systematic Review and Meta-Analysis. *Scientific Reports*. 2018/08/13 2018;8(1):12050. doi:10.1038/s41598-018-30487-6
420. Cojocaru IM, Cojocaru M, Miu G, Sapira V. Study of interleukin-6 production in Alzheimer's disease. *Rom J Intern Med*. 2011;49(1):55-8.
421. Lyra e Silva NM, Gonçalves RA, Pascoal TA, et al. Pro-inflammatory interleukin-6 signaling links cognitive impairments and peripheral metabolic alterations in Alzheimer's disease. *Translational Psychiatry*. 2021/04/28 2021;11(1):251. doi:10.1038/s41398-021-01349-z
422. Park JC, Han SH, Mook-Jung I. Peripheral inflammatory biomarkers in Alzheimer's disease: a brief review. *BMB Rep*. Jan 2020;53(1):10-19. doi:10.5483/BMBRep.2020.53.1.309
423. Kravitz BA, Corrada MM, Kawas CH. Elevated C-reactive protein levels are associated with prevalent dementia in the oldest-old. *Alzheimer's & dementia : the journal of the Alzheimer's Association*. 2009;5(4):318-323. doi:10.1016/j.jalz.2009.04.1230
424. Qin Q, Teng Z, Liu C, Li Q, Yin Y, Tang Y. TREM2, microglia, and Alzheimer's disease. *Mech Ageing Dev*. Apr 2021;195:111438. doi:10.1016/j.mad.2021.111438
425. Franzmeier N, Suárez-Calvet M, Frontzkowski L, et al. Higher CSF sTREM2 attenuates ApoE4-related risk for cognitive decline and neurodegeneration. *Molecular Neurodegeneration*. 2020/10/08 2020;15(1):57. doi:10.1186/s13024-020-00407-2
426. Sproston NR, Ashworth JJ. Role of C-Reactive Protein at Sites of Inflammation and Infection. *Frontiers in immunology*. 2018;9:754-754. doi:10.3389/fimmu.2018.00754
427. Lewis NA, Knight JE. Longitudinal associations between C-reactive protein and cognitive performance in normative cognitive ageing and dementia. *Age Ageing*. Nov 10 2021;50(6):2199-2205. doi:10.1093/ageing/afab152
428. Martiskainen H, Takalo M, Solomon A, et al. Decreased plasma C-reactive protein levels in APOE ε4 allele carriers. *Ann Clin Transl Neurol*. Oct 2018;5(10):1229-1240. doi:10.1002/acn3.639
429. O'Bryant SE, Waring SC, Hobson V, et al. Decreased C-Reactive Protein Levels in Alzheimer Disease. *J Geriatr Psychiatry Neurol*. 2010/03/01 2009;23(1):49-53. doi:10.1177/0891988709351832
430. Lu L, Li J, Moussaoui M, Boix E. Immune Modulation by Human Secreted RNases at the Extracellular Space. Review. *Frontiers in Immunology*. 2018-May-16 2018;9doi:10.3389/fimmu.2018.01012
431. Schwartz L, Cohen A, Thomas J, Spencer JD. The Immunomodulatory and Antimicrobial Properties of the Vertebrate Ribonuclease A Superfamily. *Vaccines (Basel)*. 2018;6(4):76. doi:10.3390/vaccines6040076
432. Singh-Manoux A, Dugravot A, Brunner E, et al. Interleukin-6 and C-reactive protein as predictors of cognitive decline in late midlife. *Neurology*. 2014;83(6):486-493. doi:10.1212/WNL.0000000000000665

433. Wright CB, Sacco RL, Rundek TR, Delman JB, Rabbani LE, Elkind MSV. Interleukin-6 is associated with cognitive function: the Northern Manhattan Study. *J Stroke Cerebrovasc Dis*. Jan-Feb 2006;15(1):34-38. doi:10.1016/j.jstrokecerebrovasdis.2005.08.009
434. Park S-H, Lee E-H, Kim H-J, et al. The relationship of soluble TREM2 to other biomarkers of sporadic Alzheimer's disease. *Scientific Reports*. 2021/06/22 2021;11(1):13050. doi:10.1038/s41598-021-92101-6
435. Henjum K, Almdahl IS, Årskog V, et al. Cerebrospinal fluid soluble TREM2 in aging and Alzheimer's disease. *Alzheimer's Research & Therapy*. 2016/04/27 2016;8(1):17. doi:10.1186/s13195-016-0182-1
436. Lanoiselée H-M, Nicolas G, Wallon D, et al. APP, PSEN1, and PSEN2 mutations in early-onset Alzheimer disease: A genetic screening study of familial and sporadic cases. *PLOS Medicine*. 2017;14(3):e1002270. doi:10.1371/journal.pmed.1002270
437. Tanzi RE. The genetics of Alzheimer disease. *Cold Spring Harb Perspect Med*. 2012;2(10):a006296. doi:10.1101/cshperspect.a006296
438. Ertekin-Taner N. Genetics of Alzheimer's disease: a centennial review. *Neurol Clin*. 2007;25(3):611-v. doi:10.1016/j.ncl.2007.03.009
439. Langfelder P, Horvath S. WGCNA: an R package for weighted correlation network analysis. journal article. *BMC Bioinformatics*. 2008;9(1):559. doi:10.1186/1471-2105-9-559
440. Gaiteri C, Chen M, Szymanski B, et al. Identifying robust communities and multi-community nodes by combining top-down and bottom-up approaches to clustering. *Scientific Reports*. 2015/11/09 2015;5(1):16361. doi:10.1038/srep16361
441. Gerring ZF, Gamazon ER, Derks EM, for the Major Depressive Disorder Working Group of the Psychiatric Genomics C. A gene co-expression network-based analysis of multiple brain tissues reveals novel genes and molecular pathways underlying major depression. *PLOS Genetics*. 2019;15(7):e1008245. doi:10.1371/journal.pgen.1008245
442. Langfelder P, Horvath S. Fast R Functions for Robust Correlations and Hierarchical Clustering. *Journal of Statistical Software*. 03/07 2012;46(11):1 - 17. doi:10.18637/jss.v046.i11
443. Hopkins AL, Groom CR. The druggable genome. *Nature Reviews Drug Discovery*. 2002/09/01 2002;1(9):727-730. doi:10.1038/nrd892
444. Gamazon ER, Wheeler HE, Shah KP, et al. A gene-based association method for mapping traits using reference transcriptome data. *Nature Genetics*. 2015;47(9):1091-1098.
445. Consortium G. The Genotype-Tissue Expression (GTEx) pilot analysis: Multitissue gene regulation in humans. *Science*. 2015;348(6235):648-660.
446. Bennett DA, Buchman AS, Boyle PA, Barnes LL, Wilson RS, Schneider JA. Religious Orders Study and Rush Memory and Aging Project. *Journal of Alzheimer's disease : JAD*. 2018;64(s1)(s1):S161-S189. doi:10.3233/JAD-179939
447. Mahoney ER, Dumitrescu L, Moore AM, et al. Brain expression of the vascular endothelial growth factor gene family in cognitive aging and alzheimer's disease. *Molecular psychiatry*. 2019;
448. Huckins LM, Dobbyn A, Ruderfer DM, et al. Gene expression imputation across multiple brain regions provides insights into schizophrenia risk. *Nature Genetics*. 2019/04/01 2019;51(4):659-674. doi:10.1038/s41588-019-0364-4
449. Kolberg L, Raudvere U, Kuzmin I, Vilo J, Peterson H. gprofiler2 -- an R package for gene list functional enrichment analysis and namespace conversion toolset g:Profiler. *F1000Res*. 2020;9doi:10.12688/f1000research.24956.2
450. Smedley D, Haider S, Ballester B, et al. BioMart – biological queries made easy. *BMC Genomics*. 2009/01/14 2009;10(1):22. doi:10.1186/1471-2164-10-22
451. Hastie TT, Robert; Gavin, Sherlock; Eisen, Michael; Brown, Patrick; Botstein, David. Imputing Missing Data for Gene Expression Arrays. *Technical Report*. Division of Biostatistics, Stanford University; 1999.
452. Millevoi S, Vagner S. Molecular mechanisms of eukaryotic pre-mRNA 3' end processing regulation. *Nucleic Acids Res*. May 2010;38(9):2757-74. doi:10.1093/nar/gkp1176
453. Tsolakidou A, Czibere L, Pütz B, et al. Gene expression profiling in the stress control brain region hypothalamic paraventricular nucleus reveals a novel gene network including amyloid beta precursor protein. *BMC genomics*. 2010;11:546-546. doi:10.1186/1471-2164-11-546
454. Chen X-F, Zhang Y-w, Xu H, Bu G. Transcriptional regulation and its misregulation in Alzheimer's disease. *Mol Brain*. 2013;6:44-44. doi:10.1186/1756-6606-6-44
455. Meng G, Mei H. Transcriptional Dysregulation Study Reveals a Core Network Involving the Progression of Alzheimer's Disease. Original Research. *Frontiers in Aging Neuroscience*. 2019-May-07 2019;11doi:10.3389/fnagi.2019.00101

456. Mofatteh M. Neurodegeneration and axonal mRNA transportation. *Am J Neurodegener Dis*. 2021;10(1):1-12.
457. Marques-Coelho D, Iohan LdCC, Melo de Farias AR, et al. Differential transcript usage unravels gene expression alterations in Alzheimer's disease human brains. *npj Aging and Mechanisms of Disease*. 2021/01/04 2021;7(1):2. doi:10.1038/s41514-020-00052-5
458. Shan N, Wang Z, Hou L. Identification of trans-eQTLs using mediation analysis with multiple mediators. *BMC Bioinformatics*. 2019/03/29 2019;20(3):126. doi:10.1186/s12859-019-2651-6
459. Kolberg L, Kerimov N, Peterson H, Alasoo K. Co-expression analysis reveals interpretable gene modules controlled by trans-acting genetic variants. *eLife*. 2020/09/03 2020;9:e58705. doi:10.7554/eLife.58705
460. Brynedal B, Choi J, Raj T, et al. Large-Scale trans-eQTLs Affect Hundreds of Transcripts and Mediate Patterns of Transcriptional Co-regulation. *The American Journal of Human Genetics*. 2017/04/06/ 2017;100(4):581-591. doi:https://doi.org/10.1016/j.ajhg.2017.02.004
461. Langfelder P, Mischel PS, Horvath S. When Is Hub Gene Selection Better than Standard Meta-Analysis? *PLOS ONE*. 2013;8(4):e61505. doi:10.1371/journal.pone.0061505
462. Zhao J, Fu Y, Yamazaki Y, et al. APOE4 exacerbates synapse loss and neurodegeneration in Alzheimer's disease patient iPSC-derived cerebral organoids. *Nature Communications*. 2020/11/02 2020;11(1):5540. doi:10.1038/s41467-020-19264-0
463. Therriault J, Benedet AL, Pascoal TA, et al. APOEε4 potentiates the relationship between amyloid-β and tau pathologies. *Molecular Psychiatry*. 2021/10/01 2021;26(10):5977-5988. doi:10.1038/s41380-020-0688-6
464. Rawle MJ, Davis D, Bendayan R, Wong A, Kuh D, Richards M. Apolipoprotein-E (Apoe) ε4 and cognitive decline over the adult life course. *Translational Psychiatry*. 2018/01/10 2018;8(1):18. doi:10.1038/s41398-017-0064-8
465. Gharbi-Meliani A, Dugravot A, Sabia S, et al. The association of APOE ε4 with cognitive function over the adult life course and incidence of dementia: 20 years follow-up of the Whitehall II study. *Alzheimer's Research & Therapy*. 2021/01/04 2021;13(1):5. doi:10.1186/s13195-020-00740-0
466. Moser VA, Workman MJ, Hurwitz SJ, Lipman RM, Pike CJ, Svendsen CN. Microglial transcription profiles in mouse and human are driven by APOE4 and sex. *iScience*. 2021/11/19/ 2021;24(11):103238. doi:https://doi.org/10.1016/j.isci.2021.103238
467. Theendakara V, Peters-Libeu CA, Spilman P, Poksay KS, Bredesen DE, Rao RV. Direct Transcriptional Effects of Apolipoprotein E. *J Neurosci*. 2016;36(3):685-700. doi:10.1523/JNEUROSCI.3562-15.2016
468. Lin Y-T, Seo J, Gao F, et al. APOE4 Causes Widespread Molecular and Cellular Alterations Associated with Alzheimer's Disease Phenotypes in Human iPSC-Derived Brain Cell Types. *Neuron*. 2018/06/27/ 2018;98(6):1141-1154.e7. doi:https://doi.org/10.1016/j.neuron.2018.05.008
469. Mordovkina D, Lyabin DN, Smolin EA, Sogorina EM, Ovchinnikov LP, Eliseeva I. Y-Box Binding Proteins in mRNP Assembly, Translation, and Stability Control. *Biomolecules*. 2020;10(4):591. doi:10.3390/biom10040591
470. Kleene KC. Y-box proteins combine versatile cold shock domains and arginine-rich motifs (ARMs) for pleiotropic functions in RNA biology. *Biochemical Journal*. 2018;475(17):2769-2784. doi:10.1042/BCJ20170956
471. Lyabin DN, Eliseeva IA, Smolin EA, et al. YB-3 substitutes YB-1 in global mRNA binding. *RNA Biol*. 2020;17(4):487-499. doi:10.1080/15476286.2019.1710050
472. Cooke A, Schwarzl T, Huppertz I, et al. The RNA-Binding Protein YBX3 Controls Amino Acid Levels by Regulating SLC mRNA Abundance. *Cell Reports*. 2019;27(11):3097-3106.e5. doi:10.1016/j.celrep.2019.05.039
473. GeneCards. YBX3. Accessed March 22, 2022, https://www.genecards.org/cgi-bin/carddisp.pl?gene=YBX3
474. Wadhwani AR, Affaneh A, Van Gulden S, Kessler JA. Neuronal apolipoprotein E4 increases cell death and phosphorylated tau release in alzheimer disease. *Annals of neurology*. 2019;85(5):726-739. doi:10.1002/ana.25455
475. Hashimoto Y, Jiang H, Niikura T, et al. Neuronal apoptosis by apolipoprotein E4 through low-density lipoprotein receptor-related protein and heterotrimeric GTPases. *J Neurosci*. 2000;20(22):8401-8409. doi:10.1523/JNEUROSCI.20-22-08401.2000
476. Ash PEA, Vanderweyde TE, Youmans KL, Apicco DJ, Wolozin B. Pathological stress granules in Alzheimer's disease. *Brain Res*. 2014;1584:52-58. doi:10.1016/j.brainres.2014.05.052
477. Glowacka WK, Alberts P, Ouchida R, Wang J-Y, Rotin D. LAPTM5 protein is a positive regulator of proinflammatory signaling pathways in macrophages. *The Journal of biological chemistry*. 2012;287(33):27691-27702. doi:10.1074/jbc.M112.355917

478. Fitz NF, Wolfe CM, Playso BE, et al. Trem2 deficiency differentially affects phenotype and transcriptome of human APOE3 and APOE4 mice. *Molecular Neurodegeneration*. 2020/07/23 2020;15(1):41. doi:10.1186/s13024-020-00394-4
479. Patel KR, Zhu K, Henrion MYR, et al. Single Cell-type Integrative Network Modeling Identified Novel Microglial-specific Targets for the Phagosome in Alzheimer's disease. *bioRxiv*. 2020:2020.06.09.143529. doi:10.1101/2020.06.09.143529
480. Angénieux C, Waharte F, Gidon A, et al. Lysosomal-Associated Transmembrane Protein 5 (LAPTM5) Is a Molecular Partner of CD1e. *PLOS ONE*. 2012;7(8):e42634. doi:10.1371/journal.pone.0042634
481. Salih DA, Bayram S, Guelfi S, et al. Genetic variability in response to amyloid beta deposition influences Alzheimer's disease risk. *Brain communications*. 2019;1(1):fcz022-fcz022. doi:10.1093/braincomms/fcz022
482. Forabosco P, Ramasamy A, Trabzuni D, et al. Insights into TREM2 biology by network analysis of human brain gene expression data. *Neurobiology of aging*. 2013;34(12):2699-2714. doi:10.1016/j.neurobiolaging.2013.05.001
483. Zhang B, Gaiteri C, Bodea L-G, et al. Integrated Systems Approach Identifies Genetic Nodes and Networks in Late-Onset Alzheimer’s Disease. *Cell*. 2013;153(3):707-720. doi:10.1016/j.cell.2013.03.030
484. Nam KN, Wolfe CM, Fitz NF, et al. Integrated approach reveals diet, APOE genotype and sex affect immune response in APP mice. *Biochim Biophys Acta Mol Basis Dis*. 2018;1864(1):152-161. doi:10.1016/j.bbadis.2017.10.018
485. Warner MH, Roinick KL, Arndt KM. Rtf1 is a multifunctional component of the Paf1 complex that regulates gene expression by directing cotranscriptional histone modification. *Mol Cell Biol*. Sep 2007;27(17):6103-15. doi:10.1128/mcb.00772-07
486. Yan T, Ding F, Zhao Y. Integrated identification of key genes and pathways in Alzheimer's disease via comprehensive bioinformatical analyses. *Hereditas*. 2019;156:25-25. doi:10.1186/s41065-019-0101-0
487. Wang X, Allen M, Li S, et al. Deciphering cellular transcriptional alterations in Alzheimer's disease brains. *Molecular Neurodegeneration*. 2020/07/13 2020;15(1):38. doi:10.1186/s13024-020-00392-6
488. Ciryam P, Kundra R, Freer R, Morimoto RI, Dobson CM, Vendruscolo M. A transcriptional signature of Alzheimer's disease is associated with a metastable subproteome at risk for aggregation. *Proceedings of the National Academy of Sciences*. 2016;113(17):4753. doi:10.1073/pnas.1516604113
489. Strehler EE. Plasma membrane calcium ATPases: From generic Ca2+ sump pumps to versatile systems for fine-tuning cellular Ca2+. *Biochemical and Biophysical Research Communications*. 2015/04/24/ 2015;460(1):26-33. doi:https://doi.org/10.1016/j.bbrc.2015.01.121
490. Chen M, Laursen SH, Habekost M, et al. Central and Peripheral Nervous System Progenitors Derived from Human Pluripotent Stem Cells Reveal a Unique Temporal and Cell-Type Specific Expression of PMCAs. Original Research. *Frontiers in Cell and Developmental Biology*. 2018-February-06 2018;6doi:10.3389/fcell.2018.00005
491. Feng H, Moakley DF, Chen S, McKenzie MG, Menon V, Zhang C. Complexity and graded regulation of neuronal cell-type-specific alternative splicing revealed by single-cell RNA sequencing. *Proceedings of the National Academy of Sciences of the United States of America*. 2021;118(10):e2013056118. doi:10.1073/pnas.2013056118
492. Morabito S, Miyoshi E, Michael N, Swarup V. Integrative genomics approach identifies conserved transcriptomic networks in Alzheimer's disease. *Human Molecular Genetics*. 2020;29(17):2899-2919. doi:10.1093/hmg/ddaa182
493. Baglietto-Vargas D, Forner S, Cai L, et al. Generation of a humanized Aβ expressing mouse demonstrating aspects of Alzheimer's disease-like pathology. *Nature Communications*. 2021/04/23 2021;12(1):2421. doi:10.1038/s41467-021-22624-z
494. Calcium Hypothesis of Alzheimer's disease and brain aging: A framework for integrating new evidence into a comprehensive theory of pathogenesis. *Alzheimers Dement*. Feb 2017;13(2):178-182.e17. doi:10.1016/j.jalz.2016.12.006
495. Veinbergs I, Everson A, Sagara Y, Masliah E. Neurotoxic effects of apolipoprotein E4 are mediated via dysregulation of calcium homeostasis. *J Neurosci Res*. Feb 1 2002;67(3):379-87. doi:10.1002/jnr.10138
496. Xu P-T, Li Y-J, Qin X-J, et al. A SAGE study of apolipoprotein E3/3, E3/4 and E4/4 allele-specific gene expression in hippocampus in Alzheimer disease. *Molecular and cellular neurosciences*. 2007;36(3):313-331. doi:10.1016/j.mcn.2007.06.009
497. Alonso AdC, Zaidi T, Grundke-Iqbal I, Iqbal K. Role of abnormally phosphorylated tau in the breakdown of microtubules in Alzheimer disease. *Proceedings of the National Academy of Sciences*. 1994;91(12):5562-5566.
498. Johnson ECB, Carter EK, Dammer EB, et al. Large-scale deep multi-layer analysis of Alzheimer's disease brain reveals strong proteomic disease-related changes not observed at the RNA level. *Nat Neurosci*. 2022/02/01 2022;25(2):213-225. doi:10.1038/s41593-021-00999-y

499. Holstege H, Hulsman M, Charbonnier C, et al. Exome sequencing identifies novel AD-associated genes. *medRxiv*. 2020:2020.07.22.20159251. doi:10.1101/2020.07.22.20159251
500. Peterson RE, Kuchenbaecker K, Walters RK, et al. Genome-wide Association Studies in Ancestrally Diverse Populations: Opportunities, Methods, Pitfalls, and Recommendations. *Cell*. Oct 17 2019;179(3):589-603. doi:10.1016/j.cell.2019.08.051
501. Lennon JC, Aita SL, Bene VAD, et al. Black and White individuals differ in dementia prevalence, risk factors, and symptomatic presentation. *Alzheimers Dement*. Dec 2 2021;doi:10.1002/alz.12509
502. Rajabli F, Feliciano BE, Celis K, et al. Ancestral origin of ApoE ε4 Alzheimer disease risk in Puerto Rican and African American populations. *PLoS Genet*. Dec 2018;14(12):e1007791. doi:10.1371/journal.pgen.1007791
503. Gureje O, Ogunniyi A, Baiyewu O, et al. APOE ε4 is not associated with Alzheimer's Disease in elderly Nigerians. *Annals of neurology*. 2006;59(1):182-185.
504. Barnes LL, Bennett DA. Alzheimer's disease in African Americans: risk factors and challenges for the future. *Health Aff (Millwood)*. 2014;33(4):580-586. doi:10.1377/hlthaff.2013.1353
505. 2020 Alzheimer's disease facts and figures. *Alzheimers Dement*. Mar 10 2020;doi:10.1002/alz.12068
506. Kunkle BW, Schmidt M, Klein HU, et al. Novel Alzheimer Disease Risk Loci and Pathways in African American Individuals Using the African Genome Resources Panel: A Meta-analysis. *JAMA Neurol*. Jan 1 2021;78(1):102-113. doi:10.1001/jamaneurol.2020.3536
507. Hohman TJ, Cooke-Bailey JN, Reitz C, et al. Global and local ancestry in African-Americans: Implications for Alzheimer's disease risk. *Alzheimers Dement*. Mar 2016;12(3):233-43. doi:10.1016/j.jalz.2015.02.012
508. Tosto G, Fu H, Vardarajan BN, et al. F-box/LRR-repeat protein 7 is genetically associated with Alzheimer's disease. *Ann Clin Transl Neurol*. Aug 2015;2(8):810-20. doi:10.1002/acn3.223
509. Kang S, Gim J, Gunasekaran TI, et al. APOE-stratified genome-wide association study suggests potential novel genes for late-onset Alzheimer's disease in East-Asian descent. *medRxiv*. 2021:2020.07.02.20145557. doi:10.1101/2020.07.02.20145557
510. Lee JJ, Wedow R, Okbay A, et al. Gene discovery and polygenic prediction from a genome-wide association study of educational attainment in 1.1 million individuals. *Nature Genetics*. 2018/08/01 2018;50(8):1112-1121. doi:10.1038/s41588-018-0147-3
511. Haworth CMA, Wright MJ, Luciano M, et al. The heritability of general cognitive ability increases linearly from childhood to young adulthood. *Molecular psychiatry*. 2010;15(11):1112-1120. doi:10.1038/mp.2009.55
512. Spengler M, Gottschling J, Hahn E, Tucker-Drob EM, Harzer C, Spinath FM. Does the heritability of cognitive abilities vary as a function of parental education? Evidence from a German twin sample. *PloS one*. 2018;13(5):e0196597-e0196597. doi:10.1371/journal.pone.0196597
513. Morris TT, Davies NM, Dorling D, Richmond RC, Smith GD. Examining the genetic influences of educational attainment and the validity of value-added measures of progress. *bioRxiv*. 2018:233635. doi:10.1101/233635
514. Kan KJ, Wicherts JM, Dolan CV, van der Maas HL. On the nature and nurture of intelligence and specific cognitive abilities: the more heritable, the more culture dependent. *Psychol Sci*. Dec 2013;24(12):2420-8. doi:10.1177/0956797613493292
515. Tucker-Drob EM, Briley DA, Harden KP. Genetic and Environmental Influences on Cognition Across Development and Context. *Curr Dir Psychol Sci*. Oct 2013;22(5):349-355. doi:10.1177/0963721413485087
516. Oveisgharan S, Wilson RS, Yu L, Schneider JA, Bennett DA. Association of Early-Life Cognitive Enrichment With Alzheimer Disease Pathological Changes and Cognitive Decline. *JAMA Neurology*. 2020;77(10):1217-1224. doi:10.1001/jamaneurol.2020.1941
517. Hohman TJ, Kaczorowski CC. Modifiable Lifestyle Factors in Alzheimer Disease: An Opportunity to Transform the Therapeutic Landscape Through Transdisciplinary Collaboration. *JAMA Neurology*. 2020;77(10):1207-1209. doi:10.1001/jamaneurol.2020.1114
518. Sebastiani P, Gurinovich A, Nygaard M, et al. APOE Alleles and Extreme Human Longevity. *The Journals of Gerontology: Series A*. 2019;74(1):44-51. doi:10.1093/gerona/gly174
519. Ryu S, Atzmon G, Barzilai N, Raghavachari N, Suh Y. Genetic landscape of APOE in human longevity revealed by high-throughput sequencing. *Mechanisms of ageing and development*. 2016;155:7-9. doi:10.1016/j.mad.2016.02.010
520. Whittemore K, Vera E, Martínez-Nevado E, Sanpera C, Blasco MA. Telomere shortening rate predicts species life span. *Proceedings of the National Academy of Sciences*. 2019;116(30):15122. doi:10.1073/pnas.1902452116
521. Mahoney ER, Dumitrescu L, Seto M, et al. Telomere length associations with cognition depend on Alzheimer's disease biomarkers. *Alzheimers Dement (N Y)*. 2019;5:883-890. doi:10.1016/j.trci.2019.11.003

522. Andrew MK, Tierney MC. The puzzle of sex, gender and Alzheimer's disease: Why are women more often affected than men? *Womens Health (Lond)*. 2018;14:1745506518817995. doi:10.1177/1745506518817995
523. Neu SC, Pa J, Kukull W, et al. Apolipoprotein E Genotype and Sex Risk Factors for Alzheimer Disease: A Meta-analysis. *JAMA neurology*. 2017;74(10):1178-1189.
524. Hohman TJ, Dumitrescu L, Barnes LL, et al. Sex-specific effects of Apolipoprotein E with cerebrospinal fluid levels of tau. *JAMA Neurology*. 2018;75(8):989-998. doi:10.1001/jamaneurol.2018.0821
525. Koran MEI, Wagener M, Hohman TJ, Alzheimer's Neuroimaging I. Sex differences in the association between AD biomarkers and cognitive decline. *Brain imaging and behavior*. 2017;11(1):205-213. doi:10.1007/s11682-016-9523-8
526. Barnes LL, Wilson RS, Bienias JL, Schneider JA, Evans DA, Bennett DA. Sex Differences in the Clinical Manifestations of Alzheimer Disease Pathology. *Archives of General Psychiatry*. 2005;62(6):685-691. doi:10.1001/archpsyc.62.6.685
527. Buckley RF, Mormino EC, Rabin JS, et al. Sex Differences in the Association of Global Amyloid and Regional Tau Deposition Measured by Positron Emission Tomography in Clinically Normal Older Adults. *JAMA Neurol*. May 1 2019;76(5):542-551. doi:10.1001/jamaneurol.2018.4693
528. Buckley RF, Scott MR, Jacobs HIL, et al. Sex Mediates Relationships Between Regional Tau Pathology and Cognitive Decline. *Ann Neurol*. Aug 16 2020;88(5):921-932. doi:10.1002/ana.25878
529. Deming Y, Dumitrescu L, Barnes LL, et al. Sex-specific genetic predictors of Alzheimer's disease biomarkers. *Acta Neuropathol*. Dec 2018;136(6):857-872. doi:10.1007/s00401-018-1881-4
530. Dumitrescu L, Barnes LL, Thambisetty M, et al. Sex differences in the genetic predictors of Alzheimer's pathology. *Brain*. 2019;142(9):2581-2589. doi:10.1093/brain/awz206 %J Brain
531. Dumitrescu L, Mayeda ER, Sharman K, Moore AM, Hohman TJ. Sex differences in the genetic architecture of Alzheimer's disease. *Current Genetic Medicine Reports*. 2019;7(1):13-21. doi:10.1007/s40142-019-0157-1
532. Mathys H, Davila-Velderrain J, Peng Z, et al. Single-cell transcriptomic analysis of Alzheimer's disease. *Nature*. 2019;570(7761):332-337. doi:10.1038/s41586-019-1195-2
533. Dubal DB. Chapter 16 - Sex difference in Alzheimer's disease: An updated, balanced and emerging perspective on differing vulnerabilities. In: Lanzenberger R, Kranz GS, Savic I, eds. *Handbook of Clinical Neurology*. Elsevier; 2020:261-273.
534. Langfelder P, Horvath S. Eigengene networks for studying the relationships between co-expression modules. *BMC Systems Biology*. 2007/11/21 2007;1(1):54. doi:10.1186/1752-0509-1-54
535. Langfelder P, Zhang B, Horvath S. Defining clusters from a hierarchical cluster tree: the Dynamic Tree Cut package for R. *Bioinformatics*. 2007;24(5):719-720. doi:10.1093/bioinformatics/btm563
536. Parikshak NN, Luo R, Zhang A, et al. Integrative functional genomic analyses implicate specific molecular pathways and circuits in autism. *Cell*. 2013;155(5):1008-1021. doi:10.1016/j.cell.2013.10.031